



UNIVERSITÀ DEGLI STUDI DI SALERNO



UNIVERSITÀ DEGLI STUDI DI SALERNO

Dipartimento di Farmacia

PhD Program

in **Drug Discovery and Development**

XXXII Cycle — Academic Year 2019/2020

PhD Thesis in

***Rational design, synthesis and in vitro
evaluation of cell-active chemical probes for
bromodomain-containing proteins***

Candidate

Alessandra Cipriano

Supervisor(s)

Prof. *Sabrina Castellano*

Prof. *Gianluca Sbardella*

PhD Program Coordinator: Prof. Dr. *Gianluca Sbardella*

INDEX

ABSTRACT	VII
CHAPTER I.....	1
INTRODUCTION	1
1.1 Epigenetic	3
1.2 Lysine acetylation: an important epigenetic mark.....	4
1.3 Bromodomain-containing proteins	10
1.4 BET proteins: structure and physio-pathological roles	13
1.5 BET ligands	17
1.6 Selectivity within BET family	23
1.7 Bivalent BET ligands	27
1.8 PROTAC approach.....	28
CHAPTER II	39
AIM OF WORK	39
2.1 Aim of work	41
2.2 Bisubstrate approach.....	42
2.3 Frozen analogue-approach.....	46
2.4 PROTAC approach.....	48
CHAPTER III.....	51
RESULTS AND DISCUSSION.....	51
3.1 Bivalent ligands	53

3.2 Benzimidazole-based ligands.....	57
3.3 BET PROTACs compounds	63
CHAPTER IV.....	69
CHEMISTRY	69
4.1 Synthesis of bivalent ligands.....	71
4.2 Synthesis of benzimidazole-based ligands.....	83
4.3 Synthesis of BET PROTACs	87
CHAPTER V	103
CONCLUSIONS	103
CHAPTER VI.....	107
MATERIALS AND METHODS	107
7.1 General information	109
7.2 Synthetic procedures	110
7.3 Biological protocols	211
7.4 NMR Data.....	214
REFERENCES.....	263

ABSTRACT

Bromodomains (BRDs) are epigenetic readers able to selectively recognize the acetylated lysine residues on histone and non-histone proteins. Through their activity, bromodomain-containing proteins (BRDs) are involved in a wide range of cellular events, such as chromatin remodeling and transcriptional activation. One of the most studied and druggable family of bromodomain-containing proteins is the Bromo and Extra Terminal domain (BET) family, whose members (BRD2, BRD3, BRD4, and BRDT) contain two highly homologous bromodomains: BD1 and BD2. Despite several ligands have been discovered, there is still need to identify novel classes of compounds with high potency, selectivity and in vivo activity.

This Ph. D. project is focused on the design, synthesis, biochemical and biophysical evaluation of new chemical probes for BET proteins. To this purpose, three different medicinal approaches were applied to obtain different classes of compounds. Exploiting the bisubstrate approach, bivalent ligands were designed and synthesized. Biochemical and biophysical assays allowed the identification of compound **3** (EML896), a promising bivalent compound able to bind both BD1 and BD2 bromodomain of BET proteins. Applying a frozen analogue approach, the diazobenzene core of reported diazobenzene-ligands was rigidized, yielding a benzimidazole scaffold. A small library of benzimidazole-based ligands has been designed and synthesized and compound **15** (EML765) was identified as promising BD1 selective ligand. Finally, at the University of Dundee, the attention was focused on compounds able to induce protein degradation. Specifically, proteolysis targeting chimera compounds (PROTACs) containing BD1 and BD2 selective warhead were designed, synthesized and biological evaluated.

CHAPTER I

INTRODUCTION

1.1 Epigenetic

Post-translational modifications (PTMs) on histones are key mechanisms to regulate the expression of specific genes inside the cells. Despite the identical genetic material, cells retain distinct characteristics and biological functions in the tissues and organs in which they are expressed. Epigenetics is the study of reversible and heritable changes which modulate genes activity without altering the underlying DNA sequences.¹

To minimize the space occupied in cells, DNA is organized in a multi-protein complex called chromatin. The basic element of chromatin is the nucleosome, a structure of DNA wrapped around an octamer of histone proteins composed of a tetramer, containing two copies of both H3 and H4, combined with two H2A/H2B dimers. Histones are highly conserved basic proteins, enrich of lysine and arginine both of which have a positive charge, which helps them to bind the negatively charged phosphate backbone of DNA. The differential condensation state of chromatin regulates the accessibility of transcriptional machinery to genes for their initially transcription into mRNA that finally gets translated into proteins.²

There are two major states of chromatin. Heterochromatin is densely packed and transcriptionally silent. On the other hand, euchromatin is less condensed, more accessible, and therefore transcriptionally active.

The conformation of chromatin is dynamically modified through epigenetic modifications such as methylation, acetylation, phosphorylation, sumoylation and ubiquitination. These post-translational modifications (PTMs) on histone and non-histone proteins act as epigenetic marks that regulate the expression of specific genes inside the cells and are, consequently, able to regulate different processes such as differentiation, development, proliferation and genome integrity.

Over the past years, different proteins have been identified and characterized as epigenetic actors (Figure 1.1). *Writers* are enzymes able to catalyze the insertion of chemical modifications

into either histone tails or the DNA. Epigenetic *erasers* are enzymes able to remove the added modifications. Epigenetic *readers* are domains able to selectively recognize the inserted epigenetic marks.³

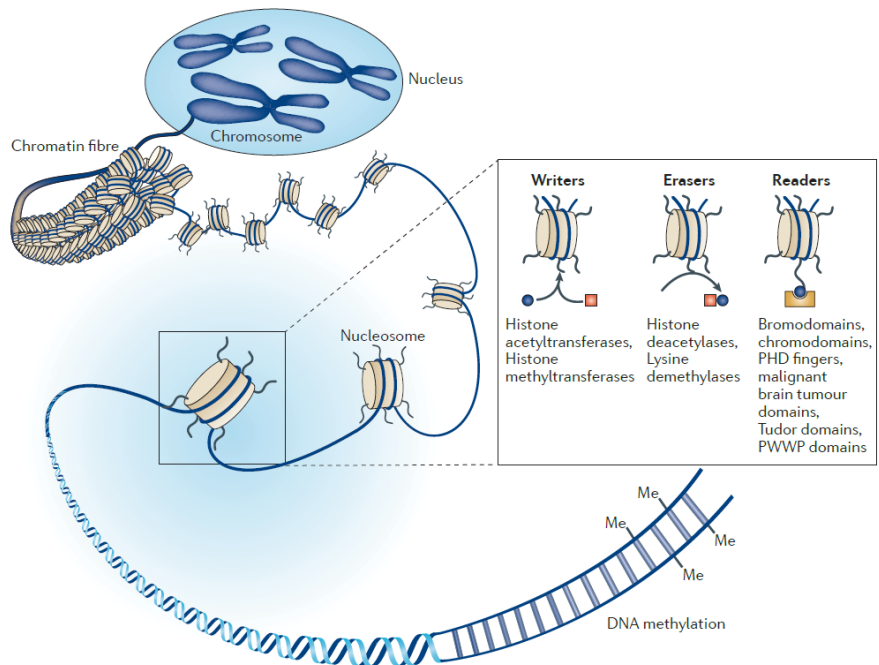


Figure 1.1 Representation of the proteins which insert (*writers*), remove (*erasers*) and read (*readers*) the epigenetic modifications.³

1.2 Lysine acetylation: an important epigenetic mark

One of the main epigenetic mechanisms in the regulation of biological processes is the protein acetylation, which occur on lysine residues of histone proteins. Three classes of epigenetic proteins act in this process: ‘*writers*’ or lysine acetyltransferases (KATs), which insert acetyl groups to proteins; ‘*erasers*’ or lysine deacetylases (KDACs), which remove acetyl groups; and ‘*readers*’ or acetyllysine binders, which selectively recognize the acetylated proteins.

1.2.1 Lysine Acetyltransferases (KATs)

Acetylation is a dynamic process, mediated by acetyltransferases (KATs), that involves the transfer of acetyl group to ϵ -amino group of lysine residues from acetyl-coenzyme A (Ac-CoA), which acts as a cofactor.⁴ Traditionally, KATs are classified into two major classes: type A and type B. To the type B class belong the cytoplasmic acetyltransferases, which add the acetyl mark on newly synthesized histone H4 at K5 and K12 (as well as certain sites within H3), driving their translocation into the nucleus and their correct deposition into chromatin. On the other hand, the type A KATs are a heterogeneous family of enzymes, located in the nucleus, which act as activators to enhance transcription.⁵⁻⁶ In fact, the acetylation neutralizes the positive charge of lysine residues of histone proteins, decreasing their binding to the negatively charged phosphate of DNA. In this way, the chromatin adopts a more open and less condensed conformation, accessible to the transcriptional machinery. Moreover, the acetyl group acts as a mark, specifically recognized by acetyllysine *readers*, forming a new surface for protein association and cellular signaling transduction (Figure 1.2).⁷

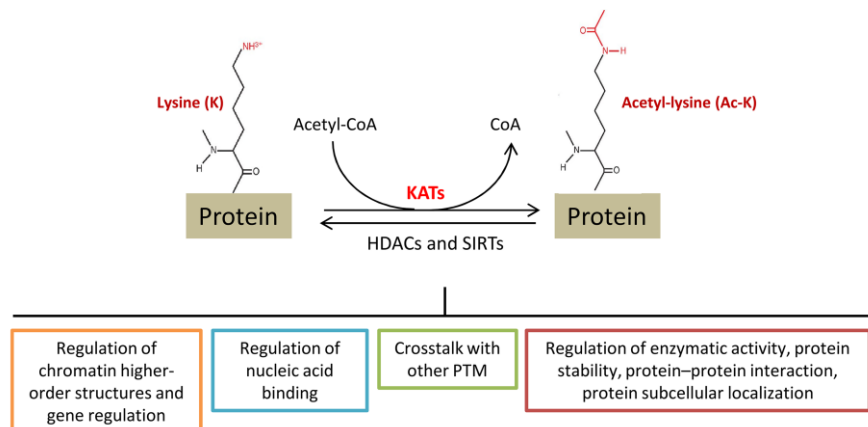


Figure 1.2 Schematic representation of acetylation process and the impact on different biological function of different proteins.⁷

Based on structure similarities in the binding pocket, the nuclear KAT are properly divided into five major families: the MOZ, Ybf2, SAS2, and Tip60 (MYST) family; the general control

non-repressible 5 (GCN5)-related N-acetyltransferase (GNAT) family; the general transcription factor HATs containing the TAF250 domain; the CREB-binding protein (CBP) and the E1A-associated protein of 300 kDa (p300) family; and the steroid/nuclear receptor co-activators (SRC/NCoA) family.⁶

Changes in the activity and/or expression levels of KATs, are related to different diseases states. Several studies suggest that CBP has a critical role in the regular development of the hematopoietic system whereas p300 has an important tumor-suppressor role. Different type of cancers such as lung, colon, breast and ovarian carcinomas are related to mutations and/or deletions of p300 and/or CBP. Chromosomal translocation occurring on p300/CBP genes are associated with leukemia and lymphomas.⁷⁻⁹ Also the GNAT and MYST family members are closely linked to the hallmarks of cancer. Outside oncology indications, several data support a role for histone acetylation in diverse neurological disorders. It has been extensively reported that the acetylation balance is important in memory storage and neuronal plasticity. Some KAT or KDAC are highly expressed in brain areas involved in learning and memory, such as the hippocampus and prefrontal cortex. Several reports shown that neurological disorders such as Parkinson's, Huntington's and Alzheimer's diseases are strictly connected to down-regulation or loss of function of p300/CBP.¹⁰⁻¹¹

Interestingly, knockout or chemical inhibition of a GNAT family member, the p300/CBP-associated factor (PCAF) improve cognitive and behavioral deficits in model of Alzheimer's disease.¹² Mutations of CBP gene result in Rubinstein–Taybi syndrome (RTS), characterized by a short stature, intellectual disability, distinctive facial features, and broad thumbs.⁸ High p300 levels induce hypertrophy in cardiomyocytes and lead to a greater accumulation of fatty acids, insulin resistance and inflammation of the liver, with an important role in cardiovascular diseases and diabetes.¹³

1.2.2 Lysine deacetylases (KDACs)

The acetyl group is specifically removed from lysine residues in histones proteins by lysine deacetylases (KDACs) or histone deacetylases (HDACs), *epigenetic erasers*. Deacetylation restores the positive charge on lysines that is related with the condensed and transcriptionally inactive state of chromatin.

HDACs are divided into five classes based on sequence similarities (Figure 1.3). Class I includes HDAC1, HDAC2, HDAC3 and HDAC8; class IIa consists of HDAC4, HDAC5, HDAC7 and HDAC9; class IIb comprises HDAC6 and HDAC10; class III comprises the sirtuins from SIRT1 to SIRT7; HDAC11 is the only member of class IV. A zinc ion is required for catalysis of enzymes from classes I, II and IV. On the other hand, sirtuins required NAD⁺ as cofactor for enzyme activity and own deacetylase and ADPribosylase activity (Figure 1.3).¹⁴

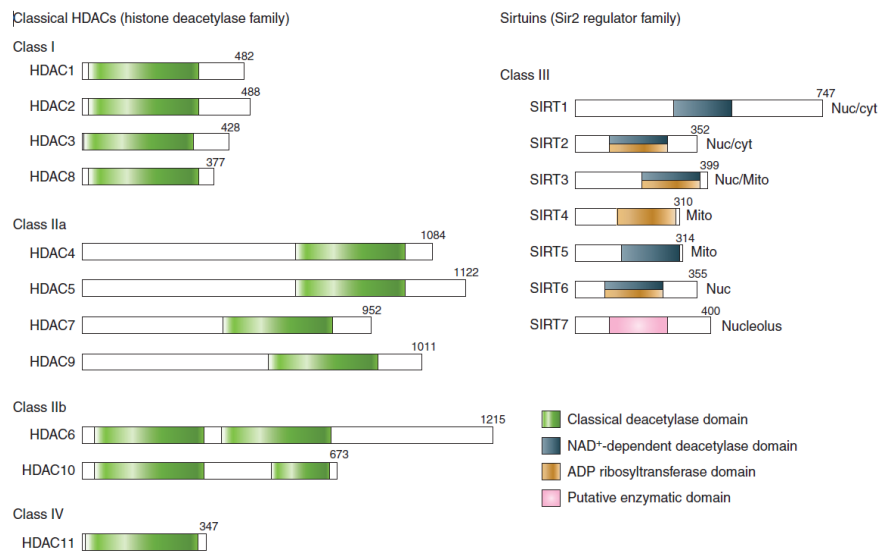


Figure 1.3 Schematic representation of deacetylases based on: number of aminoacids (on the right of each proteins); cellular localizations (Nuc, nuclear; cyt, cytoplasmic; Mito, mitochondrial); deacetylation mechanism (on the lower-right).¹⁴

As well as acetyltransferases, HDACs control the equilibrium of acetylation state and their aberrant activity has been associated with several pathological conditions such as cancer,

neurological diseases, metabolic disorders, inflammatory diseases, cardiac diseases, and pulmonary diseases.¹⁵ It is important to mention four HDAC inhibitors approved by FDA for different oncological indications. In 2006, Vorinostat was approved for the treatment of cutaneous manifestations in patients with cutaneous T cell lymphoma. Three years later, Romidepsin was firstly approved for cutaneous T-cell lymphoma and then for peripheral T-cell lymphomas. For the same lymphomas, Belinostat was approved in 2014. One years later, Panobinostat was approved for the treatment of multiple myeloma.¹⁶

1.2.3 Acetyllysine readers: bromodomain

The acetyl group on lysine residues of histone proteins is selectively recognized by epigenetic *readers*, called bromodomain (BRD). First identified in the *brahma* gene in *Drosophila melanogaster*, hence the name, bromodomains are protein-protein interactions modules of approximately 110 aminoacids.

The human proteome encodes 61 bromodomains, which are present in 46 human nuclear and cytoplasmic proteins. These include histone methyltransferases such as ASH1L and mixed lineage leukemia protein (MLL), bromodomain-containing protein (BRD9), HATs (p300/CBP associated-factor and GCN5L2), transcriptional co-activators (TRIM), ATP-dependent chromatin remodeling complexes (bromodomain adjacent to zinc finger domain protein 1B (BAZ1B)), nuclear-scaffolding proteins (polybromo 1 (PBRM1/PB1), helicases (SWI/SNF-related matrix-associated actin-dependent regulators of chromatin subfamily A (SMARCA5)) and the bromo and extra-terminal domain (BET) family. Based on sequence similarity, the BRD are divided into eight structural classes (Figure 1.4).¹⁷⁻¹⁸

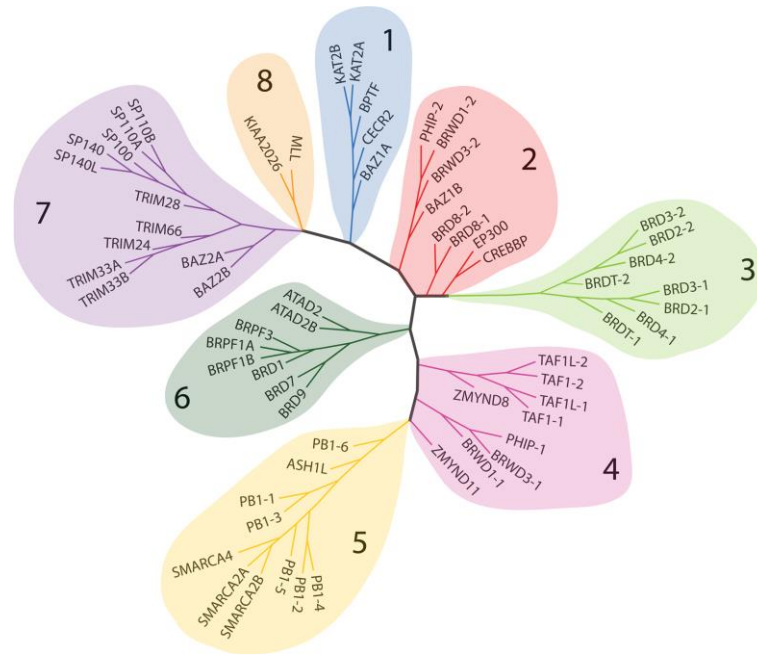


Figure 1.4 Sequence similarity-based phylogenetic tree of the 61 human bromodomains, divided into eight structural classes.¹⁸

Despite the unique architecture of each protein, bromodomains have a conserved binding pocket that comprises four α -helices (named α Z, α A, α B and α C) linked to form a large loop (the ZA loop) and a shorter loop (the BC loop). Different composition of the ZA and the BC loop allow the binding of different BRDs to distinct lysine acetylation sites.¹⁹

The ability of human BRDs to selectively recognize acetylated peptides was shown by Filippakopoulos *et al* in 2012. According to other studies, the binding of BRDs to acetylated histone peptides *in vitro* is relatively weak, suggesting that the high affinity binding *in vivo* is associated to additional interaction domains.²⁰⁻²¹

The orientation of the bound peptide can dramatically change with different domains adjacent to the BRD module. Despite that, the acetyl group is recognized in a conserved manner, involving two hydrogen bond with the carbonyl oxygen of acetyl-lysine (KAc): a direct one, with the side-chain amino group of a conserved asparagine residue in the BC loop and a water-mediated hydrogen bond with a tyrosine residue in the ZA loop.²²

BRD-containing proteins are involved in the regulation of gene expression through the modulation of transcription and have a broad range of roles in cellular homeostasis.²³

The implication of aberrant functions of BRD-containing proteins in several human diseases stimulated the development of BRD inhibitors and, over the past few years, the identification of several *chemical probes* allowed to elucidate the biological functions of these proteins.

The most important BRD-containing proteins and their ligands are summarized in the next Sections.

1.3 Bromodomain-containing proteins

1.3.1 HATs containing a bromodomain: p300/CBP and PCAF

The acetyltransferases CBP and p300 (Section 1.2.1) contain a bromodomain flanking the HAT catalytic domain that is important in binding of CBP/p300 to chromatin and in induction of histone acetylation at specific sites.^{24,25} Recently, different ligands specific for the bromodomains of CBP and p300 have been reported (Figure 1.5). **SGC-CBP30**, the first compound reported to bind CBP/p300 bromodomain with high potency (K_D values of 21 and 32 nM for CBP and p300 BRDs, respectively) and good selectivity over other bromodomain proteins, was discovered in 2014 by Structure Genomic Consortium (SGC). **CBP30** reduce immune cell production of several pro-inflammatory cytokines with further therapeutic applications not only in an oncology context but also in the treatment of autoimmune disorders.²⁶⁻²⁷

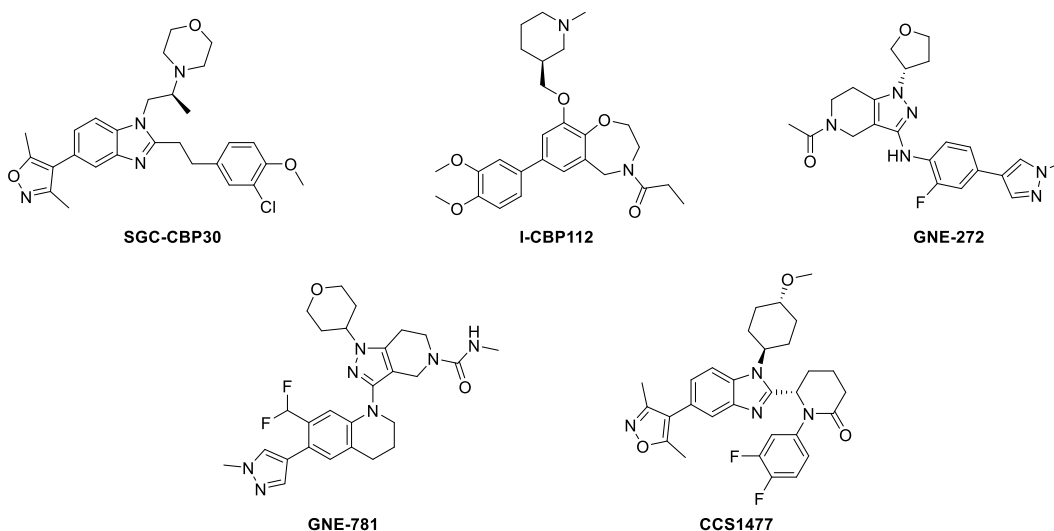


Figure 1.5 Selected ligands of p300/CBP bromodomain.

The same group developed a benzoxazine-based compound (**I-CBP112**) less potent than **CBP-30** (K_D values of 0.142 and 0.625 μM for CBP and p300, respectively) but with a better selectivity toward BET family members (IC_{50} of 15 μM for BRD4 (BD1) compared to 3.2 μM for BRD4 (BD1) of **CBP-30**). It has been shown that a synergistic combination of **I-CBP112** and **A-485**, a CBP/p300 acetyltransferase inhibitor, can decrease the transcription of androgen-dependent and pro-oncogenic prostate genes, reducing cell proliferation in prostate cancer.²⁸

In 2017, **GNE-272** was identified as promising pyrazole-based compound and further SAR studies allowed the identification of **GNE-781** with high potency (IC_{50} of 6.2 nM), selectivity over other BRD-containing proteins and anti-tumor activity in AML tumor model.²⁹⁻³⁰ CellCentric has initiated a phase I/IIa clinical trial (NCT03568656) for the **CCS1477** compound in patients with metastatic prostate cancer and other solid tumors. This compound is a potent (K_D values of 1.7 and 1.3 nM for CBP and p300 BRDs respectively), selective (approximately 170 fold over BET members) and orally bioavailable inhibitor of the bromodomain of p300 and CBP.³¹

PCAF is another multi-domain protein containing a histone acetyltransferase unit and a single bromodomain.

During transcription, this protein associates CBP and p300 and several type of diseases such as cancer, neuroinflammation and HIV infection are related to its misregulation.³²⁻³³

1.3.2 Bromodomain-containing protein 9 (BRD9)

Bromodomain-containing protein 9 and 7 (BRD9 and BRD7) are high homology components of the chromatin remodelling SWI/SNF (BAF) complex. Also these proteins are disease related (e.g. pediatric malignant rhabdoid tumors) and small molecules inhibitors are available (Figure 1.6).³⁴ The first identified BRD7/BRD9 ligand was **LP99**, which helped to better understand the role of these proteins in the regulation of inflammatory cytokines.³⁵

In 2016, GlaxoSmithKline scientists identified the first selective chemical probes for BRD9 (**I-BRD9**) with excellent selectivity over other BRD-containing proteins and a surprisingly selectivity over BRD7 (approximately 200 fold), despite the 85% sequence homology. Treatment with this ligand lead to the down-regulation of sensitive genes implicated in cancer and immunology, suggesting a role of BRD9 in this pathways.³⁶⁻³⁷ The SGC group identified two potent, selective and cell-permeable *chemical probes*, **BI-7273** (IC₅₀ of 19 nM and 117 nM for BRD9 and BRD7 respectively) and **BI-9564** (IC₅₀ of 75 nM and 3.4 μM for BRD9 and BRD7, respectively).³⁸

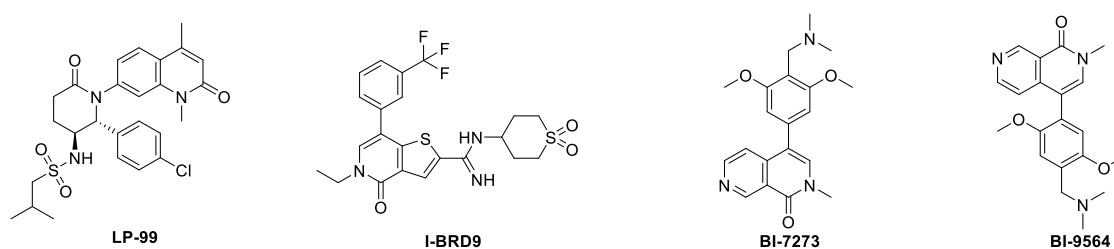


Figure 1.6 Selected ligands of BRD9/BRD7 bromodomain.

1.3.3 BAZ2A/2B, TAF1 and PBI bromodomain

Other bromodomain-containing proteins are the bromo adjacent to zinc finger 2A (BAZ2A) and 2B (BAZ2B), component of the nucleolar remodeling complex (NoRC) which play a role in the regulation of noncoding RNAs. Through their bromodomain, these proteins interact with the acetylated histone tails. High expression levels of BAZ2A have been reported in prostate cancer whereas poor outcome of pediatric B cell acute lymphoblastic leukemia is associated with high expression levels of BAZ2B. One representative BAZ ligand is **GSK2801** depicted in Figure 1.7. This compound has a nanomolar potency (K_D of 136 and 257 nM for BAZ2B and BAZ2A, respectively), selectivity over other BRDs and a good cell-permeability, showing a synergistic activity with BET inhibitors to induces apoptosis in triple-negative breast cancer.³⁹

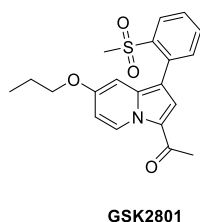


Figure 1.7 BAZ2A/BAZ2B bromodomain ligand.

TFIID, a transcription complex, contain a core subunit TAF1, which contains a tandem BRD module that recognizes multiply acetylated H4 peptides.

A subunit of the PBAF chromatin remodeling complex, PB1 interact with different acetylated lysine through its six tandem bromodomain and its mutations are often found in clear cell renal cell carcinoma.¹⁹

1.4 BET proteins: structure and physio-pathological roles

One of the most important and druggable family of BRD-containing proteins is the BET family (Bromodomain and Extra-Terminal Domain) composed by four proteins: bromodomain-containing protein 2 (BRD2), BRD3, BRD4 and the bromodomain testis-specific protein

(BRDT). With the only exception of BRDT, a tissue-specific isoform expressed in male germ cells, these proteins are ubiquitously expressed in the cell nucleus.

All the BET members share a common domain architecture featuring two evolutionarily highly conserved N-terminal bromodomains (BD1 and BD2) and an extra-terminal domain (ET). The active acetyl-lysine binding pocket has the classical architecture of bromodomain modules. Characteristic of all the BET family members is the “WPF shelf” (W81, P82, F83), a hydrophobic region of the BC loop that includes conserved Trp/Pro/Phe motif (Figure 1.8).⁴⁰

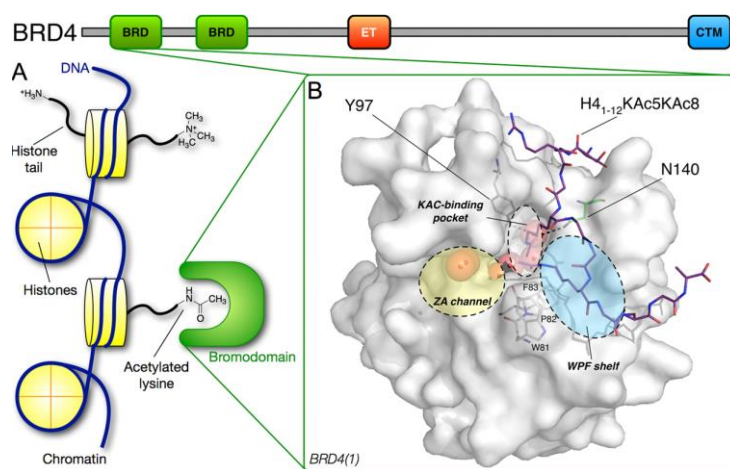


Figure 1.8 General structure of BET proteins considering BRD4 as representative of the family. Highlighted the ZA channel, the acetyl-lysine binding pocket and the WPF shelf.⁴¹

BET proteins play essential roles in different biological processes such as epigenetic memory, regulation of cell-cycle progression through gene transcription, and maintenance of chromatin architecture.

Over the past few years, the development of BET *chemical probes* allowed to better characterize their biological functions and their potential as therapeutic targets. However, the functional differences among the four BET members remain not fully elucidated.⁴²

Bromodomain-containing protein 4 (BRD4) is probably the most studied member of BET family. Through its two BRDs, BRD4 interacts with di-acetylated histone H3 and/or H4. There are three isoforms expressed in humans: one long isoform of 1362 residues (BRD4 A) which

also possess a C-terminal domain (CTD), and two shorter isoforms (BRD4 B and C) that differ by a unique 72-residue at the C terminus (Figure 1.9).⁴³

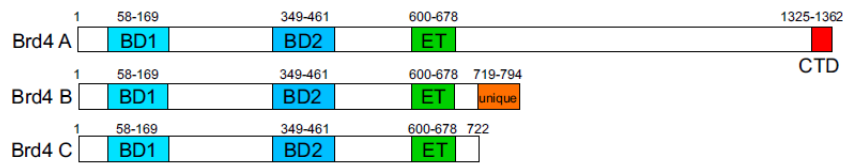


Figure 1.9 Schematic representation of the long isoform (BRD4 A) and the two short isoforms (BRD4 B and C) of BRD4. ET (Extra-terminal domain); CTD (C-terminal domain).⁴⁴

Important is the role of BRD4 in cell cycle control, affecting cell proliferation, apoptosis, transcription and other cellular processes. The C-terminal domain (CTD) and the second bromodomain of BRD4 interacts with cyclin T and CDK9, components of the positive transcription elongation factor complex (P-TEFb). Through its phosphorylation activity, this complex promotes the activation of RNA polymerase II and, consequently, transcriptional elongation. The second bromodomain (BD2) recognizes an acetylated region of cyclin T, preventing the association of P-TEFb with 7SK/HEXIM, a ribonucleoprotein complex that maintain P-TEFb in a kinase-inactive state.⁴⁵ BRD4 marks the start sites of many M/G1 genes, promotes cell-cycle progression to S phase and seems important for the G2 transition to M phase.⁴⁵⁻⁴⁶

Bromodomain-containing protein 2 (BRD2) recognize mainly the acetylated lysine 12 (K12Ac) of H4 and activates transcription (Figure 1.10). Important is the association of BRD2 with E2F, a transcription factors which play a key role during the G1/S transition, regulating the expression of several genes.^{45, 47}

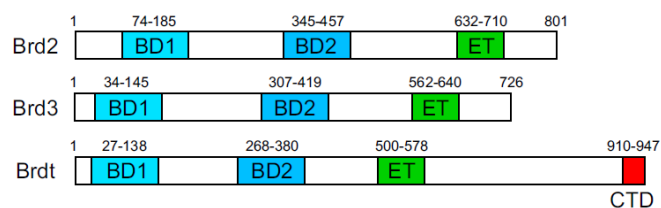


Figure 1.10 Schematic representation of BRD2, BRD3 and BRDT domain.⁴⁴

One of the main function of bromodomain-containing protein 3 (BRD3) is the binding with an acetylated lysine adjacent the *zinc finger* domain of GATA1, a transcription factor with an essential role in hematopoiesis (Figure 1.10). Mutation in the first bromodomain of BRD3 or interference in its interaction resulted in a lower ability of GATA1 to associate chromatin, inhibiting erythroid maturation.⁴⁸

BRDT binds to di-acetylated H4 and mediates the chromatin remodeling during spermatogenesis (Figure 1.10). It has been shown that this bromodomain testis-specific protein is essential for normal spermatogenesis, and mutation in its first bromodomain results in abnormal spermatids and sterility in mice.⁴⁵

The roles of BET proteins in transcriptional regulation connect these proteins to several disease states. Mutation or overexpression of BET proteins are often found in different type of cancers. Fusion of NUT (nuclear protein in testis) with BRD4 or BRD3 are found in the NUT midline carcinoma (NMC), an aggressive and poorly differentiated carcinoma that originates mainly from midline sites such as the head, neck or mediastinum. BET proteins can directly regulate the expression of MYC, a well-characterized oncogene often mutated or overexpressed in several type of malignancies, with important implications in hematologic cancer models, such as MLL-fusion leukemia, acute myeloid leukemia (AML), Burkitt's lymphoma, multiple myeloma, and B-cell acute lymphoblastic (BLL) leukemia. Different brain tumor MYC dependent or independent such as medulloblastoma, diffuse intrinsic pontine glioma (DIPG) and glioblastoma multiform (GBM) are sensitive to BET inhibition.^{46, 49}

Important is the role of BET proteins in inflammation, metabolic disorders and adipogenesis. The implication of BET inhibition in inflammatory and autoimmune disorders is due to their ability to interfere with pro-inflammatory transcription factor such as NF- κ B, STAT3, STAT5 and RORC.⁵⁰ The reduced secretion of cytokines (TNF α , IL-1b, IL-6 and IL-8) and matrix metalloproteinase (MMP-1, MMP-3 and MMP-13) can be helpful in patients with rheumatoid arthritis, osteoarthritis and psoriasis.¹⁷

BET proteins can drive the expression of PPAR γ , a transcription factor important in the adipocyte differentiation and their inhibition may have important implications in metabolic diseases related to adipose tissue dysfunction and obesity.⁵¹

BET inhibition is also investigated in the context of cardiovascular disease and atherosclerosis. At cardiac level, BRD4 expression is induced during cardiac hypertrophy. Moreover, the correlation with NF-kB and GATA4, known to direct heart failure progress, reinforce the implications of these proteins to cardiac disorders.¹⁷

1.5 BET ligands

Over the past few years, the high therapeutic implications of BET proteins prompted a growing interest in developing potent, selective and cell-active BET ligands. Typically, a BET ligand is a small molecule able to insert within the hydrophobic pocket between the ZA and BC loops displacing an acetylated peptide. From the structural point of view, the ligands feature an acetyl-lysine mimetic group, a portion able to form a hydrogen bond to the conserved asparagine and tyrosine residues, thus mimicking the interactions of the lysine-acetylated peptide.^{18, 41}

Different *chemotypes* have been identified, such as methyltriazolodiazepines and triazepines, 3,5-dimethylisoxazoles, dihydroquinazolinones, tetrahydroquinolines and 2-thiazolidinones.

1.5.1 Diazepine-based and triazepine-based compounds as BET ligands

One of the first reported ligands of BET proteins with high-affinity and selectivity share the triazolodiazepine chemical scaffold. The finding that clinically approved benzodiazepines, such as alprazolam and midazolam, bind BET bromodomains with low affinity prompted the researchers to use this versatile scaffold as template for the development of BET selective

ligands. At the same time, a patent published in 2009 by Mitsubishi Pharmaceuticals details the binding of triazolothienodiazepine-based compounds to BET proteins. These evidence drive the design of several triazolodiazepine-based compounds as BET ligands, which feature a thienodiazepine or a benzodiazepine core and a triazole as KAc mimetic group (Figure 1.11). The interactions of these compounds within the binding pocket are very similar. The two adjacent nitrogen atoms of the 1,2,4-triazole form hydrogen bonds with the conserved asparagine and tyrosine residues, whereas the methyl group binds to a small hydrophobic pocket, mimicking the interaction of the native acetyl-lysine ligand. The fused aromatic ring of the triazolodiazepine bind within a lipophilic pocket, the ZA channel, while the 5-phenyl group interacts with the WPF shelf, a critical region for good binding, affinity and selectivity for BET proteins.⁴⁷

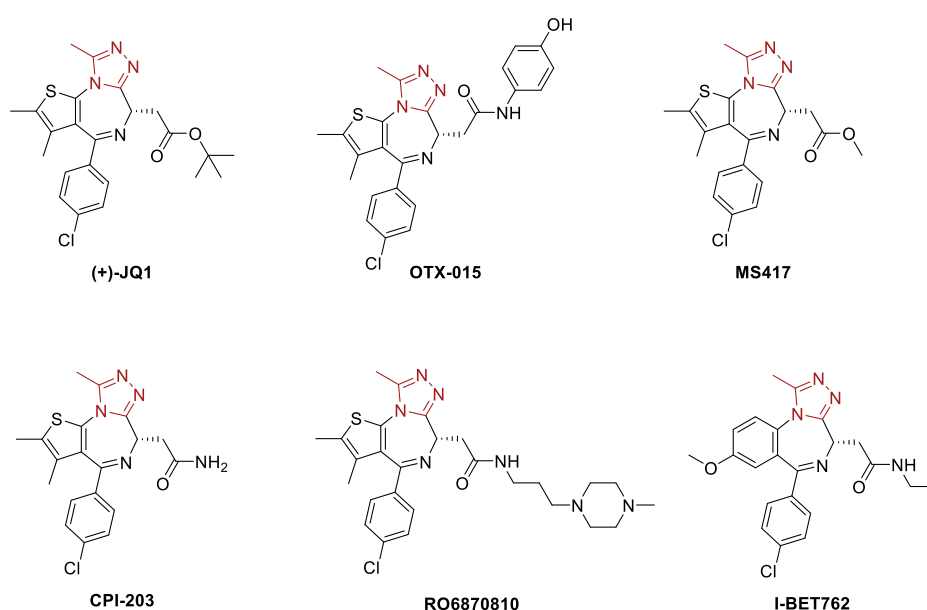


Figure 1.11 Triazolothienodiazepine and benzodiazepine BET ligands. In red, the KAc mimetic group.

One of the first published triazolothienodiazepine-based BET ligand was (+)-**JQ1**, developed by Filippakopoulos group.⁵² This compound shown a highly selectivity toward BET family over non-BET bromodomain-containing proteins with affinity for each BET proteins ranged

from 49 nM to 190 nM. Only the S enantiomer, (+)-JQ1 was active, whereas the R enantiomer (–)-JQ1 showed no significant interaction (IC₅₀ of 10.000 nM). JQ1 displayed antiproliferative effects in preclinical models of several tumor types including multiple myeloma, lymphoma, acute lymphoblastic leukemia, medulloblastoma, NMC (NUT midline carcinoma), mostly due to modulation of MYC expression.⁴⁶ In a murine model of human interstitial fibrosis, it has been shown that the myocardial expression of classical hypertrophic marker genes is reduced with the treatment of **JQ1**, preventing the development of left ventricular hypertrophy, and systolic dysfunction.¹⁷

This compound was intensively used for deepen the biological function of BET proteins but is not enter in clinical trials for its short half-life.⁵³

A structurally **JQ1**-related compound with a longer half-life is **RO6870810**. This compound enters in Phase I, multicenter, open-label study for patients with advanced solid tumors. Subcutaneous dosing is generally well tolerated, with good results in NUT-midline carcinoma (NMC) treatment associated with reversible irritation of the injection site, increases of bilirubin and anorexia.⁵⁴

The replacement of *tert*-butyl ester of **JQ1** with a methyl ester, led the formation of **MS417**, a triazolothienodiazepine-based compound, able to decrease the transcriptional activity of NF-κB in HIV-associated nephropathy. Other triazolothienodiazepine compounds related to **JQ1** are **CPI-203**, with superior oral and intraperitoneal bioavailability and **OTX-015** with high efficacy in different cancer cell lines.¹⁸ The latter has completed a Phase I trial in patients with acute myeloid leukemia (AML) and solid tumors. This compound is orally available but has different problems related to dose-limiting effects such as thrombocytopenia and gastrointestinal events in patients with or without leukemia.⁵⁵ The effects of **OTX-015** were also investigated in brain tumors in a nonrandomized, multicenter Phase IIa trial but the trial was terminated after one year.⁵³

An important triazolobenzodiazepine is **I-BET762** with high potency (IC_{50} of 32.5 – 42.5 nM) and selectivity for BET proteins.⁵⁶⁻⁵⁷ *In vivo* studies suggested that **I-BET762** can reduce MYC expression in different type of cancers. Moreover, this compound is able to suppress pro-inflammatory gene expression in LPS-stimulated macrophages such as pro-inflammatory cytokines (e.g., IFN β , IL1 β , IL6 and IL12A) and chemokines (e.g., CXCL9 and CCL12). In 2012, the compound was entered in Phase I of clinical trials for the treatment of NUT midline carcinoma, and other refractory hematologic malignancies.⁵⁴

The bioisosteric replacement of the chiral carbon in the diazepine scaffold with a nitrogen atom furnished triazolobenzotriazepine-based compounds. The most promising compound (**BzT-7**) has a good BRD4 binding affinity (K_D values of 0.64 μ M) and a similar binding mode of benzodiazepine-related compounds (Figure 1.12).⁵⁸ The chlorinated analogue (**Cl-BzT-7**) showed a similar potency of **BzT-7** and a slightly better activity toward the first bromodomain of BET (Panagis Filippakopoulos, unpublished data).

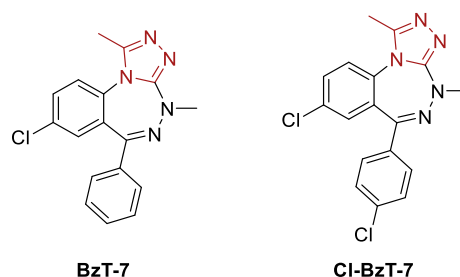


Figure 1.12 Triazolobenzotriazepine BET ligands. In red, the KAc mimetic group.

1.5.2 3,5-dimethylisoxazole-based compounds

3,5-dimethylisoxazole moiety has been shown to be an excellent KAc mimetic group. In fact, the isoxazole oxygen atom is able to mimic a hydrogen bond with the amide of asparagine residue, while the water-mediated hydrogen bond with tyrosine is formed by isoxazole nitrogen. Starting from this fragment, GSK scientist identified **I-BET151**, a 3,5-dimethylisoxazole-based compound (Figure 1.13).⁵⁹

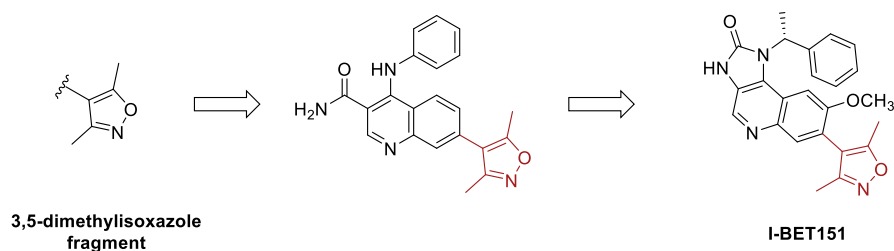


Figure 1.13 Development of 3,5-dimethylisoxazole BET ligand (I-BET151) starting from 3,5-dimethylisoxazole fragment. In red, the KAc mimetic group.

This compound revealed high selectivity for BET proteins and high potency (BRD4 $K_D = 100$ nM). This ligand is able to modulate transcriptional programs responsible for cell-cycle progression and apoptosis in MLL-fusion-driven leukemia cells.⁵⁹

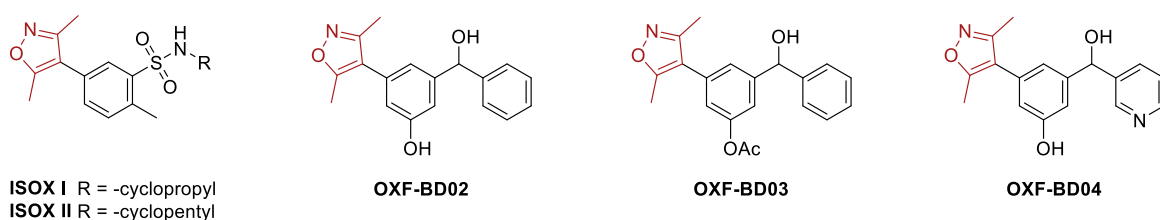


Figure 1.14 Exemplifies other 3,5-dimethylisoxazole-based BET ligands. In red, the KAc mimetic group.

From the same fragment, other 3,5-dimethylisoxazole-based BET ligands were developed (Figure 1.14). All the compounds share an aromatic ring in position 4 of isoxazole ring. On this, N-cyclopropyl or N-cyclopentyl sulfonamide is inserted to occupy the WPF shelf and improve BET selectivity (**ISOX I** and **ISOX II**).⁶⁰⁻⁶¹ On the other hand, the substitution of the aromatic ring (a phenolic or phenyl acetate group) with a phenyl methanol group afforded two different compounds, **OXFBD02** and **OXFBD03** with a good potency (IC_{50} values of 384 nM and 371 nM for BRD4 (BD1), respectively) but with a short metabolic half-life (approximately 40 min for **OXFBD02**) in human liver microsomes. The replacement of the phenyl methanol group

with a 3-pyridinemethanol furnished the related compound **OXFBD04** with higher affinity and an increased metabolic half-life (approximately 6.5 h) in human liver microsomes.⁶²⁻⁶³

1.5.3 Dihydroquinazolinones and tetrahydroquinolines

Two different fragments were identified as KAc mimetic group by different researchers in a fragment-screening campaign: the 3,4-dihydro-3-methyl-2(1H)-quinazolinone (MQZ) fragment and the N-acetyl-2-methyltetrahydroquinoline (THQ) fragment (Figure 1.15).

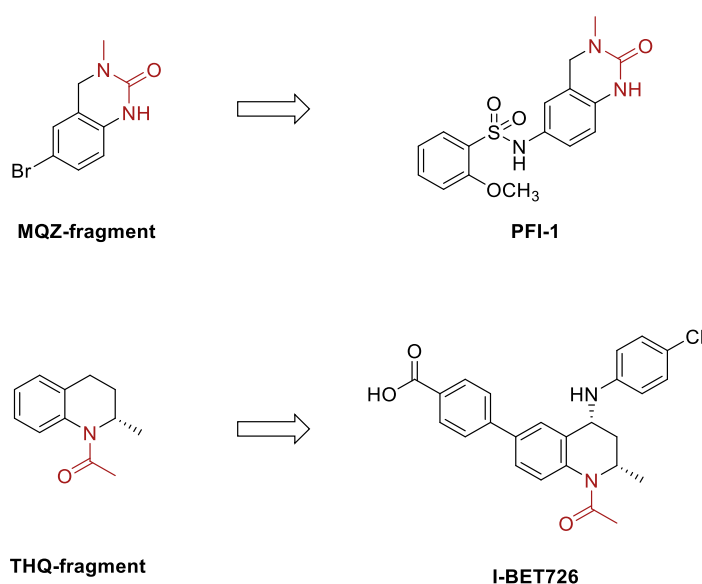


Figure 1.15 Development of BET ligands starting from MQZ and THQ fragments. In red, the KAc mimetic group.

Optimization of MQZ fragment with the insertion of different substituents able to insert in the WPF shelf, resulted in **PF-1**, a potent compound (IC_{50} value of 220 nM for BRD4) with high selectivity for the BET bromodomains. Different studies shown that the treatment of sensitive cell lines with PFI-1 caused cell-cycle block and induction of apoptosis.⁶⁴

Decoration of THQ fragment lead to **I-BET726**, a selective and potent BET ligand (K_D of 4 nM), active in the treatment of neuroblastoma tumors in vivo and with an excellent anti-proliferative activity in some solid tumor cell lines.⁶⁵

1.5.4 2-Thiazolidinones

Using a fragment-based drug discovery approach followed by docking and X-ray crystallography, Zhao *et al.* were able to screen a library of fragment, identifying 2-thiazolidinone-based ligands as strong BET binders. Structure-based optimization allowed the identification of some compounds with submicromolar IC₅₀ values, with a good potential for further optimization (Figure 1.16).⁶⁶

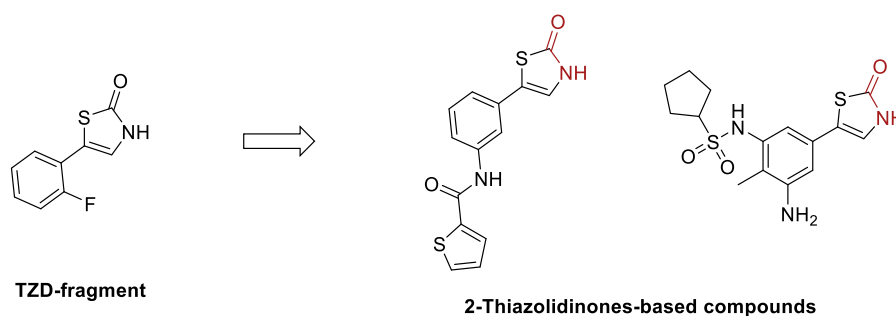


Figure 1.16 Develop of 2-thiazolidinones ligands starting from an identified fragment. In red, the KAc mimetic group.

1.6 Selectivity within BET family

One of the most challenging aspects in the BET field is the design of selective ligands for each BET proteins and also for their corresponding first and second bromodomains. Despite the excellent progress made, all the ligands mentioned above are pan-BET ligands, i.e. compounds with no selectivity within BET family members.⁶⁷

Nevertheless, the first and the second bromodomain of each BET proteins seem to have different functions. For instance, the first bromodomain of BRD4 binds di-acetylated H4K5ac/K8ac, regulating transcriptional activation thorough the attachment of this domain and its associated proteins to target gene promoter. On the other hand, the second bromodomain recruits mostly non-histone proteins such as the pTEFb complex to target genes. In BRD3, only

the first bromodomain binds to the transcription factor GATA1, suggesting a separate role of the second bromodomain of the protein.⁶⁷⁻⁶⁸

These evidences suggested that a selective targeting of singular BET and the discrimination between the first and the second bromodomain could results in distinct transcriptional outcomes, mitigating unwanted effects such as acquired-resistance of tumor cells treated with BET inhibitor, in addition to dose-limiting toxicities and limited long-term effectiveness.^{53, 69}

Unfortunately, the very high sequence identity at the KAc binding pocket (95%) of BET family members has limited the design of selective ligands and only few selective compounds are known. Three crucial residue positions that differ between the first and the second bromodomain of BRD4 close the KAc peptide-binding site are shown by sequence comparison (Figure 1.17). In particular:

- glutamine (Q85) in BD1 correspond a lysine residue (K378) in BD2;
- aspartic acid in the BC loop of BD1 (D144) is a histidine residue in BD2 (H437);
- isoleucine in BD1 (I146) is a valine residue in BD2 (V439).⁶⁷

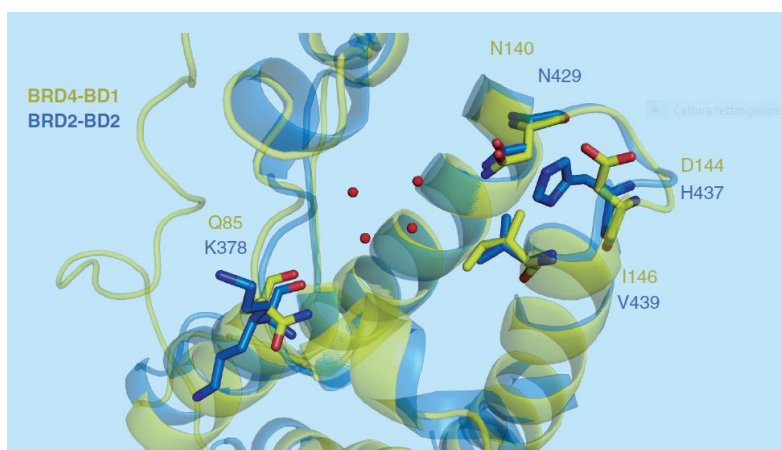
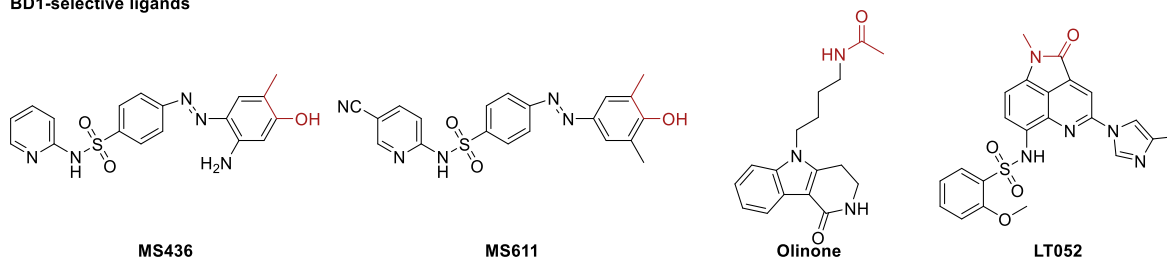


Figure 1.17 Differences between BD1 and BD2 showed by superposition of the x-ray structure of BRD4-BD1 (in yellow, PDB 4QB3) and BRD2-BD2 (in blue, PDB 4J1P).⁶⁷

Exploiting these small differences, some selective ligands have been developed (Figure 1.18).

BD1-selective ligands



BD2-selective ligands

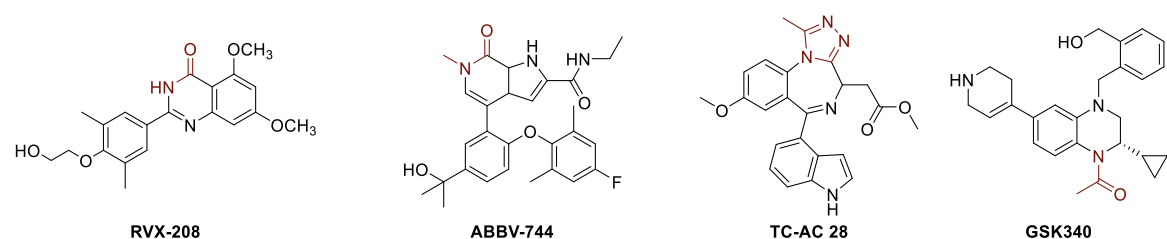


Figure 1.18 Selected ligands BD1 and BD2 selective. In red, the KAc mimetic group.

From a structural point of view, all these compounds share different KAc mimetic groups and different substituents which clash the different amino acids in BD1/BD2 domain, driving the selectivity of compounds. For example, the sulfonamide oxygen of **MS436** forms a water-mediated hydrogen bond with the side-chain amine of a lysine residue (K91) of BRD4 (BD1) mutated in alanine residue (A384) in BRD4 (BD2). These interactions favor a high potency (K_i of 30–50 nM for BRD4 (BD1) and a 10-fold selectivity for the first bromodomain.⁷⁰ A related diazobenzene-based compound, **MS611** showed 100-fold selectivity for the first bromodomain of BRD4 (K_i of 0.41 nM for BD1 of BRD4 and 41.3 μ M for BD2 of BRD4).⁶⁸

The X-ray crystal structure of Olinone in complex with BD1 of BRD4 highlighted interactions with the aspartate residue (D144) mutated in histidine (H435) in BD2 of BRD4 which would clash with the indole moiety of compound. Olinone exhibited 100-fold higher selectivity toward BD1 (K_D of 3.4 μ M) than BD2 (no detectable binding) for all of the BET bromodomains.⁶⁸

On the other hand, interactions with the typical histidine residue in BD2 allowed to gain selectivity toward the second bromodomain.

RVX-208 is packed against the histidine residue (H433), establishing π - π stacking interactions which limit the di-methyl-phenyl moiety in one fixed conformation that is not conserved in BD1, considering that the histidine is replaced in an aspartate residue. The compound displays high potency (IC_{50} values of 87 μ M and 0.51 μ M for BD1 and BD2 of BRD3, respectively) and about 170-fold selectivity for the second bromodomain.⁷¹⁻⁷²

Exploiting a ‘bump and hole’ approach, **TC-AC-28** was developed. The indole moiety establishes π - π stacking interactions with the histidine residue in the second bromodomain of BRD2 substituted by an aspartate residue in BD1 which cannot create such interactions. The compound has high affinity and approximately 20-fold selectivity for BD2 over BD1 (K_D of 800 and 40 nM against BD1 and BD2 of BRD2, respectively).⁷³

Optimization of the tetrahydroquinoline **I-BET726** (Section 1.5.3) furnished **GSK340** with nanomolar potency and approximately 50-fold selectivity over BD2 of BRD4 (pIC_{50} of 5.5 and 7.2 against BD1 and BD2 of BRD4, respectively).⁷⁴

These compounds allowed to better understand different pathways in which the two domains are involved. For instance, the BD1 selective ligand Olinone stimulated the progression of primary oligodendrocyte progenitors, while simultaneously inhibition of both BD1 and BD2 domain prevented it and retained the cells at a progenitor state, with interesting implications in disorders characterized by myelin loss such as aging and neurodegeneration stage.⁶⁸ On the other hand, the BD2 selective ligand, **RVX-208** affect the transcription of a lower number of genes toward the pan-BET inhibitor **JQ1**.⁷¹ These evidence suggested that the discrimination between BD1 and BD2 could achieve more selective transcriptional effects.

Currently, only BD2-selective ligands reach the clinical phase. **RVX-208** is in phase III trial for patients with high-risk cardiovascular disease with type 2 diabetes mellitus and low high-

density lipoprotein (HDL). Surprisingly, this compound is the only BET ligand to reach phase III trial and one of the few BET ligands for non-oncology indications.⁷⁵

ABBV-744, currently the most potent (2-5 nM) and selective BD2 ligand (approximately 250-640-fold) is in phase I of clinical trials with indications for prostate cancer and AML.⁷⁶⁻⁷⁷

In 2019, a BD1 selective ligand was developed (**LT052**) starting from a benzo[cd]indol-2(1H)-one scaffold. This compound showed nanomolar BRD4 BD1 potency and 138-fold selectivity over BRD4 BD2 with good cellular results, exploring new therapeutic approach for the treatment of acute gout arthritis.⁷⁸

1.7 Bivalent BET ligands

Beyond the classical medicinal chemistry approaches, alternative strategies can be used to develop more potent and selective chemical probes. The presence in BET proteins of two bromodomains offer the possibility to engage both domains using a bivalent ligand, designed linking two ‘warheads’ that engage distinct binding sites within proteins.

Bivalent chemical probes have the potential to exhibit a better affinity and selectivity compared to a monovalent probe, which may bind not only a structural domain of a protein of interest, but also many structurally related domains.

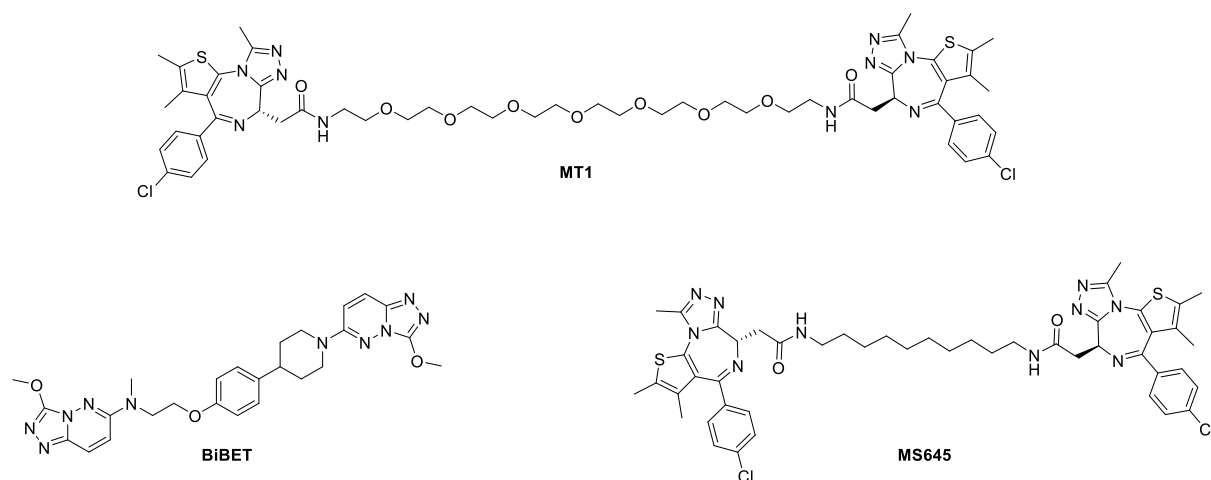


Figure 1.19 Bivalent ligands of bromodomain-containing proteins.

To date, few bivalent ligands have been developed (Figure 1.19). Bradner *et al.* designed bivalent BET ligands connecting two molecules of **JQ1** with different linker lengths.⁷⁹ The most promising compound, **MT1** has high potency (IC₅₀ of 3.09 nM toward BRD4 (BD1)) compared to the monovalent ligand JQ1 (IC₅₀ of 20.9 nM toward BRD4 (BD1)) and has a 400-fold improvement in activity in AML than the corresponding monovalent ligand **JQ1**. The better activity is probably due to the capability of **MT1** to induce dimerization of individual BET bromodomains. Interestingly, the high-resolution structure shown that one molecule of **MT1**, simultaneously recognizing two bromodomains of BRD4(BD2), creates a new hydrophobic pocket between the two bromodomain monomers.⁷⁹ Evaluation of the nature and rigidity of the linker, afforded **MS645** a bivalent compound related to **MT1**, with a shorter and lipophilic linker. Notably, **MS645** has an important effect in solid tumor, inhibiting BRD4 interactions with transcription enhancer/mediator proteins MED1 and YY1, required for accelerated proliferation of solid tumor TNBC cells.⁸⁰

Another class of bivalent ligands that induce dimerization are the **biBET** ligands. The X-ray crystal structure of a **biBET** ligand in complex with the first bromodomain of BRD4 revealed the formation of a dimer, in which both the triazolopyridazine and N-methylpiperazinone act as KAc mimic group. These compounds cause cell death in BRD4-dependent cell lines three orders of magnitude higher than **JQ1**. Remarkably, both **JQ1** and **biBETs** inhibit the acute lymphoblastic leukemia cell line RS4-11 but only bivalent ligand reach near-complete cell killing, highlighting possibly beneficial from bivalent inhibition.^{81,82}

1.8 PROTAC approach

Over the past few years, an emerging strategy to inhibit proteins activity is their selective induced-degradation using PROTACs compounds.

Proteolysis Targeting Chimeras (PROTACs) are heterobifunctional molecules able to hijack the target protein to ubiquitin-proteasome machinery (UPS) for their selective degradation.

Structurally, a PROTAC compound includes a ligand for the protein of interest (POI) and a ligand for the E3 ubiquitin ligase connected by a linker. In this way, these heterobifunctional molecules are able to bridge the target protein and an E3 ubiquitin ligase. The latter binds to an E2 enzyme, promoting the polyubiquitination of the protein. The polyubiquitinated target is recognized as a substrate by the proteasome and is consequently degraded. As the PROTAC remains unmodified, it can initiate a new degradation event (Figure 1.20).⁸³

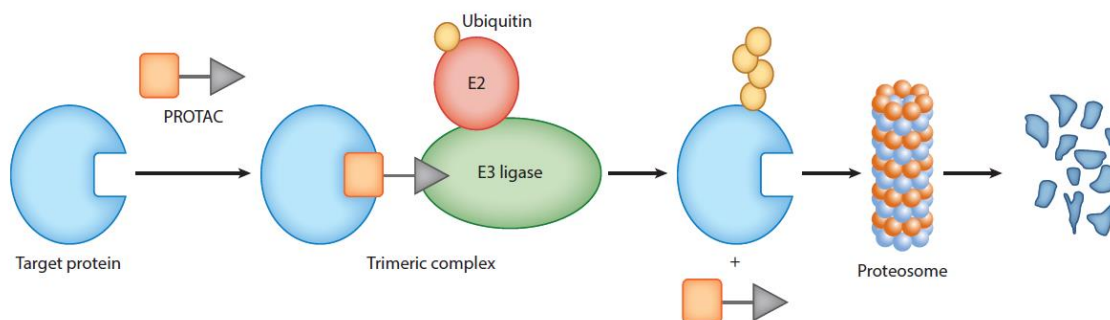


Figure 1.20 Schematic mechanism of PROTACs.

In order to better understand this process, in the following Sections will be detailed the main elements involved in this mechanism.

1.8.1 The ubiquitin/proteasome system (UPS)

One of the major mechanism for protein degradation involve the ubiquitin/proteasome system (UPS) which maintain a good balance of intracellular protein levels eliminating damaged, misfolded and mutant proteins. Proteins are covalently conjugated with ubiquitin, a highly conserved 76-residue protein. In this way, proteins are labelled and targeted into proteasome for their proteolysis into small peptides of 3–24 amino acids.

Protein ubiquitination is an ATP-dependent enzymatic reaction mediated by three enzymes: an ubiquitin-activating enzyme (E1), an ubiquitin-conjugating enzyme (E2), and an ubiquitin ligase (E3) (Figure 1.21).⁸⁴⁻⁸⁵

E1 ubiquitin-activating enzymes mediates the formation of a high-energy thioester bond between the C-terminus of ubiquitin and cysteine residues in E1, in an ATP-dependent manner. Activated ubiquitin is transferred to E2 ubiquitin-conjugating enzymes via trans-thioesterification reaction. The transfer of ubiquitin from E2 enzyme to Lys residue or the N-terminus of the substrate is mediated by an E3 ubiquitin ligase, which selectively recognize the protein substrate. Commonly, the lysine ubiquitinated are the K48- or K11- residues.⁸⁴⁻⁸⁵

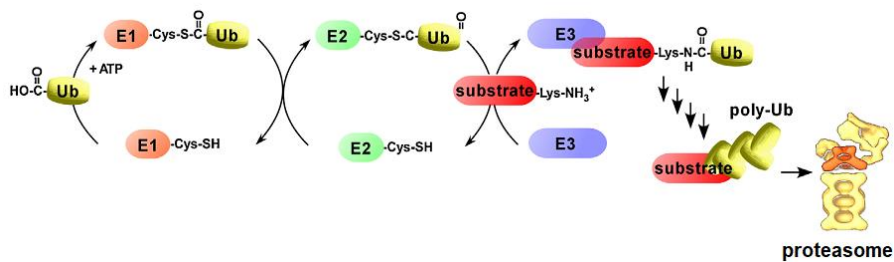


Figure 1.21 Schematic representation of the ubiquitination process.⁸⁴

1.8.2 E3 ligases

The specific recognition of target proteins for their degradation is mediated by E3 ligases, key mediator of UPS system. The high number of these ligases in mammals, approximately 500-1000, suggested a high specificity and versatility of this process.⁸⁶

Commonly, E3 ligases are divided into four major families:

- the Really Interesting New Gene (RING)-finger-type;
- the HECT (homologous to the E6-AP carboxyl terminus) type, which transfer ubiquitin to the target substrate protein after the transfer to their own cysteine residues;
- the U-box-type, which have a RING-like domain but lacking the cysteine and histidine zinc co-ordination sites;
- PHD-finger type.

The largest family of E3 ligases is the RING-finger-type, which use a zinc finger domain to interact with E2 enzyme for direct ubiquitin transfer to the substrate. One of the most important subfamilies is the cullin-RING ligase complexes (CRLs) built on Cullin proteins (Figure 1.22).

The substrate is specifically recognized through a substrate-recognition protein anchor to cullin by an adaptor protein. The binding with the ubiquitin-conjugating enzyme (E2) occurs at the RING component.⁸⁷

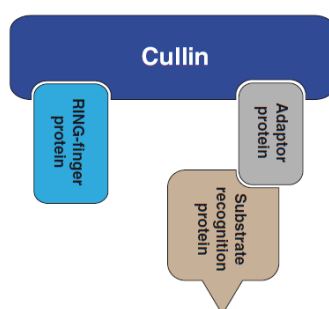


Figure 1.22 General representation of the cullin-RING ligase complexes (CRLs).⁸⁷

Considering that alterations in the correct levels of proteins or their quality are related to different type of pathological states, proteasome and E3 ligases have become interesting therapeutic target. The identification of E3 ligase ligands is important also in PROTAC compounds development. Herein, we focus the attention on the most used E3 ligase ligands for BET PROTACs: the cereblon (CRBN) and the Von Hippel–Lindau (VHL) ligand.

1.8.2.1 Cereblon (CRBN) as E3 ligase

Cereblon (CRBN) is the substrate-recognition protein of the E3 ubiquitin ligase complex containing Cullin 4 (CUL4) protein. Other member of this complex are the DNA damage-binding protein 1 (DDB1) which connect Cereblon to the cullin protein (CUL4), and Roc1

(regulator of cullin 1) which interact with E2 ubiquitin-conjugating enzyme through its RING finger domain.⁸⁸

In 2010, Handa and co-workers described for the first time the E3 ligase Cereblon as the primary target of thalidomide. Since then, thalidomide analogues, called immunomodulatory drugs (IMiDs), such as lenalidomide, pomalidomide, 4-OH-thalidomide and its chemically and biologically more manageable analogues (the 5-OH-thalidomide and the 5-piperazine-thalidomide **105**) were developed as CRBN ligands (Figure 1.23).⁸⁸⁻⁹⁰

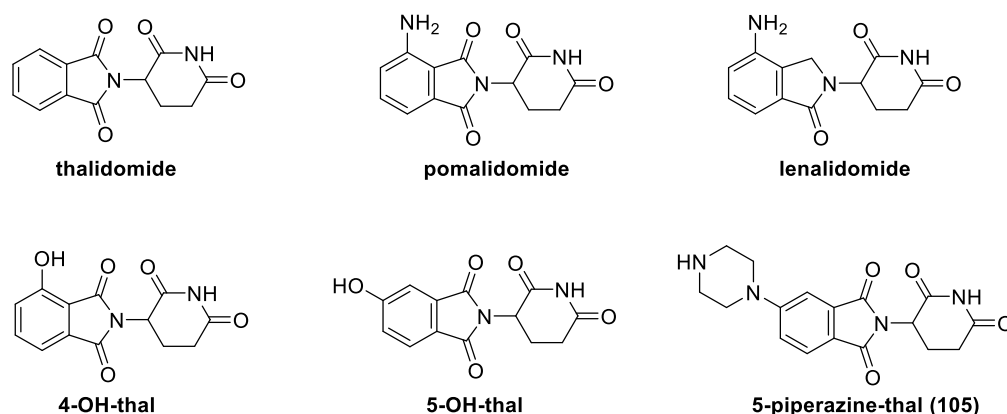


Figure 1.23 Structure of immunomodulatory drugs (IMiDs) as Cereblon binders.

The crystal structure of DDB1–CRBN complex bound to IMiDs allowed to clarify their interaction within the complex. The glutarimide ring of IMiDs is inserted within a hydrophobic tryptophan pocket, termed the thalidomide-binding domain (TBD). The phthalimide ring is exposed on the surface of the CRBN protein, modifying its ability to interact with new substrates.⁸⁸ The C4 phthalimide aniline position of thalidomide (different from lenalidomide and pomalidomide) is solvent exposed. At the same manner, the phthalimide C5 and C6 positions are fully solvent exposed, allowing modifications in this position to obtain more manageable thalidomide analogues (5-OH-thal and 5-piperazine-thal (**159**)). The binding of the (S)-enantiomer is preferred over the (R)-enantiomer but under physiological conditions thalidomide undergoes rapid racemization.⁹¹

The mechanism of IMiDs is complex and not entirely elucidated but some studies suggested two different effects. On one hand, these compounds compete with endogenous substrates, decreasing their degradation. On the other hand, IMiDs can redirect the ligase to degrade new proteins, changing CRBN's E3 ligase substrate preference. For example, these compounds are able to promote the ubiquitination and degradation of transcription factors as Ikaros (IKZF1) and Aiolos (IKZF3); lenalidomide but not thalidomide and pomalidomide can stimulate the degradation of casein kinase I α (CKI α).

Despite the progress made, the knowledge about the target proteins degraded by IMiDs are limited and further studies are needed to better elucidate their mode of action.⁸⁸

1.8.2.2 Von Hippel–Lindau (VHL) E3 ligase

Von Hippel–Lindau tumor suppressor protein (VHL) is the substrate receptor of the VHL E3 ubiquitin ligase. Other members of this complex are a RING finger protein (Rbx1), which interact with E2 enzyme and adaptor proteins (Elongin B [EloB] and Elongin C [EloC]) able to connect VHL to a cullin protein (Cul2). The most important substrate of VHL is the hypoxia inducible factor 1 α (HIF-1 α), a transcription factor constitutively expressed, which activate the transcription of several genes in response to low oxygen conditions. To balance its intracellular levels, HIF-1 α is selectively hydroxylated by prolyl hydroxylase domain (PHD) enzymes at two specific proline residues within the HIF-1 α oxygen-dependent degradation domain (ODD). Only the hydroxylated form is recognized by VHL E3 ligase complex, ubiquitinated and degraded by UPS system.⁹²

Considering that VHL interact with HIF-1 α by hydroxyproline residue, this scaffold was used as starting point for the design of selective VHL ligands (Figure 1.24).

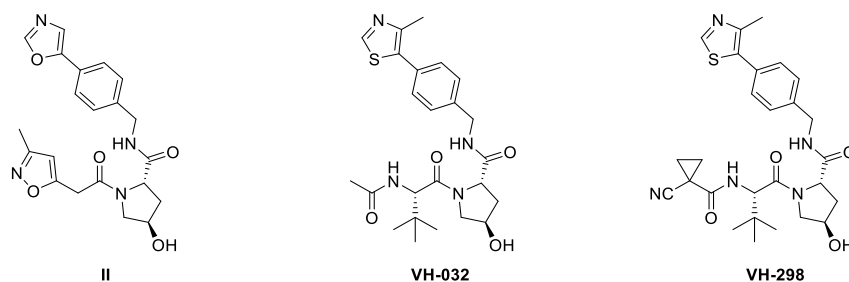


Figure 1.24 Structure of VHL-ligands.

The first VHL ligand (**II**) has a low micromolar affinity (K_D of 5.4 μM) and the same binding site of HIF-1 α .⁹³

To optimize binding affinity and lipophilicity, Ciulli group developed VHL ligands inserting different substituents on the hydroxyproline central scaffold to fill the left-hand side (LHS) and right-hand side (RHS) of the protein-protein interaction surface. Maintaining the aryl group of ligand **II**, the RHS was filled with a 4-methylthiazole, which does not alter the conformation of the protein. On the other hand, the LHS sub pocket was occupied firstly by a *t*-butyl group, then by an acetamido group, with important interactions of the carbonyl group within the pocket. In this way, **VH032** was designed as VHL ligand with improved binding affinity (K_D of 0.185 μM) and lipophilicity.⁹⁴ The replacement of the terminal methyl group of **VH032** with a cyanocyclopropyl group, which better fill the LHS pocket, furnished **VH298** ligand. This compound has affinity in the nanomolar range (K_D of 90 nM), higher passive cell permeability and good cellular activity.⁹⁵

Importantly, loss of binding specificity occurs changing the stereochemistry at the carbon atom bearing the hydroxyl group of the hydroxyproline ring.⁹⁵

1.8.3 BET degraders

The possibility of drive the degradation of a specific target was demonstrated nearly 20 years ago with the development of the first peptide-based degrader. The use of synthetic compounds

instead of a peptidic ligands prompted the development of several PROTACs as potential drugs.⁹⁶ In the BET field, several degraders have been developed (Figure 1.25).

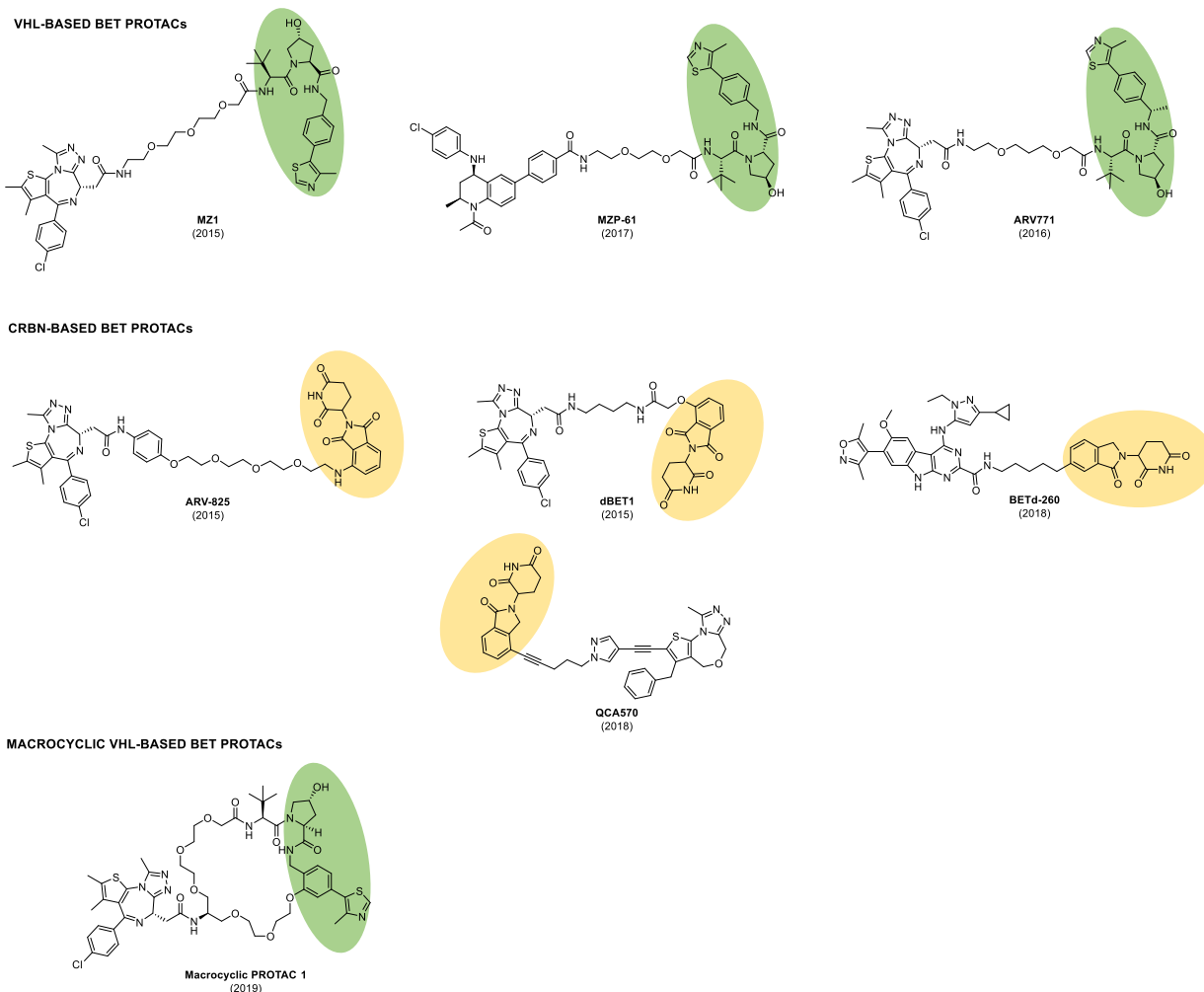


Figure 1.25 BET degraders.

In 2015, the first examples of CRBN-based BET PROTACs were reported: **dBET1** and **ARV-825**. These molecules share CRBN ligand as E3 recruiter and (+)-**JQ1** as BET warhead, differing for the nature and length of linkers.⁹⁷⁻⁹⁸ These compounds are efficient degraders of all BET proteins, resulting in anti-tumor efficacy and cell-proliferation inhibition more effective than small-molecule BRD4 ligands. In 2018, two BET degraders were developed using as E3 recruiter CRBN ligands. **dBET260** has an azacarbazole-based scaffold as BET binder, showing BET degradation at concentrations as low as 30 pM in the RS4;11 leukemia

cell line.⁹⁹ **QCA570** contain a [1,4]oxazepines-BET ligands and is able to induce degradation at low picomolar concentrations.¹⁰⁰

On the other hand, VHL-based PROTACs have been developed. Ciulli and co-workers designed **MZ1** as a potent BET degrader, connecting **JQ1** to a VHL-recruiting ligand, using a PEG3 as linker. Surprisingly, **MZ1** showed a preferential degradation for BRD4 over BRD2 and BRD3 despite **JQ1** is a pan-BET inhibitor.¹⁰¹ The crystal structure of **MZ1** in complex with VHL and the second bromodomain of BRD4 clarify that the formation of a ternary complex induce new protein–protein and protein–ligand contacts that contributing to the high stability and cooperativity of ternary complex.¹⁰² Higher selectivity for the second bromodomains over the first bromodomains of BETs is maintained by the first macrocyclic PROTAC developed by the same research group starting from **MZ1**.¹⁰³ Similar to MZ1 but with a linker of different nature and length, **ARV-771** is an effective BET degrader, offering a good therapeutic strategy in a castration-resistant prostate cancer (CRPC).¹⁰⁴

Using tetrahydroquinoline as BET ligand and VHL as E3 recruiter, **MZP-61** was developed. Despite the BET warhead has high potency, the resulting PROTAC is less potent than the related **JQ1**-based PROTACs. This is due a negative cooperativities of ternary complex formation, which can affect the activity of the degraders.¹⁰⁵

1.8.4 Advantages and limits of PROTAC approach

The good results obtained in different cellular studies suggested several potential benefits of induced-selective degradation. First of all, the chosen ligand can bind anywhere on the target protein, also if does not have the ability to block specific functions of the protein, making druggable proteins for which the design of selective small-molecule is challenging. Through targeted protein degradation, the selectivity of a ligand can be modulated, taking advantages from the new protein-protein interactions within the ternary complex.¹⁰⁶

The catalytic mode of action of PROTACs is associated with low level of target protein occupancy at concentrations much lower than classical small-molecules, avoiding off-target effects due to high occupancy of targets or high doses. Once that PROTACs restore proteins to basal levels, its action is limited to a smaller pool of the novo resynthesized proteins, involving low tissue concentrations of degraders. In some cell, the time to recover the sufficient pool of proteins to reintroduce physiological signaling may be long, increasing the duration of action of PROTACs. The low drug exposures, low doses, and long dosing interval can overcome the possibly low oral absorption with the development of formulations for controlled release.¹⁰⁶

On the other hand, PROTACs have several limits due to their structure, physicochemical properties and their mode of action.

Most of the compounds have a high molecular weight and a complex structure, which complicate their synthesis and purifications. The nature and the length of the linkers should be choosing carefully, considering the high oxidative metabolism especially at this level and possibly secondary interactions.¹⁰⁷ Physicochemical properties such as solubility, chemical stability and non-specific binding to protein in media should be considered also for the quality and the interpretation of data.

Moreover, the complex mode of action of PROTACs should be examined. First of all, the designed degraders must access the proper intracellular compartment in which both the targeted protein and the E3 ligase are located. Often, cell permeability is a big limitation, considering the high molecular weight and total polar surface area of compounds. Once inside, the degraders must bind at the same time both with the target protein and the E3 ligase, forming a stable ternary complex (POI-PROTACs-E3 LIGASE).¹⁰⁶ High concentrations of PROTAC can promote the binary complex instead the ternary system. This aspect, called 'hook effect', could inhibit substrate degradation and make dosing of PROTACs in patients a tricky challenge.¹⁰⁶

Once formed, the ternary complex must allow the two partners to adopt an appropriate conformation suitable for the transfer of ubiquitin(s) to the right acceptor site and with sufficient

efficiency, faster than the lifetime of the ternary complex and the action of deubiquitinase enzymes. The ubiquitin transferred should be accessible and detectable by proteasome to start the degradation process. Protein ubiquitination could be not sufficient for protein degradation: modifications in protein conformation can alter the recognition by the proteasome, avoiding the degradation process. Moreover, the rate of protein degradation should be faster than the *de novo* resynthesis, an important aspect to be considered.¹⁰⁶

CHAPTER II
AIM OF WORK

2.1 Aim of work

Despite the excellent progress made in the BET field, there is still a need to clarify all the pathways in which BET proteins are involved and their connections with pathological states in different cell types.

Although the promising results, the outcomes obtained from BET ligands in clinical trials reveal critical points, suggesting different responses in clinical efficacy from preclinical models. Efficacy, dose optimization, metabolism, toxic effects, mechanisms of resistance and limited long-term efficiency are key aspects to be optimized.^{22, 53}

In this context, the identification of compounds with improved selectivity toward BET family members and/or their singular bromodomain (BD1 and BD2) offers a valuable chemical tool to ascertain their role during various physiological and physio-pathological conditions.

Aim of this PhD project is the design, synthesis, biochemical and biophysical evaluation of new chemical probes for BET proteins, in order to obtain potent compounds with improved selectivity. To this purpose, three different medicinal approaches were applied to obtain different classes of compounds (Figure 2.1):

- the bisubstrate approach;
- the frozen analogue approach;
- the PROTAC approach.

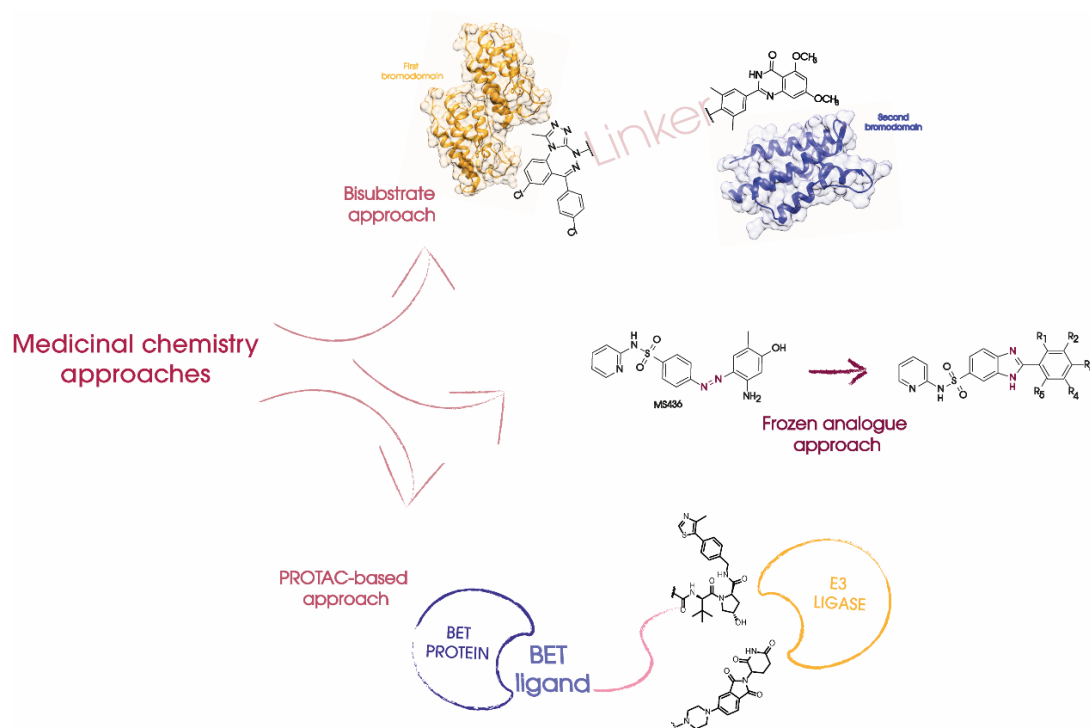


Figure 2.1 Aim of work: different medicinal chemistry approaches to obtain selective BET ligands.

2.2 Bisubstrate approach

The presence of two bromodomains in BET proteins makes these proteins suitable for the development of bivalent ligands.

Compounds presented here have been designed with the aim to bind simultaneously the first and the second bromodomain of the same BET protein. Such derivatives could allow, for the first time, the co-crystallization of both bromodomains within the same BET protein and therefore obtain important structural information for the design of selective ligands. The design strategy, illustrated in Figure 2.2, involved the connection of a BD1 and a BD2 selective ligand with proper linkers.

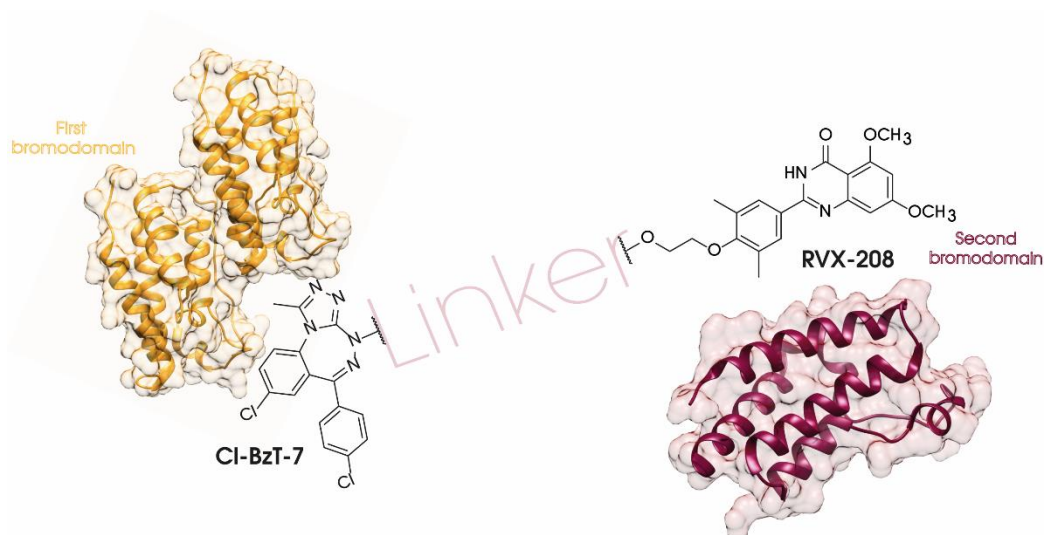


Figure 2.2 Design of bivalent ligands bridging BD1/BD2 selective ligands with proper linkers.

As depicted in Figure 2.2, **Cl-BzT-7** and **RVX-208** were selected as BD1 and BD2 selective ligands, respectively.

To define the putative proper connection position for the attachment of the linkers, the crystal structures of **BzT-7**, the deschlorinated derivative of **Cl-BzT-7**, and of **RVX-208** were considered.

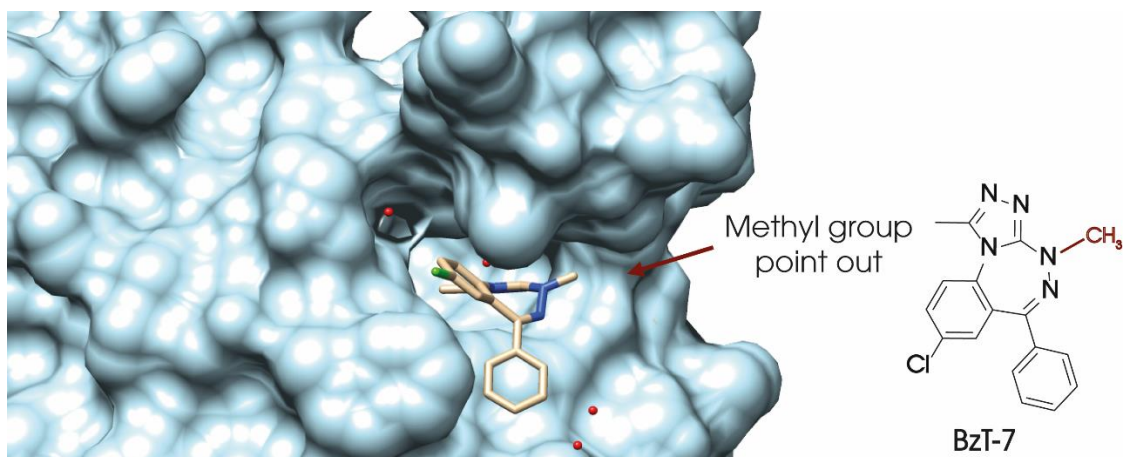


Figure 2.3 Crystal structure of the first bromodomain of human BRD4 in complex with **BzT-7** (PDB 3U5L).

As the N-methyl group of **BzT-7** points out the binding pocket, this position can be exploited to anchor the linker (Figure 2.3). Moreover, structure-activity relationships of related analogues (Section 1.5.1) indicate that this position well tolerate the presence of a carbonylic function. Therefore, a coupling reaction between the carboxylic acid analogue of **Cl-BzT-7** and an amine could be exploited to insert the linker.

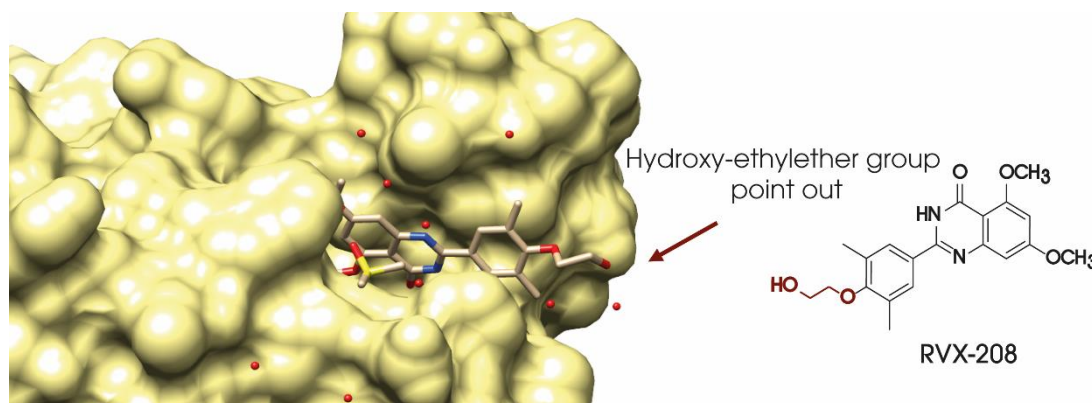


Figure 2.4 Crystal structure of the second bromodomain of human BRD2 in complex with **RVX-208** (PDB 4MR6).

For **RVX-208**, the crystal structure reveals that the hydroxy-ethylether group in 4' of **RVX-208** points out of the binding pocket and makes only a few contacts with the bromodomain surface (Figure 2.4). Therefore, this position was selected as point for the attachment of the linker.

Evaluated the proper attachment position, different linkers are chosen. Considering that the role of the linker is critical and cannot be clearly anticipated, we selected a broad range with different shape, polarity and length. The combination of these three units yielded the collection of compounds depicted in Table 2.1.

It has to be noted that, in compound **1** the BD1 and BD2 ligands were directly connected. Compound **14**, that features a different point of linker attachment on **RVX-208**, was designed in order to confirm the accuracy of the attachment point previously selected.

Table 2.1 Bivalent ligands (compounds **1–14**).

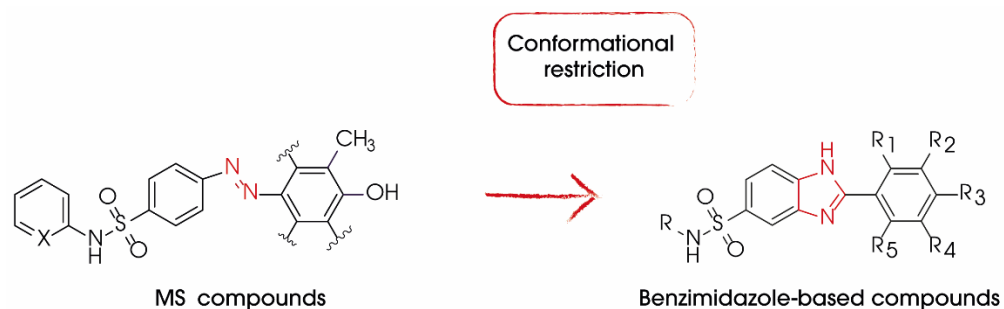
BIVALENT LIGANDS	
	R
1 (EML807)	-
2 (EML901)	
3 (EML896)	
4 (EML730)	
5 (EML897)	
6 (EML731)	
7 (EML898)	
8 (EML729)	
9 (EML742)	
10 (EML823)	
11 (EML899)	
12 (EML809)	
13 (EML900)	
14 (EML824)	

2.3 Frozen analogue-approach

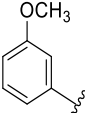
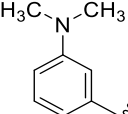
Among the selective ligands of the first bromodomain of BET proteins, SARs of diazobenzene-based compounds, **MS436** and **MS611** have been extensively investigated (Section 1.6). Despite their good potency and selectivity for BD1 over BD2 of BRD4, the presence of diazo-group makes these compound metabolic unstable and prevents their further development. Exploiting the frozen analog approach, the diazo-group of this class of compound was constrained into an imidazole yielding benzimidazole derivatives. The benzimidazole scaffold is a privileged chemotype, synthetic accessible and metabolically stable. Moreover, the conformational restriction of a flexible ligand improves drug-likeness and could positively affect potency and selectivity.¹⁰⁸⁻¹¹⁰

Taking in account also the SARs of diazobenzene-based compounds, a small library of benzimidazole-based ligands was designed (Table 2.2).

Table 2.2 Benzimidazole-based ligands (compounds **15** – **32**)



	R	R₁	R₂	R₃	R₄	R₅
15 (EML765)		-H	-CH ₃	-OH	-CH ₃	-H
16 (EML803)		-H	-CH ₃	-OH	-CH ₃	-H
17 (EML798)		-H	-CH ₃	-OH	-CH ₃	-H
18 (EML795)	-H	-H	-CH ₃	-OH	-CH ₃	-H

19 (EML796)	-CH ₃	-H	-CH ₃	-OH	-CH ₃	-H
20 (EML801)		-H	-CH ₃	-OH	-CH ₃	-H
21 (EML797)		-H	-CH ₃	-OH	-CH ₃	-H
22 (EML802)		-H	-CH ₃	-OH	-CH ₃	-H
23 (EML760)		-H	-H	-OH	-H	-H
24 (EML761)		-H	-OH	-H	-H	-H
25 (EML762)		-H	-H	-Cl	-H	-H
26 (EML763)		-OH	-H	-OH	-H	-H
27 (EML764)		-H	-OH	-OH	-H	-H
28 (EML766)		-CH ₃	-H	-OH	-H	-CH ₃
29 (EML806)		-H	-CH ₃	-OH	-H	-H
30 (EML799)			-CH ₃	-OH	-CH ₃	-H
31 (EML804)			-CH ₃	-OH	-CH ₃	-H
32 (EML805)			-CH ₃	-OH	-CH ₃	-H

First, as proof of concept of the frozen analog approach strategy, compound **15**, the corresponding benzimidazole analog of **MS436**, was synthesized.

Then, a SAR study was undertaken on the substituent on the sulfonamide nitrogen (compounds **16 – 22**). Detected the best substituent in this position, structural modifications of the phenyl ring in position 2 of the benzimidazole core were explored (compounds **23 – 32**). Bearing in mind SARs of diazobenzene-based compounds, hydroxyl and methyl groups were preferentially selected. In fact, in **MS436**, the hydroxyl group on the phenyl ring forms a hydrogen bond with the conserved asparagine residue in the KAc binding pocket and, together with the ortho methyl group, acts as KAc mimetic.

2.4 PROTAC approach

Despite the remarkable results obtained with BET PROTACs developed so far, all of them contain a pan-BET ligand as BET warhead. It is simple to speculate that using selective BET ligands the effectiveness of this type of molecules could be improved.

Therefore, using as BET warhead BD1 and BD2 selective ligands, a collection of BET PROTACs was designed (Figure 2.5). This part of the PhD project was developed at the School of Life Sciences (University of Dundee) under the supervision of Prof. Alessio Ciulli.

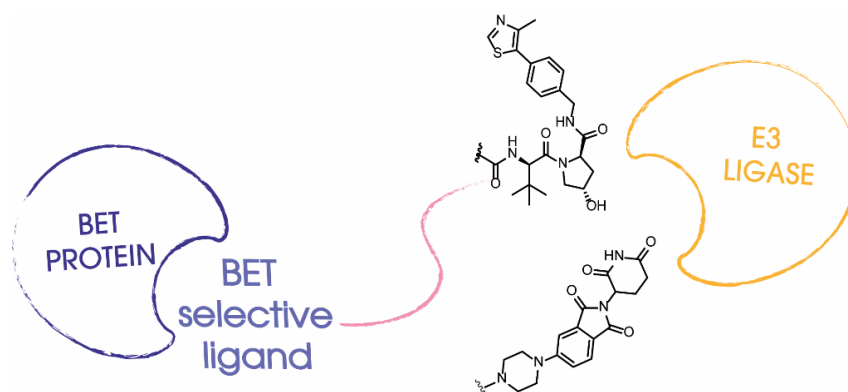


Figure 2.5 Design of PROTACs with selective BET ligands

EML765, the benzimidazole-based compound identified during this PhD project (Section 2.3), was selected as BD1-selective ligand.

To define the proper connection position for the attachment of the linker on the benzimidazole scaffold, the crystal structure of **MS436**, the diazobenzene analogue of **EML765** was exploited (Figure 2.6).

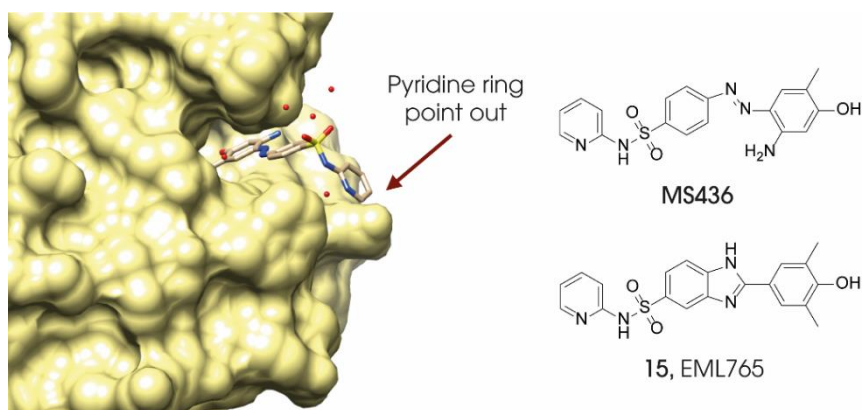


Figure 2.6 crystal Structure of the first bromodomain of human BRD4 in complex with **MS436** (PDB 4NUD).

Assuming similar binding mode for the two compounds, position 5 of the pyridine ring seems to be not involved in important interactions with the protein. Therefore, this position was identified as linker-attachment point and functionalized with an alkynyl group for proper linker connection (**15A**, Figure 2.7).

RVX-208 was again picked as BD2 selective ligand. In analogy to the design of bivalent ligands (Section 2.2), the hydroxy-ethylether group was chosen as appropriate position for linker attachment.

A derivative of thalidomide and a proline-based compound were exploited as Cereblon (CRBN) and von Hippel–Lindau (VHL) ligands, respectively. Finally, four different linkers were used.

The combination of these components yielded 16 compounds depicted in Figure 2.7.

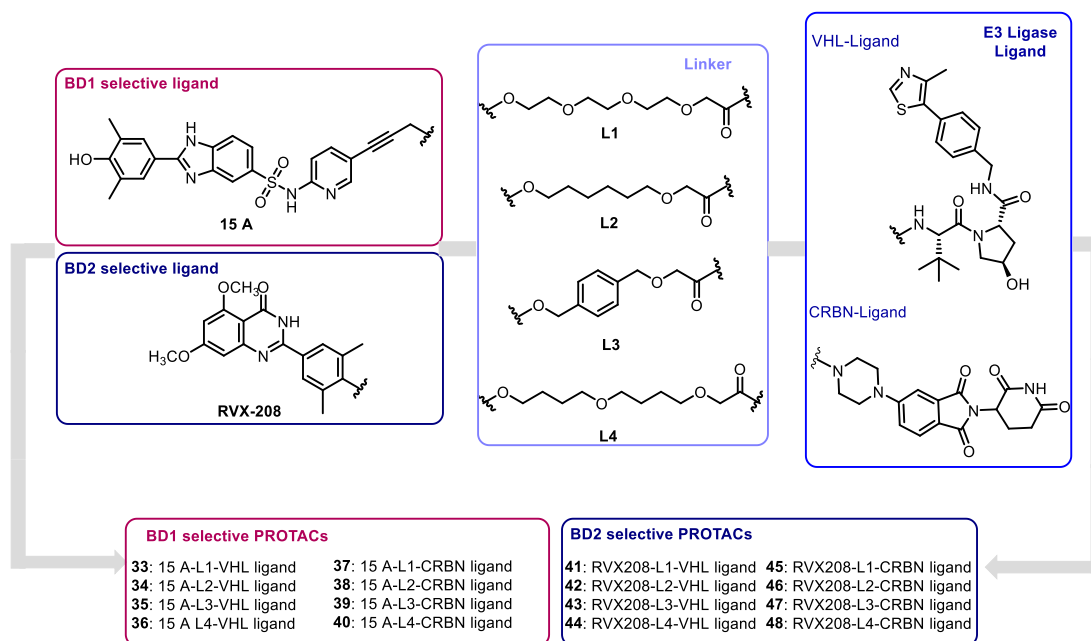


Figure 2.7 Combination of components for PROTACs design.

Biophysical, biochemical and cellular assays were exploited to evaluate the activity and the selectivity of designed compounds (Section 3). The synthetic strategies used to obtain the target compounds are detailed in Section 4.

CHAPTER III
RESULTS AND DISCUSSION

3.1 Bivalent ligands

The activity of the bivalent ligands **1 – 14** (Table 2.1) was evaluated by research group of Prof. Panagis Filippakopoulos by means of two different assays. Differential Scanning Fluorimetry (DSF) was performed for the preliminary evaluation of the binding properties. Sedimentation velocity assay was performed to investigate the ability of compounds to engage simultaneously the first and the second bromodomain.

3.1.1 Preliminary biophysical evaluation: DSF assay

DSF assay is a rapid and inexpensive screening technology helpful to identify ligands that bind the target protein. Briefly, the increase of temperature promotes the transition of a protein from the native to the unfolded state and the thermal stability of a protein is quantified as the midpoint of thermal denaturation or melting point (T_m), that is the temperature at which both native and unfolded states are equimolar. The presence of ligand that binds the protein stabilize the folded protein and, consequently, shift its T_m in concentration and potency-dependent manner. In DSF, a compound with a low fluorescence signal in a polar environment and high fluorescence in a non-polar environment is added to a protein solution and, during heating, the fluorescence of the solution is monitored. During protein unfolding, the hydrophobic core becomes exposed and the fluorescence increase until the protein is completely denatured and, thus, the T_m can be determined. The difference of T_m in the presence or in the absence of a specific ligand (ΔT_m) could be related to its affinity for the protein.¹¹¹

Compounds were screened in a panel of proteins containing the first (BD1) and the second (BD2) bromodomain of the four BET proteins and four selected bromodomain-containing proteins outside the BET family, in order to evaluate off-target effects (Figure 3.1).

Compound **2** was not evaluated in DSF assay because it is intensely colored and, consequently, could interfere in the assay. The results obtained for compound **4** were not considered because the resultant curve gave multiple transitions.

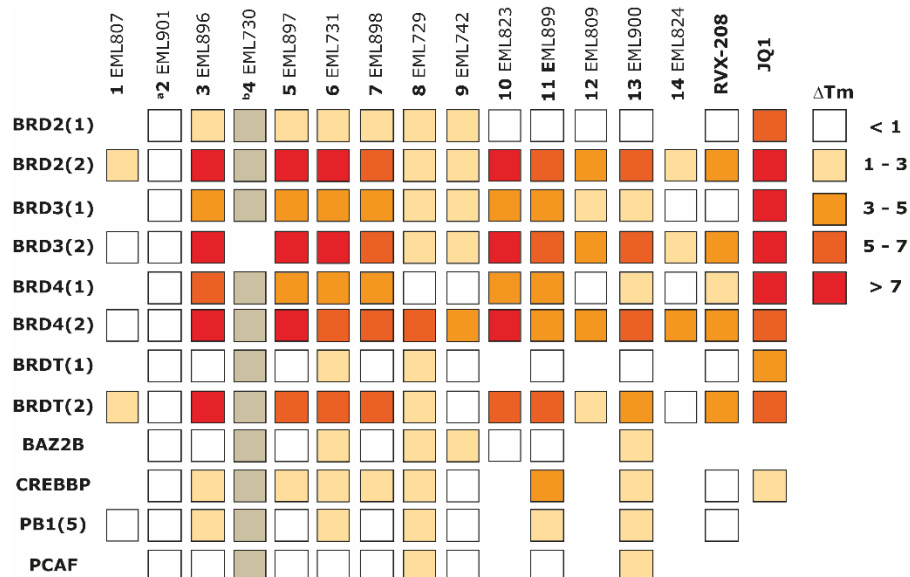


Figure 3.1 DSF data of compounds **1-14** and of **RVX-208** and **JQ1** used as reference compounds. Compounds have been initially screened at 50 μ M concentration. Temperature shift data are color coded as indicated in the figure. ^a not tested: bright yellow compound which interfere in the assay; ^b the DSF curve gave multiple transitions.

First of all, the inactivity of compounds **1** and **14**, which features no separation between the BD1 and BD2 warheads and a different point of linker attachment on BD2 ligand, respectively, confirms that a linker at 4' position of the pendant phenyl ring of **RVX-208**, is essential for activity. Moreover, all the tested compounds have no off target effects, being inactive on the selected bromodomain-containing proteins outside the BET family.

Then, we investigated the role of the linker.

Compounds **3** and **5-7**, featuring only PEGs linker, are able to bind both BD1 and BD2 domain with a preference for BD2. Generally, increasing the length of the chain decrease the affinity and compound **3** proved to be the more potent.

The presence of phenyl ring bridging the triazobenzotriazepine warhead to the PEG linker drastically decrease the affinity of compounds. In fact, compounds **8** and **9** showed only modest activity in all the proteins tested and, therefore, this type of linker was not further investigated. It is to note that his outcome was unpredicted as an aromatic amide is present in some diazepine-based compounds (i.e. **OTX-015**, Section 1.5.1)

To evaluate the role of the linker flexibility, a triazole ring was introduced as a spacer between the two BET ligands, connecting the triazolobenzotriazepine warhead with an alkyl chain (compounds **10** and **11**) or a PEG chain (compounds **12** and **13**).

Results represented in Figure 3.1 indicate that the presence of the triazole ring is generally well tolerated and, consistently to the results obtained with compounds **3–7**, increasing the distance between the two warheads decreases the affinity. Again, the shorter derivative (compound **10**) is the more potent of the series.

Thus, compounds **3** and **10** were selected for further evaluation.

3.1.2 Sedimentation velocity assay

Sedimentation velocity assay was performed to investigate the ability of compound **3** (**EML896**) and compound **10** (**EML823**) to engage simultaneously the first and the second bromodomain.

This technique is an analytical method of ultracentrifugation that measures the movement of proteins under a high centrifugal force to define the size, shape and interactions of proteins. The high speed shifts the proteins from the center to the external of the rotor until all the proteins form a layer outside. The rate of this process is function of the sedimentation coefficient of the protein, influenced by the molecular weight and by molecular shape. Linear proteins have more hydrodynamic friction and, consequently, a smaller sedimentation coefficient than a globular protein of the same molecular weight.¹¹²

Upon binding with a bivalent ligand which engage both BD1/BD2 domain, the protein adopts a more globular conformation, changing its sedimentation velocity. Moreover, changes in the molecular weight of proteins can prove if there is an intramolecular or intermolecular binding.

The sedimentation velocity assay performed with the compound **10 (EML823)** and the tandem BRD4 (the constructs that contain BD1, BD2 and the long 15kDa linker), indicated that the compound engages only one side of the protein. In fact, as illustrated in Figure 3.2, **EML823** does not distort the protein and does not change the sedimentation velocity of the tandem BRD4 (dotted black).

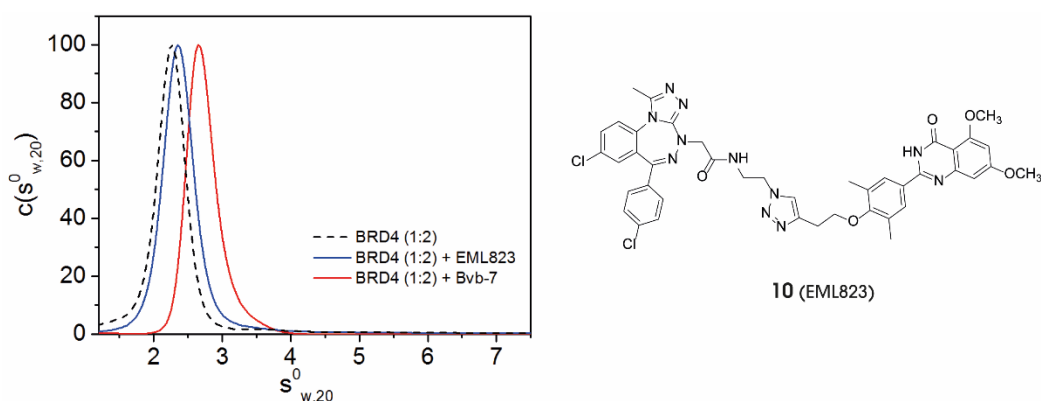


Figure 3.2 Sedimentation velocity of tandem BRD4 (1:2) with no ligand (dotted black), with **EML823** (in blue) and with a reference compound (**Bvb-7**, in red).

On the other hand, compound **3 (EML896)** gave positive results. As illustrated in Figure 3.3, the compound changes the size and shape of sedimentation velocity of all four BET proteins (the tandem constructs of BRD2, BRD3, BRD4 and BRDT). The shape change is more evident in the case of BRD2 and BRD4 (**Figure 3.3**, panel **b** and **d**). Moreover, the molecular weight of proteins is unchanged, suggesting that the both domain within the same proteins are engaged. However, it seems that the compound binds preferentially one protein site. In fact, as depicted in Figure 3.3, panel **e**, the distributions are not homogenous: the compound distorts all the protein binding to both sites, but, at the same time, binds only to one site keeping the protein

linear. Nevertheless, these results are promising for the development of bivalent compounds and compound **EML896**, together with the information on the role of the linker obtained in the present work, could be considered a valuable lead.

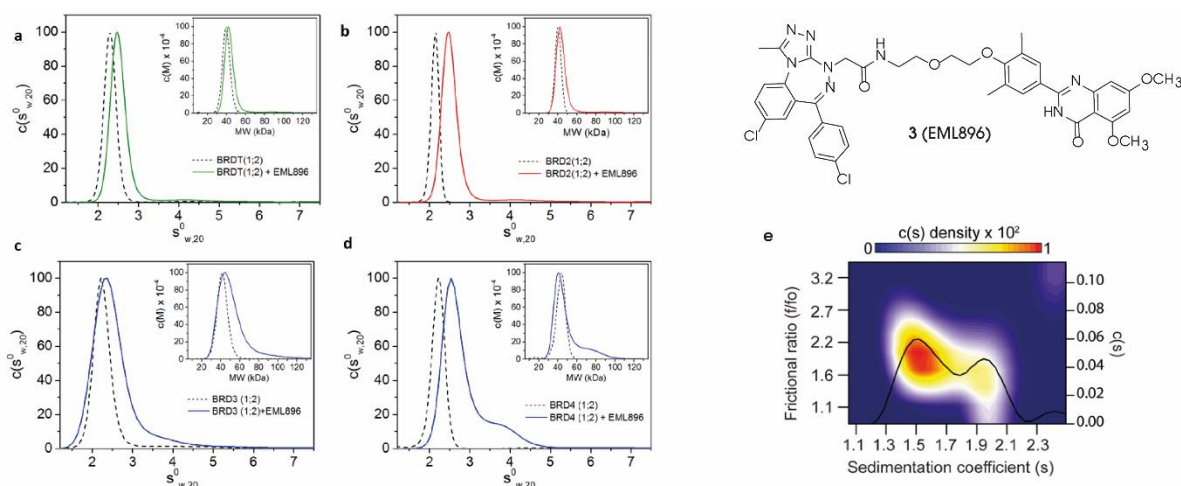


Figure 3.3 (a) sedimentation velocity of tandem BRDT (1:2) with no ligand (dotted black), with **10** (EML896) (in green); (b) sedimentation velocity of tandem BRD2 (1:2) with no ligand (dotted black), with **10** (EML896) (in red); (c) sedimentation velocity of tandem BRD3 (1:2) with no ligand (dotted black), with **10** (EML896) (in blu); (d) sedimentation velocity of tandem BRD4 (1:2) with no ligand (dotted black), with **10** (EML896) (in light blue); (e) 3D distribution. Higher f/f_0 represents the linear species and the lower one is the compacted BD1/BD2 engaged complex.

3.2 Benzimidazole-based ligands

The affinity of all benzimidazole-based ligands (compounds **15** – **32**, Table 2.2) was preliminary evaluated by DSF assay (Prof. Panagis Filippakopoulos). Subsequently, the biological profile of **15** (**EML 765**), the most potent and selective derivative was further explored by means of isothermal titration calorimetry (Prof. Panagis Filippakopoulos) and time-resolved fluorescence resonance energy transfer (Prof. Alessio Ciulli) assays.

3.2.1 Preliminary biophysical evaluation: DSF assay

The ability of benzimidazole-based ligands to bind a wide panel of bromodomain-containing proteins was preliminarily evaluated using the DSF assay (Figure 3.4).

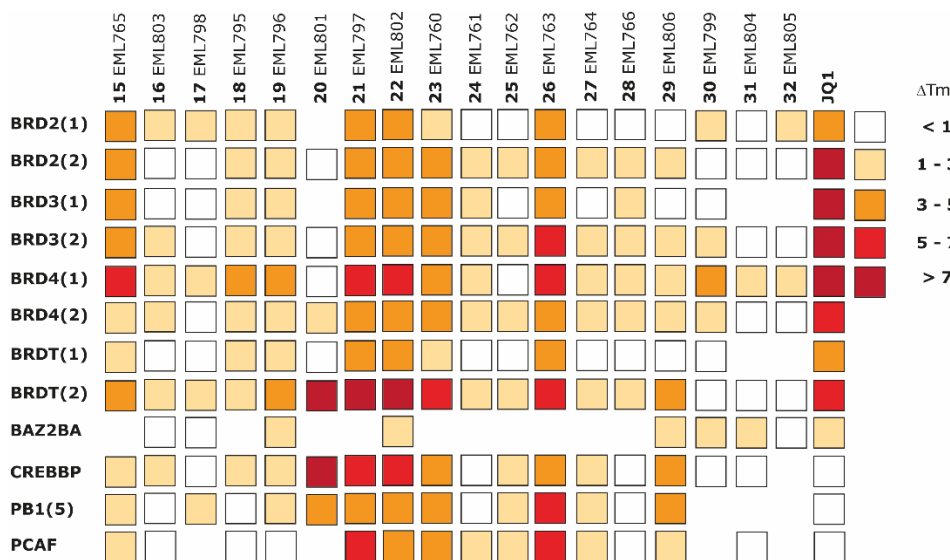


Figure 3.4 DSF data measured on compounds **15** – **32** and on **JQ1** used as reference compound. The compounds have been initially screened at 50 μ M concentration. Temperature shift data are color coded as indicated in the figure.

The binding properties of **15**, the benzimidazole analog of **MS436**, validate the efficacy of our frozen analogue approach. Indeed, even if with a lower ΔT_m than the unselective **JQ1**, compound **15** increase the melting temperature of all the BET proteins but the effect is more marked for BRD4 (1), the first bromodomain of BRD4. The investigation of the substitutions on the sulfonamide nitrogen revealed that the pyridine ring is essential for activity and selectivity. In fact, the primary sulfonamide (**18**) and the methyl sulfonamide (**19**) have no affinity toward all the BET domains considered. Similar results were observed when the pyridine ring is detached from the sulphonamide function (**16** – **17**). Surprisingly, the replacement of pyridine ring with a cyclopropyl group (**20**) results in a completely lost of activity toward BET members and a strong off-target binding on bromodomain of CBP.

Instead, the insertion of a cyclopentyl or cyclohexyl group (**21** and **22**, respectively) results in compounds with similar activity to **15** toward the first bromodomain of BRD4 but less selectivity, with activity on other non-BET bromodomain containing proteins.

Based on these data, the pyridine sulfonamide portion was maintained and a structure-activity relationship (SAR) study was undertaken on the phenyl ring in position 2 of the benzimidazole core. The main result is that the 3,5-dimethyl-4-phenolic group is fundamental for the activity. In fact, the shift of both methyl group (**28**) or the removal of one methyl (**29**) results in compounds completely inactive. The removal of both methyl group (**23**) results in compound with a weaker affinity compared to compound **15**. The replacement of the 4-hydroxyl group with a chlorine (**25**), its shift in position 3 (compound **24**) or the 3,4-dihydroxyphenyl derivative (compound **27**) results in completely inactive molecules. Instead the 2,4-dihydroxyphenyl derivative (compound **26**) acts as a promiscuous bromodomain binder. These results corroborate the hypothesis that the 3,5-dimethyl-4-phenolic group acts as KAc mimetic group and was not changed. To evaluate the impact on the activity and on selectivity of substituents with high steric hindrance, a phenyl ring was introduced in position 2 (compounds **30** – **32**). As represented in Figure 3.4, all these modifications are detrimental for the activity and the parent compound **15** remains the derivative with highest affinity.

3.2.2 ITC assay

As the DSF assay gave only qualitative information, to quantify the binding of **15** (hereafter referred to as **EML765**), Isothermal Titration Calorimetry (ITC) was performed.

This physical assay measures the thermal changes occurred when a ligand binds the target protein contained in the sample cell. The ITC instrument has two identical cells: the sample cell, containing the target protein and a reference cell, kept at the same temperature. When an interaction occurs, the instrument regulates the temperature of the reference cell to maintain the

thermal equilibrium between the two cells. In this way, the binding affinity, the enthalpy changes and the binding stoichiometry can be determined.¹¹³

We were pleased to find that **EML765** has a strong affinity (K_D of 70 nM) toward BRD4 (BD1) comparable to **JQ1** (K_D of 50 nM), used as reference compound (Figure 3.5).

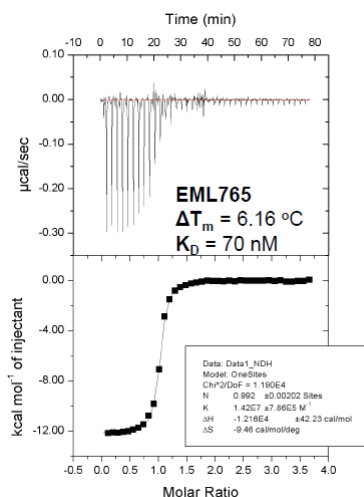


Figure 3.5 ITC data related to the binding of compound **EML765** to the first bromodomain of BRD4.

3.2.3 Selectivity profile of **EML765**

The preliminary results of **EML765** obtained with the DSF screening suggested that the compound is able to discriminate BD1 and BD2 domain of BET proteins. Thus, the selectivity of the compound was investigated.

With this aim, during the time spending at the University of Dundee, under the supervision of Prof. Alessio Ciulli, I performed a time-resolved fluorescence resonance energy transfer (TR-FRET) binding assay. This method involves an energy transfer from a donor to an acceptor chromophore. Upon excitation, the donor chromophore can transfer the acquired energy to an acceptor donor if there is a small distance between them. According to literature, in our assay 6 x His-tag BD1 or BD2 domain of each BET protein interacts with europium chelate-labeled anti-6His antibody, a donor chromophore. At the same time, the Alexa647 dye conjugated to

the BET ligand **JQ-1** is added: the binding of **JQ1** to the protein bring the acceptor (Alexa647) in close proximity to the donor chromophore. Upon excitation, there is an energy transfer from donor to acceptor resulting in the emission of a photon, showing FRET fluorescence.

In presence of a ligand able to bind the protein, there is competition with **JQ-1** conjugated to Alexa647 dye and, consequently, a decreased FRET signal (Figure 3.6).^{74, 114}

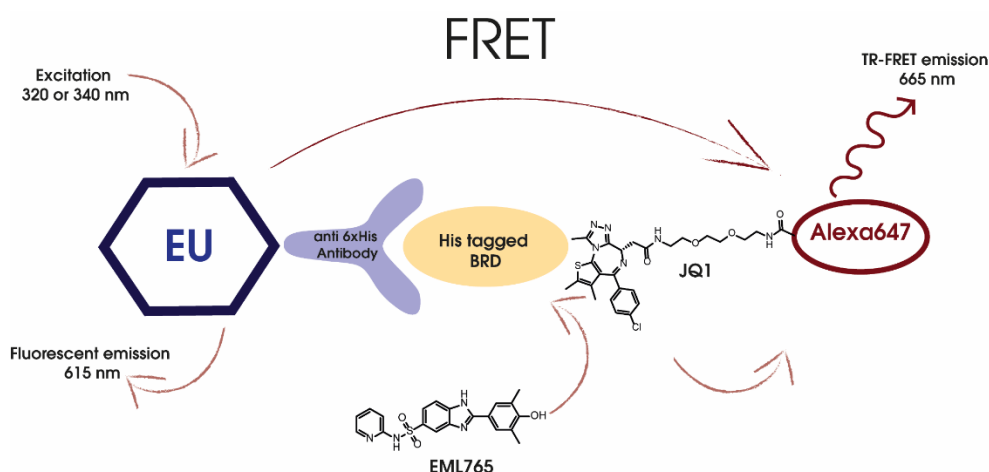


Figure 3.6 Schematic representation of TR-FRET system for BET proteins and the selected ligand (**EML765**).

Data presented in Figure 3.7 and in Table 3.3 confirms **EML765** as selective ligand of the first bromodomain of BET proteins. In fact, the affinity for BD1 ranges from 0.126 to 0.252 μM while for BD2 ranges from 2.2 to 22 μM . The best result is in BRD2, in which the selectivity ratio for the binding to BD1 and BD2 is 170 (Table 3.1).

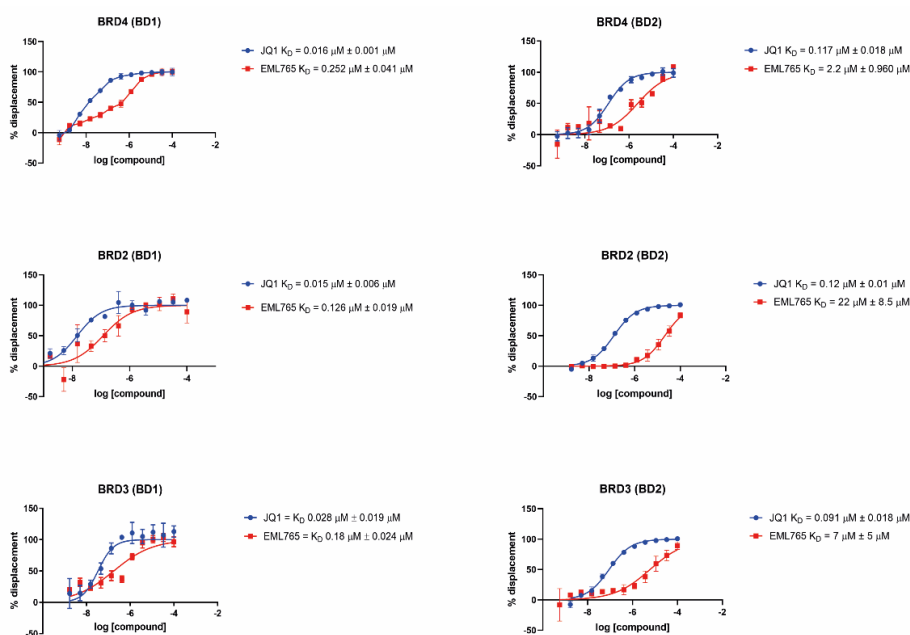


Figure 3.7 TR-FRET assay of the compound **EML765** (in red) toward the first and the second bromodomain of BET proteins. The compound **JQ1** (in blue) was used as reference compound.

Table 3.1 Selectivity profile of **EML765**

TARGET PROTEIN	EML765 (K _D μM)	BD1 SELECTIVITY INDEX
BRD4 BD1	0.252	10
BRD4 BD2	2.2	
BRD2 BD1	0.126	170
BRD2 BD2	22	
BRD3 BD1	0.18	40
BRD3 BD2	7	

Taken together, these data validate **EML765** as new lead compound for the development of potent and selective ligands for the first bromodomain of BET proteins.

3.3 BET PROTACs compounds

The ability of BET PROTACs (compounds **33** – **48**, Figure 2.7) to induce protein-degradation was evaluated in two different cell lines.

Compounds were firstly profiled in HEK-293 cells, a BET-insensitive cell line, which does not undergo to cell-death upon BET inhibition. Firstly, cells were treated for 6 h with compounds at two different concentrations (1 μ M and 0.01 μ M) and then the lysates were immunoblotted with BRD2, BRD3 and BRD4 specific antibodies. **MZ1** and the inactive **cisMZ1** were used as positive and negatively control, respectively. Unfortunately, no significant reduction in protein levels for all the compounds tested was observed (Figure 3.8). Same results were obtained with longer incubation time (16 hours) (Figure 3.9).

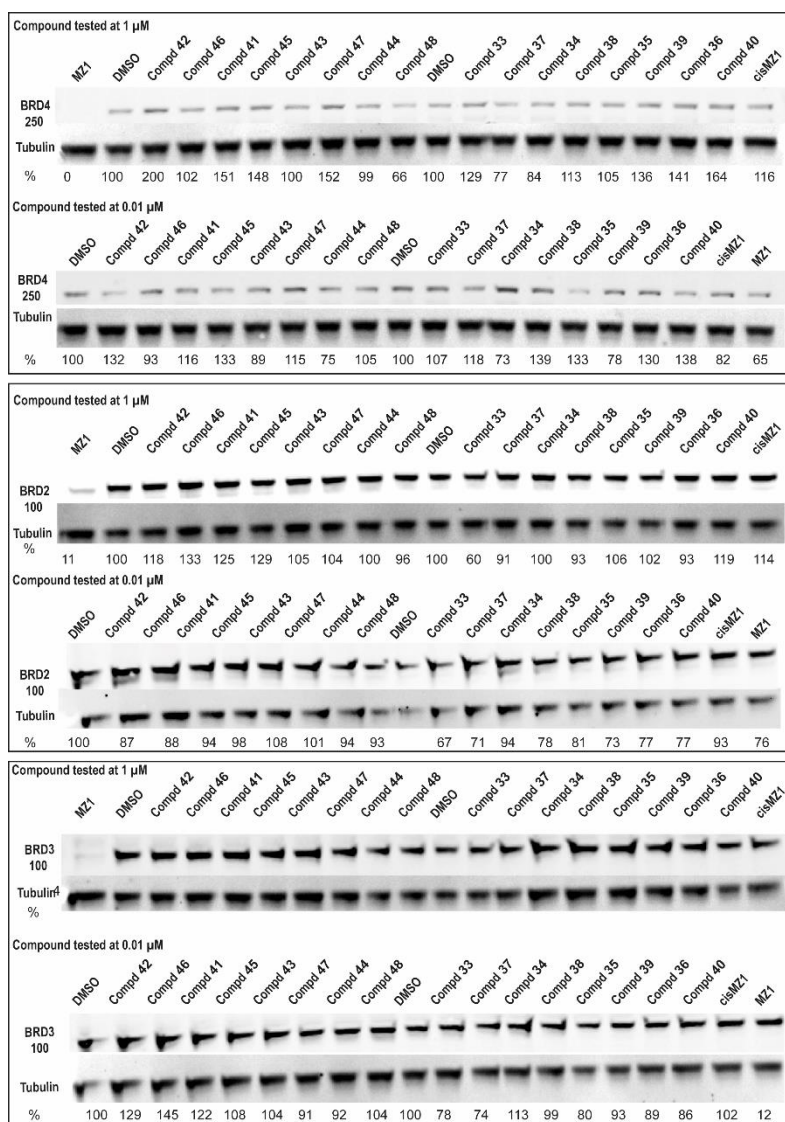


Figure 3.8 Protein degradation profile of BET degraders visualized by immunoblot using anti-BRD4, anti-BRD2 and anti-BRD3 antibody. HEK293 cells were treated for 6 h at 1 μ M and 0.01 μ M with inhibitors, positive control (**MZ1**), negative control (**cisMZ1**) and DMSO control.

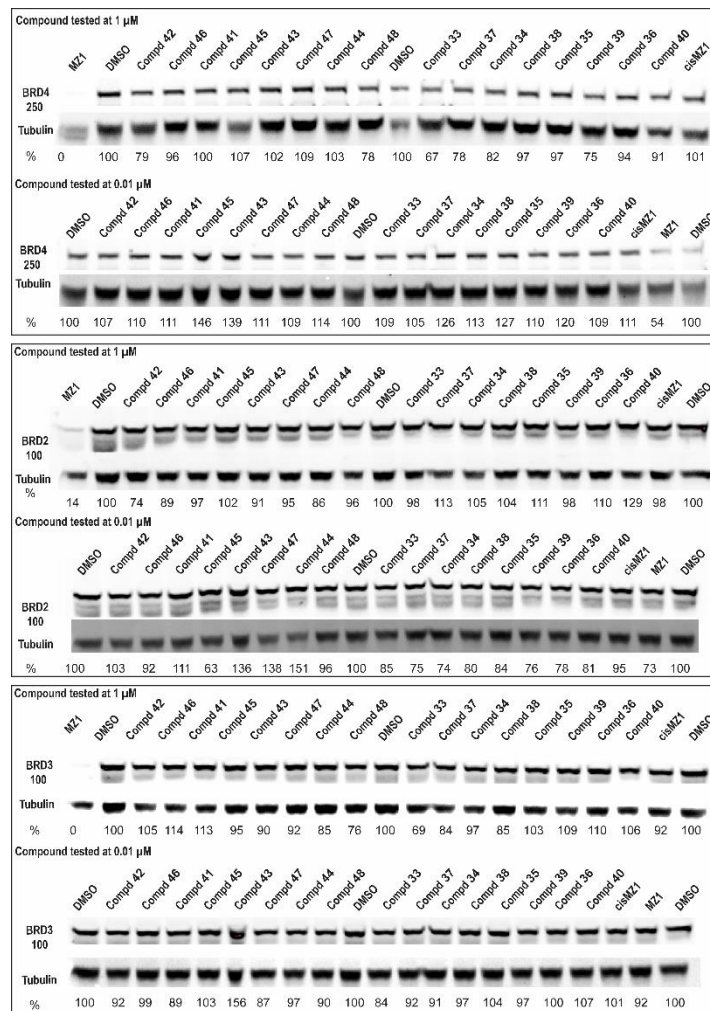


Figure 3.9 Protein degradation profile of BET degraders visualized by immunoblot using anti-BRD4, anti-BRD2 and anti-BRD3 antibody. HEK293 cells were treated for 16 h at 1 μ M and 0.01 μ M with inhibitors, positive control (**MZ1**), negative control (**cisMZ1**) and DMSO control.

In order to eliminate potential false-negatives due to the “Hook effect”, the compounds were tested also at lower concentrations (0.1 μM and 0.001 μM). Even in this case, the compounds do not induce protein degradation for BRD2 (Figure 3.10) and BRD3 (Figure 3.11).

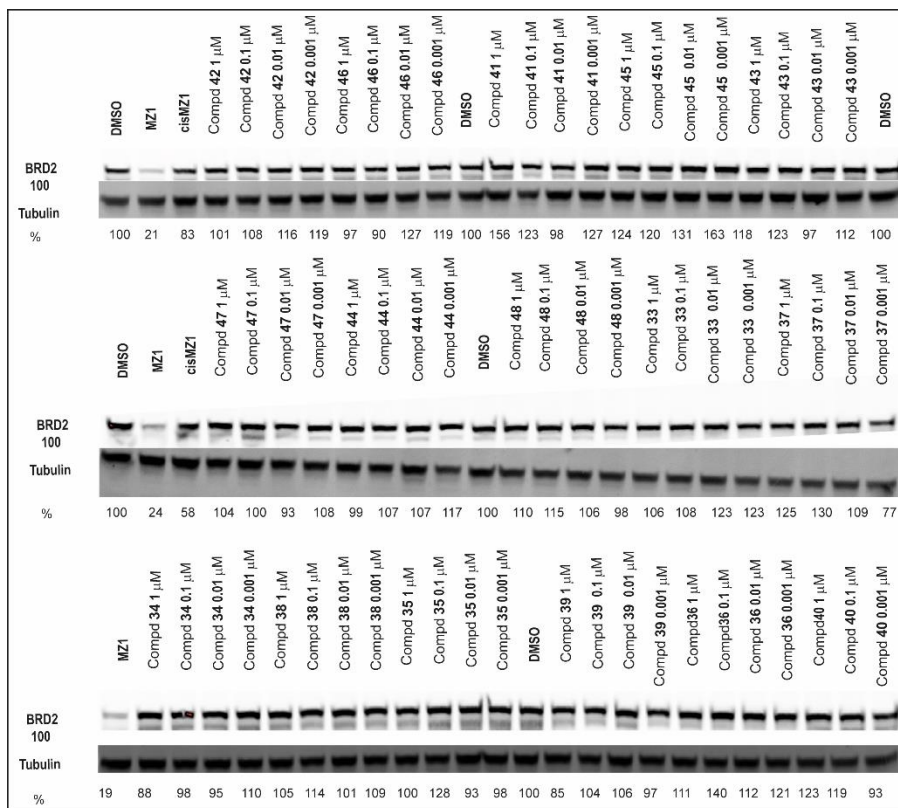


Figure 3.10 Protein degradation profile of BET degraders visualized by immunoblot using anti-BRD2 antibody. HEK293 cells were treated for 16 h at 1.0 μM , 0.1 μM , 0.01 μM and 0.001 μM with inhibitors, positive control (MZ1), negative control (cisMZ1) and DMSO control.

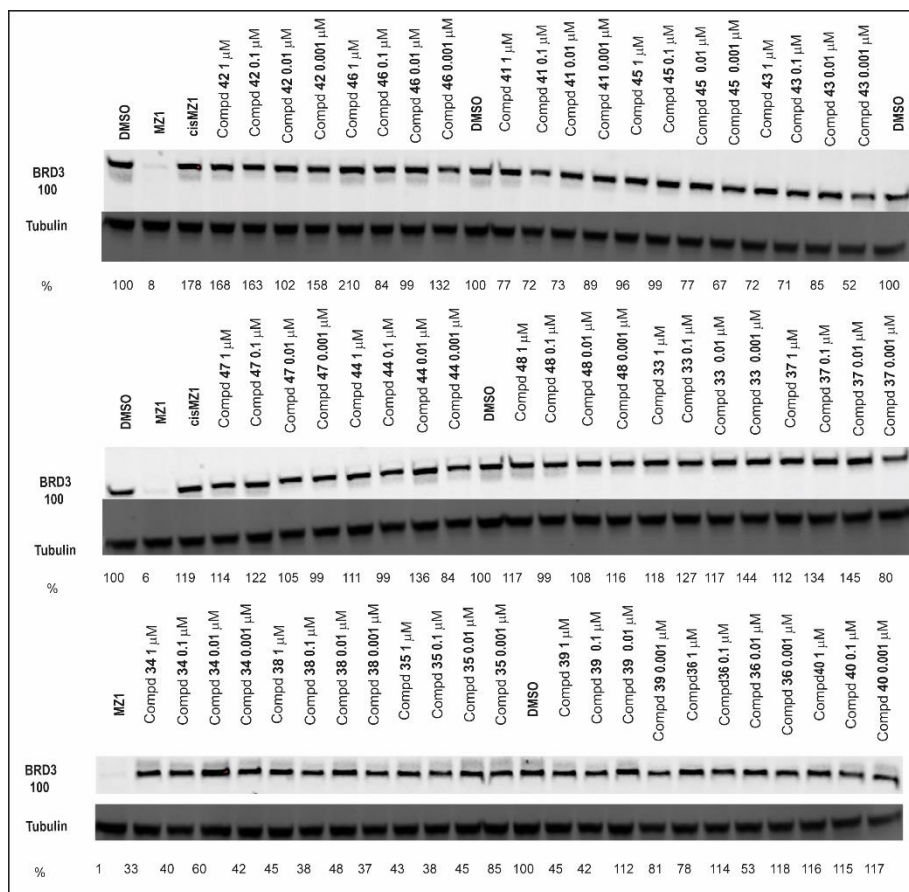


Figure 3.11 Protein degradation profile of BET degraders visualized by immunoblot using anti-BRD3 antibody. HEK293 cells were treated for 16 h at 1.0 μM , 0.1 μM , 0.01 μM and 0.001 μM with inhibitors, positive control (**MZ1**), negative control (**cisMZ1**) and DMSO control.

These results were confirmed using Simple Western™ Jess, an innovative automated capillary-based immunoassay that is supposed to be more reproducible and more sensitive than traditional method. Using an optimized method, the assay was performed only for BRD4 and the cells were treated for 16 h at four different concentrations (1.0 μM , 0.1 μM , 0.01 μM and 0.001 μM). Also in this assay, however, no protein degradation was observed (Figure 3.12).

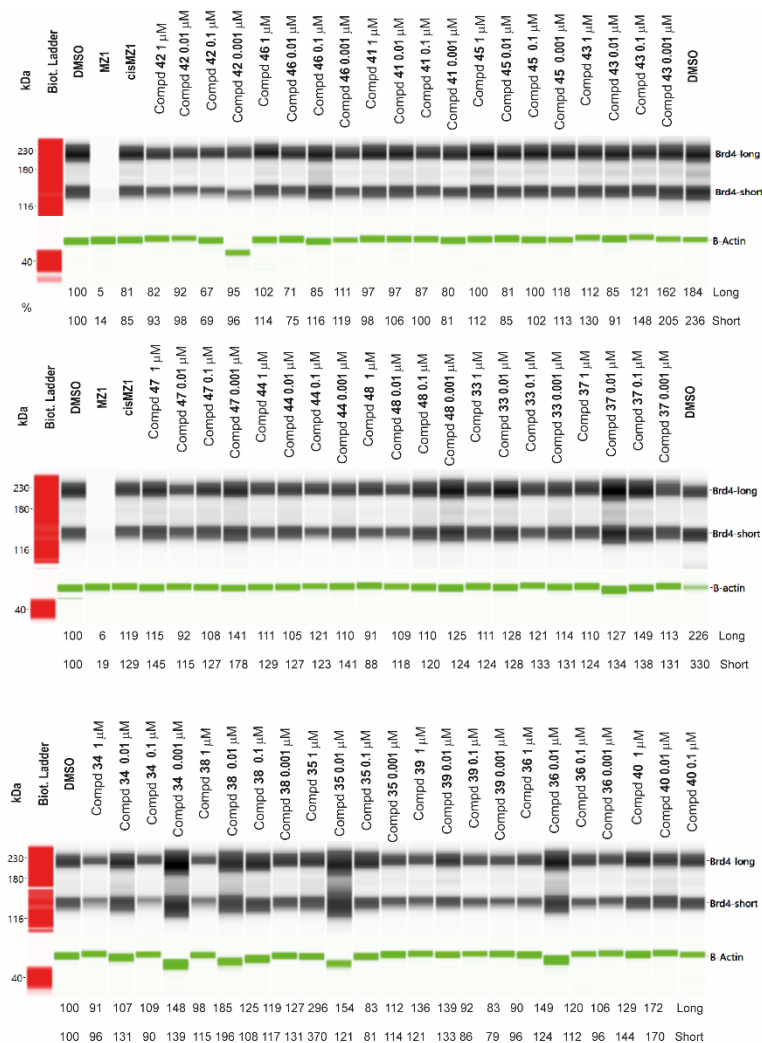


Figure 3.12 Protein degradation profile of BET degraders obtained using the Jess, an automated protein separator. HEK293 cells were treated for 16 h at 1 μ M, 0.1 μ M, 0.01 μ M and 0.001 μ M using anti-BRD4 as antibody.

Taken together, these data definitely showed that compounds **33** – **48** are not able to induce protein-degradation in HEK-293 cells.

Our PROTACs were also evaluated in MV4-11 cells, a BET-sensitive cell line which undergoes to cell-death upon BET inhibition. We evaluate the ability of compounds to induce cell-death using the cell viability assay. As depicted in Figure 3.13, compounds **33** – **48** do not induce substantial cell-death.

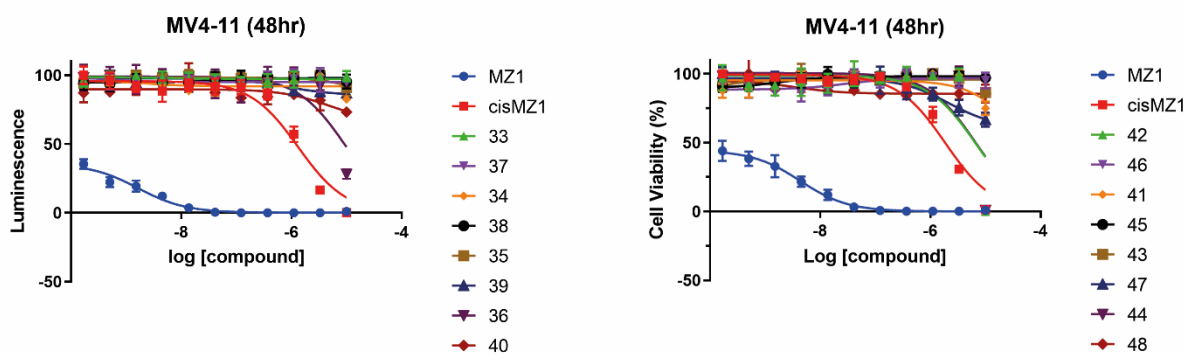


Figure 3.13 Cell viability assay. MV4-11 cells were treated with the PROTAC compounds, positive control (MZ1) and negative control (cisMZ1) for 48 h. Cell viability was measured with Promega CellTiter-Glo luminescent cell viability assay kit. Data were analyzed with Graphpad Prism software.

Despite the negative results, the designed PROTAC compounds can be considered a starting point for further evaluation and optimization. Indeed, the inactivity of compounds it is not unusual in PROTACs field, considering that several aspects can influence the activity of degraders. We suspect that the length and the nature of the linkers could be not suitable for the proper engagement of target protein and E3 ligase and can be optimized. We can also speculate that the compounds engage just one component of the system (the target protein or the E3 ligase) promoting the formation of a binary system instead the ternary complex or that they do not promote a stable ternary complex. In addition, the compounds could have a low cellular permeability.¹⁰⁵⁻¹⁰⁶

All these aspects should be better investigated. For examples, we can evaluate possible changes in cellular activity using the electroporation to increase the permeability of the cell membrane or perform *in vitro* assays to better evaluate the formation of binary and/or ternary complex.

CHAPTER IV

CHEMISTRY

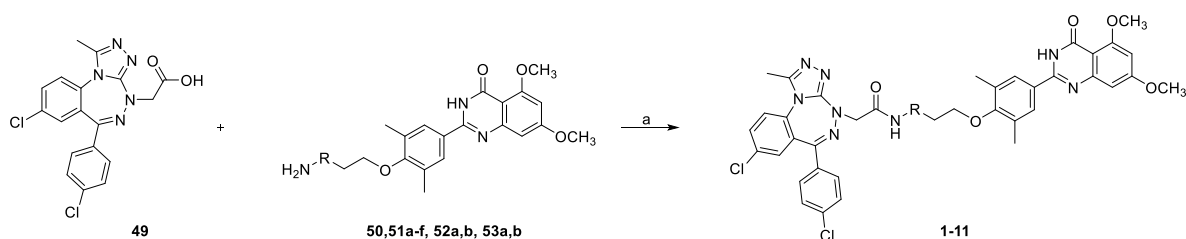
4.1 Synthesis of bivalent ligands

This Section describes the synthetic procedures adopted for the preparation of target compounds. A general synthetic approach was used for compounds **1** – **11**, while for compounds **12** – **14** other two different approaches have to be used.

4.1.1 Synthesis of bivalent ligands 1 – 11

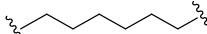
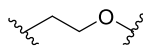
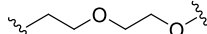
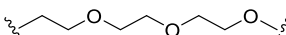
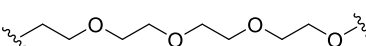
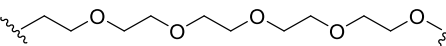
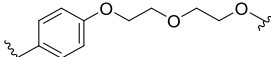
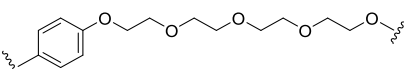
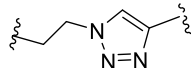
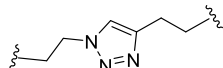
Compounds **1** – **11** were obtained by amide coupling of compound **49**, **Cl-BzT-7** featuring a carboxylic function, and the proper amino-linkers attached on hydroxy-ethylether group in 4' of **RVX-208** (**50**, **51a – f**, **52a,b** and **53a,b**) using EDC and HOBt as peptide coupling reagents (Scheme 4.1). As summarized in Table 4.1, the yields ranged from moderate to good.

Scheme 4.1 General synthetic scheme for the preparation of compounds **1** – **11**



Reagents and conditions: (a) EDC hydrochloride, HOBt, NMM, dry DMF, r. t., 4 h.

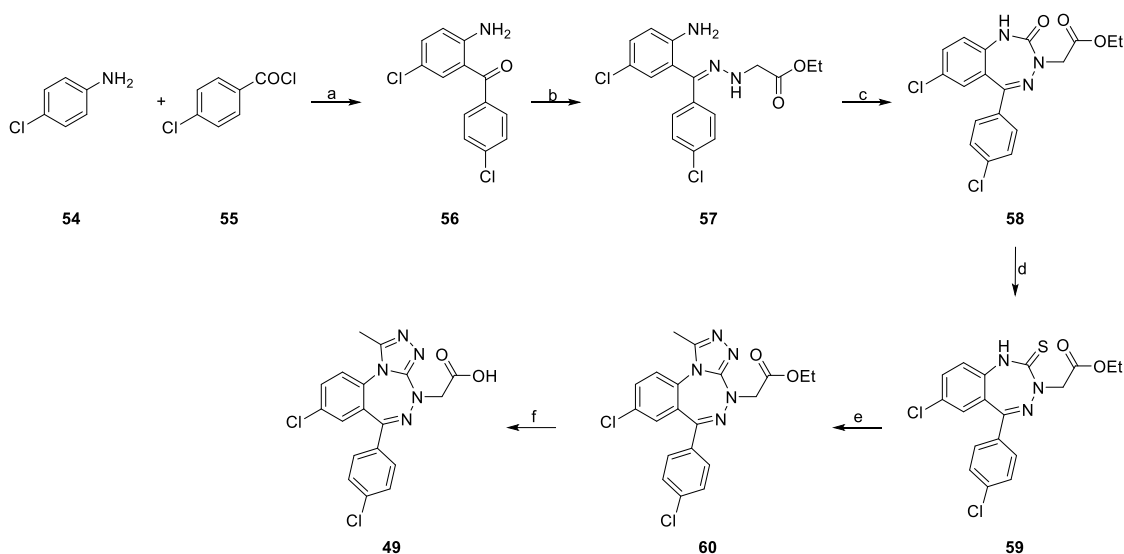
Table 4.1 Compounds 1-11

	R	YIELD
50; 1 (EML807)	-	66%
51a; 2 (EML901)		60%
51b; 3 (EML896)		60%
51c; 4 (EML730)		54%
51d; 5 (EML897)		60%
51e; 6 (EML731)		48%
51f; 7 (EML898)		49%
52a; 8 (EML729)		74%
52b; 9 (EML742)		52%
53a; 10 (EML823)		78%
53b; 11 (EML899)		57%

4.1.1.1 Synthesis of triazolobenzotriazepine scaffold **49**

The synthetic protocol for the preparation of compound **49** is reported in Scheme 4.2.

Scheme 4.2 Procedure for preparation of compound **49**



Reagents and conditions: (a) ZnCl_2 , 120 °C to 230 °C, 4 h (70%); (b) ethyl hydrazinoacetate hydrochloride, dry EtOH, reflux, 18 h (79%); (c) TEA, $(\text{CCl}_3\text{O})_2\text{CO}$, dry DCM, 0 °C to r. t., 18 h (85%); (d) Lawesson's reagent, toluene, reflux, 18 h (55%); (e) $\text{NH}_2\text{-NHAc}$, $\text{Hg}(\text{OAc})_2$, THF/AcOH (4:1), 95 °C (30%); (f) LiOH, EtOH/ H_2O (1:1) (93%).

Reaction of 2-amino-4',5-dichlorobenzophenone (**56**), prepared from 4-chloroaniline (**54**) and 4-chlorobenzoyl chloride (**55**) according to previously published procedure¹¹⁵, with ethyl hydrazinoacetate hydrochloride in anhydrous ethanol (dry EtOH) allowed the formation of the corresponding imine (**57**). Intramolecular cyclization with triphosgene¹¹⁶ ($(\text{CCl}_3\text{O})_2\text{CO}$) yields the corresponding benzotriazepinone (**58**) which is then thionated with Lawesson's reagent to afford the thioamide **59**, a more reactive derivative for the subsequent formation of triazole ring. The moderate yield (55%) is in part due to poorly soluble byproducts which complicated purification procedures as well as the presence of ethyl ester group which can compete in the thionation reaction.

The triazole ring of compound **60** was obtained by mercury-mediated cyclization in presence of acetyl hydrazine at 80 °C. The modest yield obtained in this one-step procedure is comparable to the reaction traditionally conducted in a three-step procedure,⁷³ which involves

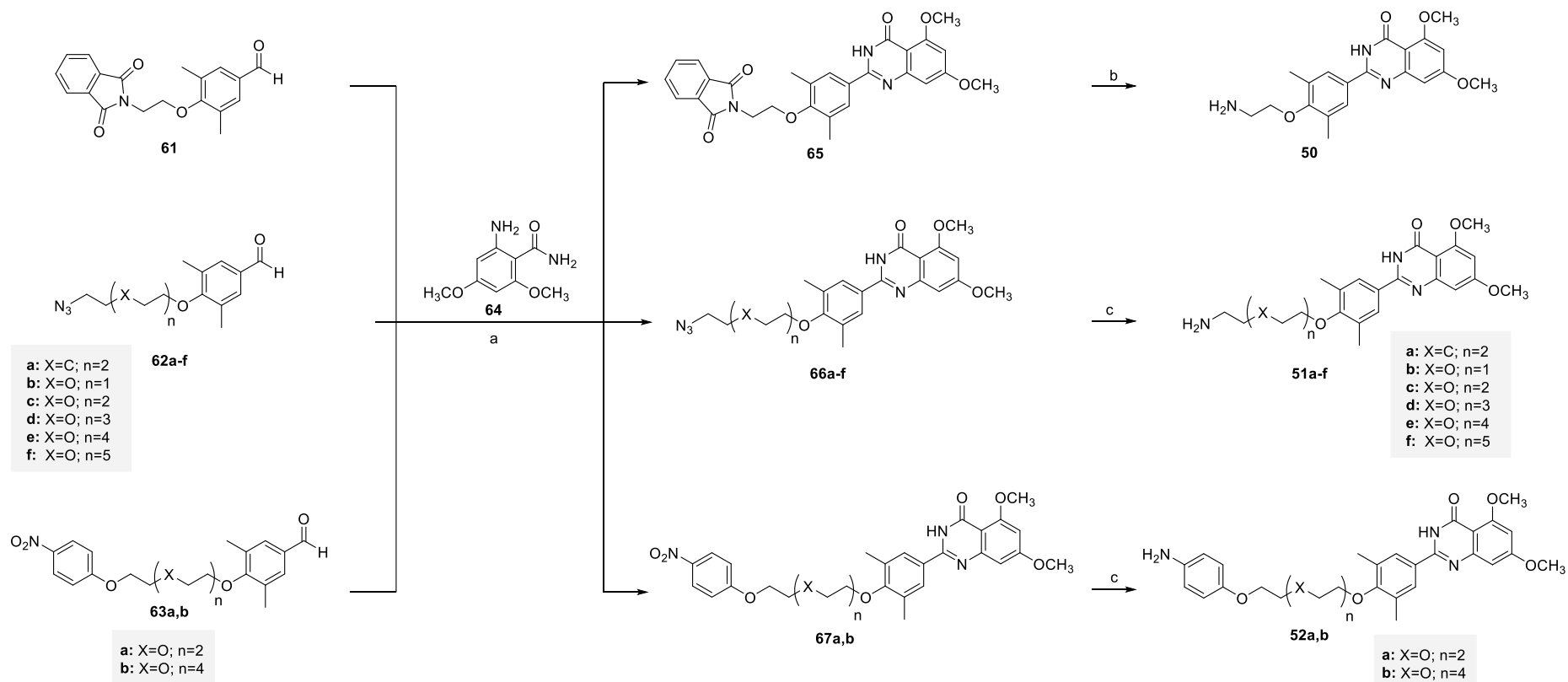
the treatment of compound **59** with hydrazine in tetrahydrofuran (THF), followed by acetylation with acetyl chloride and further cyclization in acidic conditions. Finally, hydrolysis of the ethyl ester with lithium hydroxide (LiOH) furnished the carboxylic acid derivative **49** in good yield (86%).

4.1.1.2 Synthesis of amines **50**, **51a – f** and **52a,b**

The amines **50**, **51a – f** and **52a,b** were prepared as depicted in Scheme 4.3. The quinazolinone core was formed by a direct cyclocondensation-dehydrogenation of the synthesized aldehydes **61**, **62a – f** and **63a,b** and the 2-amino-4,6-dimethoxybenzamide **64**, in presence of sodium bisulfite (NaHSO₃ 50% in mixture with Na₂S₂O₃) and a catalytic amount of p-toluenesulfonic acid (TsOH) in anhydrous N,N-dimethylacetamide (DMAc), affording the intermediates **65**, **66a – f** and **67a,b**. Hydrazinolysis of N-substituted phthalimide **65** and palladium-on-carbon hydrogenation converted the azido group of intermediates **66a – 66f** and the nitro group of intermediates **67a,b** into the corresponding amino derivatives **50**, **51a – f** and **52a,b**.

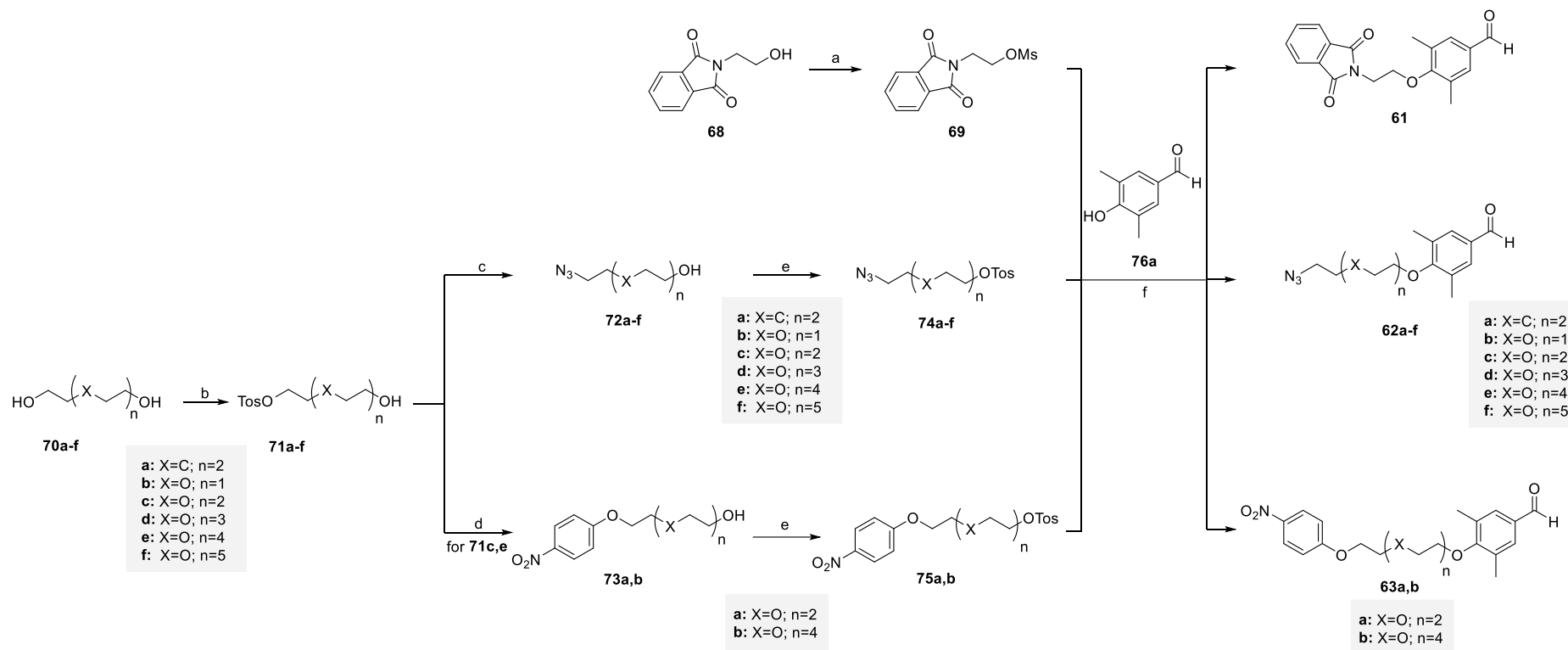
It has to be noted that the synthetic protocol involved the construction of **RVX-208** scaffold on proper linkers. This strategy was preferred considering that the direct addition of the linkers on quinazolinone scaffold could give a mixture of alkylated byproducts due to the tautomerism of this scaffold.

Scheme 4.3 Procedure for preparation of amines **50**, **51a-f**, **52a,b**



Reagents and conditions: (a) NaHSO₃ (50% in mixture), TsOH, DMAc, 120 °C, 18 h (40 – 80%); (b) NH₂NH₂, EtOH, reflux, 3 h (85%); (c) H₂, Pd/C, EtOH, 3 h (81 – 99%).

Scheme 4.4 Procedure for preparation of aldehydes **61**, **62a – f** and **63a,b**



Reagents and conditions: (a) MsCl, TEA, dry DCM 0 °C to r. t. (99%); (b) TsCl, Ag₂O, KI, toluene, 0 °C to r. t., 18 h (53 – 82%); (c) NaN₃, DMF, r. t., 18 h; (50 – 70%); (d) p-nitrophenol, K₂CO₃, dry DMF, 80 °C, 18 h (96 – 99%); (e) TsCl, TEA, dry DCM, r. t., 18 h (41 – 66%); (f) K₂CO₃, dry DMF, 80 °C, 18 h (51 – 87 %).

The aldehydes **61**, **62a – f** and **63a,b** were prepared as reported in Scheme 4.4. The general synthetic route is based on the attachment of proper linkers on 4-hydroxy-3,5-dimethylbenzaldehyde **76a**, commercially available.

All the linkers used are properly activated converting their alcoholic functions in a good leaving group. The ethyl linker of compound **1** is prepared starting from the 2-phthalimidoethanol (**68**) commercially available. The alcoholic group of **68** is converted into the corresponding mesylate compound (**69**), using mesyl chloride and triethylamine (TEA) in anhydrous dichloromethane (DCM).

Linkers used for the synthesis of compounds **2 – 9** are prepared from the commercially available 1,8-octanediol (**70a**) or the poli(ethylene glycol)s (PEGs) (**70b – f**).

The starting materials are selectively monotosylated (**71a – f**) using tosyl chloride (TsCl) in presence of silver oxide (Ag₂O) and a catalytic amount of potassium iodide (KI). This method allows a selective monotosylation of symmetrical diols using a stoichiometric amount of tosylating agent under mild conditions.¹¹⁷

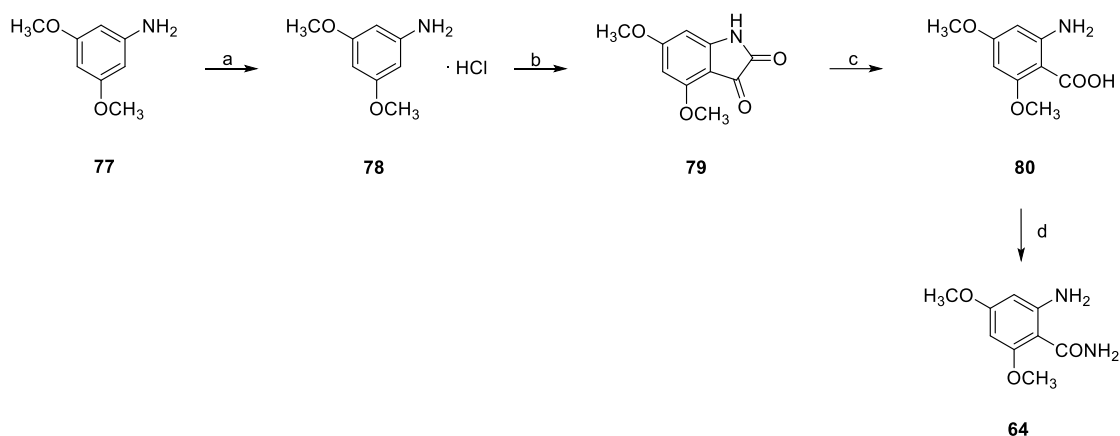
Monotosylated compounds **71a – f** reacted with sodium azide in N,N-dimethylformamide (DMF) affording the intermediates **72a – f**. On the other hand, the intermediates **73a,b** are prepared treating the monotosylated intermediates **71c,e** with 4-nitrophenol, commercially available, in presence of potassium carbonate (K₂CO₃) in anhydrous DMF.

Then, the obtained intermediates **72a – f** and **73a,b** are tosylated in presence of tosyl chloride and triethylamine in anhydrous DCM yielding the intermediates **74a – f** and **75a,b**.

The activated linkers (intermediates **69**, **74a – f** and **75a,b**) can easily undergo nucleophilic substitution with the 4-hydroxy-3,5-dimethylbenzaldehyde **76a**, commercially available, affording the corresponding aldehydes **61**, **62a – f** and **63a,b** in moderate or good yield (51 – 87%)

The 2-amino-4,6-dimethoxybenzamide (**64**) was prepared according a previously described procedure (Scheme 4.5).⁷¹

Scheme 4.5 Synthesis of 2-amino-4,6-dimethoxybenzamide **64**



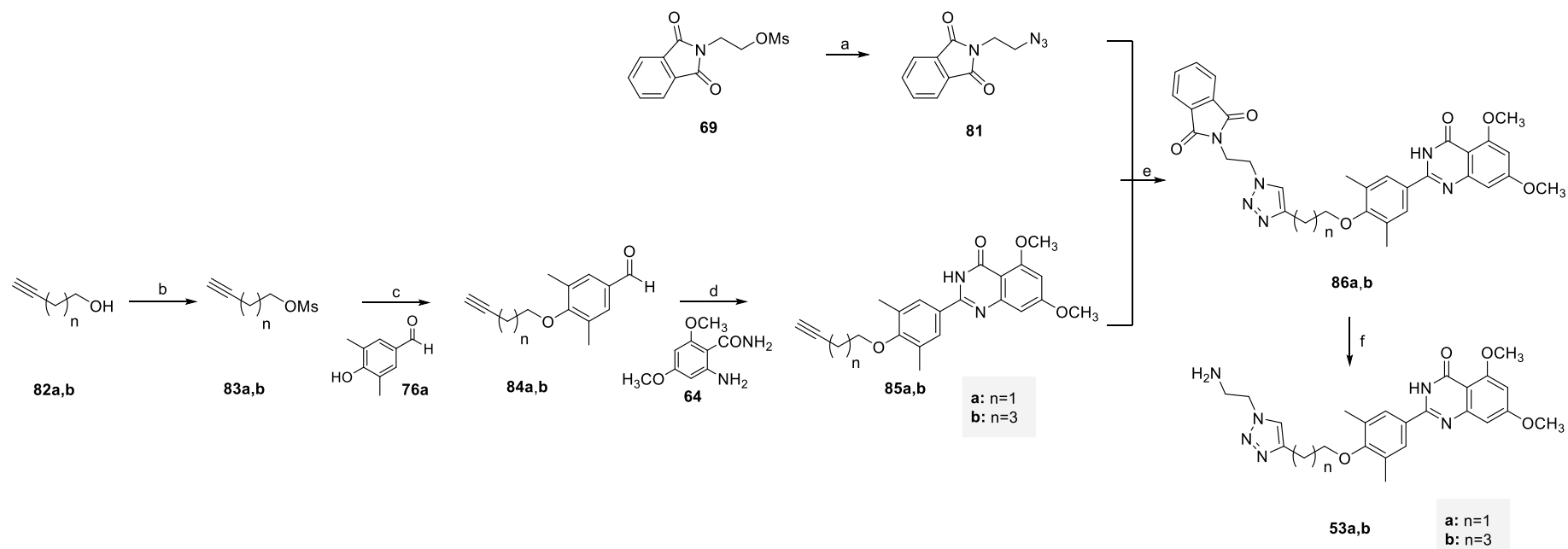
Reagents and conditions: (a) HCl_(g), Et₂O (97%); (b) (COCl)₂, 0 °C to 170 °C, 90 min (61%); (c) NaOH, H₂O₂, 70 °C to 100 °C for 2 h then r. t., 18 h (60%); (d) EDC hydrochloride, HOBT, NMM, ammonia hydroxide solution (33%), dry THF, r. t., 4 h (88%).

Briefly, the 3,5-dimethoxyaniline hydrochloride salt (**78**), obtained treating the commercially available amine (**77**) with hydrochloric acid, reacted with oxalyl chloride at high temperature leading to the formation of the 4,6-dimethoxy indolin-2,3-dione (**79**). Subsequent reaction with sodium hydroxide (NaOH) and hydrogen peroxide (H₂O₂) furnished the 2-amino-4,6-dimethoxybenzoic acid (**80**) which, reacting with ammonia hydroxide solution (33%), in coupling condition, afford the desired compound **64**.

4.1.1.3 Synthesis of amines **53a,b**

The amines **53a,b** were obtained according to a slight modification of the above-described procedure (Scheme 4.6). Indeed, the formation of 1,2,3-triazole scaffold involve a ‘click chemistry reaction’. This reaction is a copper(I)-catalyzed variant of the Huisen 1,3-dipolar cycloaddition of azides and terminal alkynes for the 1,2,3-triazole formation. Accordingly, azides intermediates and terminal alkynes have been prepared.

Scheme 4.6 Procedure for preparation of amines **53a,b**



Reagents and conditions: (a) NaN_3 , DMF, r. t., 18 h (80%); (b) MsCl , TEA, dry DCM 0 °C to r. t. 3 h; (c) K_2CO_3 , dry DMF, 80 °C, 18 h (66 – 68%); (d) NaHSO_3 (50% in mixture), TsOH , dry DMAc, 120 °C, 18 h (70 – 72%); (e) CuI , DIPEA, AcOH, DCM, r. t., 18 h (67 – 87%); (f) NH_2NH_2 , EtOH, reflux, 3 h (81 – 83%).

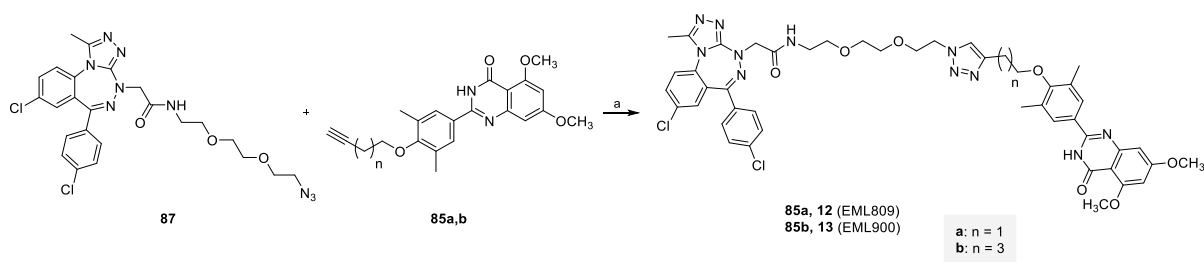
Starting from the mesylate intermediate **69**, synthesized as described in Scheme 4.3, the azide intermediate **81** is obtained under classical condition of nucleophilic substitution, using sodium azide as nucleophile. On the other hand, treatment of 3-butyne-1-ol (**82a**) and 5-hexyn-1-ol (**82b**), commercially available, with mesyl chloride (MsCl) give the mesylates **83a,b** which reacted with the 4-hydroxy-3,5-dimethylbenzaldehyde (**76a**) under classical conditions of nucleophilic substitution, affording the aldehydes **84a,b**. The latter reacted with the 2-amino-4,6-dimethoxybenzamide (**64**) by a direct cyclocondensation-dehydrogenation affording the quinazolinone-base ligands **85a,b**.

Obtained both azide (**81**) and alkyne intermediates (**85a,b**), copper iodide and catalytic amount of AcOH and DIPEA were used to obtain the triazole intermediates **86a,b** by click reaction in good yield (67 – 87%). Finally, hydrazinolysis of N-substituted phthalimides **86a,b** furnished the corresponding amines **53a,b**.

4.1.2 Synthesis of bivalent ligands 12 – 13

Compounds **12** and **13** were obtained by a final ‘click reaction’ (Scheme 4.7) between the azido group of the first portion of the linker on **Cl-BzT-7 (83)** and the alkynyl group on the second portion of the linker attached on **RVX-208 (85a,b)** prepared as previously described (Scheme 4.6).

Scheme 4.7 Procedure for preparation of compounds 12-13



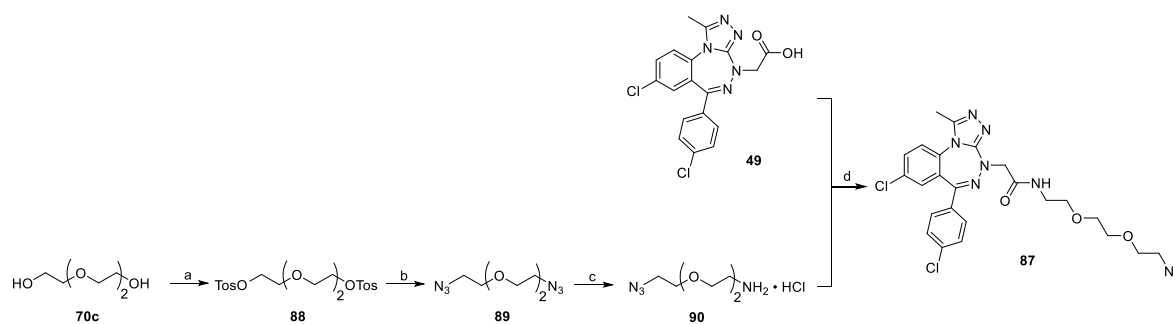
Reagents and conditions: (a) CuI, DIPEA, AcOH, DCM, r. t., 18 h (52 – 69%).

Unlike the synthetic procedures adopted for the preparation of intermediates **86a,b**, the triazole ring was formed in the last step of reaction, avoiding the use of free amine-PEG3-azide which could complicate the purification procedures.

The azide intermediate **87** was prepared as depicted in Scheme 4.8.

Key starting material is the amine-PEG3-azide **90**, prepared according to previously published procedures.¹¹⁸ Briefly, the triethylene glycol **70c**, commercially available, is tosylated (**88**) using tosyl chloride (TsCl) and potassium hydroxide (KOH). The ditosyloxy triethylene glycol **88** reacts with an excess of sodium azide forming the diazide intermediate **89**. Under Staudinger condition, the diazide intermediate **89** is selective reduced furnished the monoamine triethylene glycol as hydrochloride salt **90** in high yield (78%). The latter was coupled with the intermediate **49** using EDC and HOBT as coupling reagent affording the azide intermediate **87** in good yield (75%).

Scheme 4.8 Procedure for preparation of compound **87**

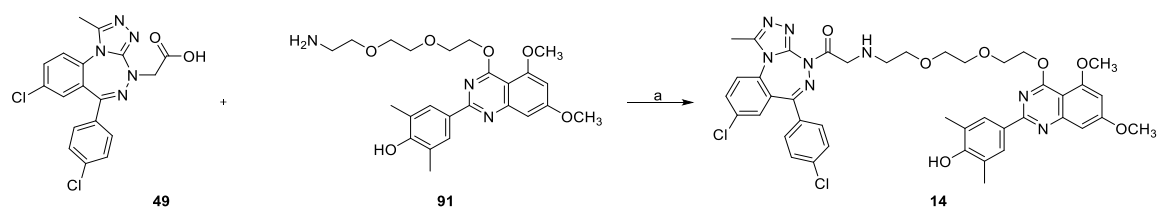


Reagents and conditions: (a) TsCl, KOH, DCM 0 °C to r. t., 3 h (93%); (b) NaN₃, TBAI, DMF, 80 °C, 18 h (99%); (c) PhP₃, HCl, AcOEt, r. t., 18 h (78%); (d) EDC hydrochloride, HOBT, NMM, dry DMF, r. t., 4 h (75%).

4.1.3 Synthesis of bivalent ligand 14

Compound **14** was obtained by a final coupling reaction between the carboxylic group of **Cl-BzT-7 (49)** and the amino group of the linker attached on quinazolinone side of **RVX-208 (91)** using EDC and HOBT as coupling reagents (Scheme 4.9).

Scheme 4.9 Procedure for preparation of bivalent ligand 14.



Reagents and conditions: (a) EDC hydrochloride, HOBT, NMM, dry DMF, r. t., 4 h (60%).

To avoid a mixture of mono- and di-alkylated intermediates, as mentioned above, the first approach involved the insertion of a proper protecting group on the phenolic portion. Tosyl and acetyl group are used as protecting group with negative results.

In both cases, we didn't recover the desired product, with different problems during the attachment of the linker and/or the de-protection steps (Figure 4.1).

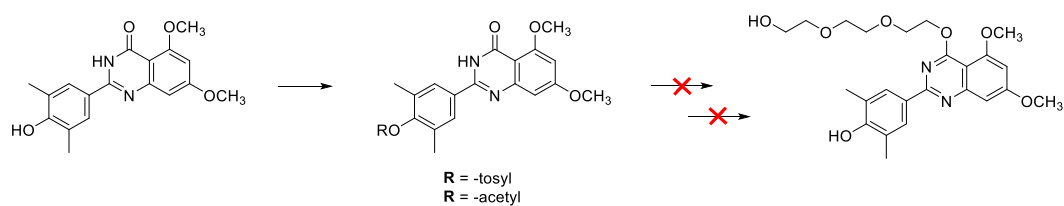
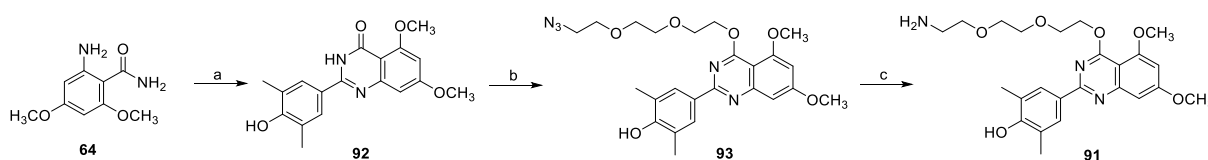


Figure 4.1 First synthetic strategy used for the attachment of the linker on quinazolinone scaffold.

These negative results prompted us to directly attach the linker on deprotected quinazolinone intermediate (Scheme 4.10).

Cyclocondensation-dehydrogenation in presence of NaHSO₃ of the 2-amino-4,6-dimethoxybenzamide (**64**) and the 4-hydroxy-3,5-dimethylbenzaldehyde **76a** allowed the formation of the quinazolinone ligand **92**. Nucleophilic substitution with the linker **74c** prepared as previously described (Scheme 4.3) allowed the attachment of the linker on quinazolinone side (**93**). As expected, the modest yield (37%) is due to the contemporary formation of mono- and di-alkylated byproducts separated by flash-chromatography. Palladium-on-carbon hydrogenation converted the azido group into the amino compounds **91**.

Scheme 4.10 Procedure for preparation of amine **91**.



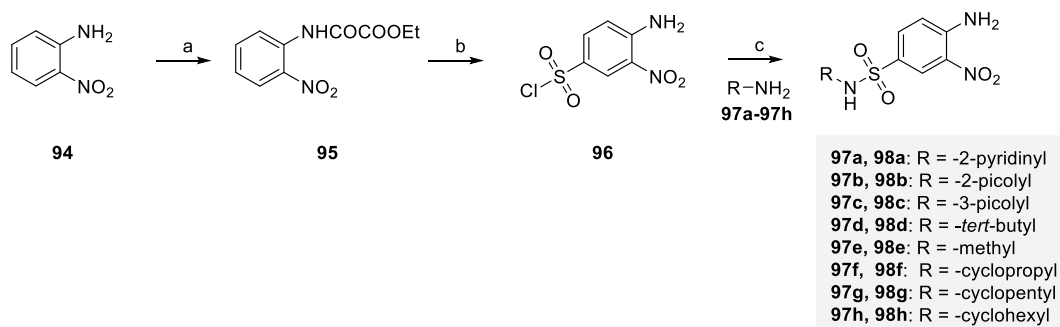
Reagents and conditions: (a) **76a**, NaHSO₃ (50% in mixture), TsOH, dry DMAc, 120 °C, 18 h (94%); (b) **74c**, K₂CO₃, dry DMF, 80 °C, 18 h (37%); (c) H₂, Pd/C, EtOH, 3 h (98 %).

4.2 Synthesis of benzimidazole-based ligands

This Section describes the synthetic procedures adopted for the preparation of benzimidazole-based ligands **15** – **32**. All the compounds were prepared following a synthetic protocol previously developed by us.¹¹⁹

Key intermediates in the preparation of benzimidazole-based ligands **15** – **32** are the N-substituted-4-amino-3-nitrobenzenesulfonamides **98a** – **h**, synthesized as illustrated in Scheme 4.11.

Scheme 4.11 Synthesis of N-substituted-4-amino-3-nitrobenzenesulfonamides **98a – h**

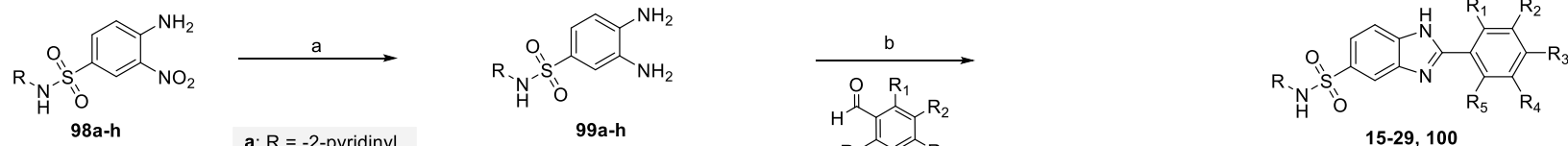


Reagents and conditions: (a) Ethyl chlorooxoacetate, Et₂O, r. t., 18 h (98%); (b) ClSO₃H, 80 °C, 3 h (99%); (c) (i) **97a**, pyridine, 0 °C to r. t. (40%); (ii) **97b – h**, THF, r. t., 18 h (60-85%);

Briefly, treatment with ethyl chlorooxoacetate of the 2-nitroaniline **94** in diethyl ether (Et₂O) furnished the protected amino compound **95** which reacted with the chlorosulfonic acid at 80 °C. Aqueous workup gave the unprotected sulfonyl chloride **96** which reacted with appropriate amines (**97a – h**) to afford the corresponding N-substituted-4-amino-3-nitrobenzenesulfonamides (**98a – h**). Preparation of *N*-aryl sulphonamide **98a** in 40% yield required the use of pyridine as a solvent at 80 °C. On the other hand, preparation of *N*-alkyl sulfonamides **98b – h** in good yields (60 – 85%) involved reaction between one equivalent of **96** and 4 equivalents of the appropriate ammine in THF at room temperature.

From nitro derivatives **98a – h**, zinc dust reduction in acetic acid or palladium-catalysed hydrogenation furnishing the corresponding 3,4-diaminobenzenesulfonamides **99a** and **99b – h**, respectively. Under oxidative conditions, the amino compounds were condensed with commercially available aldehydes **76a – h**, in dry DMF at 80 °C to afford the benzimidazole-based compounds **15 – 17**, **19 – 29** and **100**. Finally, deprotection under acidic conditions (DCM/TFA 1:1) of intermediate **100** furnished the primary sulfonamide **18** (Scheme 4.12).

Scheme 4.12 Synthesis of benzimidazole-based compounds **15 – 29**



a: R = -2-pyridinyl
b: R = -2-picolyl
c: R = -3-picolyl
d: R = -*tert*-butyl
e: R = -methyl
f: R = -cyclopropyl
g: R = -cyclopentyl
h: R = -cyclohexyl

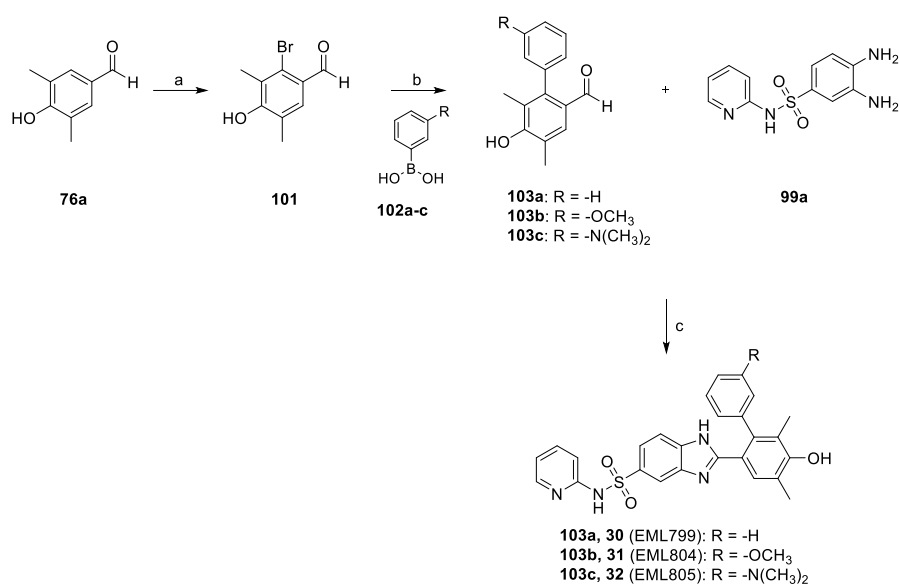
76a-h
a: R₁, R₅ = -H; R₂, R₄ = -CH₃; R₃ = -OH
b: R₁, R₂, R₄, R₅ = -H; R₃ = -OH
c: R₁, R₃, R₄, R₅ = -H; R₂ = -OH
d: R₁, R₂, R₄, R₅ = -H; R₃ = -Cl
e: R₂, R₄, R₅ = -H; R₁, R₃ = -OH
f: R₁, R₄, R₅ = -H; R₂, R₃ = -OH
g: R₂, R₄ = -H; R₁, R₅ = -CH₃; R₃ = -OH
h: R₁, R₄, R₅ = -H; R₂ = -CH₃; R₃ = -OH

15 (EML765): R = -2-pyridinyl; R₁, R₅ = -H; R₂, R₄ = -CH₃; R₃ = -OH
16 (EML803): R = -2-picolyl; R₁, R₅ = -H; R₂, R₄ = -CH₃; R₃ = -OH
17 (EML798): R = -3-picolyl; R₁, R₅ = -H; R₂, R₄ = -CH₃; R₃ = -OH
100: R = -*tert*-butyl; R₁, R₅ = -H; R₂, R₄ = -CH₃; R₃ = -OH
18: R = -H; R₁, R₅ = -H; R₂, R₄ = -CH₃; R₃ = -OH
19 (EML796): R = -methyl; R₁, R₅ = -H; R₂, R₄ = -CH₃; R₃ = -OH
20 (EML801): R = -cyclopropyl; R₁, R₅ = -H; R₂, R₄ = -CH₃; R₃ = -OH
21 (EML797): R = -cyclopentyl; R₁, R₅ = -H; R₂, R₄ = -CH₃; R₃ = -OH
22 (EML802): R = -cyclohexyl; R₁, R₅ = -H; R₂, R₄ = -CH₃; R₃ = -OH
23 (EML760): R₁, R₂, R₄, R₅ = -H; R₃ = -OH
24 (EML761): R₁, R₃, R₄, R₅ = -H; R₂ = -OH
25 (EML762): R₁, R₂, R₄, R₅ = -H; R₃ = -Cl
26 (EML763): R₂, R₄, R₅ = -H; R₁, R₃ = -OH
27 (EML764): R₁, R₄, R₅ = -H; R₂, R₃ = -OH
28 (EML766): R₂, R₄ = -H; R₁, R₅ = -CH₃; R₃ = -OH
29 (EML806): R₁, R₄, R₅ = -H; R₂ = -CH₃; R₃ = -OH

Reagents and conditions: (a) Zn dust, AcOH, 4 h (64%) or H₂, Pd/C, EtOH, 18 h (89 – 97%); (b) NaHSO₃, dry DMF, 80 °C, 18 h (54 – 85%); (c) DCM/TFA (1:1), r. t. 18 h (74%).

Preparation of compounds **30** – **32** required the preparation of not commercially available aldehydes **103a** – **c** as illustrated in Scheme 4.13. Briefly, aldehyde **76a** is selectively brominated at position 2 by means of N-bromosuccinimide (NBS). The brominated aldehyde **101** easily undergoes Suzuki-Miyaura cross-coupling with boronic acids (**102a** – **c**) affording the aldehydes **103a** – **c**. Following the synthetic procedures mentioned above, the benzimidazole-based ligands **30** – **32** were obtained in good yield (53 – 67%) using as starting material the 3,4-diaminobenzenesulfonamide **99a**.

Scheme 4.13 Synthesis of benzimidazole-based compounds **30** – **32**



Reagents and conditions: (a) NBS, H₂SO₄, 60 °C, 4 h (20%); (b) MW, TETRAKIS, K₂CO₃, EtOH, 80 °C, 30 min, (67 – 70%); (c) NaHSO₃, dry DMF, 80 °C, 18 h (53 – 67%).

4.3 Synthesis of BET PROTACs

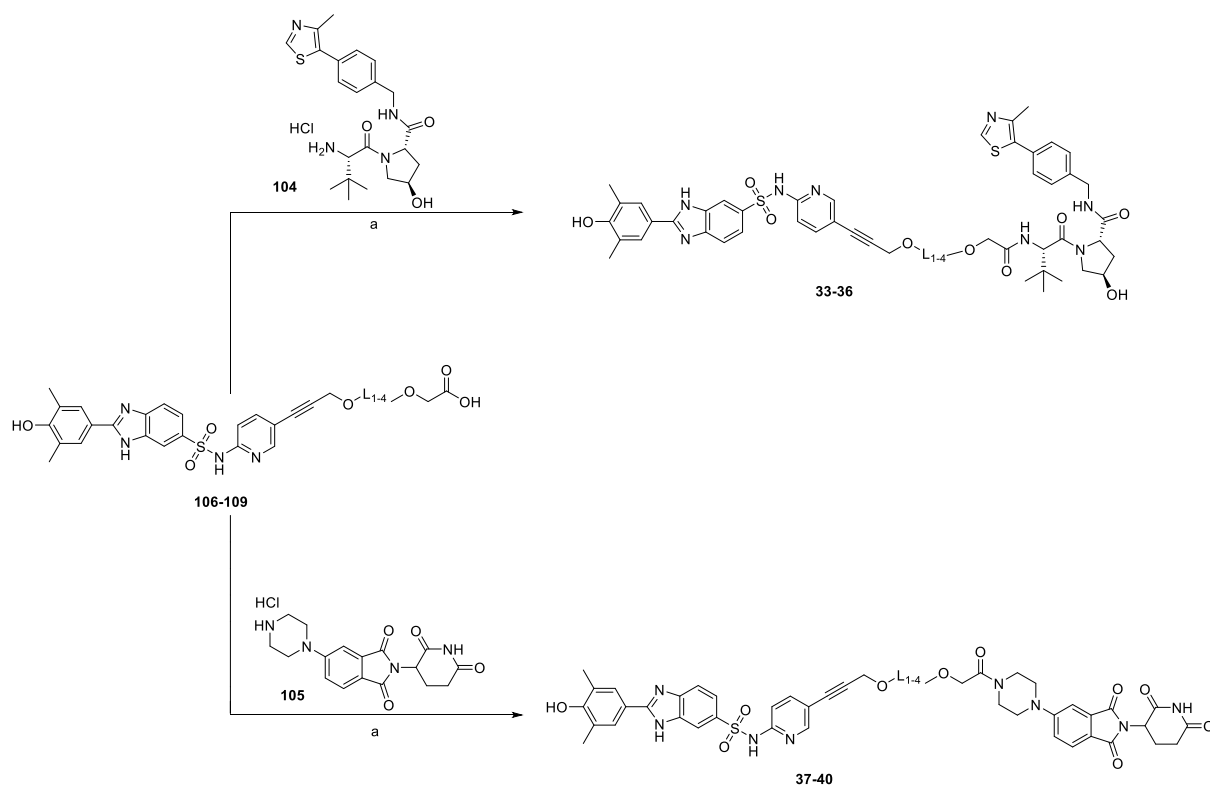
This Section describes the synthetic procedures adopted for the preparation BET PROTAC compounds **33** – **48**.

Final compounds were obtained via peptide coupling (Scheme 4.14 and Scheme 4.15) between the carboxylic function of proper linkers attached on BD1/BD2 scaffold and the primary amino group of VHL ligand (**104**) and CRBN ligand (**105**).

Compounds **33** – **40** were obtained using PyOXIM as coupling reagent, DIPEA in anhydrous DMF. On the other hand, COMU was used as coupling reagent for the synthesis of compounds **41** – **48**. As summarized in Table 4.2 and in Table 4.3, the yields are moderate.

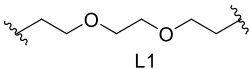
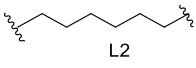
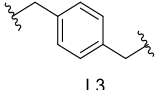
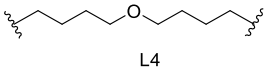
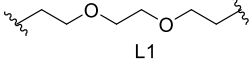
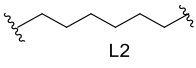
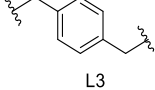
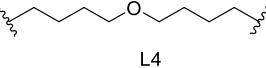
VHL ligand (**104**) and CRBN ligand (**105**) were prepared according to literature.^{101, 120} All the linkers and the functionalized BD1/BD2 ligands are prepared as described in the following Sections.

Scheme 4.14 Synthesis of BET PROTACs **33** – **40**

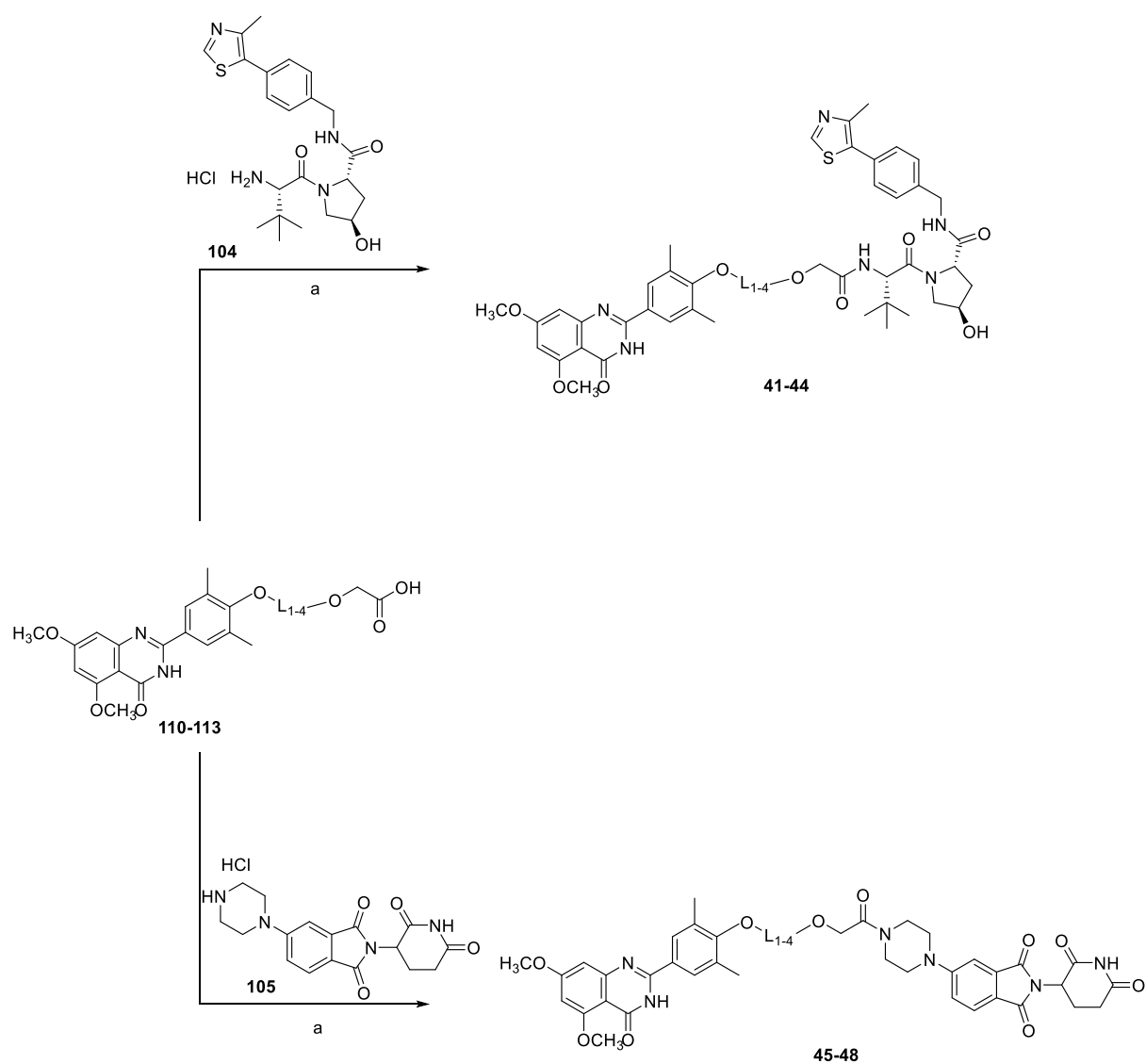


Reagents and conditions: (a) PyOXIM, DIPEA, dry DMF, r. t. 30 min – 1 h.

Table 4.2 Compounds **33-40**

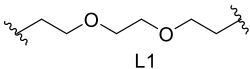
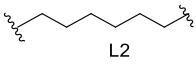
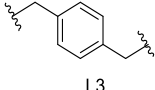
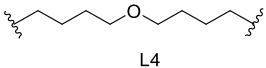
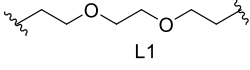
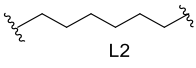
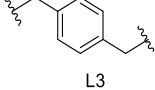
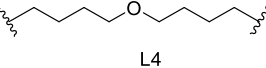
ENTRY LIGAND	ENTRY AMINE	LINKER (L1-L4)	FINAL COMPOUND	YIELD
106	104	 L1	33	50%
107	104	 L2	34	32%
108	104	 L3	35	42%
109	104	 L4	36	32%
106	105	 L1	37	28%
107	105	 L2	38	27%
108	105	 L3	39	39%
109	105	 L4	40	38%

Scheme 4.15 Synthesis of BET PROTACs **41 – 48**



Reagents and conditions: (a) COMU, DIPEA, dry DMF, r.t., 30 min – 1 h.

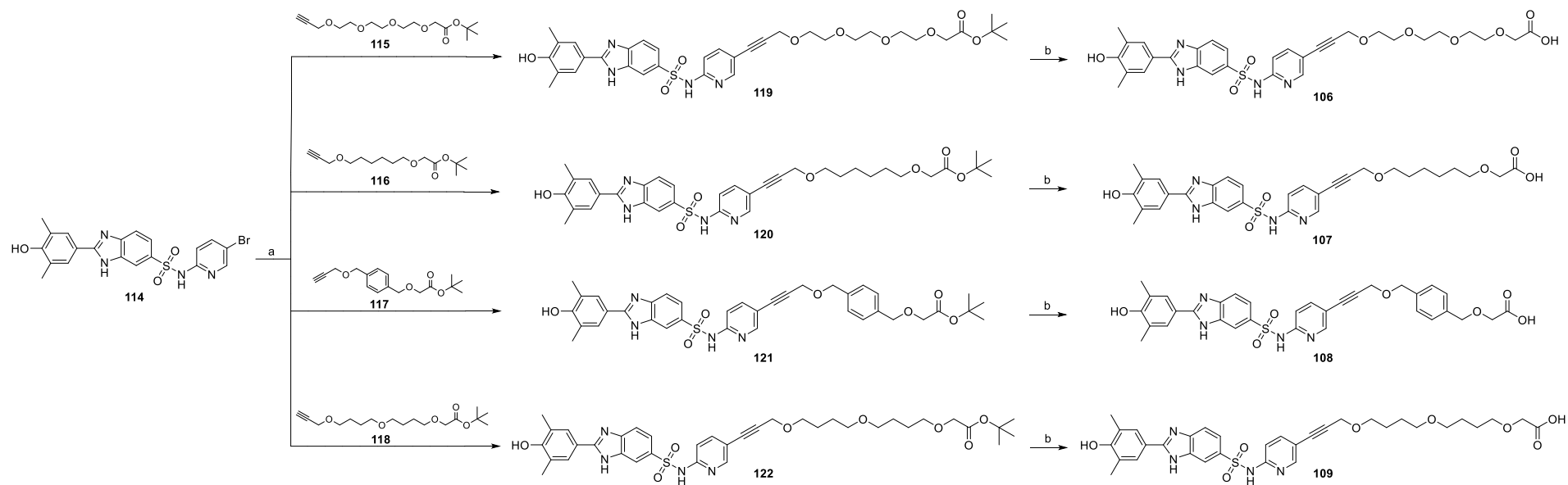
Table 4.3 Compounds **41-48**

ENTRY LIGAND	ENTRY AMINE	LINKER (L1-L4)	FINAL COMPOUND	YIELD
110	104	 L1	41	46%
111	104	 L2	42	32%
112	104	 L3	43	36%
113	104	 L4	44	37%
110	105	 L1	45	37%
111	105	 L2	46	45%
112	105	 L3	47	27%
113	105	 L4	48	31%

4.3.1 Synthesis of PROTAC compounds 33 – 40

The synthesis of PROTACs **33 – 40** required the preparation of intermediates **106 – 109**, obtained as illustrated in Scheme 4.16. These compounds containing a triple bond for proper linker connection. Under Sonogashira coupling conditions, the bromine analogue **114** reacted with the alkynyl linkers **115 – 118** opportune prepared, affording the intermediates **119 – 122**. Straightforward hydrolysis of *tert*-butyl ester with trifluoroacetic acid in DCM yielded compounds **106 – 109**.

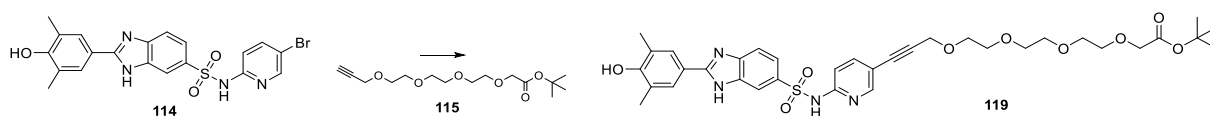
Scheme 4.16 Synthesis of intermediates 106 – 109



Reagents and conditions: (a) $\text{P}[\text{P}(\text{tBu}_3)]_2$, $\text{P}(\text{tBu}_3)$, K_2CO_3 , CuI , $100\text{ }^\circ\text{C}$, 12 h (11 – 20%); (b) DCM/TFA 9:1, r. t., 30 min (95 – 96%).

The Sonogashira reaction conditions required an optimization work. Indeed, considering that this reaction is high context-dependent and could be complex on pyridine, especially using a PEG linker as substrate, different conditions were investigated using the bromine intermediate **114** and the alkyne linker **115** as model substrate (Table 4.4).

Table 4.4 Different condition of Sonogashira tested. All reactions are set up on 10 mg and carried out at 100 °C. The reactions are monitored by LC-MS.



#	[Pd]	LIGAND	[Cu]	BASE	SOLVENT	CONVERSION
a	Pd(PPh ₃) ₄	-	CuI	K ₂ CO ₃	dry DMF	10 %
b	Pd(PPh ₃) ₄	-	CuI	K ₂ CO ₃	dry ACN	No Product
c	Pd(PPh ₃) ₄	-	CuI	DIPEA	dry DMF	No Product
d	Pd(PPh ₃) ₄	-	CuI	TEA	dry ACN	No Product
e	Pd(OAc) ₂	P(tBu) ₃	CuI	K ₂ CO ₃	dry DMF	No Product
f	Pd[P(tBu) ₃] ₂	P(tBu) ₃	CuI	K ₂ CO ₃	dry ACN	30 %
g	Pd[P(tBu) ₃] ₂	P(tBu) ₃	CuI	K ₂ CO ₃	dry DMF	100%

All the conditions differ for the palladium complex, the base and the solvent whereas in all reactions copper iodide is used (Table 4.4).

Firstly, the tetrakis(triphenylphosphine)palladium(0) complex was investigated (**a – d**), using different bases (K₂CO₃, TEA and DIPEA) and solvents (dry DMF and dry ACN). Unfortunately, trace product was observed only using K₂CO₃ as base and dry DMF as solvent (**a**). Maintaining the base (K₂CO₃), we decided to investigate different palladium complex: the bis(tri-*tert*-butylphosphine)palladium(0) and the palladium(II) acetate.

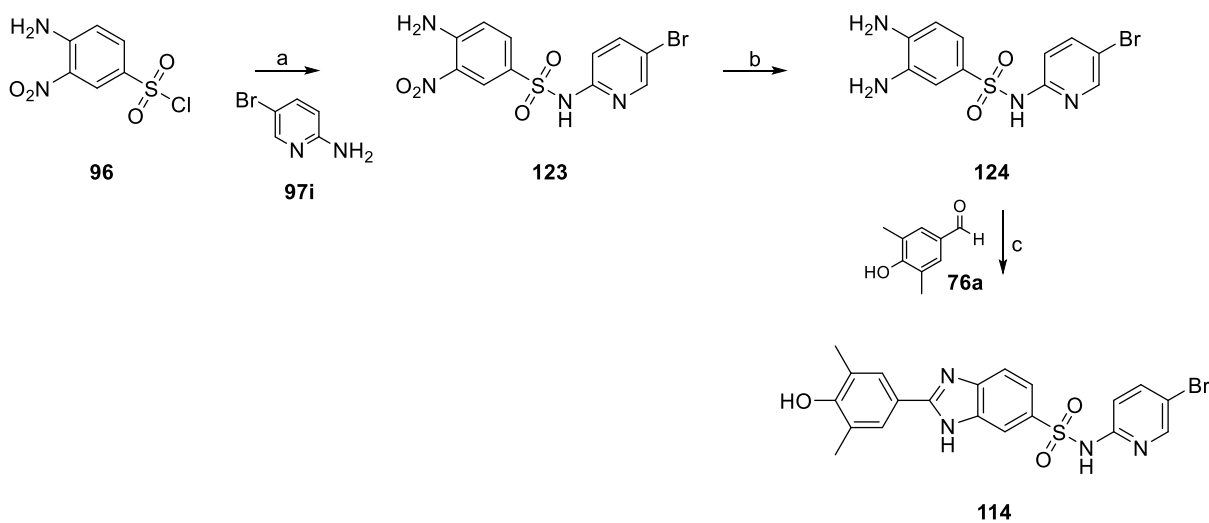
The main difference is the palladium form: palladium(II) acetate required the generation *in situ* of the reactive form (Pd0) using tri-*tert*-butylphosphine (**e**) whereas the bis(tri-*tert*-butylphosphine)palladium(0) complex has the palladium in the reactive form (Pd0) (**f-g**). Nevertheless, the bis(tri-*tert*-butylphosphine)palladium(0) is more unstable and can easily oxidize in palladium(II). To overcome this issue, tri-*tert*-butylphosphine was added (**f-g**).

Using palladium(II) acetate, we recovered only starting material (**e**). The use of bis(tri-*tert*-butylphosphine)palladium(0) gave good results. LC-MS analysis reveal the formation of 30% of product and the 70% of des-brominated starting material (**f**) using dry ACN as solvent. Surprisingly, a quantitative conversion of starting material was observed using dry DMF as solvent (**g**). The good results obtained prompted us to apply these conditions to all the alkynyl linkers **115** – **118** (Scheme 4.16). Unfortunately, despite the quantitative conversion of the starting material, we didn't recover a quantitative amount of products (**119** – **122**). As matter of fact, the insoluble palladium by-products and the low solubility of compounds complicated purification and negatively impacted the yield (11 – 20%).

4.3.1.2 Synthesis of bromine derivative **114**

Preparation of bromine analogue of the benzimidazole-based ligand was carried out according to Scheme 4.17, exploiting the same synthetic strategies previously described (Section 4.2).

Scheme 4.17 Synthesis of bromine analogue **114**



Reagents and conditions: (a) 2-amino-5-bromopyridine **97i**, dry pyridine, r. t., 18 h (23%); (b) Zn dust, acetic acid, r. t., 18 h (98%); (c) **76a**, NaHSO₃, dry DMF, 100 °C, 18 h (56%).

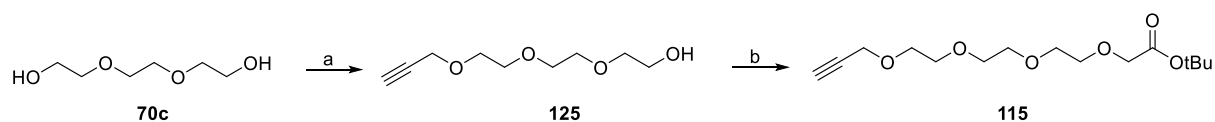
Briefly, the sulphonyl chloride **96**, synthesized as previously described (Scheme 4.11), reacted with the commercially available 2-amino-5-bromopyridine **97i** affording the corresponding N-substituted-4-amino-3-nitrobenzenesulfonamide (**123**). According to the synthesis of **98a**, the reaction featured a low yield (23%) due to solubility problems which negatively affected purification. Any attempt to optimize this reaction changing solvents (pyridine or N, N-dimethylacetamide), bases (pyridine and triethylamine) and temperatures (0 °C or room temperature) were unsuccessful. The reduction of the nitro group with zinc dust in acetic acid furnished the corresponding amino group (**124**) which reacts with the commercially available 4-hydroxy-3,5-dimethylbenzaldehyde **76a**, under oxidative condition, affording the bromine analogue **114**.

4.3.1.2 Synthesis of alkynyl linkers **115** – **118**

The four linkers chosen (L1 – L4) were properly functionalized with the alkynyl group, suitable for the subsequent Sonogashira reaction, and with a carboxylic function, required for the final coupling reaction.

The triethylene glycol **70c**, commercially available, reacted with the propargyl bromide in presence of potassium *tert*-butoxide (tBuOK) to give the alkynyl linker **125**. The latter reacted with *tert*-butyl 2-bromoacetate in presence of sodium hydride (NaH) to afford the proper functionalized PEG (L1) linker **115** (Scheme 4.18).

Scheme 4.18 Synthesis of alkynyl linker **115**

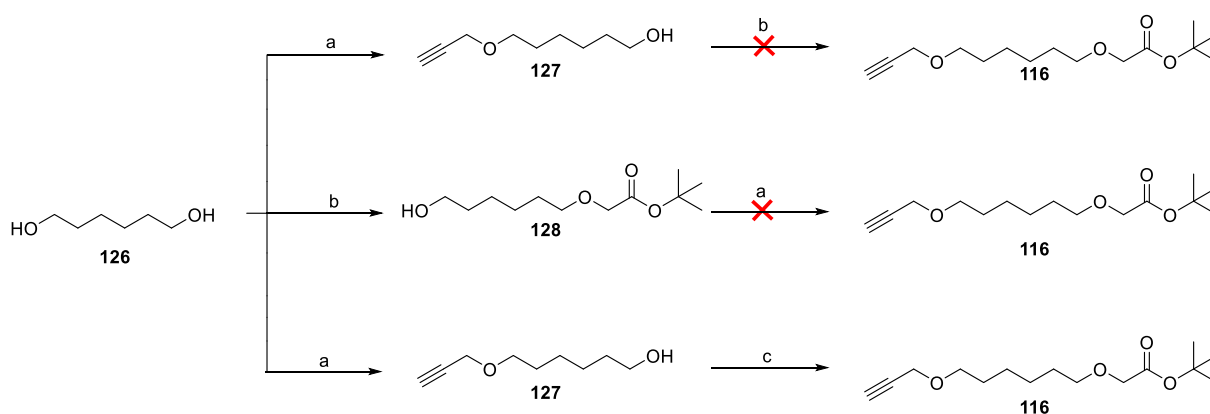


Reagents and conditions: (a) propargyl bromide, tBuOK, dry THF, r. t., 18 h (80%); (b) *tert*-butyl 2-bromoacetate, NaH (60% mineral oil), dry THF, r. t., 18 h (50%).

The same synthetic conditions were used to obtain the functionalized aliphatic L2 linker (Scheme 4.19). The commercially available 1,6-hexandiol (**126**) react with propargyl bromide in presence of sodium hydride affording the alkynyl aliphatic linker **127** in good yield (76%). Unfortunately, the subsequent reaction with *tert*-butyl 2-bromoacetate on the alkynyl aliphatic linker failed, both using anhydrous DMF and anhydrous THF as solvents. The same negative result was obtained treating, in the first instance, the 1,6-hexandiol (**126**) with *tert*-butyl 2-bromoacetate, affording the intermediate **128**, which unsuccessfully reacted with propargyl bromide. In all the conditions, we recovered starting materials and byproducts, probably due to rearrangement at alkynyl position.

Finally, using *tert*-butyl diazoacetate in a rhodium-catalyzed reaction, we were able to obtain the desired product **116**. This reaction involved the formation of a metal–carbene complex intermediate which, probably, proceeds better on this linker.

Scheme 4.19 Synthesis of alkynyl linker **116**

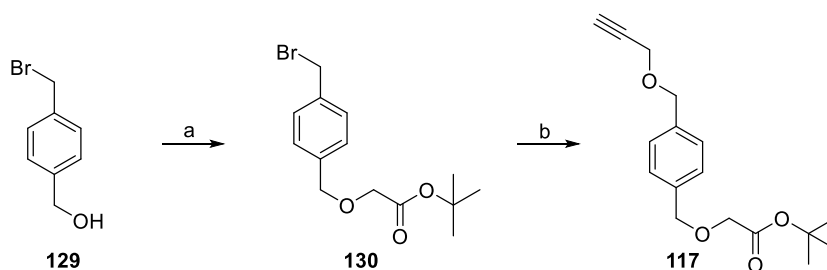


Reagents and conditions: (a) propargyl bromide, NaH, dry DMF, r. t., 18 h (76%); (b) *tert*-butyl 2-bromoacetate, NaH (60% mineral oil), dry DMF or dry THF, r. t., 18 h (40%); (c) *tert*-butyl diazoacetate, rhodium acetate, DCM, r. t., 18 h (66%).

The synthesis of functionalized linker L3 was carried out treating the 4-bromomethylbenzyl alcohol **129**, commercially available, with *tert*-butyl diazoacetate in presence of rhodium-acetate affording the intermediate **130** (Scheme 4.20).

Under nucleophilic substitution condition, the latter reacted with propargyl alcohol in presence of sodium hydride affording the proper functionalized alkynyl linker **117**.

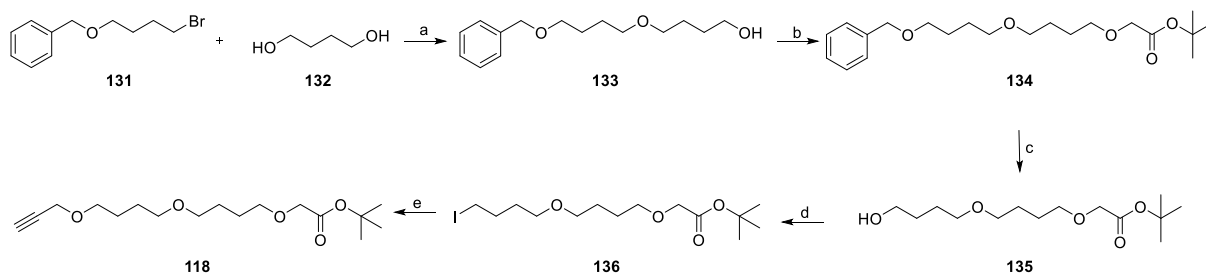
Scheme 4.20 Synthesis of alkynyl linker **117**



Reagents and conditions: (a) *tert*-Butyl diazoacetate, rhodium acetate, DCM, r. t., 18 h (67%); (b) propargyl alcohol, NaH (60% mineral oil), dry DMF, r. t., 18 h (60%).

Finally, the alkynyl L4 linker is prepared as shown in Scheme 4.21. Briefly, the benzyl 4-bromobutyl ether (**131**) reacted with the 1,4-butanediol (**132**) in presence of sodium hydride, furnishing the intermediate **133** in good yield (84%). The resulting intermediate **133** reacted with *tert*-butyl diazoacetate, in presence of rhodium acetate, forming the intermediate **134** which undergoes a palladium-catalysed hydrogenation affording the O-debenzylated compound **135**. Avoiding the issue occurred in the synthesis of linker **116**, a different strategy to insert the alkynyl group was used. The primary alcoholic function of **135** was converted into iodide in presence of triphenylphosphine, iodine and catalytic amount of imidazole by Appel reaction, affording the intermediate **136**. The latter reacted with propargyl alcohol in presence of sodium hydride affording the alkynyl linker **118**.

Scheme 4.21 Synthesis of alkynyl linker 118

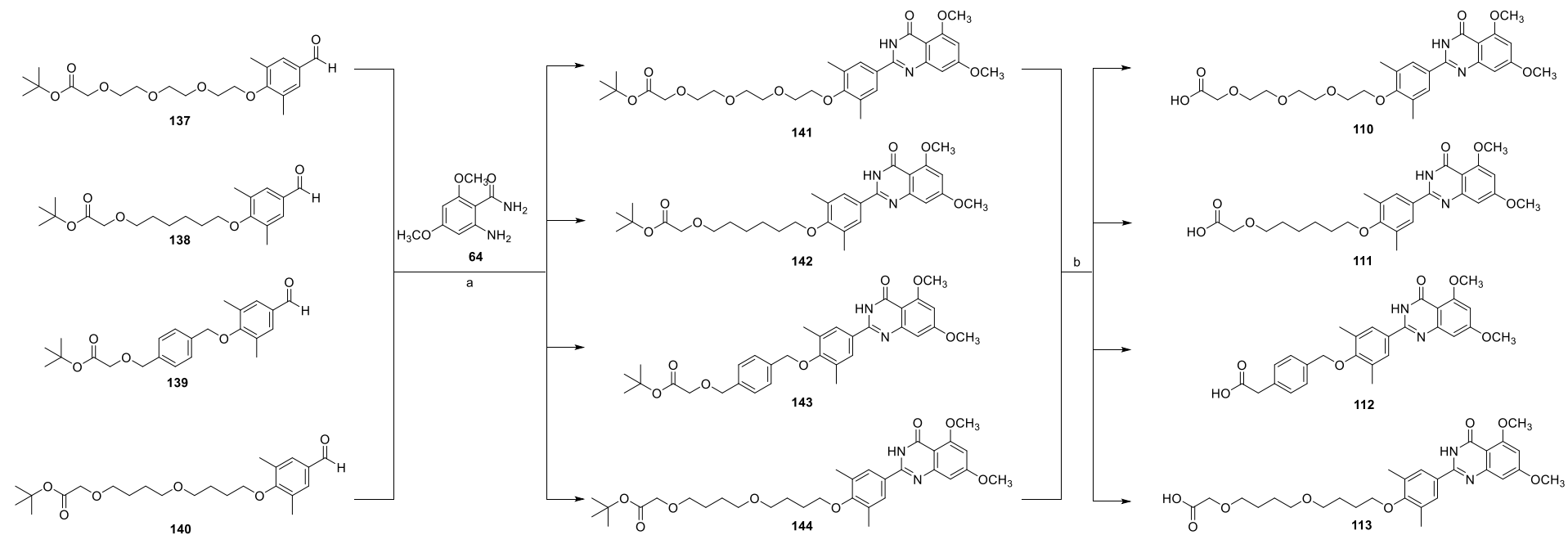


Reagents and conditions: (a) NaH (60% mineral oil), dry DMF, r. t., 18 h (84%); (b) *tert*-butyl diazoacetate, rhodium acetate, DCM, r. t., 18 h (75%); (c) H₂, Pd/C 10%, methanol, r. t., 18 h (96%) (d) I₂, Ph₃P, imidazole, dry DCM, 0 °C to r. t., 3 h (56%); (e) propargyl alcohol, NaH (60% mineral oil), dry DMF, r. t., 18 h (30%).

4.3.2 Synthesis of PROTAC compounds 41 – 48

The synthesis of PROTAC compounds **41** – **48** involved the preparation of intermediates **110** – **113** as depicted in the Scheme 4.22.

Scheme 4.22 Synthesis of intermediates **110** – **113**



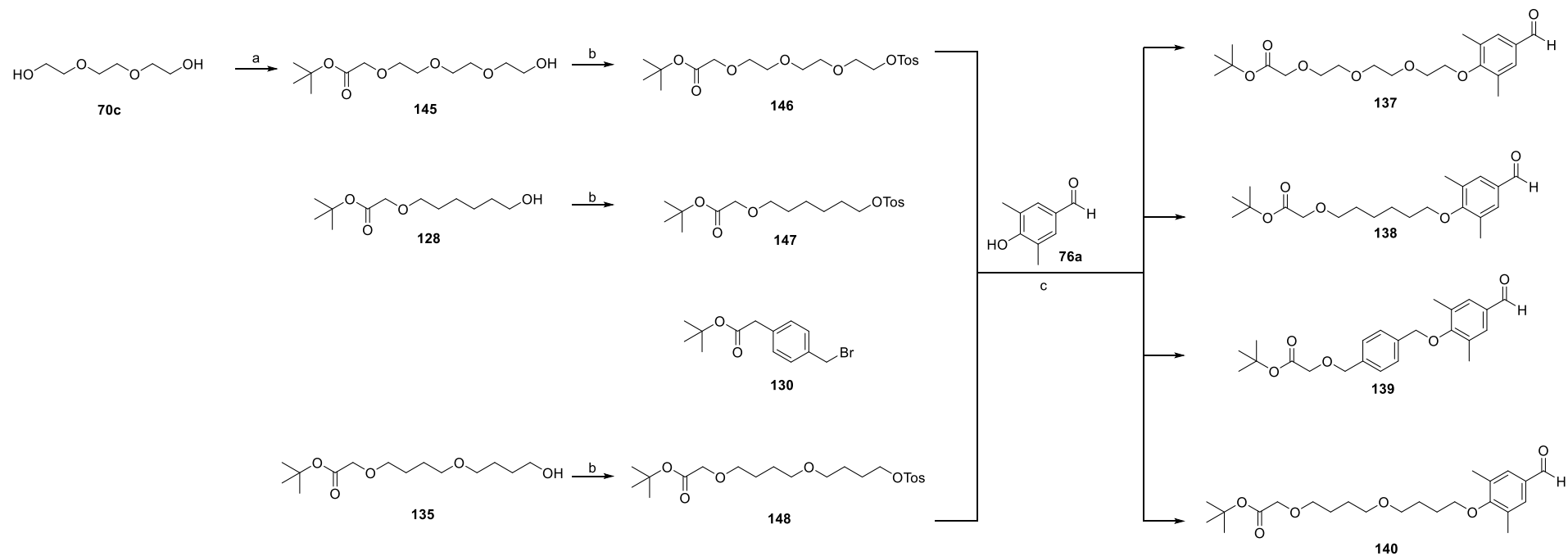
Reagents and conditions: (a) NaHSO₃, dry DMF, 100 °C, 18 h (68 – 86%); (b) DCM/TFA 9:1, r. t. 1 h (96 – 97%).

According to the synthetic strategies previously optimized (Section 4.1), we decided to build the quinazolinone scaffold on the proper linkers featuring a carboxylic function for the final coupling reaction. The opportune prepared aldehydes (**137** – **140**) reacted with 2-amino-4,6-dimethoxybenzamide **64** by cyclocondensation-dehydrogenation in presence of NaHSO₃ to afford the quinazolinone-based ligands (**141** – **144**). Unlike the synthesis of intermediates **65**, **66a** – **f** and **67a,b** (Scheme 4.3), we did not use a catalytic amount of *p*-toluenesulfonic acid to avoid acid conditions which could interfere with the acid-labile *tert*-butyl ester. Moreover, anhydrous DMF instead of anhydrous DMAc was used and, consequently, a lower temperature (100 °C). Finally, hydrolysis in acidic conditions furnished the carboxylic derivatives **110** – **113**.

The aldehydes **137** – **140** were prepared as described in Scheme 4.23.

The first step required the activation of the four linkers (L1 – L4) with a proper leaving group (-OTos or -Br). The triethylene glycol **70c**, commercially available, reacted with *tert*-butyl 2-bromoacetate in presence of sodium hydride to give the intermediate **145** in good yield (60%). Protected linkers **128** and **135**, synthesized as previously reported, and **145** were activated in the subsequent nucleophilic substitutions using tosyl chloride and triethylamine in anhydrous DCM affording the tosylated intermediates **146**, **147** and **149**. The tosylated intermediates **146**, **147** and **149** and the bromine intermediate **148**, synthesized as previously described (Scheme 4.19), easily reacted with the 4-hydroxy-3,5-dimethylbenzaldehyde **76a**, commercially available, under nucleophilic substitution conditions, affording the corresponding aldehyde intermediates **137** – **140** in good yield (70 – 96%).

Scheme 4.23 Synthesis of intermediates **137** – **140**



Reagents and conditions: (a) *tert*-butyl 2-bromoacetate, NaH (60% mineral oil), dry DMF, r. t., 18 h (60%); (b) TsCl, TEA, dry DCM, r. t., 18 h (60 – 64%); (c) K₂CO₃, dry DMF, 80 °C, 18 h (70 – 96%).

CHAPTER V

CONCLUSIONS

This PhD project reported the design, synthesis and biological evaluation of new ligands for the BET family of bromodomains, with attention on selectivity between BET protein isoforms and/or bromodomain modules. Selective ligands could offer valuable chemical probes for these epigenetic reader proteins and putative therapeutic agents. To this aim, three different approaches were applied.

Bisubstrate approach have been exploited to design compounds potentially able to bind the first and the second bromodomain of BET proteins in order to obtain structural information. The compounds were designed connecting a BD1 (**Cl-BzT-7**) and a BD2 (**RVX-208**) / selective ligand with a proper linker. A small set of compounds have been designed and synthesized, changing the length and the nature of linkers. DSF assay and sedimentation velocity assay showed that compound **EML896** is able to partially engage both BD1 and BD2 domain. These promising results are a valuable starting point for the development of new bivalent chemical probes.

To develop selective ligands for the first bromodomain of BETs, diazobenzene-based compounds were selected as lead compounds. In order to improve metabolic stability and pharmacokinetic properties, the diazobenzene core was rigidized into a benzimidazole scaffold and a small library of compounds was designed and synthesized. DSF, ITC and TR-FRET assays allowed the identification of compound **EML765** as potent BET ligand (K_D of 70 nM) with a good selectivity for the first bromodomain of BETs (170-fold for BD1 of BRD2). Taken together, the data endorse compound **EML765** as promising BD1 selective ligand. Metabolic stability and pharmacokinetic properties are currently being assessed.

Finally, BET PROTACs with BD1 and BD2 selective ligands were designed. **EML765** and **RVX-208** were chosen as BD1 and BD2 warhead, respectively, and connected with different type of linkers to VHL-based and CRBN-based E3 ligase ligands. Compounds were synthesized and their activity was evaluated in cellular assays. Unfortunately, compounds are not able to induce protein degradation. These results need to be considered in the perspective of the

complexity of protein-induced degradation mechanism and of the multifaceted aspects involved in the PROTACs design.

CHAPTER VI

MATERIALS AND METHODS

7.1 General information

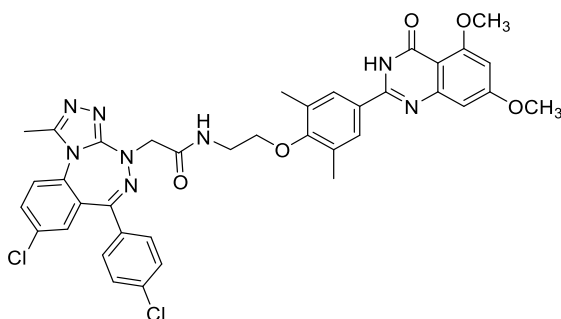
All chemicals were purchased from Sigma-Aldrich Srl (Milan, Italy) or from Fluorochem Ltd. (Hadfield, UK) and were of the highest purity. All solvents were of reagent grade and, when necessary, were purified and dried by standard methods. All reactions requiring anhydrous conditions were conducted under a positive atmosphere of nitrogen in oven-dried glassware. Standard syringe techniques were used for anhydrous addition of liquids. Reactions were routinely monitored by thin-layer chromatography (TLC) performed on aluminum-backed silica gel plates (Merck DC, Alufolien Kieselgel 60 F254) with spots visualized by UV light ($\lambda = 254, 365$ nm) or using a KMnO_4 alkaline solution. Solvents were removed using a rotary evaporator operating at a reduced pressure of ~ 10 Torr. Organic solutions were dried over anhydrous Na_2SO_4 . Chromatographic purification was done on an automated flash chromatography system (Isolera Dalton 2000, Biotage) using cartridges packed with KP-SIL, 60 Å (40–63 μm particle size). All microwave-assisted reactions were conducted in a CEM Discover SP microwave synthesizer equipped with vertically focused IR temperature sensor. Analytical high-performance liquid chromatography (HPLC) was performed on a Shimadzu SPD 20A UV/vis detector ($\lambda = 220$ and 254 nm) using C-18 column Phenomenex Synergi Fusion-RP 80A (75 \times 4.60 mm²; 4 μm) at 25 °C using mobile phases A (water + 0.1% TFA) and B (acetonitrile (ACN) + 0.1% TFA) at a flow rate of 1 mL/min. Preparative HPLC was performed using a Shimadzu Prominence LC20AP with the UV detector set to 220 and 254 nm. Samples were injected onto a Phenomenex Synergi Fusion-RP 80A (150 \times 21 mm²; 4 μm) C-18 column at room temperature. Mobile phases of A (water + 0.1% TFA) and B (ACN + 0.1% TFA) were used with a flow rate of 20 mL/min.

^1H spectra were recorded at 400 MHz on a Bruker Ascend 400 spectrometer, while ^{13}C NMR spectra were obtained by distortionless enhancement by polarization transfer quaternary

spectroscopy on the same spectrometer. Chemical shifts are reported in δ (ppm) relative to the internal reference tetramethylsilane. Due to the existence of tautomers, some ^1H and ^{13}C NMR signals could not be detected for some of the prepared benzimidazoles so only the distinct signals are reported. Low-resolution mass spectra were recorded on a Finnigan LCQ DECA ThermoQuest mass spectrometer in electrospray positive and negative ionization modes (ESI-MS). VHL ligand **104** and CRBN ligand **105** were prepared in according with the reported procedure and all the ^1H -NMR and ^{13}C -NMR spectra are consistent with those already reported to literature.^{90, 101} Only the biological experiments done by myself are reported.

7.2 Synthetic procedures

Synthesis of 2-(8-chloro-6-(4-chlorophenyl)-1-methyl-4H-benzo[e][1,2,4]triazolo[3,4-c][1,2,4]triazepin-4-yl)-N-(2-(4-(5,7-dimethoxy-4-oxo-3,4-dihydroquinazolin-2-yl)-2,6-dimethylphenoxy)ethyl)acetamide (1, EML807)



To a stirred solution of intermediate **49** (22 mg, 0.05 mmol) and amine derivative **50** (22 mg, 0.06 mmol) in 1 mL of dry DMF, EDC hydrochloride (17 mg, 0.085 mmol), HOBt (13 mg, 0.085 mmol) and 4-methylmorpholine (0.024 mL, 0.22 mmol) were added. The reaction was stirred at room temperature for 18 h. Then, water (15 mL) was added the resulting mixture was extracted with EtOAc (3 x 10 mL). The combined organic phases were washed with saturated solution of NaHCO_3 (3 x 10 mL), brine (15 mL), dried over anhydrous Na_2SO_4 , filtered and

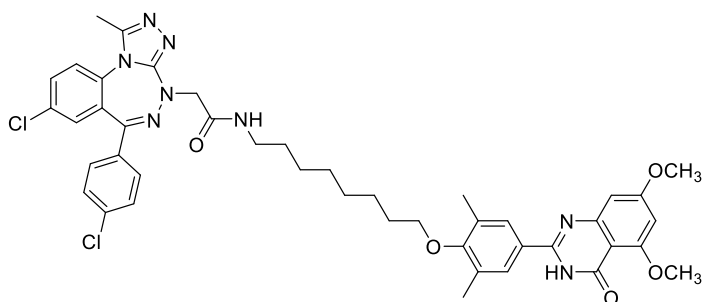
evaporated under reduced pressure. The crude was purified by silica gel chromatography (DCM-MeOH 97:3 to 90:10) yielding the title compound as white solid (25 mg, 66%).

^1H NMR (400 MHz, CDCl_3) δ 9.65 (s, 1H), 7.65 (s, 2H), 7.57 (dd, $J = 8.6, 2.4$ Hz, 1H), 7.48 (d, $J = 8.6$ Hz, 2H), 7.35 (d, $J = 8.6$ Hz, 2H), 7.29 (d, $J = 8.6$ Hz, 1H), 7.20 (d, $J = 2.4$ Hz, 1H), 7.21 – 7.15 (m, 1H), 6.81 (d, $J = 2.3$ Hz, 1H), 6.45 (d, $J = 2.3$ Hz, 1H), 4.64 – 4.57 (m, 2H), 3.96 (s, 3H), 3.92 (s, 3H), 3.90 – 3.85 (m, 2H), 3.73 – 3.64 (m, 2H), 2.60 (s, 3H), 2.18 (s, 6H).

^{13}C NMR (101 MHz, CDCl_3) δ 168.41, 165.16, 161.43, 160.76, 160.61, 159.32, 158.38, 153.82, 152.12, 148.47, 137.35, 133.65, 133.38, 133.07, 132.28, 131.61, 131.22, 130.44, 129.56, 128.97, 127.96, 127.71, 123.95, 101.39, 98.26, 70.62, 57.61, 56.40, 55.74, 39.72, 16.43, 12.66.

MS (ESI) m/z : 753 ($\text{M}+\text{H}$) $^+$

Synthesis of 2-(8-chloro-6-(4-chlorophenyl)-1-methyl-4H-benzo[e][1,2,4]triazolo[3,4-c][1,2,4]triazepin-4-yl)-N-(8-(4-(5,7-dimethoxy-4-oxo-3,4-dihydroquinazolin-2-yl)-2,6-dimethylphenoxy)octyl)acetamide (2, EML901)

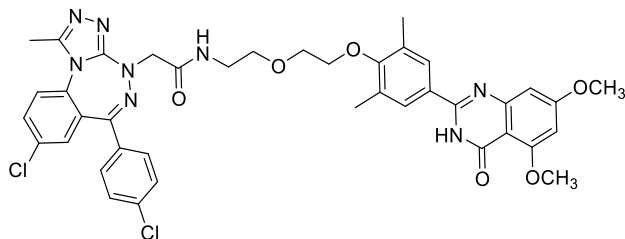


Compound **2** (EML901) was obtained as a light yellow solid (35 mg, 60%) from derivative **49** (28 mg, 0.07 mmol) and **51a** (35 mg, 0.077 mmol) according to the procedure described for **1**.

^1H NMR (400 MHz, CDCl_3) δ 9.40 (s, 1H), 7.68 (s, 2H), 7.64 (dd, $J = 8.7, 2.4$ Hz, 1H), 7.49 (d, $J = 8.7$ Hz, 2H), 7.38 (d, $J = 8.7$ Hz, 2H), 7.32 (d, $J = 8.7$ Hz, 1H), 7.27 (d, $J = 2.4$ Hz, 1H), 6.82 (d, $J = 2.3$ Hz, 1H), 6.54 (t, $J = 5.8$ Hz, 1H), 6.45 (d, $J = 2.3$ Hz, 1H), 4.54 – 4.49 (m, 2H), 3.97 (s, 3H), 3.93 (s, 3H), 3.78 (t, $J = 6.5$ Hz, 2H), 3.37 – 3.17 (m, 2H), 2.60 (s, 3H), 2.35 (s, 6H), 1.85 – 1.72 (m, 4H), 1.51 – 1.35 (m, 8H). ^{13}C NMR (101 MHz, CDCl_3) δ 167.94, 165.14,

161.43, 160.53, 159.39, 153.90, 152.26, 148.38, 137.32, 133.70, 133.33, 133.20, 132.31, 132.11, 131.10, 130.46, 129.64, 128.98, 127.46, 124.06, 101.39, 98.18, 72.49, 57.65, 56.39, 55.73, 39.26, 30.35, 29.71, 29.50, 29.40, 29.20, 26.76, 26.05, 16.54, 12.68. MS (ESI) m/z : 837 (M+H)⁺.

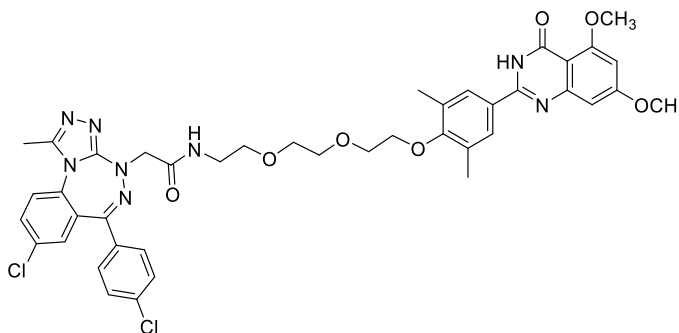
Synthesis of 2-(8-chloro-6-(4-chlorophenyl)-1-methyl-4H-benzo[e][1,2,4]triazolo[3,4-c][1,2,4]triazepin-4-yl)-N-(2-(2-(4-(5,7-dimethoxy-4-oxo-3,4-dihydroquinazolin-2-yl)-2,6-dimethylphenoxy)ethoxy)ethyl)acetamide (3, EML896)



Compound **3** (EML896) was obtained as a white solid (47 mg, 60%) from derivative **49** (40 mg, 0.1 mmol) and **51b** (46 mg, 0.11 mmol) according to the procedure described for **1**.

¹H NMR (400 MHz, CDCl₃) δ 9.62 (s, 1H), 7.68 (s, 2H), 7.57 (dd, J = 8.7, 2.3 Hz, 1H), 7.47 (d, J = 8.7 Hz, 2H), 7.35 (d, J = 8.7 Hz, 2H), 7.28 (d, J = 5.0 Hz, 1H), 6.82 (d, J = 2.3 Hz, 1H), 6.80 (d, J = 6.2 Hz, 1H), 6.46 (d, J = 2.3 Hz, 1H), 4.60 – 4.50 (m, 2H), 3.97 (s, 3H), 3.93 (s, 3H), 3.89 – 3.85 (m, 2H), 3.74 – 3.67 (m, 2H), 3.61 (t, J = 5.1 Hz, 2H), 2.57 (s, 3H), 2.30 (s, 6H). ¹³C NMR (101 MHz, CDCl₃) δ 168.13, 165.15, 161.44, 160.57, 160.49, 159.28, 158.81, 153.86, 152.20, 148.43, 137.24, 133.78, 133.22, 133.14, 132.26, 131.93, 131.19, 130.43, 129.57, 128.93, 127.83, 127.62, 124.00, 105.02, 101.40, 98.22, 71.42, 70.26, 69.91, 57.55, 56.39, 55.73, 39.31, 16.47, 12.66. MS (ESI) m/z : 797 (M+H)⁺.

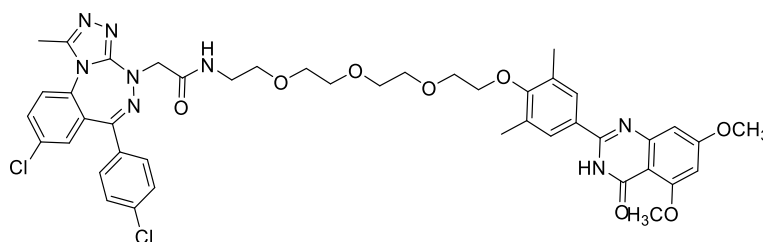
Synthesis of 2-(8-chloro-6-(4-chlorophenyl)-1-methyl-4H-benzo[e][1,2,4]triazolo[3,4-c][1,2,4]triazepin-4-yl)-N-(2-(2-(2-(4-(5,7-dimethoxy-4-oxo-3,4-dihydroquinazolin-2-yl)-2,6-dimethylphenoxy)ethoxy)ethoxy)ethyl)acetamide (4, EML730)



Compound **4** (EML730) was obtained as a white solid (45 mg, 54%) from derivative **49** (40 mg, 0.1 mmol) and **51c** (50 mg, 0.11 mmol) according to the procedure described for **1**.

^1H NMR (400 MHz, CDCl_3) δ 9.74 (s, 1H), 7.67 (s, 2H), 7.61 (d, $J = 6.8$ Hz, 1H), 7.46 (d, $J = 8.2$ Hz, 2H), 7.37 (d, $J = 8.2$ Hz, 2H), 7.28 (m, 1H), 7.25 – 7.25 (m, 1H), 6.83 (s, 1H), 6.76 (s, 1H), 6.45 (d, $J = 1.7$ Hz, 1H), 4.70 – 4.37 (m, 2H), 3.97 (s, 3H), 3.93 (s, 3H), 3.82 – 3.76 (m, 2H), 3.67 – 3.43 (m, 10H), 2.61 (s, 3H), 2.36 (s, 6H). ^{13}C NMR (101 MHz, CDCl_3) δ 167.97, 165.10, 161.43, 160.28, 137.15, 133.93, 133.20, 132.23, 131.99, 131.25, 130.49, 129.65, 128.92, 127.77, 124.06, 101.33, 98.19, 77.34, 77.02, 76.70, 71.63, 70.70, 70.42, 70.28, 69.83, 57.39, 57.39, 56.41, 39.15, 16.52, 12.73. MS (ESI) m/z : 841 (M+H) $^+$.

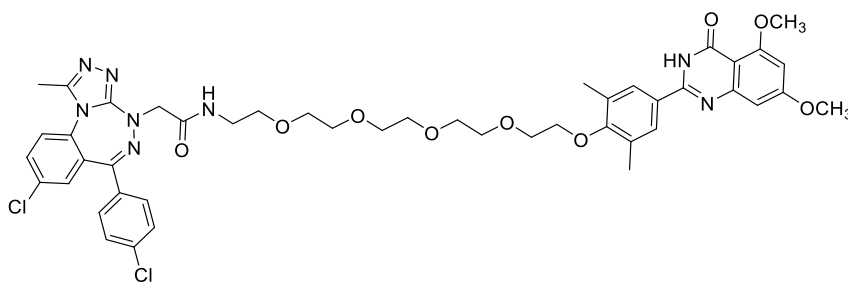
Synthesis of 2-(8-chloro-6-(4-chlorophenyl)-1-methyl-4H-benzo[e][1,2,4]triazolo[3,4-c][1,2,4]triazepin-4-yl)-N-(2-(2-(2-(2-(4-(5,7-dimethoxy-4-oxo-3,4-dihydroquinazolin-2-yl)-2,6-dimethylphenoxy)ethoxy)ethoxy)ethoxy)ethyl)acetamide (5, EML897)



Compound **5** (EML897) was obtained as a white solid (53 mg, 60%) from derivative **49** (40 mg, 0.1 mmol) and **51d** (55 mg, 0.11 mmol) according to the procedure described for **1**.

^1H NMR (400 MHz, CDCl_3) δ 9.79 (s, 1H), 7.68 (s, 2H), 7.60 (dd, $J = 8.7, 2.4$ Hz, 1H), 7.46 (d, $J = 8.6$ Hz, 2H), 7.37 (d, $J = 8.6$ Hz, 2H), 7.30 (d, $J = 8.7$ Hz, 1H), 7.24 (d, $J = 2.4$ Hz, 1H), 6.95 (t, $J = 5.4$ Hz, 1H), 6.81 (d, $J = 2.3$ Hz, 1H), 6.45 (d, $J = 2.3$ Hz, 1H), 4.56 – 4.47 (m, 2H), 4.02 – 3.96 (m, 2H), 3.97 (s, 3H), 3.92 (s, 3H), 3.85 – 3.79 (m, 2H), 3.73 – 3.69 (m, 2H), 3.66 – 3.62 (m, 2H), 3.58 – 3.45 (m, 8H), 2.61 (s, 3H), 2.37 (s, 6H). ^{13}C NMR (101 MHz, CDCl_3) δ 168.01, 165.07, 161.43, 160.54, 160.27, 159.28, 158.91, 153.86, 152.53, 148.49, 137.10, 133.97, 133.18, 133.15, 132.19, 131.99, 131.23, 130.49, 129.65, 128.90, 127.72, 105.07, 101.34, 98.15, 77.34, 71.66, 70.84, 70.63, 70.57, 70.51, 70.25, 69.82, 57.29, 56.39, 55.72, 39.18, 16.53, 12.67. MS (ESI) m/z : 885 ($\text{M}+\text{H}$) $^+$.

Synthesis of 2-(8-chloro-6-(4-chlorophenyl)-1-methyl-4H-benzo[e][1,2,4]triazolo[3,4-c][1,2,4]triazepin-4-yl)-N-(14-(4-(5,7-dimethoxy-4-oxo-3,4-dihydroquinazolin-2-yl)-2,6-dimethylphenoxy)-3,6,9,12-tetraoxatetradecyl)acetamide (6, EML731)

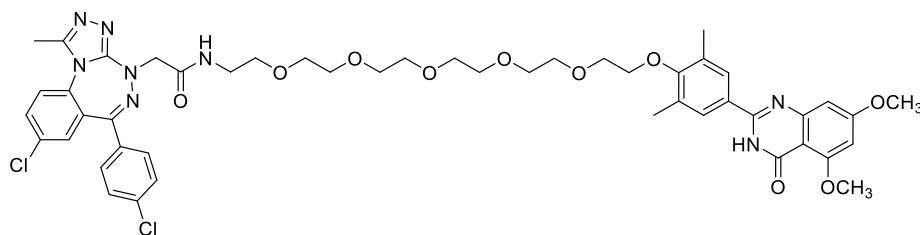


Compound **6** (EML731) was obtained as a white solid (60 mg, 48%) from derivative **49** (55 mg, 0.135 mmol) and **51e** (81 mg, 0.149 mmol) according to the procedure described for **1**.

^1H NMR (400 MHz, CDCl_3) δ 9.71 (s, 1H), 7.68 (s, 2H), 7.59 (dd, $J = 8.7, 2.4$ Hz, 1H), 7.46 (d, $J = 8.6$ Hz, 2H), 7.37 (d, $J = 8.6$ Hz, 2H), 7.30 (d, $J = 8.7$ Hz, 1H), 7.24 (d, $J = 2.4$ Hz, 1H), 6.92 (t, $J = 5.5$ Hz, 1H), 6.81 (d, $J = 2.3$ Hz, 1H), 6.44 (d, $J = 2.3$ Hz, 1H), 4.60 – 4.46 (m, 2H), 3.99 (dd, $J = 5.7, 3.7$ Hz, 2H), 3.96 (s, 3H), 3.92 (s, 3H), 3.83 (dd, $J = 5.7, 3.7$ Hz, 2H), 3.72

(dd, $J = 5.7, 3.2$ Hz, 2H), 3.67 (dd, $J = 6.3, 3.7$ Hz, 2H), 3.63 (dd, $J = 5.7, 3.7$ Hz, 2H), 3.59 (dd, $J = 6.3, 3.7$ Hz, 2H), 3.53 (s, 8H), 2.59 (s, 3H), 2.36 (s, 6H). ^{13}C NMR (101 MHz, CDCl_3) δ 168.05, 165.09, 163.35, 161.43, 160.54, 160.29, 159.29, 159.00, 153.86, 152.42, 148.37, 137.11, 133.96, 133.17, 132.20, 132.03, 131.23, 130.49, 129.62, 128.91, 127.62, 124.02, 105.06, 101.34, 98.15, 71.67, 70.91, 70.65, 70.56, 70.47, 70.22, 69.80, 57.36, 56.38, 55.72, 39.18, 16.52, 12.67. MS (ESI) m/z : 929 (M+H) $^+$.

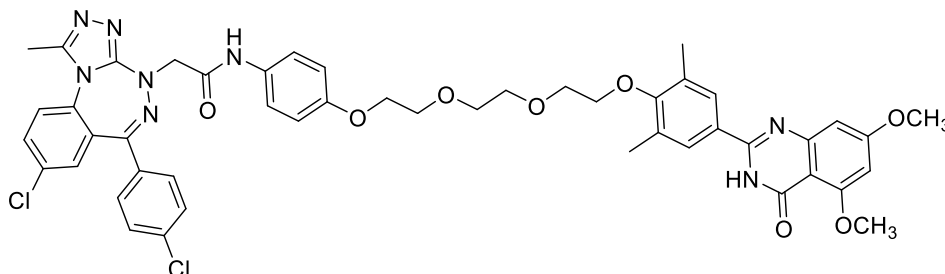
Synthesis of 2-(8-chloro-6-(4-chlorophenyl)-1-methyl-4H-benzo[e][1,2,4]triazolo[3,4-c][1,2,4]triazepin-4-yl)-N-(17-(4-(5,7-dimethoxy-4-oxo-3,4-dihydroquinazolin-2-yl)-2,6-dimethylphenoxy)-3,6,9,12,15-pentaoxaheptadecyl)acetamide (7, EML898)



Compound **7** (EML898) was obtained as a white solid (20 mg, 49%) from derivative **49** (17 mg, 0.042 mmol) and **51f** (25 mg, 0.042 mmol) according to the procedure described for **1**.

^1H NMR (400 MHz, CDCl_3) δ 9.85 (s, 1H), 7.71 (s, 2H), 7.60 (dd, $J = 8.7, 2.4$ Hz, 1H), 7.46 (d, $J = 8.6$ Hz, 2H), 7.37 (d, $J = 8.6$ Hz, 2H), 7.30 (d, $J = 8.7$ Hz, 1H), 7.24 (d, $J = 2.4$ Hz, 1H), 6.90 (t, $J = 5.4$ Hz, 1H), 6.81 (d, $J = 2.3$ Hz, 1H), 6.44 (d, $J = 2.3$ Hz, 1H), 4.59 – 4.48 (m, 2H), 3.99 (dd, $J = 5.8, 3.7$ Hz, 2H), 3.96 (s, 3H), 3.92 (s, 3H), 3.82 (dd, $J = 5.8, 3.7$ Hz, 2H), 3.74 – 3.55 (m, 20H), 2.58 (s, 3H), 2.36 (s, 6H). ^{13}C NMR (101 MHz, CDCl_3) δ 168.03, 165.09, 161.43, 160.69, 160.31, 159.29, 159.03, 153.89, 152.43, 148.36, 137.11, 133.95, 133.16, 132.22, 132.00, 131.22, 130.49, 128.91, 127.66, 124.04, 105.03, 101.33, 98.15, 71.67, 70.90, 70.67, 70.60, 70.53, 70.46, 70.44, 70.20, 69.78, 57.37, 56.37, 55.72, 39.17, 29.70, 16.51, 12.66. MS (ESI) m/z : 973 (M+H) $^+$.

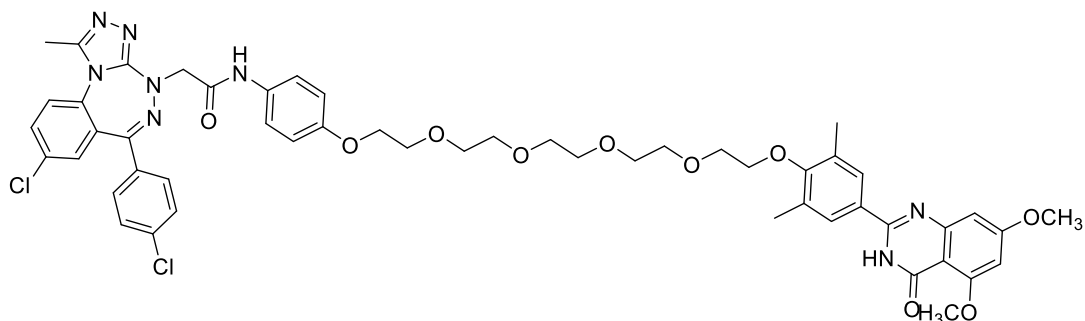
Synthesis of 2-(8-chloro-6-(4-chlorophenyl)-1-methyl-4H-benzo[e][1,2,4]triazolo[3,4-c][1,2,4]triazepin-4-yl)-N-(4-(2-(2-(2-(4-(5,7-dimethoxy-4-oxo-3,4-dihydroquinazolin-2-yl)-2,6-dimethylphenoxy)ethoxy)ethoxy)ethoxy)phenyl)acetamide (8, EML729)



Compound **8** (EML729) was obtained as a white solid (35 mg, 74%) from derivative **49** (20 mg, 0.051 mmol) and **52a** (31 mg, 0.056 mmol) according to the procedure described for **1**.

^1H NMR (400 MHz, CDCl_3) δ 10.08 (s, 1H), 8.87 (s, 1H), 7.71 (s, 2H), 7.62 (dd, $J = 8.7, 2.4$ Hz, 1H), 7.47 (d, $J = 8.2$ Hz, 2H), 7.34 (d, $J = 7.9$ Hz, 3H), 7.31 (d, $J = 8.6$ Hz, 2H), 7.26 (d, $J = 2.8$ Hz, 1H), 6.83 – 6.80 (m, 2H), 6.43 (d, $J = 2.4$ Hz, 1H), 4.64 (s, 2H), 4.09 (t, $J = 4.9$ Hz, 2H), 3.97 (d, $J = 4.4$ Hz, 2H), 3.94 (s, 3H), 3.91 (s, 3H), 3.84 (t, $J = 4.9$ Hz, 4H), 3.77 – 3.69 (m, 4H), 2.59 (s, 3H), 2.33 (s, 6H). ^{13}C NMR (101 MHz, CDCl_3) δ 166.26, 165.07, 161.39, 160.88, 160.76, 159.43, 158.98, 155.59, 153.92, 152.53, 148.47, 137.28, 133.69, 133.41, 133.07, 132.34, 131.96, 131.25, 131.08, 130.51, 129.65, 128.96, 127.75, 124.09, 121.61, 114.96, 105.02, 101.33, 98.12, 71.62, 70.95, 70.50, 69.83, 67.79, 65.85, 58.31, 56.33, 55.72, 16.46, 12.65. MS (ESI) m/z : 933 ($\text{M}+\text{H}$) $^+$.

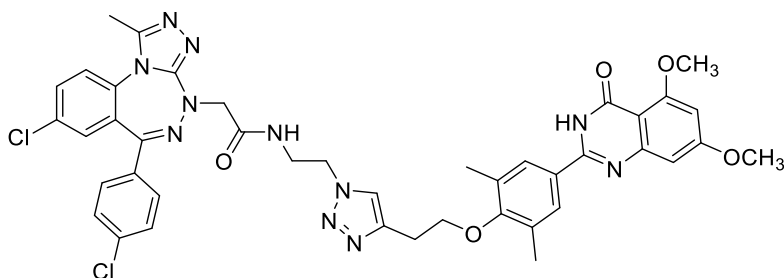
Synthesis of 2-(8-chloro-6-(4-chlorophenyl)-1-methyl-4H-benzo[e][1,2,4]triazolo[3,4-c][1,2,4]triazepin-4-yl)-N-(4-((14-(4-(5,7-dimethoxy-4-oxo-3,4-dihydroquinazolin-2-yl)-2,6-dimethylphenoxy)-3,6,9,12-tetraoxatetradecyl)oxy)phenyl)acetamide (9, EML742)



Compound **9** (EML742) was obtained as a white solid (64 mg, 52%) from derivative **49** (49 mg, 0.121 mmol) and **52b** (85 mg, 0.133 mmol) according to the procedure described for **1**.

^1H NMR (400 MHz, CDCl_3) δ 9.70 (s, 1H), 8.79 (s, 1H), 7.69 (s, 2H), 7.63 (dd, $J = 8.7, 2.4$ Hz, 1H), 7.48 (d, $J = 8.6$ Hz, 2H), 7.36 (d, $J = 8.6$ Hz, 2H), 7.35 – 7.29 (m, 2H), 7.28 (d, $J = 2.4$ Hz, 1H), 6.81 (d, $J = 2.1$ Hz, 2H), 6.79 (s, 1H), 6.44 (d, $J = 2.3$ Hz, 1H), 4.63 (s, 2H), 4.06 (dd, $J = 5.8, 3.9$ Hz, 2H), 3.98 (d, $J = 4.4$ Hz, 2H), 3.96 (s, 3H), 3.92 (s, 3H), 3.86 – 3.78 (m, 4H), 3.75 – 3.64 (m, 12H), 2.60 (s, 3H), 2.35 (s, 6H). ^{13}C NMR (101 MHz, CDCl_3) δ 166.19, 165.09, 161.41, 160.80, 160.60, 159.44, 159.04, 155.60, 153.88, 152.40, 148.47, 137.31, 133.67, 133.44, 133.08, 132.35, 132.04, 131.27, 131.03, 130.52, 129.66, 128.97, 127.63, 124.07, 121.52, 114.93, 101.35, 98.14, 71.66, 70.92, 70.85, 70.69, 70.65, 70.47, 69.74, 67.76, 61.49, 58.37, 56.37, 55.72, 16.50, 12.67. MS (ESI) m/z : 1022 ($\text{M}+\text{H}$) $^+$.

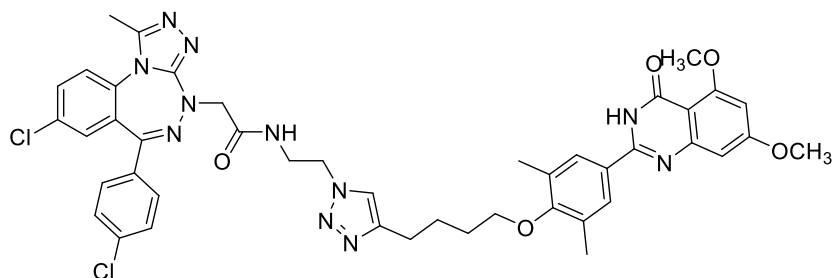
Synthesis of 2-(8-chloro-6-(4-chlorophenyl)-1-methyl-4H-benzo[e][1,2,4]triazolo[3,4-c][1,2,4]triazepin-4-yl)-N-(2-(4-(2-(4-(5,7-dimethoxy-4-oxo-3,4-dihydroquinazolin-2-yl)-2,6-dimethylphenoxy)ethyl)-1H-1,2,3-triazol-1-yl)ethyl)acetamide (10, EML823)



Compound **10** (EML823) was obtained as a white solid (45 mg, 78%) from derivative **49** (27 mg, 0.068 mmol) and **53a** (32 mg, 0.075 mmol) according to the procedure described for **1**.

^1H NMR (400 MHz, CDCl_3) δ 9.69 (s, 1H), 7.67 (s, 2H), 7.62 (dd, $J = 8.6, 2.4$ Hz, 1H), 7.49 (s, 1H), 7.44 (d, $J = 8.6$ Hz, 2H), 7.39 (d, $J = 7.3$ Hz, 2H), 7.36 (d, $J = 8.6$ Hz, 2H), 7.12 (t, $J = 5.9$ Hz, 1H), 6.81 (d, $J = 2.3$ Hz, 1H), 6.45 (d, $J = 2.3$ Hz, 1H), 4.60 (s, 2H), 4.44 (t, $J = 5.6$ Hz, 2H), 4.04 (t, $J = 6.6$ Hz, 2H), 3.96 (s, 3H), 3.92 (s, 3H), 3.85 – 3.72 (m, 2H), 3.13 (t, $J = 6.6$ Hz, 2H), 2.58 (s, 3H), 2.24 (s, 6H). ^{13}C NMR (101 MHz, CDCl_3) δ 168.82, 165.13, 161.42, 160.81, 160.60, 159.10, 158.85, 153.85, 152.27, 148.62, 144.27, 137.20, 133.87, 133.37, 132.93, 132.38, 131.90, 131.70, 130.46, 129.33, 128.91, 127.77, 124.17, 122.86, 105.01, 101.37, 98.21, 70.92, 57.47, 56.38, 55.73, 49.30, 39.27, 26.98, 16.50, 12.65. MS (ESI) m/z : 848 (M+H) $^+$

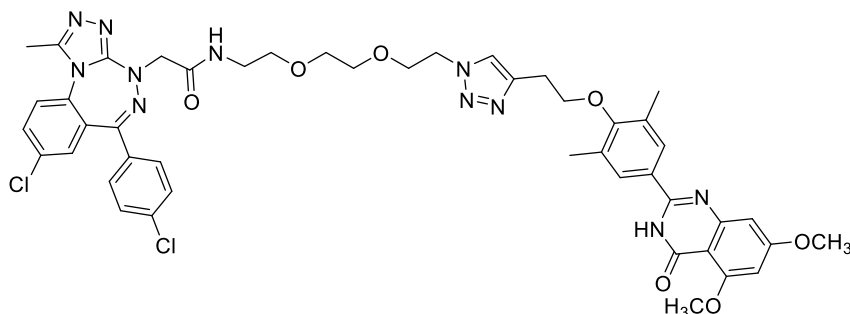
Synthesis of 2-(8-chloro-6-(4-chlorophenyl)-1-methyl-4H-benzo[e][1,2,4]triazolo[3,4-c][1,2,4]triazepin-4-yl)-N-(2-(4-(4-(4-(5,7-dimethoxy-4-oxo-3,4-dihydroquinazolin-2-yl)-2,6-dimethylphenoxy)butyl)-1H-1,2,3-triazol-1-yl)ethyl)acetamide (11, EML899)



Compound **11** (EML899) was obtained as a white solid (37 mg, 57%) from derivative **49** (30 mg, 0.074 mmol) and **53b** (40 mg, 0.081 mmol) according to the procedure described for **1**.

^1H NMR (400 MHz, CDCl_3) δ 9.58 (s, 1H), 7.69 (s, 2H), 7.64 (dd, $J = 8.6, 2.4$ Hz, 1H), 7.43 (d, $J = 8.6$ Hz, 2H), 7.40 (d, $J = 2.5$ Hz, 1H), 7.36 (d, $J = 8.6$ Hz, 2H), 7.29 (s, 1H), 7.10 (t, $J = 5.9$ Hz, 1H), 6.82 (d, $J = 2.3$ Hz, 1H), 6.45 (d, $J = 2.3$ Hz, 1H), 4.68 – 4.45 (m, 2H), 4.40 (t, $J = 5.5$ Hz, 2H), 3.97 (s, 3H), 3.92 (s, 3H), 3.82 (d, $J = 5.0$ Hz, 4H), 2.73 – 2.65 (m, 2H), 2.59 (s, 3H), 2.34 (s, 6H), 1.90 – 1.81 (m, 4H). ^{13}C NMR (101 MHz, CDCl_3) δ 168.80, 165.14, 161.43, 160.85, 160.58, 159.25, 159.10, 153.89, 152.29, 148.59, 147.72, 137.19, 133.89, 133.38, 132.95, 132.40, 132.02, 131.71, 130.45, 129.32, 128.91, 127.57, 124.12, 121.57, 105.00, 101.38, 98.19, 72.04, 57.47, 56.39, 55.73, 49.24, 39.13, 29.96, 29.70, 25.95, 25.41, 16.56, 12.67. MS (ESI) m/z : 876 ($\text{M}+\text{H}$) $^+$.

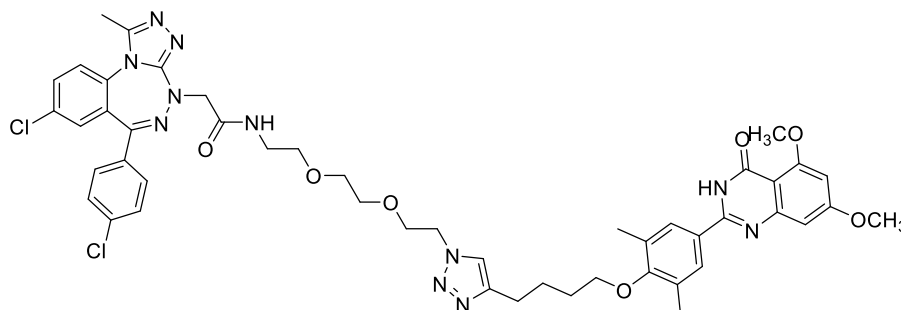
Synthesis of 2-(8-chloro-6-(4-chlorophenyl)-1-methyl-4H-benzo[e][1,2,4]triazolo[3,4-c][1,2,4]triazepin-4-yl)-N-(2-(2-(2-(4-(2-(4-(5,7-dimethoxy-4-oxo-3,4-dihydroquinazolin-2-yl)-2,6-dimethylphenoxy)ethyl)-1H-1,2,3-triazol-1-yl)ethoxy)ethoxy)ethyl)acetamide (12, EML809)



A solution of compound **87** (30 mg, 0.054 mmol) in 0.050 mL of dry DCM was added to a solution of CuI (1 mg, 0.0012 mmol), DIPEA (0.0036 mL, 0.0021 mmol) and AcOH (0.0012 mL, 0.0021 mmol) in 0.015 mL of dry DCM. After 5 min, **85a** (20 mg, 0.053 mmol) was added and the resulting mixture was stirred at room temperature for 18 h. Then, the solvent was evaporated and the crude was purified by silica gel chromatography (DCM/MeOH 95:5 to 80:20) to give the title compound **12** as white solid (34 mg, 69%).

^1H NMR (400 MHz, CDCl_3) δ 7.66 (s, 2H), 7.64 (s, 1H), 7.59 (dd, $J = 8.6, 2.4$ Hz, 1H), 7.46 (d, $J = 8.7$ Hz, 2H), 7.36 (d, $J = 8.7$ Hz, 2H), 7.30 (d, $J = 8.6$ Hz, 1H), 7.22 (d, $J = 2.4$ Hz, 1H), 6.93 (t, $J = 5.4$ Hz, 1H), 6.81 (d, $J = 2.3$ Hz, 1H), 6.44 (d, $J = 2.3$ Hz, 1H), 4.54 – 4.46 (m, 4H), 4.08 (t, $J = 6.4$ Hz, 2H), 3.96 (s, 3H), 3.92 (s, 3H), 3.83 (t, $J = 5.1$ Hz, 2H), 3.51 – 3.37 (m, 8H), 3.23 (t, $J = 6.4$ Hz, 2H), 2.59 (s, 3H), 2.25 (s, 6H). ^{13}C NMR (101 MHz, CDCl_3) δ 168.23, 165.07, 161.40, 160.53, 160.37, 159.25, 158.80, 153.83, 152.40, 148.51, 144.34, 137.17, 133.87, 133.23, 133.08, 132.25, 131.94, 131.20, 130.64, 130.49, 129.59, 128.92, 124.10, 123.26, 105.05, 101.35, 98.17, 71.04, 70.43, 70.16, 69.74, 69.54, 57.52, 56.38, 55.72, 50.15, 39.13, 27.10, 16.48, 12.72. MS (ESI) m/z : 876 ($\text{M}+\text{H}$) $^+$

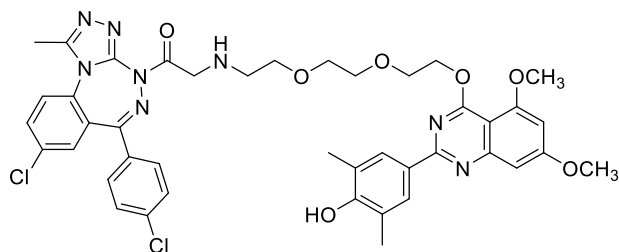
Synthesis of 2-(8-chloro-6-(4-chlorophenyl)-1-methyl-4H-benzo[e][1,2,4]triazolo[3,4-c][1,2,4]triazepin-4-yl)-N-(2-(2-(2-(4-(4-(4-(5,7-dimethoxy-4-oxo-3,4-dihydroquinazolin-2-yl)-2,6-dimethylphenoxy)butyl)-1H-1,2,3-triazol-1-yl)ethoxy)ethoxy)ethyl)acetamide (13, EML900)



Compound **13** (EML900) was obtained as a white solid (38 mg, 52%) from derivative **87** (45 mg, 0.081 mmol) and **85b** (31 mg, 0.077 mmol) according to the procedure described for **12**.

^1H NMR (400 MHz, CDCl_3) δ 9.63 (s, 1H), 7.69 (s, 2H), 7.60 (dd, $J = 8.7, 2.4$ Hz, 1H), 7.47 (d, $J = 8.7$ Hz, 2H), 7.43 (s, 1H), 7.37 (d, $J = 8.7$ Hz, 2H), 7.31 (d, $J = 8.7$ Hz, 1H), 7.23 (d, $J = 2.4$ Hz, 1H), 6.93 (d, $J = 5.7$ Hz, 1H), 6.82 (d, $J = 2.3$ Hz, 1H), 6.45 (d, $J = 2.3$ Hz, 1H), 4.71 – 4.48 (m, 2H), 4.47 (t, $J = 5.1$ Hz, 2H), 3.96 (s, 3H), 3.92 (s, 3H), 3.88 – 3.78 (m, 4H), 3.56 – 3.39 (m, 8H), 2.85 – 2.71 (m, 2H), 2.59 (s, 3H), 2.34 (s, 6H), 1.97 – 1.86 (m, 4H). ^{13}C NMR (101 MHz, CDCl_3) δ 168.15, 165.10, 161.42, 160.55, 160.38, 159.22, 153.88, 152.36, 137.20, 133.87, 133.23, 133.13, 132.27, 131.99, 131.21, 130.49, 129.60, 128.94, 127.60, 124.31, 121.91, 101.36, 98.16, 72.07, 70.42, 70.18, 69.77, 69.57, 57.55, 56.38, 55.72, 50.09, 39.15, 29.89, 26.11, 25.49, 16.55, 12.71. MS (ESI) m/z : 964 ($\text{M}+\text{H}$) $^+$.

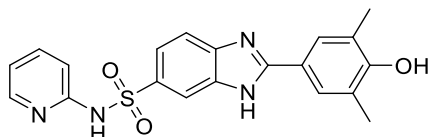
Synthesis of 1-(8-chloro-6-(4-chlorophenyl)-1-methyl-4H-benzo[e][1,2,4]triazolo[3,4-c][1,2,4]triazepin-4-yl)-2-((2-(2-(2-((2-(4-hydroxy-3,5-dimethylphenyl)-5,7-dimethoxyquinazolin-4-yl)oxy)ethoxy)ethoxy)ethyl)amino)ethan-1-one (14, EML824)



Compound **14** (EML824) was obtained as a white solid (25 mg, 60%) from derivative **49** (20 mg, 0.050 mmol) and **91** (25 mg, 0.055 mmol) according to the procedure described for **1**.

^1H NMR (400 MHz, CDCl_3) δ 8.15 (s, 2H), 7.55 (dd, $J = 8.6, 2.4$ Hz, 1H), 7.44 (d, $J = 8.7$ Hz, 2H), 7.36 (d, $J = 8.7$ Hz, 2H), 7.25 (d, $J = 2.4$ Hz, 1H), 7.22 (d, $J = 8.6$ Hz, 1H), 4.83 – 4.76 (m, 2H), 4.56 – 4.46 (m, 2H), 3.94 (s, 3H), 3.93 – 3.91 (m, 2H), 3.89 (s, 3H), 3.68 (d, $J = 5.5$ Hz, 2H), 3.58 – 3.41 (m, 6H), 2.53 (s, 3H), 2.35 (s, 6H). ^{13}C NMR (101 MHz, CDCl_3) δ 167.98, 166.17, 164.07, 160.49, 160.43, 159.20, 158.34, 156.45, 154.81, 148.33, 137.18, 133.85, 133.17, 133.09, 132.23, 131.21, 130.46, 129.81, 129.55, 129.01, 128.92, 123.98, 123.02, 99.51, 98.57, 70.66, 70.41, 69.84, 69.34, 66.02, 57.44, 56.10, 55.69, 39.16, 16.12, 12.59. MS (ESI) m/z : 841 ($\text{M}+\text{H}$) $^+$.

Synthesis of 2-(4-hydroxy-3,5-dimethylphenyl)-N-(pyridin-2-yl)-1H-benzo[d]imidazole-6-sulfonamide (15, EML765)

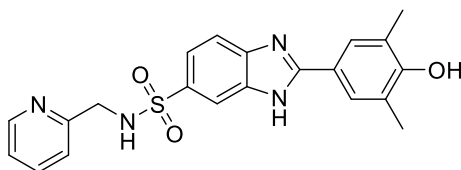


3,4-diamino-*N*-(pyridin-2-yl)benzenesulfonamide **99a** (200 mg, 0.75 mmol) was solubilized in 6 mL of dry DMF and 4-hydroxy-3,5-dimethylbenzaldehyde **76a** (114 mg, 0.75 mmol) and $\text{Na}_2\text{S}_2\text{O}_5$ (187 mg, 0.98 mmol) were added. The resulting mixture was heated at 80 °C and

stirred at this temperature for 18 h. After cooling at room temperature, water was added. The brown precipitate formed was recovered by filtration and washed several times with water. After recrystallization from EtOH, compound **15** was obtained as light yellow solid (250 mg, 85%).

^1H NMR (400 MHz, DMSO- d_6) δ 8.98 (s, 1H), 8.07 – 8.00 (m, 2H), 7.78 (s, 2H), 7.74 – 7.64 (m, 2H), 7.68 – 7.60 (m, 1H), 7.18 (d, J = 8.6 Hz, 1H), 6.87 (t, J = 6.2 Hz, 1H), 2.26 (s, 6H). ^{13}C NMR (101 MHz, DMSO- d_6) δ 156.60, 154.92, 140.40, 127.78, 125.30, 121.17, 119.76, 113.87, 17.17. MS (ESI) m/z : 395 (M+H) $^+$

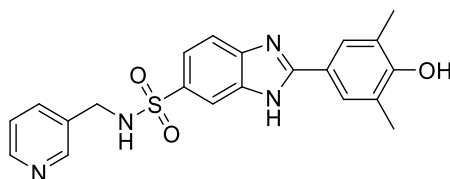
Synthesis of 2-(4-hydroxy-3,5-dimethylphenyl)-N-(pyridin-2-ylmethyl)-1H-benzof[d]imidazole-6-sulfonamide (16, EML803)



Compound **16** (EML803) was obtained as a light yellow solid (245 mg, 56%) from derivative **99b** (298 mg, 1.07 mmol) and 4-hydroxy-3,5-dimethylbenzaldehyde **76a** (161 mg, 1.07 mmol) according to the procedure described for **15**.

^1H NMR (400 MHz, DMSO- d_6) δ 13.01 (s, 1H), 8.88 (s, 1H), 8.43 – 8.39 (m, 1H), 8.13 (s, 1H), 8.04 – 7.85 (m, 1H), 7.80 (s, 2H), 7.74 – 7.67 (m, 1H), 7.61 (s, 1H), 7.37 (d, J = 7.9 Hz, 1H), 7.21 (dd, J = 7.5, 4.9 Hz, 1H), 4.05 (d, J = 5.8 Hz, 2H), 2.27 (s, 6H). ^{13}C NMR (101 MHz, DMSO- d_6) δ 157.80, 156.22, 149.15, 137.10, 133.82, 127.63, 125.21, 122.78, 122.07, 120.69, 48.53, 17.19. MS (ESI) m/z : 409 (M+H) $^+$

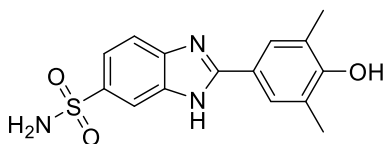
Synthesis of 2-(4-hydroxy-3,5-dimethylphenyl)-N-(pyridin-3-ylmethyl)-1H-benzo[d]imidazole-6-sulfonamide (17, EML798)



Compound **17** (EML798) was obtained as a light yellow solid (68 mg, 72%) from derivative **99c** (64 mg, 0.230 mmol) and 4-hydroxy-3,5-dimethylbenzaldehyde **76a** (34 mg, 0.230 mmol) according to the procedure described for **15**.

^1H NMR (400 MHz, $\text{DMSO-}d_6$) δ 13.03 (s, 1H), 8.89 (s, 1H), 8.45 – 8.37 (m, 1H), 8.12 (t, J = 6.3 Hz, 1H), 7.95 (s, 1H), 7.81 (s, 2H), 7.70 – 7.57 (m, 3H), 7.28 (dd, J = 7.9, 4.8 Hz, 1H), 4.02 (d, J = 6.3 Hz, 2H), 2.28 (s, 7H). ^{13}C NMR (101 MHz, $\text{DMSO-}d_6$) δ 156.24, 149.33, 148.75, 135.83, 133.89, 127.64, 125.21, 123.74, 120.67, 120.61, 44.26, 17.19. MS (ESI) m/z : 409 ($\text{M}+\text{H}$) $^+$.

Synthesis of 2-(4-hydroxy-3,5-dimethylphenyl)-1H-benzo[d]imidazole-6-sulfonamide (18, EML795)

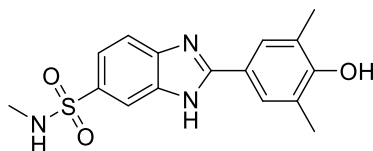


N-(tert-butyl)-2-(4-hydroxy-3,5-dimethylphenyl)-1H-benzo[d]imidazole-6-sulfonamide **100** (136 mg, 0.364 mmol) was dissolved in 3.6 mL of a solution DCM/TFA (1:1) and the mixture was stirred for 18 h. The solvent was evaporated, and the resulting solid was crystallized with ethanol to give the title compound as a light brown solid (85 mg, 74%).

^1H NMR (400 MHz, $\text{DMSO-}d_6$) δ 12.98 (s, 1H), 8.87 (s, 1H), 8.06 – 7.87 (m, 1H), 7.79 (d, J = 2.8 Hz, 2H), 7.74 – 7.56 (m, 2H), 7.28 – 7.22 (m, 2H), 2.27 (d, J = 2.9 Hz, 6H). ^{13}C NMR (101 MHz, $\text{DMSO-}d_6$) δ 156.18, 156.09, 155.35, 154.84, 146.49, 143.63, 138.01, 137.92, 137.53,

134.60, 127.56, 125.18, 120.76, 120.04, 119.68, 118.63, 116.57, 111.48, 109.56, 17.17. MS (ESI) m/z : 318 (M+H)⁺

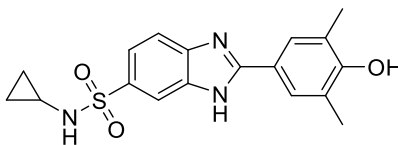
Synthesis of 2-(4-hydroxy-3,5-dimethylphenyl)-N-methyl-1H-benzo[d]imidazole-6-sulfonamide (19, EML796)



Compound **19** (EML796) was obtained as a white solid (60 mg, 73%) from derivative **99e** (50 mg, 0.248 mmol) and 4-hydroxy-3,5-dimethylbenzaldehyde **76a** (37 mg, 0.248 mmol) according to the procedure described for **15**.

¹H NMR (400 MHz, DMSO-*d*₆) δ 7.91 (s, 1H), 7.79 (s, 2H), 7.68 (d, *J* = 8.5 Hz, 1H), 7.57 (dd, *J* = 8.5, 1.7 Hz, 1H), 7.36 – 7.28 (m, 1H), 2.40 (d, *J* = 4.8 Hz, 3H), 2.27 (s, 6H). ¹³C NMR (101 MHz, DMSO-*d*₆) δ 156.23, 132.61, 127.63, 125.21, 120.68, 29.22, 17.19. MS (ESI) m/z : 332 (M+H)⁺.

Synthesis of N-cyclopropyl-2-(4-hydroxy-3,5-dimethylphenyl)-1H-benzo[d]imidazole-6-sulfonamide (20, EML801)

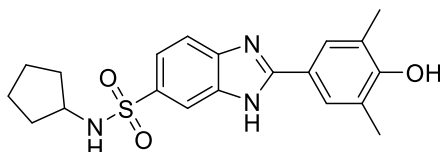


Compound **20** (EML801) was obtained as a light yellow solid (64 mg, 63%) from derivative **99f** (64 mg, 0.281 mmol) and 4-hydroxy-3,5-dimethylbenzaldehyde **76a** (25 mg, 0.281 mmol) according to the procedure described for **15**.

¹H NMR (400 MHz, DMSO-*d*₆) δ 13.02 (s, 1H), 8.88 (s, 1H), 8.01 – 7.88 (m, 1H), 7.79 (s, 2H), 7.73 – 7.62 (m, 1H), 7.61 (d, *J* = 8.2 Hz, 1H), 2.27 (s, 6H), 2.07 (dd, *J* = 6.5, 3.5 Hz, 1H), 0.49

-0.41 (m, 2H), 0.41 – 0.34 (m, 2H). ¹³C NMR (101 MHz, DMSO-*d*₆) δ 156.22, 133.69, 127.62, 125.21, 120.69, 24.64, 17.19, 5.56. MS (ESI) *m/z*: 358 (M+H)⁺

Synthesis of N-cyclopentyl-2-(4-hydroxy-3,5-dimethylphenyl)-1H-benzo[d]imidazole-6-sulfonamide (21, EML797)



Compound **21** (EML797) was obtained as a yellow solid (345 mg, 58%) from derivative **99g** (390 mg, 1.53 mmol) and 4-hydroxy-3,5-dimethylbenzaldehyde **76a** (230 mg, 1.53 mmol) according to the procedure described for **15**.

¹H NMR (400 MHz, DMSO-*d*₆) δ 9.25 – 9.11 (m, 1H), 7.99 (d, *J* = 1.7 Hz, 1H), 7.82 (s, 2H), 7.77 (d, *J* = 8.5 Hz, 1H), 7.72 (dd, *J* = 8.5, 1.7 Hz, 1H), 7.66 (d, *J* = 6.9 Hz, 1H), 3.45 – 3.35 (m, 1H), 2.28 (s, 6H), 1.60 – 1.49 (m, 4H), 1.39 – 1.26 (m, 4H). ¹³C NMR (101 MHz, DMSO-*d*₆) δ 157.40, 154.22, 136.55, 128.19, 125.56, 121.94, 118.01, 114.96, 113.79, 65.38, 54.97, 32.92, 23.27, 17.18. MS (ESI) *m/z*: 386 (M+H)⁺

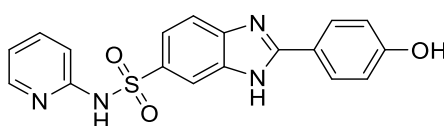
Synthesis of N-cyclohexyl-2-(4-hydroxy-3,5-dimethylphenyl)-1H-benzo[d]imidazole-6-sulfonamide (22, EML802)



Compound **22** (EML802) was obtained as a yellow solid (160 mg, 54%) from derivative **99h** (200 mg, 0.742 mmol) and 4-hydroxy-3,5-dimethylbenzaldehyde **76a** (111 mg, 0.742 mmol) according to the procedure described for **15**.

^1H NMR (400 MHz, $\text{DMSO-}d_6$) δ 13.00 (s, 1H), 8.88 (s, 1H), 8.06 – 7.85 (m, 1H), 7.79 (s, 2H), 7.73 – 7.41 (m, 3H), 2.91 (s, 1H), 2.27 (s, 6H), 1.59 – 1.34 (m, 5H), 1.19 – 0.95 (m, 5H). ^{13}C NMR (101 MHz, DMSO) δ 156.19, 135.76, 127.60, 125.20, 120.72, 33.67, 25.36, 24.82, 17.19. MS (ESI) m/z : 400 ($\text{M}+\text{H}$) $^+$.

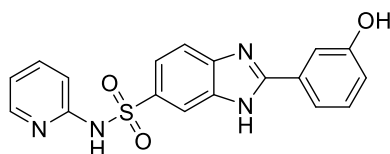
Synthesis of 2-(4-hydroxyphenyl)-N-(pyridin-2-yl)-1H-benzo[d]imidazole-6-sulfonamide (23, EML760)



Compound **23** (EML760) was obtained as a white solid (180 mg, 65%) from derivative **99a** (200 mg, 0.757 mmol) and 4-hydroxybenzaldehyde **76b** (92 mg, 0.757 mmol) according to the procedure described for **15**.

^1H NMR (400 MHz, $\text{DMSO-}d_6$) δ 13.04 (s, 1H), 10.06 (s, 1H), 8.12 – 8.01 (m, 2H), 8.00 (d, J = 8.7 Hz, 2H), 7.72 – 7.55 (m, 3H), 7.17 (d, J = 8.6 Hz, 1H), 6.92 (d, J = 8.7 Hz, 2H), 6.86 (t, J = 6.3 Hz, 1H). ^{13}C NMR (101 MHz, $\text{DMSO-}d_6$) δ 160.21, 129.04, 120.76, 116.28. MS (ESI) m/z : 367 ($\text{M}+\text{H}$) $^+$.

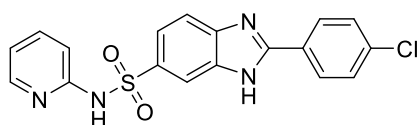
Synthesis of 2-(3-hydroxyphenyl)-N-(pyridin-2-yl)-1H-benzo[d]imidazole-6-sulfonamide (24, EML761)



Compound **24** (EML761) was obtained as a white solid (270 mg, 65%) from derivative **99a** (300 mg, 1.13 mmol) and 3-hydroxybenzaldehyde **76c** (137 mg, 1.13 mmol) according to the procedure described for **15**.

^1H NMR (400 MHz, $\text{DMSO-}d_6$) δ 9.91 (s, 1H), 8.14 (d, $J = 1.7$ Hz, 1H), 8.01 (dd, $J = 5.5, 1.7$ Hz, 1H), 7.80 (dd, $J = 8.6, 1.7$ Hz, 1H), 7.76 (d, $J = 8.5$ Hz, 1H), 7.74 – 7.67 (m, 1H), 7.62 – 7.55 (m, 2H), 7.41 (t, $J = 7.9$ Hz, 1H), 7.20 (d, $J = 8.6$ Hz, 1H), 7.04 – 6.96 (m, 1H), 6.87 (t, $J = 6.4$ Hz, 1H). ^{13}C NMR (101 MHz, $\text{DMSO-}d_6$) δ 158.41, 153.98, 153.47, 140.73, 130.87, 129.34, 122.03, 119.02, 118.35, 114.35, 114.06. MS (ESI) m/z : 367 ($\text{M}+\text{H}$) $^+$

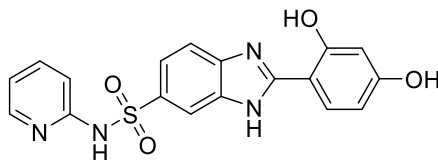
Synthesis of 2-(4-chlorophenyl)-N-(pyridin-2-yl)-1H-benzo[d]imidazole-6-sulfonamide (25, EML762)



Compound **25** (EML762) was obtained as a pale yellow solid (135 mg, 52%) from derivative **99a** (180 mg, 0.681 mmol) and 4-chlorobenzaldehyde **76d** (100 mg, 0.681 mmol) according to the procedure described for **15**.

^1H NMR (400 MHz, $\text{DMSO-}d_6$) δ 8.18 (d, $J = 8.6$ Hz, 2H), 8.13 – 8.12 (m, 1H), 8.02 (dd, $J = 5.4, 1.9$ Hz, 1H), 7.77 – 7.73 (m, 2H), 7.72 – 7.69 (m, 1H), 7.67 (d, $J = 8.6$ Hz, 2H), 7.22 – 7.16 (m, 1H), 6.91 – 6.84 (m, 1H). ^{13}C NMR (101 MHz, $\text{DMSO-}d_6$) δ 153.38, 140.43, 135.86, 129.72, 129.04, 128.53, 121.51, 113.86. MS (ESI) m/z : 385 ($\text{M}+\text{H}$) $^+$

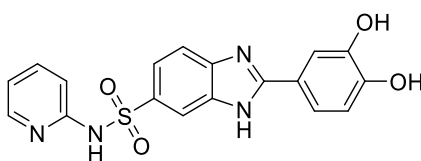
Synthesis of 2-(2,4-dihydroxyphenyl)-N-(pyridin-2-yl)-1H-benzo[d]imidazole-6-sulfonamide (26, EML763)



Compound **26** (EML763) was obtained as a light yellow solid (260 mg, 60%) from derivative **99a** (300 mg, 1.13 mmol) and 2,4-dihydroxybenzaldehyde **76e** (157 mg, 1.13 mmol) according to the procedure described for **15**.

^1H NMR (400 MHz, $\text{DMSO-}d_6$) δ 10.26 (s, 2H), 8.12 (s, 1H), 8.01 (d, $J = 5.4$ Hz, 1H), 7.87 (d, $J = 8.6$ Hz, 1H), 7.77 (d, $J = 8.6$ Hz, 1H), 7.76 – 7.66 (m, 3H), 7.19 (d, $J = 8.6$ Hz, 1H), 6.86 (t, $J = 6.4$ Hz, 1H), 6.52 – 6.45 (m, 2H). ^{13}C NMR (101 MHz, $\text{DMSO-}d_6$) δ 162.48, 160.25, 140.72, 129.22, 121.88, 114.08, 108.73, 103.48. MS (ESI) m/z : 383 ($\text{M}+\text{H}$) $^+$

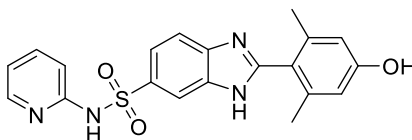
Synthesis of 2-(3,4-dihydroxyphenyl)-N-(pyridin-2-yl)-1H-benzo[d]imidazole-6-sulfonamide (27, EML764)



Compound **27** (EML764) was obtained as a pale yellow solid (255 mg, 59%) from derivative **99a** (300 mg, 1.14 mmol) and 3,4-dihydroxybenzaldehyde **76f** (157 mg, 1.14 mmol) according to the procedure described for **15**.

^1H NMR (400 MHz, $\text{DMSO-}d_6$) δ 10.01 (s, 1H), 9.52 (s, 1H), 8.10 (d, $J = 1.6$ Hz, 1H), 8.01 (dd, $J = 5.7, 1.9$ Hz, 1H), 7.81 (dd, $J = 8.5, 1.7$ Hz, 1H), 7.78 – 7.67 (m, 2H), 7.58 (d, $J = 2.2$ Hz, 1H), 7.51 (dd, $J = 8.3, 2.2$ Hz, 1H), 7.20 (d, $J = 8.6$ Hz, 1H), 6.97 (d, $J = 8.3$ Hz, 1H), 6.91 – 6.83 (m, 1H). ^{13}C NMR (101 MHz, $\text{DMSO-}d_6$) δ 153.94, 153.58, 150.24, 146.43, 140.91, 122.34, 120.31, 116.60, 116.20, 115.16, 114.83, 114.20, 113.77. MS (ESI) m/z : 383 ($\text{M}+\text{H}$) $^+$

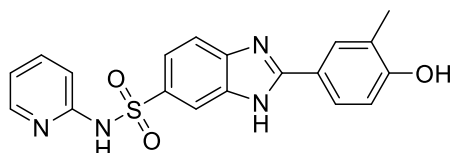
Synthesis of 2-(4-hydroxy-2,6-dimethylphenyl)-N-(pyridin-2-yl)-1H-benzo[d]imidazole-6-sulfonamide (28, EML766)



Compound **28** (EML766) was obtained as a pale yellow solid (190 mg, 67%) from derivative **99a** (190 mg, 0.719 mmol) and 4-hydroxy-2,6-dimethylbenzaldehyde **76g** (108 mg, 0.719 mmol) according to the procedure described for **15**.

^1H NMR (400 MHz, DMSO- d_6) δ 12.83 (d, $J = 5.6$ Hz, 1H), 9.60 (d, $J = 3.8$ Hz, 1H), 8.19 – 7.98 (m, 2H), 7.79 – 7.66 (m, 2H), 7.59 (d, $J = 8.5$ Hz, 1H), 7.25 – 7.16 (m, 1H), 6.88 (t, $J = 6.4$ Hz, 1H), 6.58 (s, 2H), 2.01 (s, 6H). ^{13}C NMR (101 MHz, DMSO- d_6) δ 158.48, 143.10, 122.21, 121.02, 120.13, 119.23, 118.27, 114.71, 111.89, 20.41. MS (ESI) m/z : 395 (M+H) $^+$

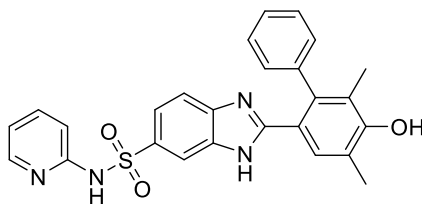
Synthesis of 2-(4-hydroxy-3-methylphenyl)-N-(pyridin-2-yl)-1H-benzo[d]imidazole-6-sulfonamide (29, EML806)



Compound **29** (EML806) was obtained as a light yellow solid (130 mg, 54%) from derivative **99a** (167 mg, 0.632 mmol) and 4-hydroxy-3-methylbenzaldehyde **76h** (86 mg, 0.632 mmol) according to the procedure described for **15**.

^1H NMR (400 MHz, DMSO- d_6) δ 10.39 (s, 1H), 8.10 (d, $J = 1.7$ Hz, 1H), 8.01 (dd, $J = 5.6, 1.9$ Hz, 1H), 7.94 (d, $J = 2.3$ Hz, 1H), 7.87 (dd, $J = 8.4, 2.3$ Hz, 1H), 7.82 (dd, $J = 8.6, 1.7$ Hz, 1H), 7.75 (d, $J = 8.8$ Hz, 1H), 7.75 – 7.67 (m, 1H), 7.21 (d, $J = 8.6$ Hz, 1H), 7.00 (d, $J = 8.6$ Hz, 1H), 6.91 – 6.83 (m, 1H), 2.23 (s, 3H). ^{13}C NMR (101 MHz, DMSO) δ 159.91, 153.88, 153.59, 140.94, 130.55, 127.36, 125.70, 122.39, 116.30, 116.15, 114.78, 114.75, 113.72, 16.45. MS (ESI) m/z : 381 (M+H) $^+$

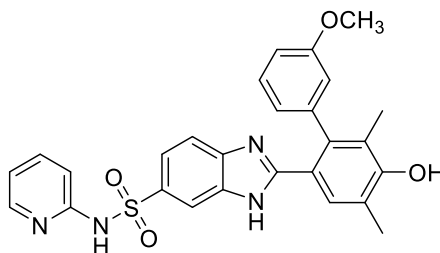
Synthesis of 2-(5-hydroxy-4,6-dimethyl-[1,1'-biphenyl]-2-yl)-N-(pyridin-2-yl)-1H-benzo[d]imidazole-6-sulfonamide (30, EML799)



Compound **30** (EML799) was obtained as a yellow solid (85 mg, 53%) from derivative **99a** (91 mg, 0.345 mmol) and the intermediate **103a** (78 mg, 0.345 mmol) according to the procedure described for **15**.

^1H NMR (400 MHz, DMSO- d_6) δ 11.96 – 11.86 (m, 2H), 8.80 (d, $J = 6.7$ Hz, 1H), 8.04 – 7.91 (m, 2H), 7.66 (s, 1H), 7.60 – 7.47 (m, 2H), 7.34 (t, $J = 8.7$ Hz, 1H), 7.27 – 7.18 (m, 3H), 7.14 – 7.03 (m, 3H), 6.86 (s, 1H), 2.28 (s, 3H), 1.95 (s, 3H). ^{13}C NMR (101 MHz, DMSO) δ 190.79, 159.28, 155.38, 140.49, 139.70, 137.26, 130.36, 130.27, 130.17, 128.67, 128.26, 128.03, 127.50, 127.23, 124.53, 123.88, 123.77, 17.02, 14.58, 13.86. MS (ESI) m/z : 471 ($\text{M}+\text{H}$) $^+$

Synthesis of 2-(5-hydroxy-3'-methoxy-4,6-dimethyl-[1,1'-biphenyl]-2-yl)-N-(pyridin-2-yl)-1H-benzo[d]imidazole-6-sulfonamide (31, EML804)

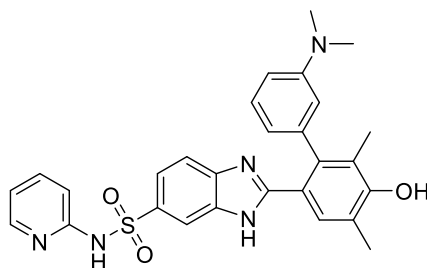


Compound **31** (EML804) was obtained as a pale yellow solid (95 mg, 65%) from derivative **99a** (77 mg, 0.291 mmol) and the intermediate **103b** (75 mg, 0.291 mmol) according to the procedure described for **15**.

^1H NMR (400 MHz, DMSO- d_6) δ 11.95 – 11.82 (m, 1H), 8.81 (d, $J = 7.2$ Hz, 1H), 8.06 – 7.94 (m, 1H), 7.69 – 7.62 (m, 1H), 7.62 – 7.55 (m, 2H), 7.41 – 7.26 (m, 2H), 7.17 – 7.08 (m, 2H),

6.89 – 6.83 (m, 1H), 6.81 – 6.73 (m, 1H), 6.64 – 6.63 (m, 1H), 6.60 (d, $J = 7.6$ Hz, 1H), 3.61 (dd, $J = 8.0, 2.0$ Hz, 3H), 2.27 (s, 3H), 1.97 (s, 3H). ^{13}C NMR (101 MHz, DMSO) δ 159.04, 158.96, 157.34, 156.49, 155.91, 155.26, 155.19, 146.15, 142.82, 141.06, 141.01, 140.18, 140.14, 133.91, 130.23, 129.38, 129.28, 123.88, 123.62, 122.53, 121.97, 120.74, 119.97, 118.91, 118.04, 116.13, 112.66, 111.71, 111.04, 55.32, 17.00, 14.57. MS (ESI) m/z : 501 (M+H)⁺.

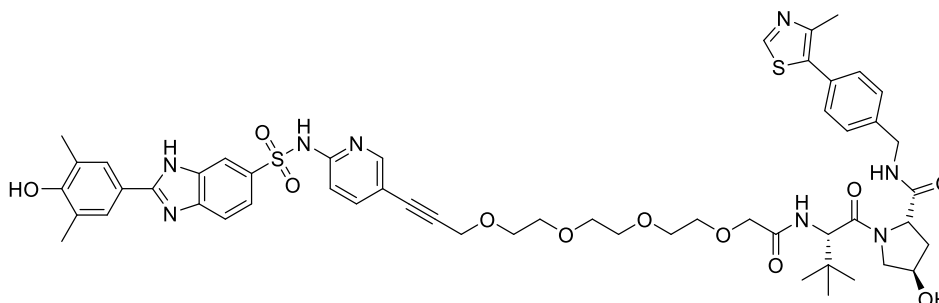
Synthesis of 2-(3'-(dimethylamino)-5-hydroxy-4,6-dimethyl-[1,1'-biphenyl]-2-yl)-N-(pyridin-2-yl)-1H-benzotimidazole-6-sulfonamide (32, EML805)



Compound **32** (EML805) was obtained as a yellow solid (60 mg, 67%) from derivative **99a** (54 mg, 0.204 mmol) and the intermediate **103c** (55 mg, 0.204 mmol) according to the procedure described for **15**.

^1H NMR (400 MHz, DMSO- d_6) δ 11.69 – 11.57 (m, 1H), 8.74 (d, $J = 7.9$ Hz, 1H), 8.04 – 7.95 (m, 1H), 7.71 – 7.62 (m, 1H), 7.57 (d, $J = 5.4$ Hz, 1H), 7.39 – 7.24 (m, 2H), 7.18 – 7.00 (m, 2H), 6.87 (s, 1H), 6.61 – 6.50 (m, 1H), 6.42 – 6.34 (m, 2H), 2.71 (s, 3H), 2.68 (s, 3H), 2.26 (s, 3H), 1.99 (s, 3H). ^{13}C NMR (101 MHz, DMSO) δ 156.88, 156.19, 155.23, 155.16, 150.27, 146.14, 142.79, 141.14, 130.14, 128.85, 128.74, 123.56, 123.49, 122.05, 120.70, 119.96, 118.83, 118.37, 118.27, 117.99, 114.59, 114.48, 111.41, 40.48, 16.98, 14.65. MS (ESI) m/z : 514 (M+H)⁺.

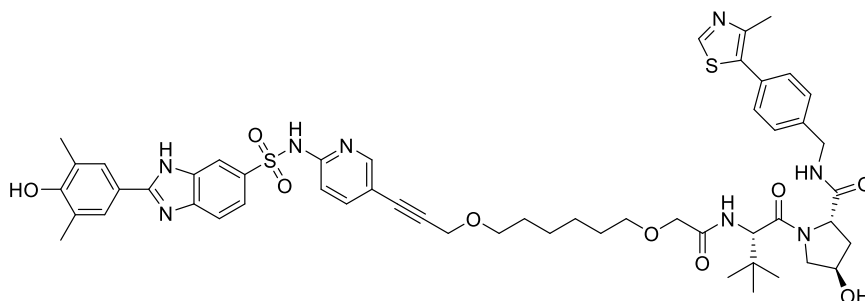
Synthesis of (2S,4R)-1-((S)-2-(tert-butyl)-18-(6-((2-(4-hydroxy-3,5-dimethylphenyl)-1H-benzimidazole)-6-sulfonamido)pyridin-3-yl)-4-oxo-6,9,12,15-tetraoxa-3-azaocadec-17-ynoyl)-4-hydroxy-N-(4-(4-methylthiazol-5-yl)benzyl)pyrrolidine-2-carboxamide (33)



To a solution of compound **106** (3.45 mg, 0.0054 mmol) in dry 0.300 mL DMF mL, a solution of compound **104** (2.52 mg, 0.0054 mmol) in 0.100 mL of dry DMF, PyOXIM (2.65 mg, 0.0054 mmol), and DIPEA (0.009 mL, 0.0504 mmol) were added. The reaction mixture was left to stir for 1 h and monitored by LC-MS (acidic method). When completed, the crude reaction was purified by HPLC with a gradient from 5% to 90% v/v acetonitrile with 0.01% v/v aqueous solution of formic acid over 20 min to yield the title compound (2.81 mg, 50%).

^1H NMR (500 MHz, CD_3OD) δ 8.82 (s, 1H), 8.18 (s, 1H), 8.14 (s, 1H), 7.81 (dd, $J = 8.6, 1.8$ Hz, 1H), 7.71 (s, 2H), 7.66 – 7.59 (m, 2H), 7.43 – 7.38 (m, 2H), 7.35 (d, $J = 8.3$ Hz, 2H), 7.17 (d, $J = 8.6$ Hz, 1H), 4.66 (s, 1H), 4.59 – 4.54 (m, 1H), 4.52 – 4.46 (m, 2H), 4.33 (s, 2H), 4.32 – 4.26 (m, 1H), 4.04 – 3.94 (m, 2H), 3.89 – 3.82 (m, 1H), 3.80 – 3.73 (m, 1H), 3.67 – 3.57 (m, 12H), 2.43 (s, 3H), 2.30 (s, 6H), 2.21 – 2.18 (m, 1H), 2.06 – 2.03 (m, 1H), 1.00 (s, 9H). ^{13}C NMR (126 MHz, CD_3OD) δ 173.00, 170.73, 170.31, 156.40, 151.42, 147.59, 138.77, 132.00, 130.05, 128.94, 127.51, 127.21, 124.93, 121.15, 119.59, 87.41, 81.87, 70.88, 70.23, 70.19, 70.05, 70.02, 69.67, 69.65, 68.86, 59.42, 58.19, 56.73, 45.96, 42.30, 37.54, 35.69, 26.00, 15.42, 14.43. LC/MS 3.5-3.8 min, m/z : 526.2072, 1051.2073 ($\text{M}+\text{H}$) $^+$.

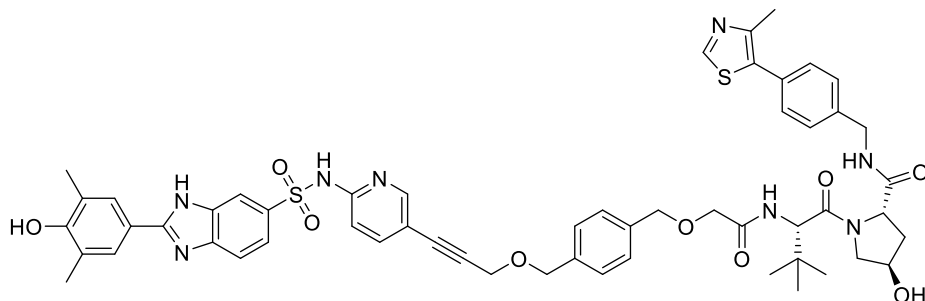
Synthesis of (2S,4R)-4-hydroxy-1-((S)-2-(2-((6-((3-(6-((2-(4-hydroxy-3,5-dimethylphenyl)-1H-benzo[d]imidazole)-6-sulfonamido)pyridin-3-yl)prop-2-yn-1-yl)oxy)hexyl)oxy)acetamido)-3,3-dimethylbutanoyl)-N-(4-(4-methylthiazol-5-yl)benzyl)pyrrolidine-2-carboxamide (34)



Compound **34** was obtained as a white solid (1.5 mg, 32%) from derivative **107** (3 mg, 0.0045 mmol) and the intermediate **104** (2.31 mg, 0.0045 mmol) according to the procedure described for **33**.

¹H NMR (500 MHz, CD₃OD) δ 8.80 (s, 1H), 8.23 – 8.15 (m, 1H), 8.14 – 8.09 (m, 1H), 7.81 (dd, J = 8.6, 1.8 Hz, 1H), 7.70 (s, 2H), 7.58 (dd, J = 8.7, 2.3 Hz, 2H), 7.42 – 7.38 (m, 2H), 7.37 – 7.31 (m, 2H), 7.16 – 7.12 (m, 1H), 4.66 (s, 1H), 4.61 – 4.55 (m, 1H), 4.53 – 4.46 (m, 2H), 4.30 (d, J = 1.3 Hz, 1H), 4.26 (s, 2H), 3.97 – 3.88 (m, 2H), 3.88 – 3.83 (m, 2H), 3.53 – 3.47 (m, 6H), 2.42 (s, 3H), 2.30 (s, 6H), 2.25 – 2.17 (m, 1H), 2.10 – 2.02 (m, 1H), 1.65 – 1.53 (m, 6H), 0.99 (s, 9H). ¹³C NMR (126 MHz, CD₃OD) δ 172.96, 170.63, 170.27, 151.39, 147.56, 138.74, 132.01, 130.04, 128.92, 127.50, 127.27, 124.92, 119.66, 71.44, 69.68, 69.55, 69.31, 59.42, 57.89, 56.73, 56.56, 42.30, 37.53, 35.83, 29.17, 29.08, 25.58, 25.55, 25.49, 15.41, 14.42. LC/MS 3.7-3.9 min, *m/z*: 510.2151, 1019.4473 (M+H)⁺.

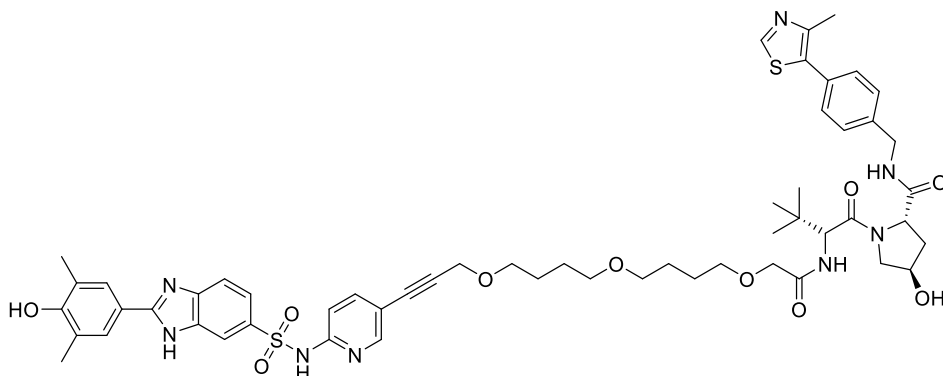
Synthesis of (2S,4R)-4-hydroxy-1-((S)-2-(2-((4-(((3-(6-((2-(4-hydroxy-3,5-dimethylphenyl)-1H-benzodimidazole)-6-sulfonamido)pyridin-3-yl)prop-2-yn-1-yl)oxy)methyl)benzyl)oxy)acetamido)-3,3-dimethylbutanoyl)-N-(4-(4-methylthiazol-5-yl)benzyl)pyrrolidine-2-carboxamide (35)



Compound **35** was obtained as a white solid (1.52 mg, 42%) from derivative **108** (2.2 mg, 0.0035 mmol) and the intermediate **104** (1.64 mg, 0.0035 mmol) according to the procedure described for **33**.

^1H NMR (500 MHz, CD_3OD) δ 8.80 (s, 1H), 8.22 – 8.13 (m, 1H), 8.12 (d, $J = 2.2$ Hz, 1H), 7.81 (dd, $J = 8.5, 1.8$ Hz, 1H), 7.70 (s, 2H), 7.62 (dd, $J = 8.7, 2.3$ Hz, 2H), 7.44 – 7.39 (m, 2H), 7.40 – 7.34 (m, 2H), 7.36 – 7.30 (m, 4H), 7.17 (d, $J = 8.6$ Hz, 1H), 4.68 (s, 1H), 4.64 – 4.58 (m, 1H), 4.58 (s, 2H), 4.56 (s, 2H), 4.55 – 4.47 (m, 2H), 4.32 (s, 2H), 4.31 – 4.24 (m, 1H), 4.06 – 3.93 (m, 2H), 3.90 – 3.84 (m, 1H), 3.82 – 3.75 (m, 1H), 2.41 (s, 3H), 2.30 (s, 6H), 2.26 – 2.17 (m, 1H), 2.11 – 2.05 (m, 1H), 1.00 (s, 9H). ^{13}C NMR (126 MHz, CD_3OD) δ 172.97, 170.33, 156.38, 151.38, 147.57, 138.76, 137.58, 136.86, 132.02, 130.02, 128.90, 128.02, 127.77, 127.50, 127.20, 124.92, 119.61, 87.24, 72.81, 71.06, 69.70, 68.53, 59.48, 57.18, 56.76, 56.69, 42.28, 37.53, 35.84, 35.13, 31.68, 29.43, 29.22, 29.07, 28.96, 28.84, 26.73, 25.49, 15.41, 14.42, 13.05. LC/MS 3.7-3.9 min, m/z : 520.2514, 1039.5043 ($\text{M}+\text{H}$) $^+$.

Synthesis of (2S,4R)-1-((S)-2-(tert-butyl)-19-(6-((2-(4-hydroxy-3,5-dimethylphenyl)-1H-benzo[d]imidazole)-6-sulfonamido)pyridin-3-yl)-4-oxo-6,11,16-trioxa-3-azanonadec-18-ynoyl)-4-hydroxy-N-(4-(4-methylthiazol-5-yl)benzyl)pyrrolidine-2-carboxamide (36)



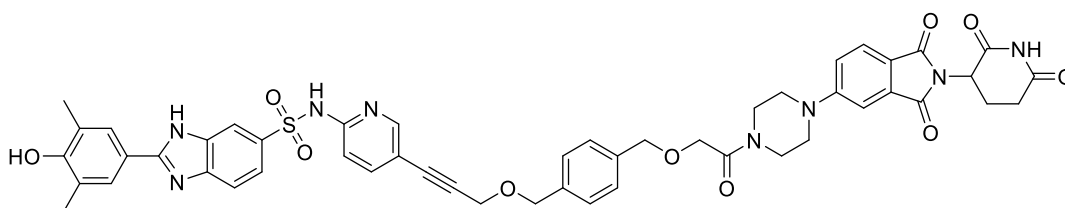
Compound **36** was obtained as a white solid (2.41 mg, 32%) from derivative **109** (4.75 mg, 0.0073 mmol) and the intermediate **104** (3.4 mg, 0.0073 mmol) according to the procedure described for **33**.

^1H NMR (500 MHz, CD_3OD) δ 8.83 (s, 1H), 8.23 – 8.15 (m, 1H), 8.14 (d, $J = 2.2$ Hz, 1H), 7.81 (dd, $J = 8.6, 1.8$ Hz, 1H), 7.70 (s, 2H), 7.62 (dd, $J = 8.7, 2.3$ Hz, 2H), 7.42 (d, $J = 3.0$ Hz, 1H), 7.40 (s, 1H), 7.38 – 7.33 (m, 2H), 7.16 (d, $J = 8.7$ Hz, 1H), 4.68 (s, 1H), 4.62 – 4.55 (m, 1H), 4.52 – 4.48 (m, 2H), 4.31 (d, $J = 6.3$ Hz, 1H), 4.28 (s, 2H), 3.97 – 3.90 (m, 2H), 3.89 – 3.84 (m, 1H), 3.82– 3.75 (m, 1H), 3.53 – 3.50 (m, 2H), 3.48 (t, $J = 5.8$ Hz, 2H), 3.40 – 3.36 (m, 4H), 2.43 (s, 3H), 2.30 (s, 6H), 2.26 – 2.19 (m, 1H), 2.11 – 2.05 (m, 1H), 1.62 – 1.57 (m, 8H), 1.01 (s, 9H). ^{13}C NMR (126 MHz, CD_3OD) δ 172.95, 170.59, 170.33, 156.37, 151.41, 147.58, 140.88, 138.76, 132.02, 130.05, 128.93, 128.09, 127.51, 127.19, 124.92, 119.63, 87.56, 81.71, 71.25, 70.09, 70.04, 69.68, 69.42, 69.27, 59.45, 57.87, 56.76, 56.60, 42.30, 37.55, 35.81, 26.05, 25.98, 25.97, 25.94, 25.52, 15.42, 14.43. LC/MS 3.7-3.9 min, m/z : 532.2278, 1063.4492 ($\text{M}+\text{H}$) $^+$.

Compound **38** was obtained as a yellow solid (1.5 mg, 27%) from derivative **107** (3.64 mg, 0.006 mmol) and the intermediate **105** (2.49 mg, 0.006 mmol) according to the procedure described for **33**.

¹H NMR (400 MHz, DMSO-*d*₆) δ 11.08 (s, 1H), 8.90 (s, 1H), 8.22 (s, 1H), 8.06 (s, 1H), 7.77 (s, 2H), 7.73 (dd, *J* = 8.7, 2.3 Hz, 1H), 7.72 – 7.65 (m, 2H), 7.64 (s, 1H), 7.34 (d, *J* = 2.3 Hz, 1H), 7.22 (dd, *J* = 8.7, 2.3 Hz, 1H), 7.12 (d, *J* = 8.8 Hz, 1H), 5.13 – 5.02 (m, 1H), 4.29 (s, 2H), 4.12 (s, 2H), 3.59 – 3.53 (m, 4H), 3.52 – 3.45 (m, 4H), 2.94 – 2.81 (m, 2H), 2.69 – 2.60 (m, 2H), 2.25 (s, 6H), 2.07 – 1.93 (m, 4H), 1.53 – 1.44 (m, 4H), 1.34 – 1.26 (m, 4H). ¹³C NMR (126 MHz, (CD₃)₂CO) δ 171.84, 171.80, 169.45, 168.34, 167.57, 167.00, 155.37, 152.89, 150.86, 141.24, 134.40, 128.77, 125.61, 124.72, 124.17, 119.88, 118.18, 114.41, 108.20, 88.75, 81.63, 70.85, 69.90, 69.25, 57.97, 49.20, 47.44, 41.01, 40.46, 31.10, 25.60, 25.49, 22.53, 15.78. LC/MS 3.6-3.7 min, *m/z*: 931.3247 (M+H)⁺.

Synthesis of N-(5-(3-(((4-((2-(4-(2-(2,6-dioxopiperidin-3-yl)-1,3-dioxoisindolin-5-yl)piperazin-1-yl)-2-oxoethoxy)methyl)benzyl)oxy)prop-1-yn-1-yl)pyridin-2-yl)-2-(4-hydroxy-3,5-dimethylphenyl)-1H-benzo[d]imidazole-6-sulfonamide (39)

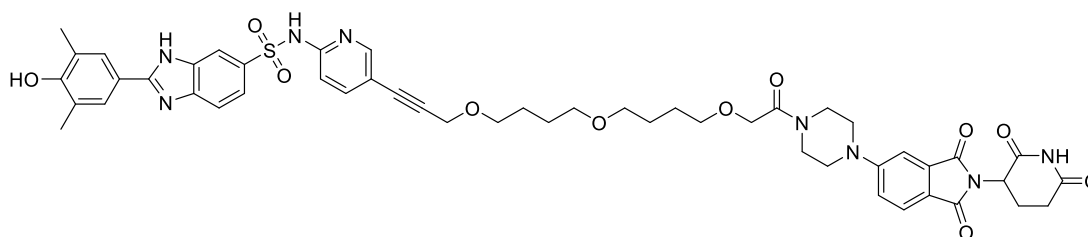


Compound **39** was obtained as a yellow solid (2.53 mg, 76%) from derivative **108** (2.2 mg, 0.0035 mmol) and the intermediate **105** (1.45 mg, 0.0035 mmol) according to the procedure described for **33**.

¹H NMR (400 MHz, DMSO-*d*₆) δ 11.05 (s, 1H), 8.82 (s, 1H), 8.19 (d, *J* = 7.5 Hz, 1H), 8.08 (s, 1H), 7.96 (s, 1H), 7.76 (s, 2H), 7.71 – 7.53 (m, 4H), 7.33 (d, *J* = 8.8 Hz, 4H), 7.23 (dd, *J* = 8.6,

2.3 Hz, 1H), 7.08 – 6.99 (m, 1H), 5.10 – 5.01 (m, 1H), 4.54 (s, 2H), 4.52 (s, 2H), 4.37 (s, 2H), 4.24 (s, 2H), 3.59 (s, 4H), 3.49 (s, 4H), 2.94 – 2.82 (m, 2H), 2.26 (s, 6H), 2.07 – 1.95 (m, 2H). ^{13}C NMR (126 MHz, $(\text{CD}_3)_2\text{CO}$) δ 171.87, 169.41, 167.59, 167.44, 167.03, 155.86, 155.44, 151.33, 150.78, 140.91, 137.59, 134.41, 133.43, 127.93, 127.41, 124.71, 124.51, 120.99, 120.85, 119.83, 118.18, 111.41, 108.22, 87.87, 82.41, 72.38, 71.07, 69.41, 57.42, 49.21, 47.48, 47.01, 44.16, 40.83, 31.13, 22.54, 15.83. LC/MS 3.4-3.6 min, m/z : 951.2 (M+H) $^+$.

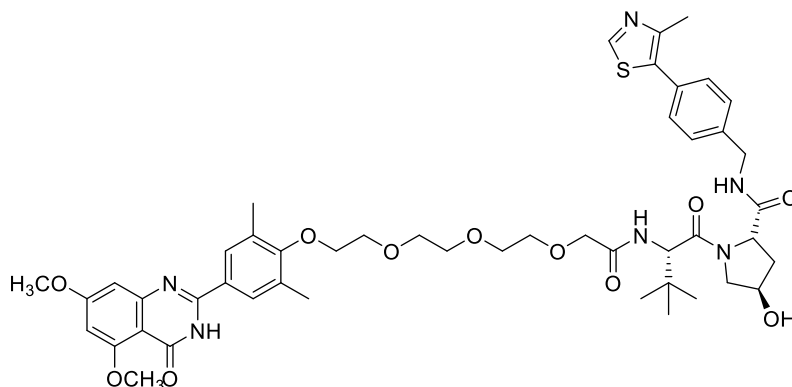
Synthesis of N-(5-(3-(4-(4-(2-(4-(2-(2,6-dioxopiperidin-3-yl)-1,3-dioxoisindolin-5-yl)piperazin-1-yl)-2-oxoethoxy)butoxy)butoxy)prop-1-yn-1-yl)pyridin-2-yl)-2-(4-hydroxy-3,5-dimethylphenyl)-1H-benzof[d]imidazole-6-sulfonamide (40)



Compound **40** was obtained as a yellow solid (2.67 mg, 38%) from derivative **109** (4.75 mg, 0.0073 mmol) and the intermediate **105** (3.03 mg, 0.0073 mmol) according to the procedure described for **33**.

^1H NMR (500 MHz, DMSO- d_6) δ 11.04 (s, 1H), 8.81 (s, 1H), 8.17 – 8.11 (m, 1H), 8.06 (s, 1H), 7.94 (s, 1H), 7.76 (s, 2H), 7.68 (d, J = 8.3 Hz, 1H), 7.64 – 7.48 (m, 2H), 7.34 (s, 1H), 7.23 (d, J = 8.6 Hz, 1H), 7.03 – 6.93 (m, 1H), 5.11 – 5.01 (m, 1H), 4.28 (s, 2H), 4.13 (s, 2H), 3.60 – 3.56 (m, 4H), 3.53 – 3.38 (m, 8H), 3.35 – 3.31 (m, 4H), 2.96 – 2.81 (m, 2H), 2.25 (s, 6H), 2.08 – 1.96 (m, 2H), 1.51 (s, 8H). ^{13}C NMR (126 MHz, DMSO) δ 173.21, 170.49, 168.12, 167.98, 167.43, 155.34, 134.34, 130.12, 127.56, 125.38, 125.17, 120.79, 119.06, 118.31, 108.47, 70.74, 70.07, 69.84, 69.52, 58.39, 49.30, 47.36, 46.95, 44.05, 35.60, 31.46, 26.42, 26.32, 22.66, 17.14. LC/MS 3.5-3.7 min, m/z : 975.3739 (M+H) $^+$.

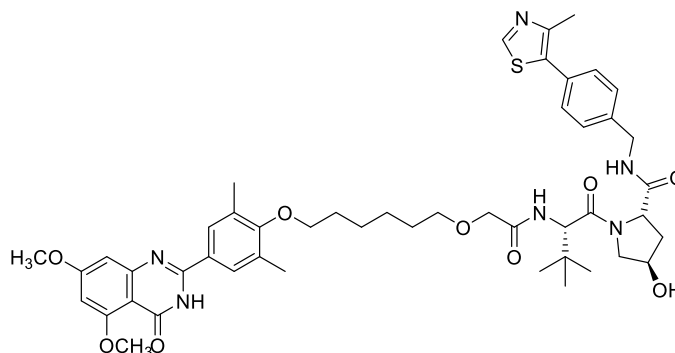
Synthesis of (2S,4R)-1-((S)-2-(tert-butyl)-14-(4-(5,7-dimethoxy-4-oxo-3,4-dihydroquinazolin-2-yl)-2,6-dimethylphenoxy)-4-oxo-6,9,12-trioxa-3-azatetradecanoyl)-4-hydroxy-N-(4-(4-methylthiazol-5-yl)benzyl)pyrrolidine-2-carboxamide (41)



To a solution of carboxylic compound **110** (25 mg, 0.047 mmol) in dry 0.300 mL DMF mL COMU (20 mg, 0.047 mmol), compound **104** (22 mg, 0.047 mmol) in 0.100 mL of dry DMF and DIPEA (0.033 mL, 0.188 mmol) were added. The reaction mixture was left to stir for 1 h and monitored by LC-MS (acidic method). When completed, the crude reaction was purified by HPLC with a gradient from 5% to 90% v/v acetonitrile with 0.01% v/v aqueous solution of formic acid over 15 min to yield the title compound (20 mg, 46%).

^1H NMR (500 MHz, CD_3OD) δ 8.87 (s, 1H), 7.66 (s, 2H), 7.42 (d, $J = 8.8$ Hz, 2H), 7.38 (d, $J = 8.2$ Hz, 2H), 6.76 (d, $J = 2.2$ Hz, 1H), 6.60 (d, $J = 2.2$ Hz, 1H), 4.69 (s, 1H), 4.62 – 4.54 (m, 1H), 4.54 – 4.47 (m, 2H), 4.36 – 4.30 (m, 1H), 4.04 (d, $J = 6.6$ Hz, 2H), 3.93 (s, 6H), 3.90 – 3.84 (m, 2H), 3.84 – 3.76 (m, 2H), 3.76 – 3.66 (m, 10H), 2.44 (s, 3H), 2.36 (s, 6H), 2.22 (s, 1H), 2.17 – 2.04 (m, 1H), 1.04 (s, 9H). ^{13}C NMR (126 MHz, CD_3OD) δ 172.93, 170.68, 170.33, 166.06, 161.78, 160.08, 159.86, 155.34, 151.49, 148.76, 147.39, 138.90, 132.12, 129.98, 129.06, 128.94, 128.62, 128.09, 127.56, 124.81, 103.46, 98.15, 97.89, 71.80, 71.00, 70.48, 70.43, 70.21, 69.76, 69.67, 59.44, 56.77, 56.71, 55.35, 55.13, 42.33, 37.55, 35.69, 25.61, 15.43, 14.36. LC/MS 3.7-3.9 min, m/z : 465.2115, 929.4130 ($\text{M}+\text{H}$) $^+$.

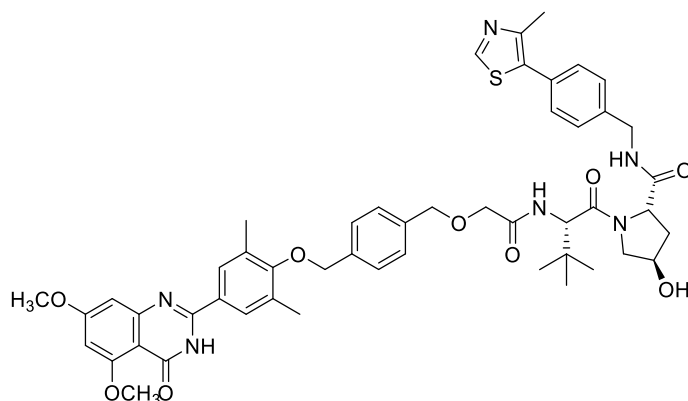
Synthesis of (2S,4R)-1-((S)-2-(2-((6-(4-(5,7-dimethoxy-4-oxo-3,4-dihydroquinazolin-2-yl)-2,6-dimethylphenoxy)hexyl)oxy)acetamido)-3,3-dimethylbutanoyl)-4-hydroxy-N-(4-(4-methylthiazol-5-yl)benzyl)pyrrolidine-2-carboxamide (42)



Compound **42** was obtained as a white solid (20.5 mg, 42%) from derivative **111** (27 mg, 0.055 mmol) and the intermediate **104** (26 mg, 0.055 mmol) according to the procedure described for **41**.

¹H NMR (500 MHz, CD₃OD) δ 8.81 (s, 1H), 7.64 (s, 2H), 7.45 – 7.39 (m, 2H), 7.36 (d, J = 8.3 Hz, 2H), 6.74 (d, J = 2.3 Hz, 1H), 6.52 (d, J = 2.3 Hz, 1H), 4.73 – 4.67 (m, 1H), 4.62 – 4.55 (m, 1H), 4.53 – 4.47 (m, 2H), 4.36 – 4.28 (m, 1H), 3.97 (d, J = 7.8 Hz, 2H), 3.90 (d, J = 1.4 Hz, 6H), 3.80 (dd, J = 7.8, 5.1 Hz, 2H), 3.58 (t, J = 6.3 Hz, 2H), 2.42 (s, 3H), 2.29 (s, 6H), 2.27 – 2.20 (m, 1H), 2.15 – 2.04 (m, 1H), 1.87 – 1.80 (m, 2H), 1.74 – 1.67 (m, 2H), 1.62 – 1.52 (m, 6H), 1.03 (s, 9H). ¹³C NMR (126 MHz, CD₃OD) δ 172.87, 170.68, 170.61, 170.34, 165.61, 161.45, 161.08, 161.04, 159.45, 154.20, 151.85, 151.34, 147.57, 138.79, 131.99, 131.57, 130.09, 129.10, 128.92, 128.23, 128.09, 127.54, 126.68, 103.96, 99.74, 97.53, 72.01, 71.49, 69.68, 69.41, 59.71, 59.44, 56.75, 56.69, 56.61, 55.14, 54.93, 42.35, 37.55, 35.81, 30.03, 29.25, 25.76, 25.65, 25.57, 15.34, 14.44. LC/MS 4.1- 4.3 min, *m/z*: 449.2164, 897.4281 (M+H)⁺.

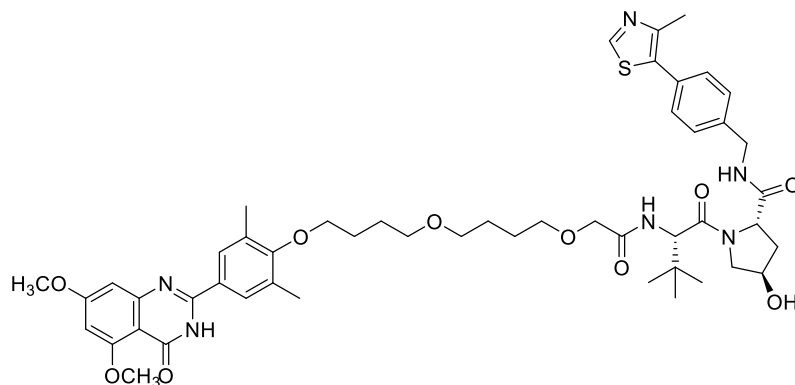
Synthesis of (2S,4R)-1-((S)-2-(2-((4-((4-(5,7-dimethoxy-4-oxo-3,4-dihydroquinazolin-2-yl)-2,6-dimethylphenoxy)methyl)benzyl)oxy)acetamido)-3,3-dimethylbutanoyl)-4-hydroxy-N-(4-(4-methylthiazol-5-yl)benzyl)pyrrolidine-2-carboxamide (43)



Compound **43** was obtained as a white solid (15 mg, 36%) from derivative **112** (23 mg, 0.045 mmol) and the intermediate **104** (21 mg, 0.045 mmol) according to the procedure described for **41**.

¹H NMR (500 MHz, CD₃OD) δ 8.81 (s, 1H), 7.70 (s, 2H), 7.46 (d, J = 3.1 Hz, 4H), 7.43 (d, J = 4.1 Hz, 2H), 7.38 (d, J = 8.3 Hz, 2H), 6.81 (d, J = 2.3 Hz, 1H), 6.56 (d, J = 2.3 Hz, 1H), 4.89 (s, 2H), 4.72 (d, J = 7.1 Hz, 1H), 4.66 (d, J = 1.6 Hz, 2H), 4.58 (d, J = 4.6 Hz, 1H), 4.55 – 4.48 (m, 2H), 4.36 – 4.29 (m, 1H), 4.12 – 4.02 (m, 2H), 3.93 (s, 3H), 3.93 (s, 3H), 3.91 – 3.85 (m, 1H), 3.84 – 3.78 (m, 1H), 2.43 (s, 3H), 2.31 (s, 6H), 2.27 – 2.21 (m, 1H), 2.14 – 2.06 (m, 1H), 1.03 (s, 9H). ¹³C NMR (126 MHz, CD₃OD) δ 172.93, 170.41, 170.32, 165.58, 161.41, 151.34, 147.66, 138.84, 137.29, 137.22, 132.00, 131.76, 130.13, 128.95, 128.17, 128.06, 127.88, 127.54, 100.65, 97.49, 73.70, 72.87, 69.70, 68.67, 59.48, 56.76, 55.09, 54.87, 42.35, 37.55, 35.81, 25.53, 15.44, 14.41. LC/MS 4.0-4.1 min, *m/z*: 459.2432, 917.4872 (M+H)⁺.

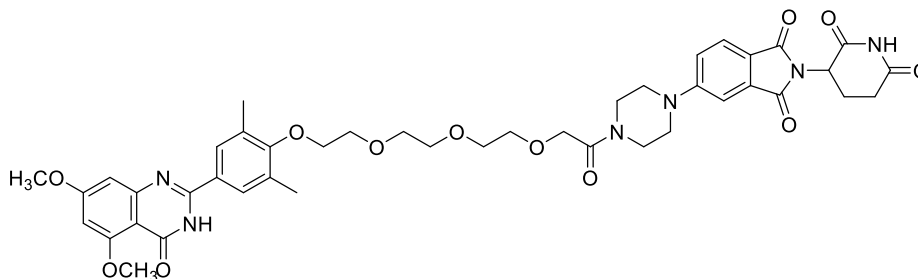
Synthesis of (2S,4R)-1-((S)-2-(2-(4-(4-(4-(5,7-dimethoxy-4-oxo-3,4-dihydroquinazolin-2-yl)-2,6-dimethylphenoxy)butoxy)butoxy)acetamido)-3,3-dimethylbutanoyl)-4-hydroxy-N-(4-(4-methylthiazol-5-yl)benzyl)pyrrolidine-2-carboxamide (44)



Compound **44** was obtained as a white solid (15 mg, 37%) from derivative **113** (22.2 mg, 0.042 mmol) and the intermediate **104** (19.6 mg, 0.042 mmol) according to the procedure described for **41**.

¹H NMR (500 MHz, CD₃OD) δ 8.84 (s, 1H), 7.68 (s, 2H), 7.45 – 7.40 (m, 2H), 7.38 (d, *J* = 8.3 Hz, 2H), 6.78 (d, *J* = 2.3 Hz, 1H), 6.57 (d, *J* = 2.3 Hz, 1H), 4.69 (s, 1H), 4.62 – 4.54 (m, 1H), 4.53 – 4.46 (m, 2H), 4.36 – 4.30 (m, 1H), 3.96 (d, *J* = 7.9 Hz, 2H), 3.93 (d, *J* = 1.2 Hz, 6H), 3.88 (d, *J* = 7.1 Hz, 1H), 3.85 (d, *J* = 6.5 Hz, 2H), 3.82 – 3.78 (m, 1H), 3.58 (t, *J* = 5.8 Hz, 2H), 3.53 – 3.47 (m, 4H), 2.45 (s, 3H), 2.34 (s, 6H), 2.29 – 2.19 (m, 1H), 2.14 – 2.07 (m, 1H), 1.92 – 1.85 (m, 2H), 1.82 – 1.76 (m, 2H), 1.74 – 1.68 (m, 4H), 1.03 (s, 9H). ¹³C NMR (126 MHz, CD₃OD) δ 171.44, 169.13, 168.91, 164.32, 161.60, 160.11, 159.46, 158.16, 153.11, 149.92, 146.13, 137.38, 130.58, 130.24, 128.64, 127.64, 127.49, 126.88, 126.64, 126.10, 124.97, 102.43, 98.00, 96.17, 70.63, 69.95, 68.79, 68.23, 67.93, 57.99, 55.29, 55.18, 53.74, 53.52, 40.89, 36.09, 34.33, 25.59, 24.72, 24.65, 24.10, 13.90. LC/MS 4.1-4.3 min, *m/z*: 471.2740, 941.5496 (M+H)⁺.

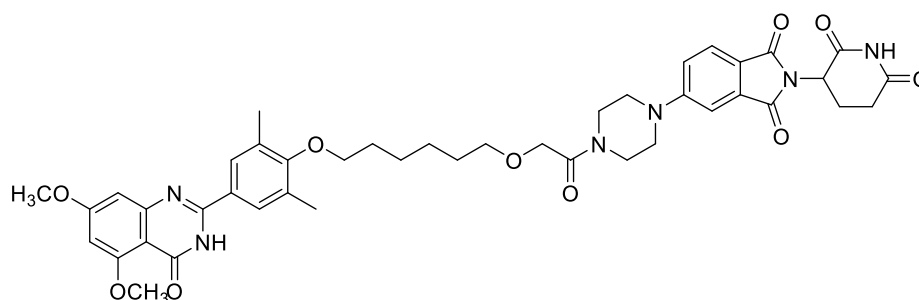
Synthesis of 5-(4-(2-(2-(2-(2-(4-(5,7-dimethoxy-4-oxo-3,4-dihydroquinazolin-2-yl)-2,6-dimethylphenoxy)ethoxy)ethoxy)ethoxy)acetyl)piperazin-1-yl)-2-(2,6-dioxopiperidin-3-yl)isoindoline-1,3-dione (45)



Compound **45** was obtained as a white solid (15 mg, 37%) from derivative **110** (25 mg, 0.047 mmol) and the intermediate **105** (18 mg, 0.047 mmol) according to the procedure described for **41**.

^1H NMR (500 MHz, CDCl_3) δ 9.74 (s, 1H), 7.71 (s, 2H), 7.65 (d, $J = 8.4$ Hz, 1H), 7.20 (d, $J = 2.3$ Hz, 1H), 7.03 (dd, $J = 8.5, 2.4$ Hz, 1H), 6.79 (d, $J = 2.3$ Hz, 1H), 6.43 (d, $J = 2.3$ Hz, 1H), 5.03 – 4.95 (m, 1H), 4.27 (d, $J = 2.0$ Hz, 2H), 3.96 (s, 3H), 3.91 (s, 3H), 3.86 (t, $J = 4.8$ Hz, 2H), 3.83 – 3.75 (m, 6H), 3.75 – 3.62 (m, 8H), 3.51 – 3.40 (m, 4H), 2.96 – 2.68 (m, 4H), 2.18 (s, 6H). ^{13}C NMR (126 MHz, CDCl_3) δ 169.20, 168.10, 166.31, 165.85, 165.23, 163.37, 161.38, 159.65, 156.92, 153.24, 152.12, 150.52, 132.50, 129.74, 125.86, 123.56, 118.45, 116.32, 106.90, 103.03, 99.42, 96.35, 69.71, 69.44, 69.10, 68.88, 68.75, 68.70, 54.48, 53.85, 47.49, 45.94, 45.44, 43.05, 42.75, 39.56, 29.72, 20.92, 14.38. LC/MS 3.5-3.7 min, m/z : 841.3401 ($\text{M}+\text{H}$) $^+$.

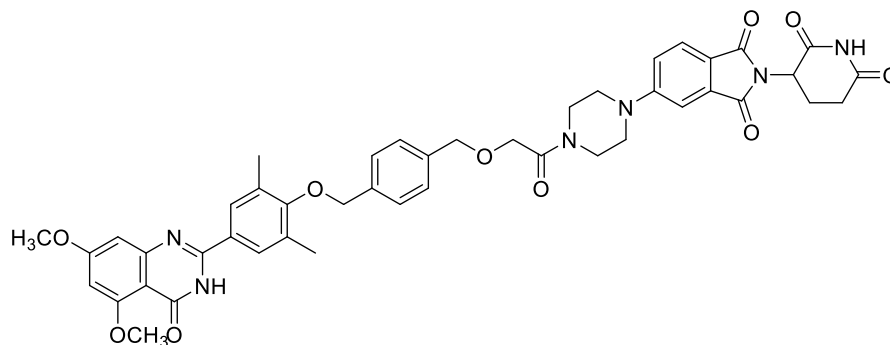
Synthesis of 5-(4-(2-((6-(4-(5,7-dimethoxy-4-oxo-3,4-dihydroquinazolin-2-yl)-2,6-dimethylphenoxy)hexyl)oxy)acetyl)piperazin-1-yl)-2-(2,6-dioxopiperidin-3-yl)isoindoline-1,3-dione (46)



Compound **46** was obtained as a white solid (20 mg, 45%) from derivative **111** (27 mg, 0.055 mmol) and the intermediate **105** (21 mg, 0.055 mmol) according to the procedure described for **41**.

^1H NMR (500 MHz, CDCl_3) δ 9.75 (s, 1H), 7.81 (s, 2H), 7.69 (d, $J = 8.4$ Hz, 1H), 7.25 (d, $J = 3.0$ Hz, 2H), 7.08 (dd, $J = 8.5, 2.4$ Hz, 1H), 6.45 (d, $J = 2.2$ Hz, 1H), 5.06 – 4.93 (m, 1H), 4.27 – 4.13 (m, 2H), 3.94 (s, 3H), 3.94 (s, 3H), 3.87 – 3.75 (m, 4H), 3.72 (t, $J = 7.3$ Hz, 2H), 3.55 (t, $J = 5.8$ Hz, 3H), 3.50 – 3.36 (m, 4H), 2.96 – 2.71 (m, 4H), 2.14 (s, 6H), 1.81 – 1.72 (m, 2H), 1.71 – 1.62 (m, 2H), 1.56 – 1.40 (m, 4H). ^{13}C NMR (126 MHz, CDCl_3) δ 170.99, 170.13, 168.31, 167.65, 161.55, 155.28, 134.28, 132.00, 128.51, 125.44, 120.64, 118.52, 108.98, 98.79, 72.30, 71.40, 71.24, 56.39, 56.01, 49.31, 48.29, 47.34, 44.77, 41.29, 31.54, 30.41, 29.50, 26.01, 25.76, 22.76, 16.19. LC/MS 4.0-4.2 min, m/z : 809.3522 ($\text{M}+\text{H}$) $^+$.

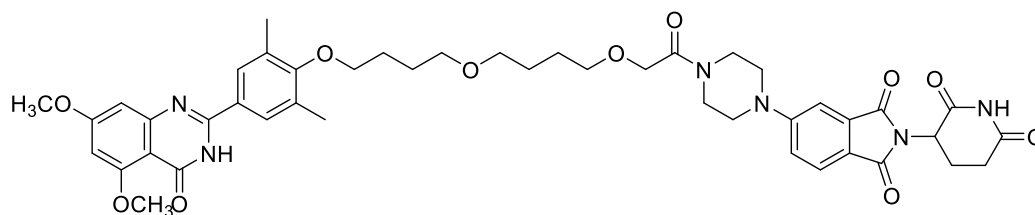
Synthesis of 5-(4-(2-((4-((4-(5,7-dimethoxy-4-oxo-3,4-dihydroquinazolin-2-yl)-2,6-dimethylphenoxy)methyl)benzyl)oxy)acetyl)piperazin-1-yl)-2-(2,6-dioxopiperidin-3-yl)isoindoline-1,3-dione
(47)



Compound **47** was obtained as a white solid (10 mg, 27%) from derivative **112** (23 mg, 0.045 mmol) and the intermediate **105** (19 mg, 0.045 mmol) according to the procedure described for **41**.

¹H NMR (500 MHz, CDCl₃) δ 10.07 (s, 1H), 7.74 (s, 2H), 7.65 (d, J = 8.4 Hz, 1H), 7.43 (d, J = 8.1 Hz, 2H), 7.40 (d, J = 8.2 Hz, 2H), 7.22 (d, J = 2.3 Hz, 1H), 6.98 (dd, J = 8.5, 2.3 Hz, 1H), 6.83 (d, J = 2.3 Hz, 1H), 6.45 (d, J = 2.3 Hz, 1H), 5.02 – 4.94 (m, 1H), 4.74 (s, 2H), 4.72 – 4.58 (m, 2H), 4.34 – 4.23 (m, 2H), 3.97 (s, 3H), 3.92 (s, 3H), 3.77 – 3.56 (m, 4H), 3.31 – 3.16 (m, 2H), 3.14 – 3.05 (m, 2H), 2.98 – 2.69 (m, 4H), 2.15 (s, 6H). ¹³C NMR (126 MHz, CDCl₃) δ 170.93, 170.21, 168.22, 167.60, 167.01, 165.30, 161.53, 161.43, 158.79, 155.24, 152.48, 137.43, 137.21, 134.23, 131.77, 129.01, 128.00, 127.71, 125.36, 120.58, 118.17, 109.10, 104.79, 101.10, 98.30, 73.72, 73.53, 70.81, 56.34, 55.73, 49.31, 47.34, 47.12, 44.42, 41.19, 41.02, 31.59, 22.73, 16.25. LC/MS 3.9-4.0 min, *m/z*: 829.3174 (M+H)⁺.

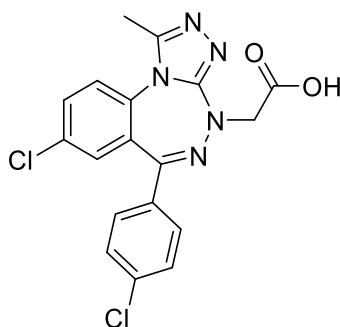
Synthesis of 5-(4-(2-(4-(4-(4-(5,7-dimethoxy-4-oxo-3,4-dihydroquinazolin-2-yl)-2,6-dimethylphenoxy)butoxy)butoxy)acetyl)piperazin-1-yl)-2-(2,6-dioxopiperidin-3-yl)isoindoline-1,3-dione (48)



Compound **48** was obtained as a white solid (11 mg, 31%) from derivative **113** (23 mg, 0.042 mmol) and the intermediate **105** (16 mg, 0.042 mmol) according to the procedure described for **41**.

¹H NMR (500 MHz, CDCl₃) δ 9.61 (s, 1H), 7.74 (s, 2H), 7.70 (d, J = 8.5 Hz, 1H), 7.28 (d, J = 2.6 Hz, 1H), 7.07 (dd, J = 8.5, 2.4 Hz, 1H), 6.87 (d, J = 2.3 Hz, 1H), 6.47 (d, J = 2.3 Hz, 1H), 5.04 – 4.96 (m, 1H), 4.21 (d, J = 1.1 Hz, 2H), 3.98 (s, 3H), 3.95 (s, 3H), 3.81 (q, J = 5.2 Hz, 4H), 3.76 (t, J = 6.4 Hz, 2H), 3.58 (t, J = 6.1 Hz, 2H), 3.54 – 3.45 (m, 6H), 2.98 – 2.72 (m, 4H), 2.22 (s, 6H), 1.92 – 1.85 (m, 2H), 1.83 – 1.76 (m, 2H), 1.73 – 1.62 (m, 6H). ¹³C NMR (126 MHz, CDCl₃) δ 171.04, 169.72, 168.32, 167.64, 167.02, 165.45, 161.51, 161.01, 159.49, 155.02, 152.84, 134.33, 131.90, 127.98, 125.43, 120.37, 118.20, 108.82, 104.55, 100.59, 98.43, 72.18, 71.31, 71.05, 70.52, 70.41, 56.35, 55.82, 49.28, 47.85, 47.33, 44.64, 41.35, 41.01, 31.52, 29.68, 29.14, 27.42, 26.57, 26.47, 26.40, 22.75, 16.23, 14.08. LC/MS 3.9-3.1 min, *m/z*: 853.4184 (M+H)⁺.

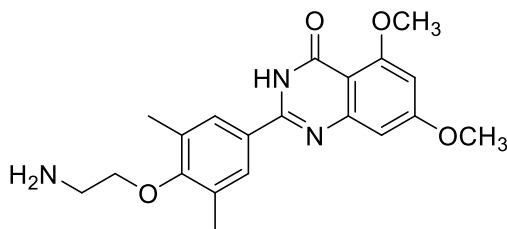
Synthesis of 2-(8-chloro-6-(4-chlorophenyl)-1-methyl-4H-benzo[e][1,2,4]triazolo[3,4-c][1,2,4]triazepin-4-yl)acetic acid (49)



An aqueous solution (3.5 mL) of LiOH (12 mg, 0.488 mmol) was added to a solution of compound **60** (105 mg, 0.244 mmol) in 3.5 mL of EtOH and the mixture was stirring for 1 h at room temperature. Then, the mixture was concentrated in vacuo: the aqueous phase was washed with CHCl₃ (3 x 10 mL), acidified with HCl 3 N until pH 3 and extracted with EtOAc (3 x 10 mL). The collected organic phases were washed with brine, dried over Na₂SO₄, filtered and concentrated under reduced pressure. The title compound (**49**) was obtained as white solid (91 mg, 93%).

¹H NMR (400 MHz, CDCl₃) δ 7.64 (dd, J = 8.7, 2.4 Hz, 1H), 7.52 – 7.43 (m, 2H), 7.39 (d, J = 8.7 Hz, 2H), 7.32 (d, J = 8.6 Hz, 1H), 6.74 (s, 1H), 4.62 (s, 2H), 2.59 (s, 3H). MS (ESI) *m/z*: 402 (M+H)⁺

Synthesis of 2-(4-(2-aminoethoxy)-3,5-dimethylphenyl)-5,7-dimethoxyquinazolin-4(3H)-one (50)

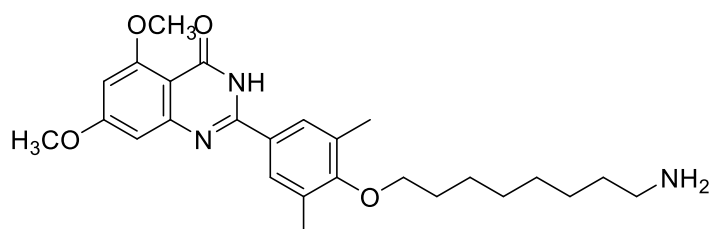


To a solution of compound **65** (50 mg, 0.111 mmol) in 1 mL of EtOH, hydrazine monohydrate (0.022 mL, 0.444 mmol) was added and the resulting mixture was stirred for 6 h at 90 °C. After cooling at room temperature, the reaction mixture was concentrated under reduced pressure.

The residual semisolid was taken up with HCl 3 N (10 mL): the aqueous phase was washed with CHCl₃ (3 x 10 mL), basified until pH 10 and extracted with EtOAc (3 x 10 mL). The collected organic phases were washed with brine, dried over sodium sulfate, filtered and concentrate under reduced pressure to give the title compound as white solid (35 mg, 85%)

¹H NMR (400 MHz, CDCl₃) δ 7.67 (s, 2H), 6.83 (d, *J* = 2.3 Hz, 1H), 6.46 (d, *J* = 2.3 Hz, 1H), 3.98 (s, 3H), 3.93 (s, 3H), 3.87 (t, *J* = 5.2 Hz, 2H), 3.13 (t, *J* = 5.2 Hz, 2H), 2.38 (s, 6H). MS (ESI) *m/z*: 370 (M+H)⁺.

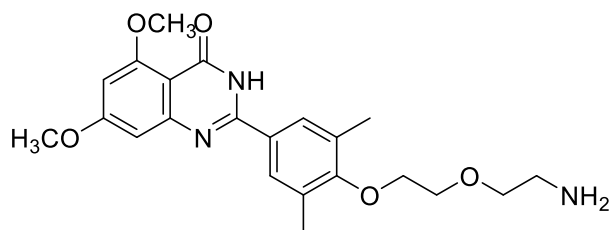
Synthesis of 2-(4-((8-aminooctyl)oxy)-3,5-dimethylphenyl)-5,7-dimethoxyquinazolin-4(3H)-one (51a)



Compound **66a** (42 mg, 0.087 mmol) was solubilized in 3 mL of EtOH and 10% Pd/C was added. The mixture was stirred under a hydrogen atmosphere (balloon) for 18 h. Then, the mixture was filtered and the filtrate evaporated to give the title compound as white solid (35 mg, 89%).

¹H NMR (400 MHz, CDCl₃) δ 7.67 (s, 2H), 6.82 (s, 1H), 6.45 (s, 1H), 3.98 (s, 3H), 3.93 (s, 3H), 3.83 – 3.74 (m, 2H), 2.74 (t, *J* = 7.1 Hz, 2H), 2.35 (s, 6H), 1.86 – 1.76 (m, 4H), 1.56 – 1.30 (m, 8H). MS (ESI) *m/z*: 454 (M+H)⁺.

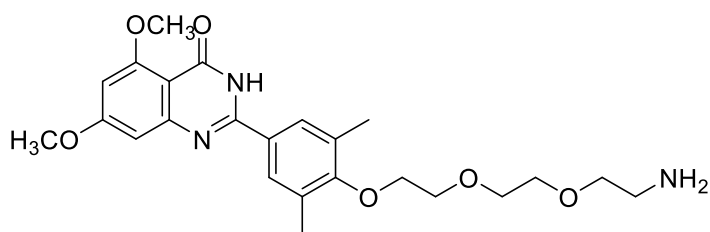
Synthesis of 2-(4-(2-(2-aminoethoxy)ethoxy)-3,5-dimethylphenyl)-5,7-dimethoxyquinazolin-4(3H)-one (51b)



Compound **51b** was obtained as a white solid (55 mg, 98%) from derivative **66b** (60 mg, 0.136 mmol) according to the procedure described for **51a**.

^1H NMR (400 MHz, CDCl_3) δ 7.66 (s, 2H), 6.82 (d, $J = 2.5$ Hz, 1H), 6.46 (d, $J = 2.3$ Hz, 1H), 4.03 – 4.00 (m, 2H), 3.98 (s, 3H), 3.93 (s, 3H), 3.83 (t, $J = 4.6$ Hz, 2H), 3.61 (t, $J = 5.2$ Hz, 2H), 2.94 (t, $J = 5.2$ Hz, 2H), 2.39 (s, 6H). MS (ESI) m/z : 414 ($\text{M}+\text{H}$) $^+$.

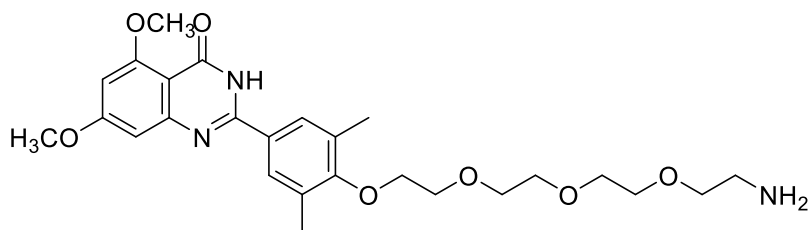
Synthesis of 2-(4-(2-(2-(2-aminoethoxy)ethoxy)ethoxy)ethoxy)-3,5-dimethylphenyl)-5,7-dimethoxyquinazolin-4(3H)-one (51c)



Compound **51c** was obtained as a white solid (50 mg, 81%) from derivative **66c** (65 mg, 0.134 mmol) according to the procedure described for **51a**.

^1H NMR (400 MHz, CDCl_3) δ 7.69 (s, 2H), 6.81 (d, $J = 2.3$ Hz, 1H), 6.44 (d, $J = 2.3$ Hz, 1H), 4.03 – 3.99 (m, 2H), 3.96 (s, 3H), 3.92 (s, 3H), 3.84 (t, $J = 4.6$ Hz, 2H), 3.76 – 3.70 (m, 3H), 3.69 – 3.63 (m, 3H), 3.54 (d, $J = 4.8$ Hz, 2H), 2.37 (s, 6H). MS (ESI) m/z : 458 ($\text{M}+\text{H}$) $^+$.

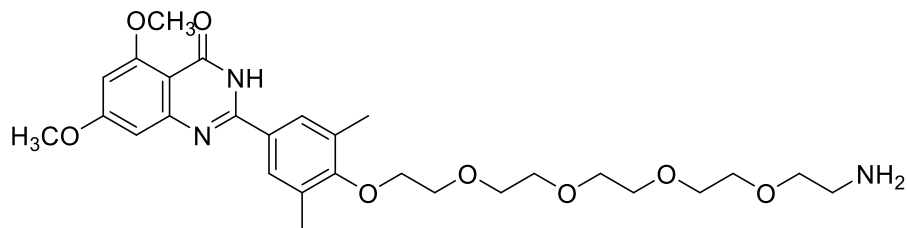
Synthesis of 2-(4-(2-(2-(2-(2-aminoethoxy)ethoxy)ethoxy)ethoxy)ethoxy)-3,5-dimethylphenyl)-5,7-dimethoxyquinazolin-4(3H)-one (51d)



Compound **51d** was obtained as a yellow oil (57 mg, 99%) from derivative **66d** (60 mg, 0.114 mmol) according to the procedure described for **51a**.

^1H NMR (400 MHz, CDCl_3) δ 7.66 (s, 2H), 6.82 (d, $J = 2.6$ Hz, 1H), 6.45 (d, $J = 2.9$ Hz, 1H), 4.03 (t, $J = 4.7$ Hz, 2H), 3.98 (s, 3H), 3.93 (s, 3H), 3.83 (d, $J = 4.5$ Hz, 2H), 3.75 – 3.61 (m, 8H), 3.52 (t, $J = 5.2$ Hz, 2H), 2.88 (t, $J = 5.2$ Hz, 2H), 2.38 (s, 6H). MS (ESI) m/z : 502 ($\text{M}+\text{H}$) $^+$.

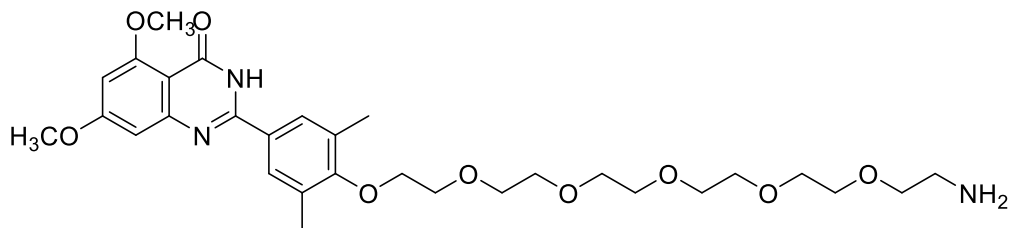
Synthesis of 2-(4-((14-amino-3,6,9,12-tetraoxatetradecyl)oxy)-3,5-dimethylphenyl)-5,7-dimethoxyquinazolin-4(3H)-one (51e)



Compound **51e** was obtained as a yellow oil (81 mg, 99 %.) from derivative **66e** (85 mg, 0.149 mmol) according to the procedure described for **51a**.

^1H NMR (400 MHz, CDCl_3) δ 7.69 (s, 2H), 6.82 (d, $J = 2.3$ Hz, 1H), 6.45 (d, $J = 2.3$ Hz, 1H), 4.01 (m, 2H), 3.97 (s, 3H), 3.92 (s, 3H), 3.85 (t, $J = 4.6$ Hz, 2H), 3.78 – 3.52 (m, 16H), 2.39 (s, 6H). MS (ESI) m/z : 546 ($\text{M}+\text{H}$) $^+$

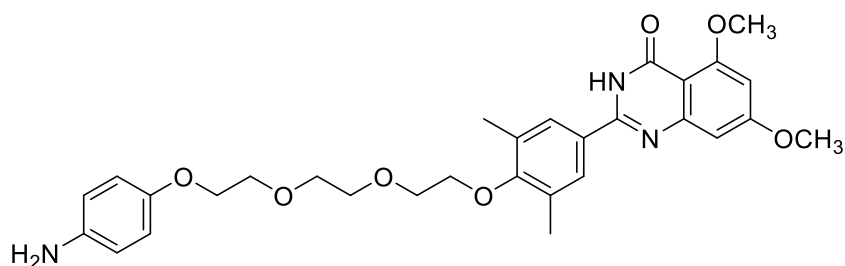
Synthesis of 2-(4-((17-amino-3,6,9,12,15-pentaoxaheptadecyl)oxy)-3,5-dimethylphenyl)-5,7-dimethoxyquinazolin-4(3H)-one (51f)



Compound **51f** was obtained as a yellow oil (45 mg, 94%) from derivative **66f** (50 mg, 0.081 mmol) according to the procedure described for **51a**.

^1H NMR (400 MHz, CDCl_3) δ 7.71 (s, 2H), 6.81 (s, 1H), 6.44 (s, 1H), 4.02 – 3.99 (m, 2H), 3.96 (s, 3H), 3.92 (s, 3H), 3.83 (d, $J = 4.5$ Hz, 2H), 3.75 – 3.59 (m, 18H), 3.53 (t, $J = 5.2$ Hz, 2H), 2.38 (s, 6H). MS (ESI) m/z : 590 ($\text{M}+\text{H}$) $^+$.

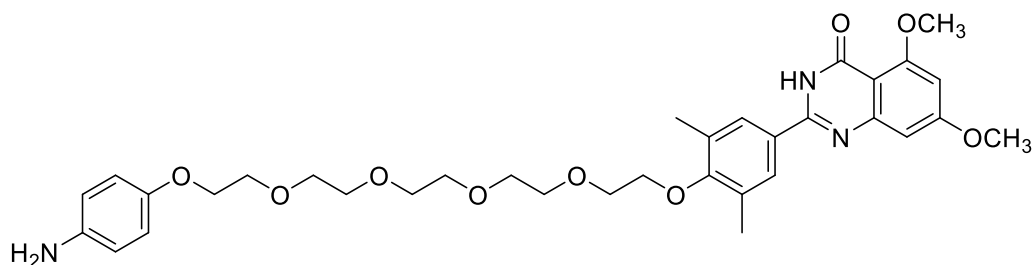
Synthesis of 2-(4-(2-(2-(2-(4-aminophenoxy)ethoxy)ethoxy)ethoxy)-3,5-dimethylphenyl)-5,7-dimethoxyquinazolin-4(3H)-one (52a)



Compound **52a** was obtained as a yellow oil (40 mg, 99%) from derivative **67a** (43 mg, 0.074 mmol) according to the procedure described for **51a**.

^1H NMR (400 MHz, CDCl_3) δ 7.74 (s, 2H), 6.81 (d, $J = 2.3$ Hz, 1H), 6.73 (d, $J = 8.3$ Hz, 2H), 6.62 (d, $J = 8.3$ Hz, 2H), 6.42 (d, $J = 2.3$ Hz, 1H), 4.04 (m, 2H), 3.97 (m, 2H), 3.92 (s, 3H), 3.91 (s, 3H), 3.83 (m, 4H), 3.75 (m, 4H), 2.33 (s, 6H). MS (ESI) m/z : 550 ($\text{M}+\text{H}$) $^+$.

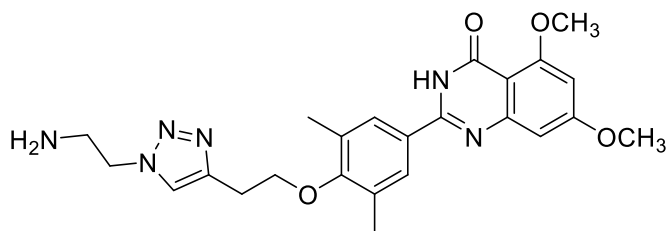
Synthesis of 2-(4-((14-(4-aminophenoxy)-3,6,9,12-tetraoxatetradecyl)oxy)-3,5-dimethylphenyl)-5,7-dimethoxyquinazolin-4(3H)-one (52b)



Compound **52b** was obtained as a yellow oil (80 mg, 84%) from derivative **67b** (100 mg, 0.150 mmol) according to the procedure described for **51a**.

^1H NMR (400 MHz, CDCl_3) δ 7.63 (s, 2H), 6.82 (d, $J = 2.3$ Hz, 1H), 6.75 (d, $J = 8.8$ Hz, 2H), 6.63 (d, $J = 8.8$ Hz, 2H), 6.46 (d, $J = 2.3$ Hz, 1H), 4.07 – 4.03 (m, 2H), 3.98 (s, 3H), 3.92 (s, 3H), 3.86 – 3.79 (m, 4H), 3.75 – 3.63 (m, 14H), 2.33 (s, 6H). MS (ESI) m/z : 638 ($\text{M}+\text{H}$) $^+$.

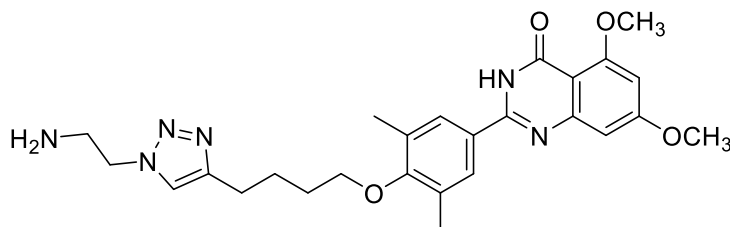
Synthesis of 2-(4-(2-(1-(2-aminoethyl)-1H-1,2,3-triazol-4-yl)ethoxy)-3,5-dimethylphenyl)-5,7-dimethoxyquinazolin-4(3H)-one (53a)



Compound **53a** was obtained as a yellow oil (52 mg, 83%) from derivative **86a** (80 mg, 0.134 mmol) according to the procedure described for **50**.

^1H NMR (400 MHz, CDCl_3) δ 7.63 (s, 2H), 7.55 (d, $J = 1.8$ Hz, 1H), 6.82 (d, $J = 2.3$ Hz, 1H), 6.46 (d, $J = 2.3$ Hz, 1H), 4.41 – 4.37 (m, 2H), 4.16 – 4.10 (m, 2H), 3.98 (s, 3H), 3.92 (s, 3H), 3.32 – 3.18 (m, 4H), 2.28 (s, 6H). MS (ESI) m/z : 465 ($\text{M}+\text{H}$) $^+$.

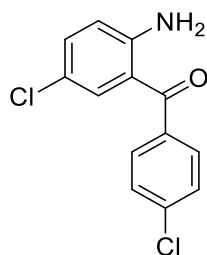
Synthesis of 2-(4-(4-(1-(2-aminoethyl)-1H-1,2,3-triazol-4-yl)butoxy)-3,5-dimethylphenyl)-5,7-dimethoxyquinazolin-4(3H)-one (53b)



Compound **53b** was obtained as a yellow oil (45 mg, 81 %) from derivative **86b** (70 mg, 0.112 mmol) according to the procedure described for **50**.

^1H NMR (400 MHz, CDCl_3) δ 7.67 (s, 2H), 7.38 (s, 1H), 6.82 (d, $J = 2.3$ Hz, 1H), 6.45 (d, $J = 2.3$ Hz, 1H), 4.38 (t, $J = 5.9$ Hz, 2H), 3.97 (s, 3H), 3.93 (s, 3H), 3.85 (t, $J = 5.9$ Hz, 2H), 3.21 (t, $J = 5.9$ Hz, 2H), 2.83 (t, $J = 7.1$ Hz, 2H), 2.35 (s, 6H), 1.96 – 1.86 (m, 4H). MS (ESI) m/z : 493 ($\text{M}+\text{H}$) $^+$.

Synthesis of (2-amino-5-chlorophenyl)(4-chlorophenyl)methanone (56)

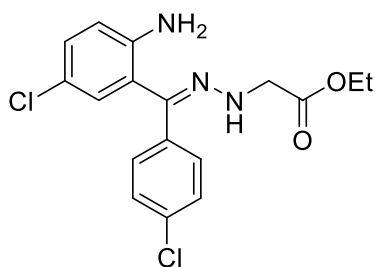


A stirred solution of 4-chlorobenzoyl chloride **55** (41.00 mL, 319 mmol) was heated at 120 °C and p-chloroaniline **54** (5.1 g, 39.98 mmol) was added slowly. Once the p-chloroaniline dissolved, zinc chloride (5.45 g, 39.98 mmol) was added, increasing the temperature up to 200-230 °C. The reaction mixture was heated at reflux for 4 hours, after which the reaction mixture was cooled to 120 °C and washed with water. The residual semisolid was dissolved with a mixture of sulfuric acid (250 mL), acetic acid (120mL) and water (120mL) and the solution was heated at reflux for 5 hours. Then, the reaction mixture was poured into ice-water, extracted with dichloromethane (3 x 200 mL) and washed with water (3 x 100 mL), 15% aqueous ammonium hydroxide solution (3 x 100 mL) and brine.

The organic phase was dried over sodium sulfate, filtered and evaporated under reduced pressure. Compound **56** was obtained as yellow solid (7.45 g, 70%) after crystallization with EtOH.

¹H NMR (400 MHz, CDCl₃) δ 7.59 (d, *J* = 8.2 Hz, 2H), 7.46 (d, *J* = 8.2 Hz, 2H), 7.36 (d, *J* = 2.5 Hz, 1H), 7.26 (dd, *J* = 2.5 Hz 1H), 6.70 (d, *J* = 8.8 Hz, 1H), 6.06 (s, 2H). MS (ESI) *m/z*: 266 (M + H)⁺

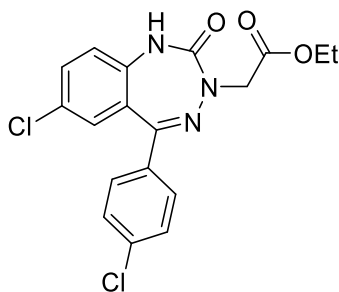
Synthesis of ethyl (E)-(((2-amino-5-chlorophenyl)(4-chlorophenyl) methylene) amino) glycinate (57)



A mixture of compound **56** (1 g, 4.42 mmol) and ethyl hydrazinoacetate hydrochloride (889 mg, 5.75 mmol) was refluxed in 10 mL of dry EtOH for 18 h. After cooling, EtOAc and saturated solution of NaHCO₃ were added and the mixture was stirred for 10 min. Then, the aqueous phase was extracted with EtOAc (3 x 15 mL): the organic phases were collected, washed with brine, dried over sodium sulfate, filtered and concentrated. The product **57** was obtained after purification on silica gel flash-chromatography column (hex-EtOAc 90:10 to 60:40) to yield a yellow oil (1.27 g, 79%).

¹H NMR (400 MHz, CDCl₃) δ 7.50 (d, *J* = 1.3 Hz, 2H), 7.47 (d, 2H), 7.46 (s, 1H), 7.45 (d, *J* = 1.3 Hz, 1H), 6.73 (d, *J* = 7.5 Hz, 1H), 4.19 (q, *J* = 8.0 Hz, 2H), 3.81 (s, 2H), 1.25 (t, *J* = 8.0 Hz, 3H). MS (ESI) *m/z*: 366 (M+H)⁺

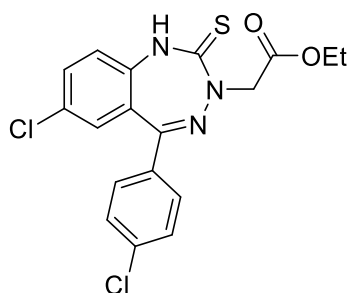
Synthesis of ethyl 2-(7-chloro-5-(4-chlorophenyl)-2-oxo-1,2-dihydro-3H-benzo[e][1,2,4]triazepin-3-yl)acetate (58)



Compound **57** (888 mg, 2.42 mmol) was dissolved in 13.30 mL of dry DCM and TEA (0.506 mL, 3.63 mmol) was added. After cooling at 0 °C, (CClO₃)₂CO (359 mg, 1.21 mmol) was added and the reaction mixture was stirring for 18 h at room temperature and, then, the solvent was evaporated. The crude was purified on a silica gel flash-chromatography column (hex-EtOAc 90:10 to 70:30) to yield compound **58** as white solid (800 mg, 85%).

¹H NMR (400 MHz, CDCl₃) δ 7.66 (s, 1H), 7.43 (d, *J* = 8.7 Hz, 1H), 7.38 (d, *J* = 8.5 Hz, 2H), 7.03 (d, *J* = 2.4 Hz, 1H), 6.95 (d, *J* = 8.5 Hz, 2H), 4.45 (s, 2H), 4.23 (q, *J* = 7.1 Hz, 2H), 1.27 (t, *J* = 7.1 Hz, 3H). MS (ESI) *m/z*: 392 (M+H)⁺

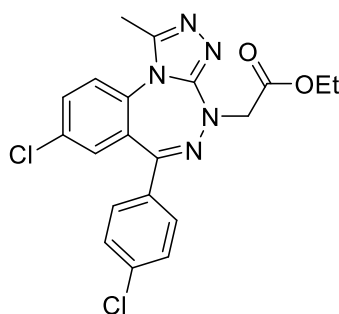
Synthesis of ethyl 2-(7-chloro-5-(4-chlorophenyl)-2-thioxo-1,2-dihydro-3H-benzo[e][1,2,4]triazepin-3-yl)acetate (59)



Lawesson's reagent (1.54 g, 3.82 mmol) was added to a solution of compound **58** (750 mg, 1.91 mmol) in 50 mL of toluene and the resulting mixture was heated at reflux for 18 h. Then, the solvent was evaporated and the crude was purified with a silica gel flash chromatography column (hex-EtOAc 95:5 to 70:30) to yield the title compound (**59**) as yellow oil (440 mg, 55%).

^1H NMR (400 MHz, CDCl_3) δ 7.59 (d, $J = 1.5$ Hz, 1H), 7.55 (d, $J = 8.1$ Hz, 2H), 7.50 (d, $J = 8.1$ Hz, 2H), 7.40 (d, $J = 7.6$ Hz, 1H), 7.33 (dd, $J = 7.6, 1.5$ Hz, 1H), 4.62 (s, 2H), 4.19 (q, $J = 7.9$ Hz, 2H), 1.25 (t, $J = 8.0$ Hz, 3H). MS (ESI) m/z : 408 ($\text{M}+\text{H}$) $^+$

Synthesis of ethyl 2-(8-chloro-6-(4-chlorophenyl)-1-methyl-4H-benzo[e][1,2,4]triazolo[3,4-c][1,2,4]triazepin-4-yl)acetate (60)

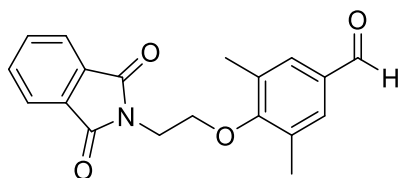


To a solution of compound **59** (499 mg, 1.17 mmol) in 20 mL of THF/AcOH (4:1,) acetylhydrazide (173 mg, 2.34 mmol) and $\text{Hg}(\text{OAc})_2$ (561 mg, 1.76 mmol) were added. The mixture was heated at 95 °C and stirring for 4 h. The crude reaction was filtered through a pad

of Celite, which was rinsed with MeOH. The filtrate was evaporated and purified with a silica gel flash chromatography column (hex-EtOAc 20:80 to 0:100) to yield a yellow oil (**60**) (146 mg, 30%).

$^1\text{H NMR}$ (400 MHz, CDCl_3) δ 7.66 (s, 1H), 7.43 (d, $J = 8.7$ Hz, 1H), 7.38 (d, $J = 8.7$ Hz, 2H), 7.03 (d, $J = 2.4$ Hz, 1H), 6.95 (d, $J = 8.7$ Hz, 2H), 4.45 (s, 2H), 4.23 (q, $J = 7.1$ Hz, 2H), 2.82 (s, 3H) 1.27 (t, $J = 7.1$ Hz, 3H). MS (ESI) m/z : 430 ($\text{M}+\text{H}$) $^+$

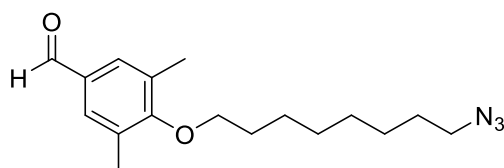
Synthesis of 4-(2-(1,3-dioxoisindolin-2-yl)ethoxy)-3,5-dimethylbenzaldehyde (61)



To a solution of **69** (540 mg, 2 mmol) in 8 mL of dry DMF, 4-hydroxy-3,5-dimethylbenzaldehyde **76a** (330 mg, 2.2 mmol) and K_2CO_3 (304 mg, 2.2 mmol) were added under nitrogen atmosphere. The resulting mixture was stirred at 80 °C for 18 h. Then, water (20 mL) was added and the aqueous phase was extracted with EtOAc (3 x 15 mL). The collected organic phases were washed with saturated solution of NaHCO_3 (3 x 15 mL), brine, dried over sodium sulfate, filtered and concentrated under reduced pressure. The title compound was obtained as yellow solid after purification on silica gel flash chromatography column (hex-EtOAc 80:20 to 70:30) (330 mg, 51%).

$^1\text{H NMR}$ (400 MHz, CDCl_3) δ 9.85 (s, 1H), 7.89 (dd, $J = 5.4, 3.1$ Hz, 2H), 7.75 (dd, $J = 5.4, 3.1$ Hz, 2H), 7.50 (s, 2H), 4.18 – 4.13 (m, 2H), 4.12 – 4.07 (m, 2H), 2.25 (s, 6H). MS (ESI) m/z : 324 ($\text{M}+\text{H}$) $^+$.

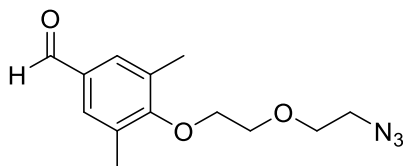
Synthesis of 4-((8-azidooctyl)oxy)-3,5-dimethylbenzaldehyde (62a)



Compound **62a** was obtained as a pale yellow solid (53 mg, 73%) from derivative **74a** (80 mg, 0.240 mmol) and **76a** (40 mg, 0.264 mmol) according to the procedure described for **61**.

^1H NMR (400 MHz, CDCl_3) δ 9.87 (s, 1H), 7.55 (s, 2H), 3.82 (t, $J = 6.4$ Hz, 2H), 3.31 – 3.23 (m, 2H), 2.33 (s, 6H), 1.88 – 1.77 (m, 2H), 1.66 – 1.58 (m, 2H), 1.56 – 1.48 (m, 8H). MS (ESI) m/z : 304 (M+H) $^+$.

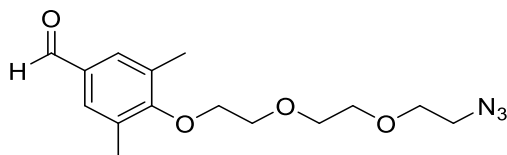
Synthesis of 4-(2-(2-azidoethoxy)ethoxy)-3,5-dimethylbenzaldehyde (62b)



Compound **62b** was obtained as a pale yellow solid (134 mg, 73%) from derivative **74b** (200 mg, 0.700 mmol) and **76a** (116 mg, 0.770 mmol) according to the procedure described for **61**.

^1H NMR (400 MHz, CDCl_3) δ 9.88 (s, 1H), 7.56 (s, 2H), 4.05 – 4.00 (m, 2H), 3.89 – 3.84 (m, 2H), 3.76 (t, $J = 5.1$ Hz, 2H), 3.44 (t, $J = 5.1$ Hz, 2H), 2.36 (s, 6H). MS (ESI) m/z : 264 (M+H) $^+$.

Synthesis of 4-(2-(2-(2-azidoethoxy)ethoxy)ethoxy)-3,5-dimethylbenzaldehyde (62c)

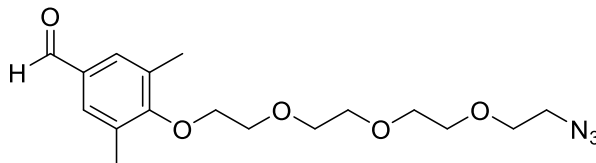


Compound **62c** was obtained as a pale yellow solid (91 mg, 78%) from derivative **74c** (125 mg, 0.379 mmol) and **76a** (63 mg, 0.417 mmol) according to the procedure described for **61**.

^1H NMR (400 MHz, CDCl_3) δ 9.88 (s, 1H), 7.55 (s, 2H), 4.04 – 3.99 (m, 2H), 3.87 – 3.84 (m, 2H), 3.78 – 3.74 (m, 2H), 3.73 – 3.66 (m, 4H), 3.39 (t, $J = 5.1$ Hz, 2H), 2.36 (s, 6H).

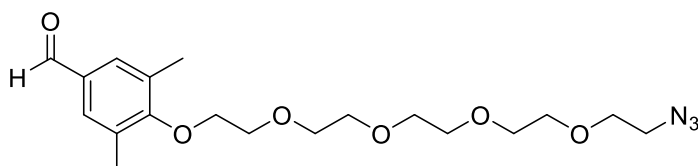
MS (ESI) m/z : 308 (M+H)⁺.

Synthesis of 4-(2-(2-(2-(2-azidoethoxy)ethoxy)ethoxy)ethoxy)-3,5-dimethylbenzaldehyde (62d)



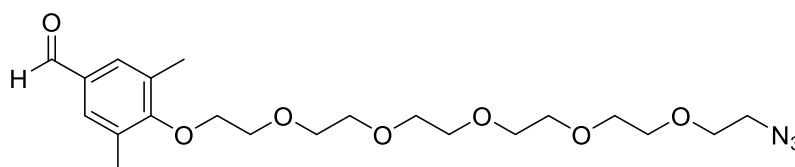
Compound **62d** was obtained as a pale yellow solid (207 mg, 85%) from derivative **74d** (260 mg, 0.690 mmol) and **76a** (114 mg, 0.760 mmol) according to the procedure described for **61**. ¹H NMR (400 MHz, CDCl₃) δ 9.87 (s, 1H), 7.55 (s, 2H), 4.01 (dd, J = 5.8, 3.7 Hz, 2H), 3.84 (dd, J = 5.9, 3.6 Hz, 2H), 3.76 – 3.70 (m, 10H), 3.42 – 3.34 (m, 2H), 2.35 (s, 6H). MS (ESI) m/z : 352 (M+H)⁺.

Synthesis of 4-((14-azido-3,6,9,12-tetraoxatetradecyl)oxy)-3,5-dimethylbenzaldehyde (62e)



Compound **62e** was obtained as a pale yellow solid (160 mg, 87%) from derivative **74e** (192 mg, 0.460 mmol) and **76a** (76 mg, 0.506 mmol) according to the procedure described for **61**. ¹H NMR (400 MHz, CDCl₃) δ 9.87 (s, 1H), 7.55 (s, 2H), 4.01 (dd, J = 5.7, 3.7 Hz, 2H), 3.84 (dd, J = 5.7, 3.7 Hz, 2H), 3.72 – 3.65 (m, 14H), 3.38 (t, J = 5.0 Hz, 2H), 2.35 (s, 6H). MS (ESI) m/z : 396 (M+H)⁺.

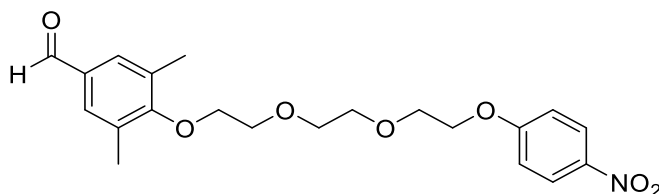
Synthesis of 4-((17-azido-3,6,9,12,15-pentaoxaheptadecyl)oxy)-3,5-dimethylbenzaldehyde (62f)



Compound **62f** was obtained as a pale yellow solid (150 mg, 63%) from derivative **74f** (250 mg, 0.541 mmol) and **76a** (89 mg, 0.595 mmol) according to the procedure described for **61**.

^1H NMR (400 MHz, CDCl_3) δ 9.87 (s, 1H), 7.54 (s, 2H), 4.02 – 3.98 (m, 2H), 3.86 – 3.80 (m, 2H), 3.75 – 3.59 (m, 20H), 2.35 (s, 6H). MS (ESI) m/z : 440 (M+H) $^+$

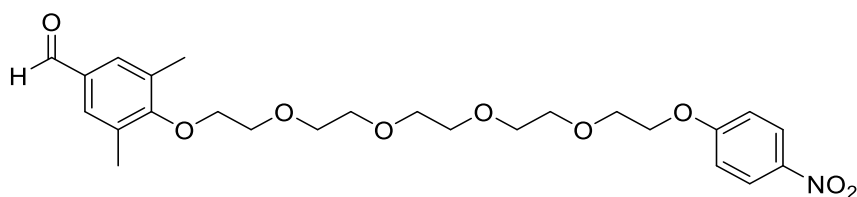
Synthesis of 3,5-dimethyl-4-(2-(2-(2-(4-nitrophenoxy)ethoxy)ethoxy)ethoxy)benzaldehyde (63a)



Compound **63a** was obtained as a pale yellow solid (174 mg, 87%) from derivative **75a** (212 mg, 0.498 mmol) and **76a** (82 mg, 0.548 mmol) according to the procedure described for **61**.

^1H NMR (400 MHz, CDCl_3) δ 9.85 (s, 1H), 8.16 (d, $J = 9.2$ Hz, 2H), 7.52 (s, 2H), 6.96 (d, $J = 9.2$ Hz, 2H), 4.26 – 4.18 (m, 2H), 4.02 – 3.98 (m, 2H), 3.92 – 3.88 (m, 2H), 3.86 – 3.82 (m, 2H), 3.76 (s, 4H), 2.33 (s, 6H). MS (ESI) m/z : 404 (M+H) $^+$.

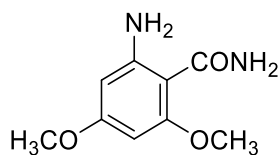
Synthesis of 3,5-dimethyl-4-((14-(4-nitrophenoxy)-3,6,9,12-tetraoxatetradecyl)oxy)benzaldehyde (63b)



Compound **63b** was obtained as a pale yellow solid (137 mg, 85%) from derivative **75b** (169 mg, 0.329 mmol) and **76a** (54 mg, 0.362 mmol) according to the procedure described for **61**.

^1H NMR (400 MHz, CDCl_3) δ 9.87 (s, 1H), 8.18 (d, $J = 9.3$ Hz, 2H), 7.54 (s, 2H), 6.97 (d, $J = 9.3$ Hz, 2H), 4.26 – 4.16 (m, 2H), 4.05 – 3.95 (m, 2H), 3.93 – 3.84 (m, 2H), 3.88 – 3.79 (m, 2H), 3.77 – 3.65 (m, 12H), 2.34 (s, 6H). MS (ESI) m/z : 492 (M+H) $^+$.

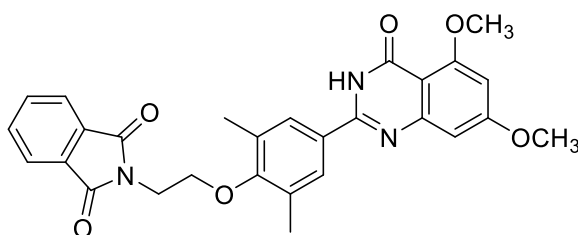
Synthesis of 2-amino-4,6-dimethoxybenzamide (64)



EDC (1.05 g, 5.47 mmol), HOBt (740 mg, 5.47 mmol) and NMM (553 mg, 5.47 mmol) were added to a solution of compound **80** (720 mg, 3.65 mmol) in 35 mL of dry THF and the mixture was stirred for 4 h. Then, 0.500 mL of hydroxide ammonium solution (33 % NH₃ in water) were added and the solution was stirred for 1 h. Water was added and the aqueous layer was extracted with EtOAc. The organic layers were collected, washed with saturated solution of NaHCO₃ and brine, dried and concentrated in under reduced pressure. The product was obtained after purification on silica gel flash chromatography column (DCM-MeOH 100:0 to 90:10) yielding the title compound as yellow solid (464 mg, 65 %).

¹H NMR (400 MHz, DMSO-d₆) δ 7.46 (s, 1H), 7.02 (s, 1H), 6.90 (s, 2H), 5.88 (d, J = 2.4 Hz, 1H), 5.76 (d, J = 2.4 Hz, 1H), 3.77 (s, 3H), 3.69 (s, 3H). MS (ESI) *m/z*: 197 (M+H)⁺.

Synthesis of 2-(2-(4-(5,7-dimethoxy-4-oxo-3,4-dihydroquinazolin-2-yl))-2,6-dimethylphenoxy)ethyl isoindoline-1,3-dione (65)

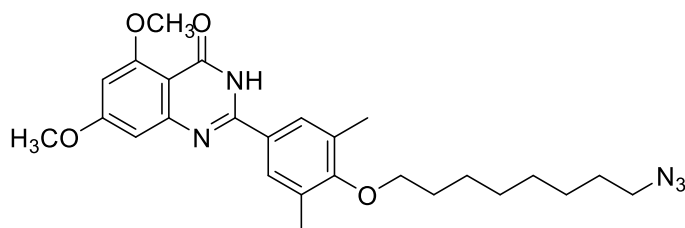


To a stirred solution of **61** (180 mg, 0.556 mmol) in 3.5 mL of dry DMAc, 2-amino-4,6-dimethoxybenzamide **64** (100 mg, 0.556 mmol), Na₂S₂O₅ (139 mg, 0.667 mmol), TsOH (21 mg, 0.111 mmol) were added. The resulting mixture was stirred at 120 °C for 18 h. After cooling at room temperature, water (30 mL) was added. The aqueous phase was extracted with EtOAc (3 x 15 mL) and the collected organic phases were washed with saturated solution of

NaHCO₃ (3 x 15 mL), brine, dried over sodium sulfate and filtered. After evaporation, the crude was purified with a silica gel flash chromatography column (DCM-MeOH 95:5 to 90:10) to give a pale yellow solid (158 mg, 63%).

¹H NMR (400 MHz, CDCl₃) δ 9.04 (s, 1H), 7.90 (dd, *J* = 5.5, 3.1 Hz, 2H), 7.76 (dd, *J* = 5.5, 3.1 Hz, 2H), 7.61 (s, 2H), 6.81 (d, *J* = 2.3 Hz, 1H), 6.45 (d, *J* = 2.3 Hz, 1H), 4.16 (t, *J* = 5.7 Hz, 2H), 4.08 (t, *J* = 5.8 Hz, 2H), 3.97 (s, 3H), 3.92 (s, 3H), 2.28 (s, 6H). MS (ESI) *m/z*: 500 (M+H)⁺.

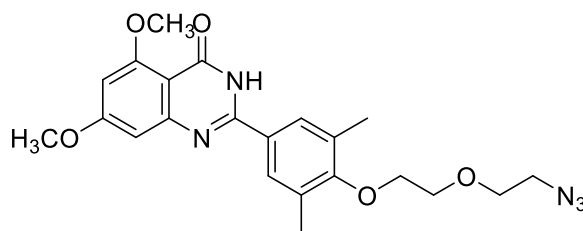
Synthesis of 2-(4-((8-azidoethyl)oxy)-3,5-dimethylphenyl)-5,7-dimethoxyquinazolin-4(3H)-one (66a)



Compound **66a** was obtained as a pale yellow solid (42 mg, 53%) from derivative **62a** (50 mg, 0.165 mmol) and **64** (32 mg, 0.165 mmol) according to the procedure described for **65**.

¹H NMR (400 MHz, CDCl₃) δ 9.34 (s, 1H), 7.67 (s, 2H), 6.82 (d, *J* = 2.4 Hz, 1H), 6.46 (d, *J* = 2.4 Hz, 1H), 3.98 (s, 3H), 3.93 (s, 3H), 3.80 (t, *J* = 6.5 Hz, 2H), 3.27 (t, *J* = 6.5 Hz, 2H), 2.36 (s, 6H), 1.87 – 1.78 (m, 2H), 1.55 – 1.48 (m, 2H), 1.39 (d, *J* = 4.1 Hz, 8H). MS (ESI) *m/z*: 480 (M+H)⁺.

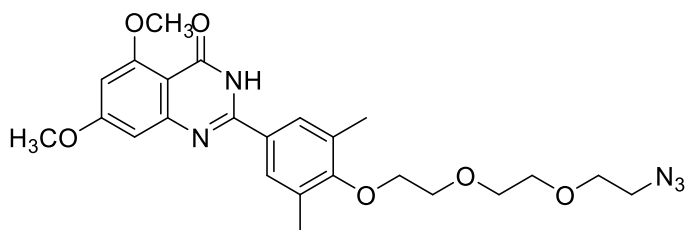
Synthesis of 2-(4-(2-(2-azidoethoxy)ethoxy)-3,5-dimethylphenyl)-5,7-dimethoxyquinazolin-4(3H)-one (66b)



Compound **66b** was obtained as a pale yellow solid (130 mg, 58%) from derivative **71b** (134 mg, 0.510 mmol) and **64** (100 mg, 0.510 mmol) according to the procedure described for **65**.

^1H NMR (400 MHz, CDCl_3) δ 9.28 (s, 1H), 7.67 (s, 2H), 6.83 (d, $J = 2.3$ Hz, 1H), 6.46 (d, $J = 2.3$ Hz, 1H), 4.01 (t, $J = 4.6$ Hz, 2H), 3.98 (s, 3H), 3.93 (s, 3H), 3.87 (t, $J = 4.6$ Hz, 2H), 3.77 (t, $J = 5.1$ Hz, 2H), 3.45 (t, $J = 5.1$ Hz, 2H), 2.39 (s, 6H) MS (ESI) m/z : 440 ($\text{M}+\text{H}$) $^+$.

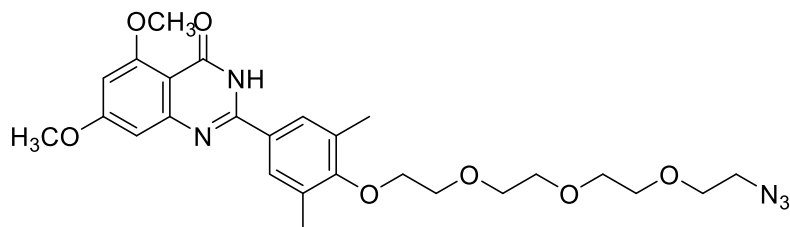
Synthesis of 2-(4-(2-(2-(2-azidoethoxy)ethoxy)ethoxy)ethoxy)-3,5-dimethylphenyl)-5,7-dimethoxyquinazolin-4(3H)-one (66c)



Compound **66c** was obtained as a pale yellow solid (65 mg, 46%) from derivative **62c** (91 mg, 0.296 mmol) and **64** (58 mg, 0.296 mmol) according to the procedure described for **65**.

^1H NMR (400 MHz, CDCl_3) δ 7.66 (s, 2H), 6.82 (d, $J = 2.3$ Hz, 1H), 6.46 (d, $J = 2.3$ Hz, 1H), 4.03 – 3.99 (m, 2H), 3.98 (s, 3H), 3.93 (s, 3H), 3.88 – 3.85 (m, 2H), 3.78 – 3.75 (m, 2H), 3.74 – 3.69 (m, 4H), 3.40 (t, $J = 5.1$ Hz, 2H), 2.38 (s, 6H). MS (ESI) m/z : 484 ($\text{M}+\text{H}$) $^+$.

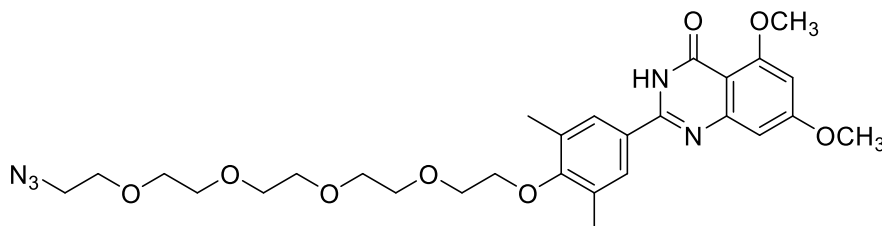
Synthesis of 2-(4-(2-(2-(2-(2-azidoethoxy)ethoxy)ethoxy)ethoxy)ethoxy)-3,5-dimethylphenyl)-5,7-dimethoxyquinazolin-4(3H)-one (66d)



Compound **66d** was obtained as a pale yellow solid (200 mg, 70%) from derivative **62d** (190 mg, 0.541 mmol) and **64** (106 mg, 0.541 mmol) according to the procedure described for **65**.

^1H NMR (400 MHz, CDCl_3) δ 9.39 (s, 1H), 7.68 (s, 2H), 6.82 (d, $J = 2.5$ Hz, 1H), 6.46 (d, $J = 2.5$ Hz, 1H), 4.03 – 3.99 (m, 2H), 3.97 (s, 3H), 3.93 (s, 3H), 3.85 (t, $J = 4.8$ Hz, 2H), 3.76 – 3.65 (m, 10H), 3.39 (t, $J = 5.0$ Hz, 2H), 2.38 (s, 6H). MS (ESI) m/z : 528 ($\text{M}+\text{H}$) $^+$.

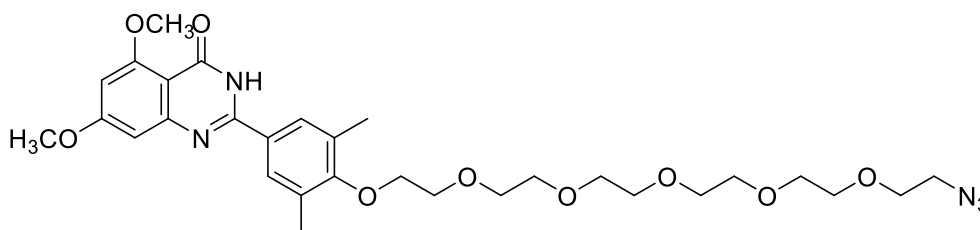
Synthesis of 2-(4-((14-azido-3,6,9,12-tetraoxatetradecyl)oxy)-3,5-dimethylphenyl)-5,7-dimethoxyquinazolin-4(3H)-one (66e)



Compound **66e** was obtained as a pale yellow solid (160 mg, 40%) from derivative **62e** (160 mg, 0.404 mmol) and **64** (79 mg, 0.404 mmol) according to the procedure described for **65**.

^1H NMR (400 MHz, CDCl_3) δ 7.66 (s, 2H), 6.82 (d, $J = 2.4$ Hz, 1H), 6.45 (d, $J = 2.4$ Hz, 1H), 3.98 (s, 3H), 3.92 (s, 3H), 3.84 (t, $J = 4.8$ Hz, 2H), 3.78 – 3.62 (m, 16H), 3.39 (t, $J = 5.1$ Hz, 2H), 2.38 (s, 6H). MS (ESI) m/z : 571 ($\text{M}+\text{H}$) $^+$.

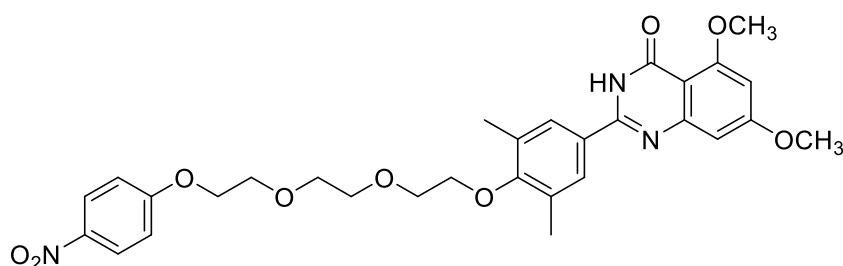
Synthesis of 2-(4-((17-azido-3,6,9,12,15-pentaoxaheptadecyl)oxy)-3,5-dimethylphenyl)-5,7-dimethoxyquinazolin-4(3H)-one (66f)



Compound **66f** was obtained as a pale yellow solid (130 mg, 62%) from derivative **62f** (150 mg, 0.341 mmol) and **64** (67 mg, 0.341 mmol) according to the procedure described for **65**.

^1H NMR (400 MHz, CDCl_3) δ 9.14 (s, 1H), 7.66 (s, 2H), 6.82 (d, $J = 2.2$ Hz, 1H), 6.46 (d, $J = 2.2$ Hz, 1H), 4.03 – 3.99 (m, 2H), 3.98 (s, 3H), 3.93 (s, 3H), 3.84 (t, $J = 4.9$ Hz, 2H), 3.74 – 3.64 (m, 18H), 3.42 – 3.34 (m, 2H), 2.38 (s, 6H). MS (ESI) m/z : 616 (M+H) $^+$.

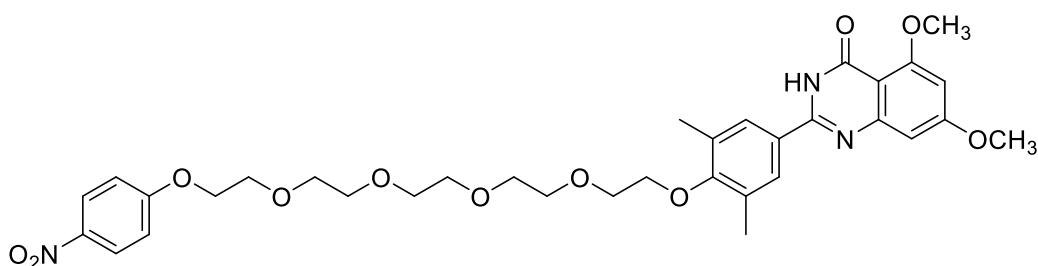
Synthesis of 2-(3,5-dimethyl-4-(2-(2-(2-(4-nitrophenoxy)ethoxy)ethoxy)ethoxy)phenyl)-5,7-dimethoxyquinazolin-4(3H)-one (67a)



Compound **67a** was obtained as a pale yellow solid (43 mg, 64 %) from derivative **63a** (47 mg, 0.116 mmol) and **64** (23 mg, 0.116 mmol) according to the procedure described for **65**.

^1H NMR (400 MHz, CDCl_3) δ 8.14 (d, $J = 9.2$ Hz, 2H), 7.78 (s, 2H), 6.93 (d, $J = 9.2$ Hz, 2H), 6.80 (d, $J = 2.3$ Hz, 1H), 6.42 (d, $J = 2.3$ Hz, 1H), 4.23 – 4.16 (m, 2H), 3.97 (dd, $J = 5.8, 3.6$ Hz, 2H), 3.93 (s, 3H), 3.90 (s, 3H), 3.88 (dd, $J = 3.7, 2.5$ Hz, 2H), 3.84 – 3.80 (m, 2H), 3.76 (s, 4H), 2.35 (s, 6H). MS (ESI) m/z : 580 (M+H) $^+$.

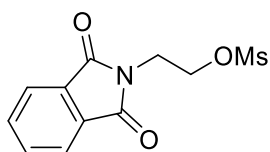
Synthesis of 2-(3,5-dimethyl-4-((14-(4-nitrophenoxy)-3,6,9,12-tetraoxatetradecyl)oxy)phenyl)-5,7-dimethoxyquinazolin-4(3H)-one (67b)



Compound **67b** was obtained as a pale yellow solid (503 mg, 80 %) from derivative **63b** (464 mg, 0.944 mmol) and **64** (185 mg, 0.944 mmol) according to the procedure described for **65**.

^1H NMR (400 MHz, CDCl_3) δ 8.16 (d, $J = 9.2$ Hz, 2H), 7.67 (s, 2H), 6.94 (d, $J = 9.2$ Hz, 2H), 6.81 (d, $J = 2.4$ Hz, 1H), 6.45 (d, $J = 2.4$ Hz, 1H), 4.26 – 4.16 (m, 2H), 4.03 – 3.98 (m, 2H), 3.98 (s, 3H), 3.92 (s, 3H), 3.91 – 3.87 (m, 2H), 3.83 (m, 2H), 3.75 – 3.64 (m, 12H), 2.37 (s, 6H). MS (ESI) m/z : 668 (M+H) $^+$.

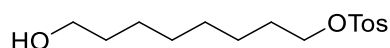
Synthesis of 2-(1,3-dioxoisindolin-2-yl)ethyl methanesulfonate (69)



Compound **68** (300 mg, 1.57 mmol) was dissolved in 15 mL of dry DCM and TEA (0.544 mL, 3.45 mmol) was added. The solution was cooling at 0 °C and mesyl chloride (0.236 mL, 3.45 mmol) was added. The reaction mixture was stirring for 2 h at room temperature under nitrogen atmosphere. Then, the mixture was diluted with DCM (10mL) and the organic phase was washed with brine (3 x 20 mL), dried over sodium sulfate, filtered and concentrated under reduced pressure. The product (**69**) was obtained as white solid (470 mg, 99 %).

^1H NMR (400 MHz, CDCl_3) δ 7.88 (dd, $J = 5.5, 3.1$ Hz, 2H), 7.75 (dd, $J = 5.5, 3.1$ Hz, 2H), 4.49 (t, $J = 5.3$ Hz, 2H), 4.05 (t, $J = 5.3$ Hz, 2H), 3.02 (s, 3H). MS (ESI) m/z : 270 (M+H) $^+$

Synthesis of 8-hydroxyoctyl 4-methylbenzenesulfonate (71a)

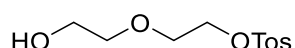


To an ice-cold solution of 1,8-octanediol **70a** (500 mg, 3.42 mmol) and Ag_2O (1.19 g, 5.13 mmol) in 31 mL of toluene, TsCl (717 mg, 3.76 mmol) and KI (57 mg, 0.342 mmol) were added. The resulting mixture was stirred at room temperature for 18 h. The precipitated silver salt was removed by filtration on silica gel, which was rinsed with EtOAc . The filtered was concentrated under reduced pressure. Then, the crude was taken up with EtOAc (40 mL). The organic phase was washed with water (3 x 20 mL), brine (40 mL), dried over sodium sulfate,

filtered and concentrated. The residue was purified by silica gel chromatography (hex-EtOAc 20:80 to 100%) to give the title compound **71a** as a pale yellow oil (600 mg, 58%).

^1H NMR (400 MHz, CDCl_3) δ 7.77 (d, J = 8.0 Hz, 2H), 7.33 (d, J = 8.0 Hz, 2H), 4.03 (t, J = 6.3 Hz, 2H), 3.65 (t, J = 6.8 Hz, 2H), 2.45 (s, 3H), 1.63-1.50 (m, 4H) 1.25-1.27 (m, 8H). MS (ESI) m/z : 301 ($\text{M}+\text{H}$) $^+$.

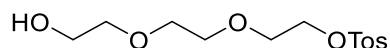
Synthesis of 2-(2-hydroxyethoxy)ethyl 4-methylbenzenesulfonate (71b)



Compound **71b** was obtained as a colorless oil (1.85 g, 75%) from derivative **70b** (1 g, 9.42 mmol) according to the procedure described for **71a**.

^1H NMR (400 MHz, CDCl_3) δ 7.80 (d, J = 7.8 Hz, 2H), 7.35 (d, J = 7.8 Hz, 2H), 4.20 (t, J = 4.6 Hz, 2H), 3.73 – 3.65 (m, 4H), 3.56 – 3.51 (m, 2H), 2.45 (s, 3H). MS (ESI) m/z : 261 ($\text{M}+\text{H}$) $^+$.

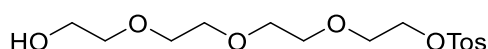
Synthesis of 2-(2-(2-hydroxyethoxy)ethoxy)ethyl 4-methylbenzenesulfonate (71c)



Compound **71c** was obtained as a colorless oil (2.43 g, 67%) from derivative **70c** (1.8 g, 11.98 mmol) according to the procedure described for **71a**.

^1H NMR (400 MHz, CDCl_3) δ 7.80 (d, J = 8.0 Hz, 2H), 7.34 (d, J = 8.0 Hz, 2H), 4.17 (t, J = 4.9 Hz, 2H), 3.71 (d, J = 4.9 Hz, 2H), 3.64 – 3.53 (m, 8H), 2.44 (s, 3H). MS (ESI) m/z : 305 ($\text{M}+\text{H}$) $^+$.

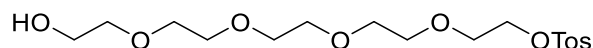
Synthesis of 2-(2-(2-(2-hydroxyethoxy)ethoxy)ethoxy)ethyl 4-methylbenzenesulfonate (71d)



Compound **71d** was obtained as a pale yellow oil (1.47 g, 82%) from derivative **70d** (1 g, 5.15 mmol) according to the procedure described for **71a**.

^1H NMR (400 MHz, CDCl_3) δ 7.82 – 7.78 (d, $J = 7.9$ Hz, 2H), 7.34 (d, $J = 7.9$ Hz, 2H), 4.19 – 4.11 (m, 2H), 3.72 – 3.55 (m, 14H), 2.45 (s, 3H). MS (ESI) m/z : 349 (M+H) $^+$.

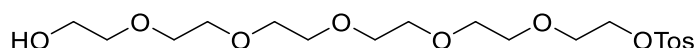
Synthesis of 14-hydroxy-3,6,9,12-tetraoxatetradecyl 4-methylbenzenesulfonate (71e)



Compound **71e** was obtained as a pale yellow oil (2.17 g, 66%) from derivative **70e** (2 g, 8.4 mmol) according to the procedure described for **71a**.

^1H NMR (400 MHz, CDCl_3) δ 7.80 (d, $J = 8.3$ Hz, 2H), 7.34 (d, $J = 8.3$ Hz, 2H), 4.19 – 4.12 (m, 2H), 3.73 – 3.55 (m, 18H), 2.45 (s, 3H). MS (ESI) m/z : 393 (M+H) $^+$.

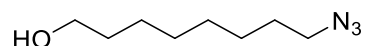
Synthesis of 17-hydroxy-3,6,9,12,15-pentaoxaheptadecyl 4-methylbenzenesulfonate (71f)



Compound **71f** was obtained as a pale yellow oil (410 mg, 53%) from derivative **70f** (500 mg, 1.77 mmol) according to the procedure described for **71a**.

^1H NMR (400 MHz, CDCl_3) δ 7.79 (d, $J = 8.2$ Hz, 2H), 7.35 (d, $J = 8.2$ Hz, 2H), 4.16 – 4.11 (m, 2H), 3.67 – 3.55 (m, 22H), 2.43 (s, 3H). MS (ESI) m/z : 437 (M+H) $^+$.

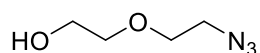
Synthesis of 8-azidoctan-1-ol (72a)



To a solution of **71a** (600 mg, 2 mmol) in 7 mL of DMF, sodium azide (390 mg, 6 mmol) was added and the mixture was stirred for 18 h. Then, water (30mL) was added: the aqueous phase was extracted with EtOAc (3 x 15 mL) and the collected organic phases were washed with a saturated solution of NaHCO_3 (3 x 15 mL), brine and dried over sodium sulfate. After filtration and evaporation, the product was obtained as pale yellow oil (240 mg, 70%).

^1H NMR (400 MHz, CDCl_3) δ 3.63 (t, $J = 7.0$ Hz, 2H), 3.25 (t, $J = 7.0$ Hz, 2H), 1.61-1.52 (m, 4H), 1.39-1.32 (m, 8H). MS (ESI) m/z : 172 (M+H) $^+$.

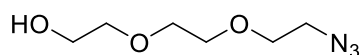
Synthesis of 2-(2-azidoethoxy)ethan-1-ol (72b)



Compound **72b** was obtained as a colorless oil (250 mg, 50%) from derivative **71b** (1 g, 3.84 mmol) according to the procedure described for **72a**.

¹H NMR (400 MHz, CDCl₃) δ 3.76 (t, *J* = 4.4 Hz, 2H), 3.70 (t, *J* = 4.9 Hz, 2H), 3.64 – 3.59 (m, 2H), 3.41 (t, *J* = 4.9 Hz, 2H). MS (ESI) *m/z*: 132 (M+H)⁺.

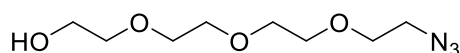
Synthesis of 2-(2-(2-azidoethoxy)ethoxy)ethan-1-ol (72c)



Compound **72c** was obtained as a colorless oil (122 mg, 53%) from derivative **71c** (400 mg, 1.31 mmol) according to the procedure described for **72a**.

¹H NMR (400 MHz, CDCl₃) δ 3.74 (t, *J* = 4.3 Hz, 2H), 3.71 – 3.66 (m, 6H), 3.64 – 3.60 (m, 2H), 3.40 (t, *J* = 5.0 Hz, 2H). MS (ESI) *m/z*: 176 (M+H)⁺.

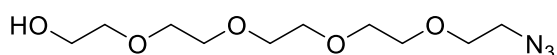
Synthesis of 2-(2-(2-(2-azidoethoxy)ethoxy)ethoxy)ethan-1-ol (72d)



Compound **72d** was obtained as a pale yellow solid (573 mg, 62%) from derivative **71d** (1.47 g, 4.22 mmol) according to the procedure described for **72a**.

¹H NMR (400 MHz, CDCl₃) δ 3.73 (t, *J* = 4.5 Hz, 2H), 3.69 – 3.66 (m, 10H), 3.62 (d, *J* = 4.6 Hz, 2H), 3.42 – 3.36 (m, 2H). MS (ESI) *m/z*: 220 (M+H)⁺.

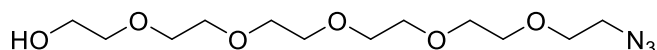
Synthesis of 14-azido-3,6,9,12-tetraoxatetradecan-1-ol (72e)



Compound **72e** was obtained as a pale yellow oil (411 mg, 62%) from derivative **71e** (1 g, 2.55 mmol) according to the procedure described for **72a**.

^1H NMR (400 MHz, CDCl_3) δ 3.73 – 3.70 (m, 2H), 3.69 – 3.63 (m, 12H), 3.62 – 3.58 (m, 4H), 3.41 – 3.36 (m, 2H). MS (ESI) m/z : 264 (M+H) $^+$.

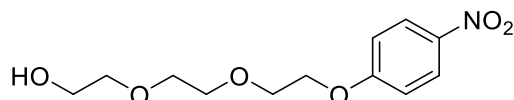
Synthesis of 17-azido-3,6,9,12,15-pentaoxaheptadecan-1-ol (72f)



Compound **72f** was obtained as a colorless oil (122 mg, 53%) from derivative **71f** (400 mg, 1.31 mmol) according to the procedure described for **72a**.

^1H NMR (400 MHz, CDCl_3) δ 3.73 (t, $J = 4.2$ Hz, 2H), 3.70 – 3.65 (m, 18H), 3.58 (t, $J = 4.4$ Hz, 2H), 3.38 (t, $J = 5.1$ Hz, 2H). MS (ESI) m/z : 308 (M+H) $^+$.

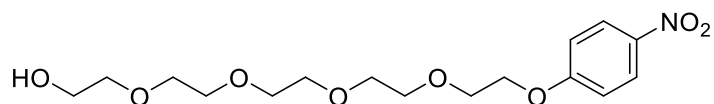
Synthesis of 2-(2-(2-(4-nitrophenoxy)ethoxy)ethoxy)ethan-1-ol (73a)



4-nitrophenol (640 mg, 4.6 mmol) and K_2CO_3 (635 mg, 4.6 mmol) were added to a solution of **71c** (700 mg, 2.30 mmol) in 2.5 mL of dry DMF and the mixture was stirring at 85 °C for 18 h. Then, H_2O (30 mL) was added: the aqueous phase was extracted by EtOAc (3 x 15 mL). The collected organic phases were washed with saturated solution of K_2CO_3 (3 x 15 mL), brine and dried (Na_2SO_4). Filtration and evaporation gave compound **73a** as yellow oil (656 mg, 2.30 mmol, 99%).

^1H NMR (400 MHz, CDCl_3) δ 8.19 (d, $J = 9.2$ Hz, 2H), 6.98 (d, $J = 9.2$ Hz, 2H), 4.24 – 4.21 (m, 2H), 3.92 – 3.88 (m, 2H), 3.75 – 3.68 (m, 6H), 3.63 – 3.60 (m, 2H). MS (ESI) m/z : 272 (M+H) $^+$.

Synthesis of 14-(4-nitrophenoxy)-3,6,9,12-tetraoxatetradecan-1-ol (73b)

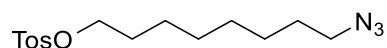


Compound **73b** was obtained as a pale yellow solid (883 mg, 96%) from derivative **71e** (857 mg, 2.18 mmol) according to the procedure described for **73a**.

$^1\text{H NMR}$ (400 MHz, CDCl_3) δ 8.19 (d, $J = 9.2$ Hz, 2H), 6.98 (d, $J = 9.2$ Hz, 2H), 4.26 – 4.18 (m, 2H), 3.92 – 3.84 (m, 2H), 3.77 – 3.68 (m, 2H), 3.71 – 3.62 (m, 12H), 3.64 – 3.57 (m, 2H).

MS (ESI) m/z : 360 ($\text{M}+\text{H}$) $^+$.

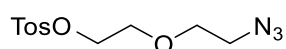
Synthesis of 8-azidooctyl 4-methylbenzenesulfonate (74a)



To a solution of **72a** (400 mg, 2.34 mmol) in 26 mL of dry DCM, TEA (0.391 mL, 2.81 mmol) and TsCl (536 mg, 2.81 mmol) were added. The resulting mixture was stirred for 18 h at room temperature under nitrogen atmosphere. Then, DCM was added (40 mL): the organic phase was washed with HCl 1N (3 x 20 mL), saturated solution of NaHCO_3 (3 x 20 mL), brine and dried over sodium sulfate. After filtration and evaporation, the crude was purified with a silica gel flash chromatography column (hex-EtOAc 80:20 to 50:50) to give a yellow oil (500 mg, 66%).

$^1\text{H NMR}$ (400 MHz, CDCl_3) δ 7.81 (d, $J = 8.3$ Hz, 2H), 7.37 (d, $J = 8.3$ Hz, 2H), 4.04 (t, $J = 6.5$ Hz, 2H), 3.27 (t, $J = 6.9$ Hz, 2H), 2.48 (s, 3H), 1.68 – 1.61 (m, 2H), 1.38 – 1.26 (m, 10H). MS (ESI) m/z : 326 ($\text{M}+\text{H}$) $^+$.

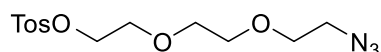
Synthesis of 2-(2-azidoethoxy)ethyl 4-methylbenzenesulfonate (74b)



Compound **74b** was obtained as a pale yellow oil (220 mg, 51%) from derivative **72b** (200 mg, 1.52 mmol) according to the procedure described for **74a**.

^1H NMR (400 MHz, CDCl_3) δ 7.81 (d, $J = 7.9$ Hz, 2H), 7.35 (d, $J = 7.9$ Hz, 2H), 4.19 – 4.16 (m, 2H), 3.73 – 3.68 (m, 2H), 3.61 (t, $J = 5.0$ Hz, 2H), 3.32 (t, $J = 5.0$ Hz, 2H), 2.45 (s, 3H). MS (ESI) m/z : 286 (M+H) $^+$.

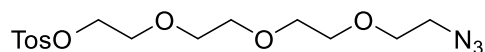
Synthesis of 2-(2-(2-azidoethoxy)ethoxy)ethyl 4-methylbenzenesulfonate (74c)



Compound **74c** was obtained as a pale yellow oil (125 mg, 54%) from derivative **72c** (123 mg, 0.700 mmol) according to the procedure described for **74a**.

^1H NMR (400 MHz, CDCl_3) δ 7.80 (d, $J = 8.3$ Hz, 2H), 7.34 (d, $J = 8.3$ Hz, 2H), 4.19 – 4.14 (m, 3H), 3.73 – 3.69 (m, 3H), 3.64 (m, 3H), 3.36 (m, 3H), 2.45 (s, 3H). MS (ESI) m/z : 330 (M+H) $^+$.

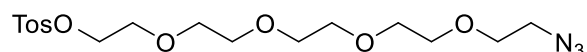
Synthesis of 2-(2-(2-(2-azidoethoxy)ethoxy)ethoxy)ethyl 4-methylbenzenesulfonate (74d)



Compound **74d** was obtained as a pale yellow oil (420 mg, 54%) from derivative **72d** (460 mg, 2.10 mmol) according to the procedure described for **74a**.

^1H NMR (400 MHz, CDCl_3) δ 7.80 (d, $J = 8.2$ Hz, 2H), 7.34 (d, $J = 8.2$ Hz, 2H), 4.16 (t, $J = 4.8$, 2H), 3.72 – 3.57 (m, 12H), 3.38 (t, $J = 5.0$ Hz, 2H), 2.45 (s, 3H). MS (ESI) m/z : 374 (M+H) $^+$.

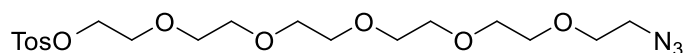
Synthesis of 14-azido-3,6,9,12-tetraoxatetradecyl 4-methylbenzenesulfonate (74e)



Compound **74e** was obtained as a pale yellow oil (300 mg, 49%) from derivative **72e** (391 mg, 1.48 mmol) according to the procedure described for **74a**.

^1H NMR (400 MHz, CDCl_3) δ 7.80 (d, $J = 8.3$ Hz, 2H), 7.34 (d, $J = 8.3$ Hz, 2H), 4.19 – 4.14 (m, 3H), 3.72 – 3.61 (m, 14H), 3.38 (m, 3H), 2.45 (s, 3H). MS (ESI) m/z : 418 (M+H) $^+$.

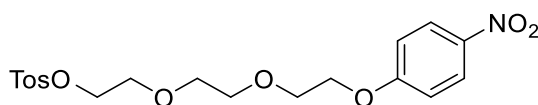
Synthesis of 17-azido-3,6,9,12,15-pentaoxaheptadecyl 4-methylbenzenesulfonate (74f)



Compound **74f** was obtained as a pale yellow oil (450 mg, 60%) from derivative **72f** (500 mg, 1.63 mmol) according to the procedure described for **74a**.

¹H NMR (400 MHz, CDCl₃) δ 7.79 (d, *J* = 7.8 Hz, 2H), 7.34 (d, *J* = 7.8 Hz, 2H), 4.19 – 4.12 (m, 2H), 3.71 – 3.58 (m, 18H), 3.51 – 3.34 (m, 4H), 2.45 (s, 3H). MS (ESI) *m/z*: 462 (M+H)⁺.

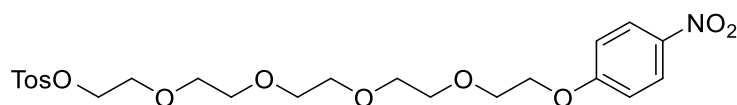
Synthesis of 2-(2-(2-(4-nitrophenoxy)ethoxy)ethoxy)ethyl 4-methylbenzenesulfonate (75a)



To a solution of **73a** (656 mg, 2.30 mmol) in 25 mL of dry DCM, TEA (730 mg, 2.76 mmol) and TsCl (526 mg, 2.76 mmol) were added. The resulting solution was stirred for 18 h at room temperature. Then, DCM was added (20 mL): the organic phase was washed with HCl 1N (3 x 15 mL), saturated solution of NaHCO₃ (3 x 15 mL), brine and dried over sodium sulfate. After filtration and evaporation, the crude was purified with a silica gel flash chromatography column (hex-EtOAc 80:20 to 70:30) to give a yellow oil (400 mg, 41 %).

¹H NMR (400 MHz, CDCl₃) δ 8.19 (d, *J* = 9.2 Hz, 2H), 7.79 (d, *J* = 8.2 Hz, 2H), 7.33 (d, *J* = 8.2 Hz, 2H), 6.98 (d, *J* = 9.2 Hz, 2H), 4.25 – 4.18 (m, 2H), 4.19 – 4.12 (m, 2H), 3.91 – 3.84 (m, 2H), 3.74 – 3.64 (m, 4H), 3.67 – 3.59 (m, 2H), 2.44 (s, 3H). MS (ESI) *m/z*: 426 (M+H)⁺.

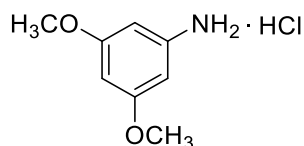
Synthesis of 1-(4-nitrophenoxy)-14-tosyl-3,6,9,12-tetraoxatetradecane (75b)



Compound **75b** was obtained as a pale yellow solid (550 mg, 50%) from derivative **73b** (865 mg, 2.18 mmol) according to the procedure described for **75a**.

^1H NMR (400 MHz, CDCl_3) δ 8.18 (d, $J = 9.2$ Hz, 2H), 7.79 (d, $J = 8.2$ Hz, 2H), 7.33 (d, $J = 8.2$ Hz, 2H), 6.98 (d, $J = 9.2$ Hz, 2H), 4.25 – 4.19 (m, 2H), 4.17 – 4.11 (m, 2H), 3.92 – 3.84 (m, 2H), 3.73 – 3.61 (m, 14H), 2.44 (s, 3H). MS (ESI) m/z : 514 ($\text{M}+\text{H}$) $^+$.

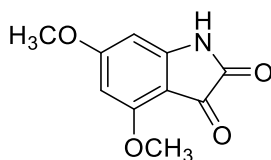
Synthesis of 3,5-dimethoxyaniline hydrochloride (78)



3,5-dimethoxyaniline **77** (5 g, 32.64 mmol) was dissolved in 150 mL of Et_2O and the reaction mixture was cooled at $0\text{ }^\circ\text{C}$. HCl (gas) was bubbled into the mixture for 1 h.

The corresponding hydrochloride salt (**78**) was obtained after filtration like white solid (6 g, 31.64 mmol, 97%). Product was used for the next step without further purification.

Synthesis of 4,6-dimethoxyindoline-2,3-dione (79)



The hydrochloride salt of 3,5-dimethoxyaniline **78** (6 g, 31.64 mmol) was dissolved in 10.71 mL of oxalyl chloride at $0\text{ }^\circ\text{C}$ and the reaction mixture was heated at $170\text{ }^\circ\text{C}$ for 90 min. The solvent was removed under reduced pressure. The semisolid residue was dissolved in MeOH at $0\text{ }^\circ\text{C}$ and then heated to reflux for 30 min. The reaction mixture was hot filtered and the precipitate was washed with MeOH to give a green solid **79** (4.13 g, 61 %). Product was used for the next step without further purification.

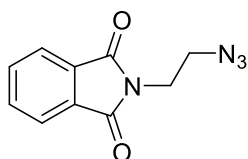
Synthesis of 2-amino-4,6-dimethoxybenzoic acid (80)



Compound **79** (4.13 g, 19.94 mmol) was dissolved in NaOH (33 % in water, 24.53 mL) and the resulting solution was heated to 70 °C. 6.70 mL of H₂O₂ were added to solution dropwise and the mixture was stirred for 3 h increasing up the temperature to 100 °C. The reaction mixture was adjusted to pH 8 with HCl and then to pH 5 with AcOH. The precipitate formed was filtered, washed with water and dried to give the compound **80** (2.31 g, 59%).

¹H NMR (400 MHz, DMSO-*d*₆) δ 6.71 (brs, 2H), 5.93 (d, *J* = 2.3 Hz, 1H), 5.78 (d, *J* = 2.4 Hz, 1H), 3.76 (s, 3H), 3.70 (s, 3H). MS (ESI) *m/z*: 197 (M+H)⁺.

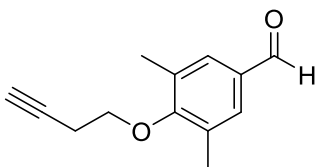
Synthesis of 2-(2-azidoethyl)isoindoline-1,3-dione (81)



To a solution of compound **69** (300 mg, 1.11 mmol) in 11 mL of DMF, sodium azide (362 mg, 5.57 mmol) was added. The resulting solution was stirred at room temperature for 18 h. Then water (20 mL) was added: the aqueous phase was extracted with EtOAc (3 x 15 mL), the collected organic phases were washed with saturated solution of NaHCO₃ (3 x 15 mL), brine and dried over sodium sulfate. After filtration and evaporation, the title compound was obtained as pale yellow solid (180 mg, 80%)

¹H NMR (400 MHz, CDCl₃) δ 7.88 (dd, *J* = 5.4, 2.9 Hz, 2H), 7.74 (dd, *J* = 5.4, 2.9 Hz, 2H), 3.90 (m, 2H), 3.59 (m, 2H). MS (ESI) *m/z*: 217 (M+H)⁺.

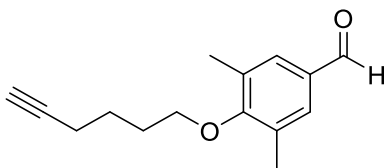
Synthesis of 4-(but-3-yn-1-yloxy)-3,5-dimethylbenzaldehyde (84a)



Compound **84a** was obtained as a pale yellow oil (950 mg, 66%) from derivative **83a** (1.05 g, 7.13 mmol) and intermediate **76a** (1.18 g, 7.84 mmol) according to the procedure described for **61**.

^1H NMR (400 MHz, CDCl_3) δ 9.88 (s, 1H), 7.55 (s, 2H), 3.95 (t, $J = 6.7$ Hz, 2H), 2.72 (t, $J = 6.8, 2.9$ Hz, 2H), 2.08-2.06 (m, 1H). MS (ESI) m/z : 203 ($\text{M}+\text{H}$) $^+$.

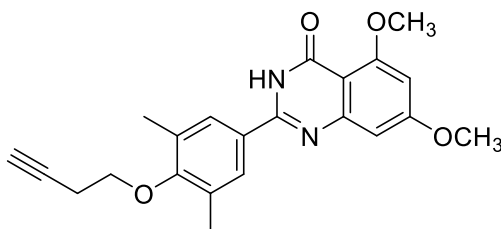
Synthesis of 4-(hex-5-yn-1-yloxy)-3,5-dimethylbenzaldehyde (84b)



Compound **84b** was obtained as a pale yellow solid (800 mg, 68%) from derivative **83b** (987 mg, 5.09 mmol) and intermediate **76** (764 mg, 5.09 mmol) according to the procedure described for **70**.

^1H NMR (400 MHz, CDCl_3) δ 9.88 (s, 1H), 7.55 (s, 2H), 3.85 (t, $J = 6.3$ Hz, 3H), 2.34 (s, 6H), 2.32 – 2.29 (m, 1H), 2.00 – 1.91 (m, 3H), 1.83 – 1.75 (m, 3H). MS (ESI) m/z : 231 ($\text{M}+\text{H}$) $^+$.

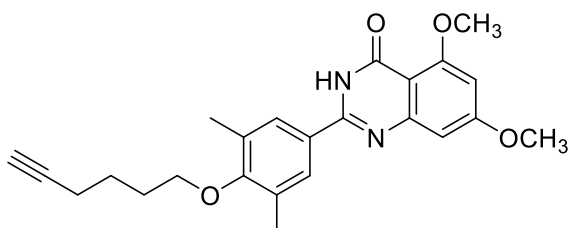
Synthesis of 2-(4-(but-3-yn-1-yloxy)-3,5-dimethylphenyl)-5,7-dimethoxyquinazolin-4(3H)-one (85a)



Compound **85a** was obtained as a pale yellow solid (270 mg, 72%) from derivative **84a** (200 mg, 0.990 mmol) and intermediate **64** (194 mg, 0.990 mmol) according to the procedure described for **65**.

^1H NMR (400 MHz, DMSO- d_6) δ 11.83 (s, 1H), 7.90 (s, 2H), 6.74 (d, $J = 2.3$ Hz, 1H), 6.51 (d, $J = 2.3$ Hz, 1H), 3.91 – 3.87 (m, 5H), 3.84 (s, 3H), 2.94 – 2.92 (m, 1H), 2.70 – 2.62 (m, 2H), 2.32 (s, 6H). MS (ESI) m/z : 379 (M+H) $^+$.

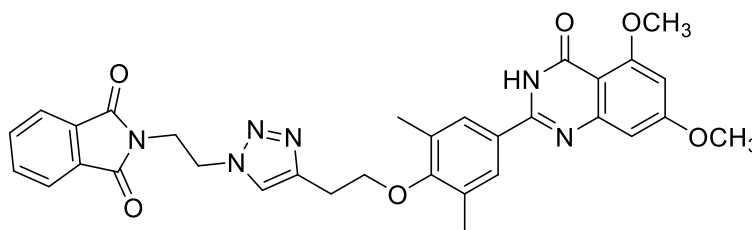
Synthesis of 2-(4-(hex-5-yn-1-yloxy)-3,5-dimethylphenyl)-5,7-dimethoxyquinazolin-4(3H)-one (85b)



Compound **85b** was obtained as a pale yellow solid (618 mg, 70%) from derivative **84b** (500 mg, 2.17 mmol) according to the procedure described for **65**.

^1H NMR (400 MHz, CDCl $_3$) δ 9.14 (s, 1H), 7.66 (s, 2H), 6.83 (d, $J = 2.3$ Hz, 1H), 6.46 (d, $J = 2.3$ Hz, 1H), 3.98 (s, 3H), 3.93 (s, 3H), 3.84 (t, $J = 6.3$ Hz, 2H), 2.36 (s, 6H), 2.34 – 2.29 (m, 1H), 2.02 – 1.93 (m, 3H), 1.86 – 1.75 (m, 3H). MS (ESI) m/z : 407 (M+H) $^+$.

Synthesis of 2-(2-(4-(2-(4-(5,7-dimethoxy-4-oxo-3,4-dihydroquinazolin-2-yl)-2,6-dimethylphenoxy)ethyl)-1H-1,2,3-triazol-1-yl)ethyl)isoindoline-1,3-dione (86a)

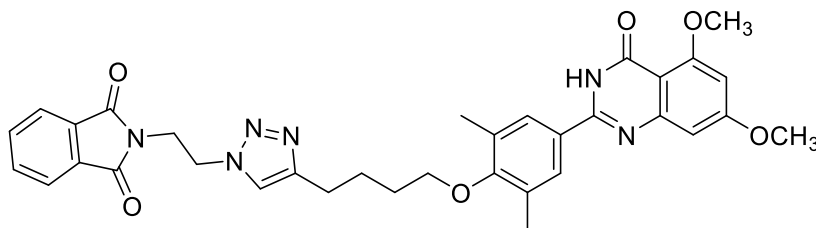


A solution of compound **81** (60 mg, 0.277 mmol) in 0.500 mL of dry DCM was added to a solution of CuI (1 mg, 0.005 mmol), DIPEA (0.0057 mL, 0.010 mmol) and AcOH (0.0017 mL, 0.010 mmol) in 0.300 mL of dry DCM. After 5 min, **85a** (100 mg, 0.264 mmol) was added

and the resulting mixture was stirred at room temperature for 18 h. Then, the solvent was evaporated and the crude was purified by silica gel chromatography (DCM/EtOAc 70:30 to 20:80) to give the title compound **86a** as white solid (144 mg, 87%).

¹H NMR (400 MHz, DMSO-*d*₆) δ 11.82 (s, 1H), 8.06 (s, 1H), 7.87 (s, 2H), 7.83 – 7.81 (m, 4H), 6.73 (s, 1H), 6.51 (s, 1H), 4.63 (t, *J* = 5.8 Hz, 2H), 4.07 – 3.94 (m, 4H), 3.88 (s, 3H), 3.84 (s, 3H), 3.15 – 2.98 (m, 2H), 2.19 (s, 6H). MS (ESI) *m/z*: 595 (M+H)⁺.

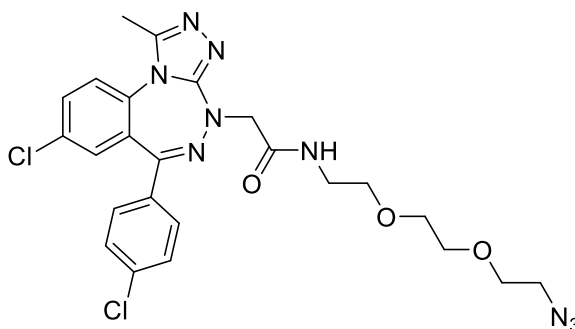
Synthesis 2-(2-(4-(4-(4-(5,7-dimethoxy-4-oxo-3,4-dihydroquinazolin-2-yl)-2,6-dimethylphenoxy)butyl)-1H-1,2,3-triazol-1-yl)ethyl)isoindoline-1,3-dione (86b)



Compound **86b** was obtained as a pale yellow solid (193 mg, 67%) from derivative **85b** (179 mg, 0.440 mmol) and intermediate 81 (100 mg, 0.462 mmol) according to the procedure described for **86a**.

¹H NMR (400 MHz, CDCl₃) δ 9.23 (s, 1H), 7.82 (dd, *J* = 5.8, 2.7 Hz, 2H), 7.74 – 7.69 (m, 2H), 7.66 (s, 2H), 7.37 (s, 1H), 6.82 (s, 1H), 6.46 (s, 1H), 4.67 (t, *J* = 6.0 Hz, 2H), 4.15 (t, *J* = 6.0 Hz, 2H), 3.97 (s, 3H), 3.93 (s, 3H), 3.84 – 3.80 (m, 2H), 2.80 (t, *J* = 6.9 Hz, 2H), 2.35 (s, 6H), 1.94 – 1.82 (m, 4H). MS (ESI) *m/z*: 623 (M+H)⁺.

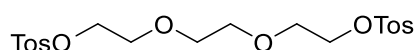
Synthesis of N-(2-(2-(2-azidoethoxy)ethoxy)ethyl)-8-chloro-6-(4-chlorophenyl)-1-methyl-4H-benzo[e][1,2,4]triazolo[3,4-c][1,2,4]triazepine-4-carboxamide (87)



To a solution of **49** (30 mg, 0.074 mmol) in 2 mL of dry DMF, compound **90** (17 mg, 0.081 mmol) was added. Then, EDC (24 mg, 0.126 mmol), HOBT (20 mg, 0.126 mmol) and NMM (0.036 mL, 0.325 mmol) were added. The resulting mixture was stirred at room temperature for 18 h. Then, water was added (10 mL): the aqueous organic phase was extracted with EtOAc (3 x 15 mL). The collected organic phases were washed with saturated solution of NaHCO₃ (3 x 15 mL), brine, dried over sodium sulfate, filtered and concentrated under reduced pressure. After purification on a silica gel flash-chromatography column (DCM-MeOH 97:3 to 90:1), the title compound was obtained as yellow solid (31 mg, 75%)

¹H NMR (400 MHz, CDCl₃) δ 7.64 (dd, *J* = 8.6, 2.4 Hz, 1H), 7.48 (d, *J* = 8.6 Hz, 2H), 7.39 (d, *J* = 8.6 Hz, 2H), 7.32 (d, *J* = 8.7 Hz, 1H), 7.28 (s, 1H), 6.80 – 6.68 (m, 1H), 3.64 – 3.58 (m, 2H), 3.55 – 3.43 (m, 8H), 3.34 (t, *J* = 5.0 Hz, 2H), 2.60 (s, 3H). MS (ESI) *m/z*: 544 (M+H)⁺.

Synthesis of (ethane-1,2-diylbis(oxy))bis(ethane-2,1-diyl) bis(4-methylbenzenesulfonate) (88)

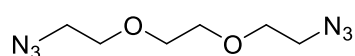


To a cooled solution of compound **70c** (3 g, 19.98 mmol) in 40 mL of DCM, TsCl (7.62 g, 39.95 mmol) and KOH powder (8.97 g, 159.84 mmol) were added in three portions at 0°C. The resulting mixture was warm up at room temperature and stirred for 18 h. Then, water (80 mL) was added: the aqueous phase was extracted with DCM (3 x 40 mL). The collected organic

phases were washed with NaHCO₃ (3 x 40 mL), brine and dried over sodium sulfate. After filtration and evaporation under reduced pressure, the title compound was obtained as white solid (8.5 g, 93%).

¹H NMR (400 MHz, CDCl₃) δ 7.79 (d, *J* = 7.9 Hz, 4H), 7.34 (d, *J* = 7.9 Hz, 4H), 4.18 – 4.11 (m, 4H), 3.68 – 3.62 (m, 4H), 3.57 – 3.52 (m, 4H), 2.45 (s, 6H). MS (ESI) *m/z*: 459 (M+H)⁺.

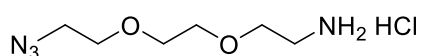
Synthesis of 1,2-bis(2-azidoethoxy)ethane (89)



To a solution of compound **88** (3 g, 6.54 mmol) in 22 mL of DMF, sodium azide (850 mg, 13.08 mmol) and tetrabutylammonium iodide (121 mg, 0.327 mmol) were added. The resulting mixture was stirred at 80 °C for 18 h. Then the mixture was concentrated under vacuo and the insoluble salts were filtered and the filtrate concentrated yielding the title compounds as colorless liquid (1.3 g, 99 %)

¹H NMR (400 MHz, CDCl₃) δ 3.71 – 3.62 (m, 8H), 3.37 (q, *J* = 4.7 Hz, 4H). MS (ESI) *m/z*: 201 (M+H)⁺.

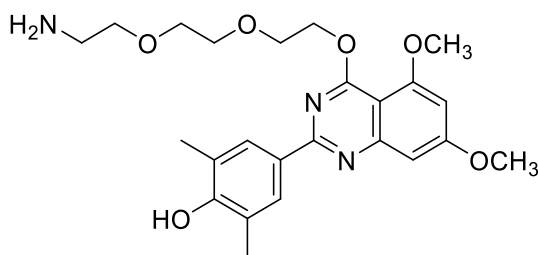
Synthesis of 2-(2-(2-azidoethoxy)ethoxy)ethan-1-amine hydrochloride (90)



To a solution of compound **89** (1.31 g, 6.54 mmol) in 40 mL of EtOAc, Ph₃P (1.71 g, 6.54 mmol) and 8 mL of HCl 1 M were added. The resulting mixture was stirred at room temperature for 18 h. Then the mixture was diluted with acidified water (40 mL): the aqueous phase was washed with EtOAc (3 x 20 mL) and then concentrated under reduced pressure to give the title compound as yellow oil (1.08 g, 78%).

¹H NMR (400 MHz, CDCl₃) δ 3.83 (t, *J* = 5.0 Hz, 2H), 3.74 – 3.67 (m, 6H), 3.46 (d, *J* = 5.1 Hz, 2H), 3.25 (d, *J* = 5.2 Hz, 2H).

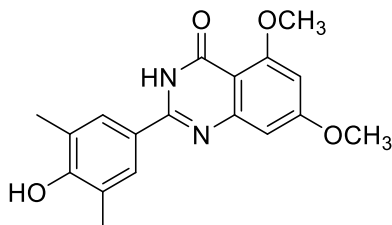
Synthesis of 4-(4-(2-(2-(2-aminoethoxy)ethoxy)ethoxy)ethoxy)-5,7-dimethoxyquinazolin-2-yl)-2,6-dimethyl phenol (91)



Compound **91** was obtained as a yellow oil (26 mg, 98 %) from derivative **93** (30 mg, 0.058 mmol) according to the procedure described for **51a**.

^1H NMR (400 MHz, CDCl_3) δ 8.16 (s, 2H), 6.93 (s, 1H), 6.44 (s, 1H), 4.83 (t, $J = 5.1$ Hz, 2H), 4.06 – 3.99 (m, 2H), 3.94 (s, 3H), 3.93 (s, 3H), 3.86 – 3.81 (m, 2H), 3.71 – 3.66 (m, 2H), 3.55 – 3.51 (m, 2H), 2.90 – 2.82 (m, 2H), 2.35 (s, 6H). MS (ESI) m/z : 458 ($\text{M}+\text{H}$) $^+$

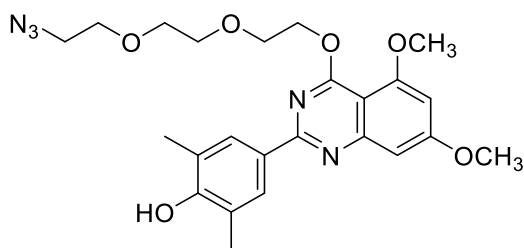
Synthesis of 2-(4-hydroxy-3,5-dimethylphenyl)-5,7-dimethoxyquinazolin-4(3H)-one (92)



Compound **92** was obtained as a yellow solid (573 mg, 94%) from derivative **64** (370 mg, 1.88 mmol) and intermediate **76a** (282 mg, 1.88 mmol) according to the procedure described for **65**.

^1H NMR (400 MHz, $\text{DMSO}-d_6$) δ 11.66 (s, 1H), 8.93 (s, 1H), 7.85 (s, 2H), 6.70 (d, $J = 1.7$ Hz, 1H), 6.48 (d, $J = 2.3$ Hz, 1H), 3.88 (s, 3H), 3.83 (s, 3H), 2.23 (s, 6H). MS (ESI) m/z : 327 ($\text{M}+\text{H}$) $^+$.

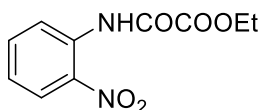
Synthesis of 4-(4-(2-(2-(2-azidoethoxy)ethoxy)ethoxy)ethoxy)-5,7-dimethoxyquinazolin-2-yl)-2,6-dimethyl phenol (93)



Compound **93** was obtained as a yellow oil (80 mg, 37%) from derivative **92** (150 mg, 0.455 mmol) and intermediate **74c** (165 mg, 0.500 mmol) according to the procedure described for **61**.

^1H NMR (400 MHz, CDCl_3) δ 8.16 (s, 2H), 6.92 (d, $J = 2.1$ Hz, 1H), 6.43 (d, $J = 2.1$ Hz, 1H), 4.94 (s, 1H), 4.85 – 4.82 (m, 2H), 4.06 – 4.01 (m, 2H), 3.94 (s, 3H), 3.92 (s, 3H), 3.89 – 3.85 (m, 2H), 3.74 – 3.64 (m, 4H), 3.39 – 3.34 (m, 2H), 2.35 (s, 6H). MS (ESI) m/z : 484 ($\text{M}+\text{H}$) $^+$.

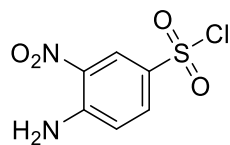
Synthesis of ethyl 2-((2-nitrophenyl)amino)-2-oxoacetate (95)



To a solution of 2-nitroaniline **94** (2.00 g, 14.48 mmol) in Et_2O (100 ml), ethyl chlorooxoacetate (1.78 ml, 15.93 mmol) was added in 4 portions and the resulting yellow suspension was stirred at room temperature for 18 h. Then the solvent was evaporated: the crude residue was taken up with EtOAc (100 mL), washed with saturated NaHCO_3 (3 x 30 mL), brine (30 mL), dried over sodium sulfate and evaporated to dryness, giving the title compound as a yellow solid (3.38 g, 98%).

^1H NMR (400 MHz, $\text{DMSO}-d_6$) δ 11.38 (s, 1H), 8.17–8.05 (m, 2H), 7.85–7.76 (m, 1H), 7.52–7.41 (m, 1H), 4.34 (q, $J = 7.0$ Hz, 2H), 1.33 (t, $J = 7.0$ Hz, 3H). MS (ESI) m/z : 239 ($\text{M}+\text{H}$) $^+$.

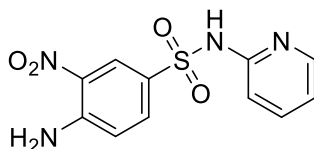
Synthesis of 4-amino-3-nitrobenzenesulfonyl chloride (96)



A solution of ethyl 2-(2-nitrophenylamino)-2-oxoacetate **95** (3 g, 12.55 mmol) in 6.7 ml of chlorosulfonic acid was heated at 80 °C for 3 h. The red mixture was poured slowly into ice water (200 ml) and stirred for 30 min. The product was extracted from the aqueous solution using Et₂O (3 x 40 mL). The combined organic phases were washed with brine (10 mL), dried over sodium sulfate, filtered, and concentrated in vacuo to give the title compound as a brown solid which was immediately used for the next reaction without purification.

¹H NMR (400 MHz, DMSO-*d*₆) δ 8.16 (d, *J* = 2.0 Hz, 1H), 7.56 (dd, *J* = 8.8, 2.0 Hz, 1H), 6.96 (d, *J* = 8.8 Hz, 1H).

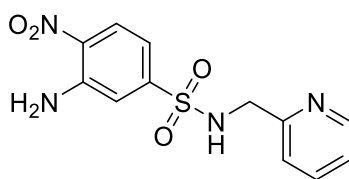
Synthesis of 4-amino-3-nitro-N-(pyridin-2-yl)benzenesulfonamide (98a)



To a stirred solution at 0 °C of crude **96** (1.41 g, 5.98 mmol) in dry pyridine (6 mL) was added dropwise, under nitrogen atmosphere, 2-aminopyridine **97a** (506 mg, 5.38 mmol). The reaction was kept at 0° C for 3 hours until starting material disappearance. Then, water was added (10 mL): the resulting solid was filtered and washed several time with water affording the title compound as orange solid (700 mg, 40%).

¹H NMR (400 MHz, DMSO-*d*₆) δ 8.47 (d, *J* = 2.2 Hz, 1H), 8.04 – 8.00 (m, 1H), 7.94 (s, 2H), 7.80 – 7.68 (m, 2H), 7.09 (dd, *J* = 16.2, 8.8 Hz, 2H), 6.87 (d, *J* = 6.5 Hz, 1H). **MS** (ESI) *m/z*: 295 (M+H)⁺.

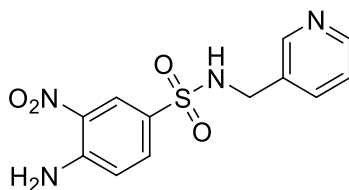
Synthesis of 4-amino-3-nitro-N-(pyridin-2-ylmethyl)benzenesulfonamide (98b)



To a stirred solution at 0 °C of crude **96** (765 mg, 3.24 mmol) in dry THF (30 mL), 2-picolylamine **97b** (1.33 mL, 12.93 mmol) was added dropwise, under nitrogen atmosphere, and the reaction was stirred for 18 h at room temperature. Then, the reaction mixture was concentrated under reduced pressure and the residue was taken up with 50 ml of water. The aqueous phase was extracted with EtOAc (3 x 20 mL), the combined organic phases were washed with brine, dried over Na₂SO₄, filtered and evaporated under reduced pressure. The title compound was obtained as yellow solid after crystallization with EtOH (590 mg, 60%).

¹H NMR (400 MHz, DMSO-*d*₆) δ 8.40 – 8.38 (m, 1H), 8.26 (d, *J* = 2.2 Hz, 1H), 7.95 (s, 2H), 7.72 – 7.61 (m, 2H), 7.33 (d, *J* = 7.9 Hz, 1H), 7.23 – 7.18 (m, 1H), 7.06 (d, *J* = 9.0 Hz, 1H), 4.09 (s, 2H). MS (ESI) *m/z*: 309 (M+H)⁺.

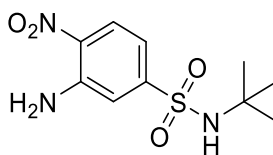
Synthesis of 4-amino-3-nitro-N-(pyridin-3-ylmethyl)benzenesulfonamide (98c)



Compound **98c** was obtained as a yellow solid (560 mg, 62%) from derivative **96** (700 mg, 2.96 mmol) and the 3-picolylamine **97c** (1.20 mL, 11.83 mmol) according to the procedure described for **98b**.

¹H NMR (400 MHz, DMSO-*d*₆) δ 8.39 (d, *J* = 1.9 Hz, 1H), 8.28 (d, *J* = 2.2 Hz, 1H), 8.16 (s, 1H), 7.97 (s, 1H), 7.66 – 7.61 (m, 1H), 7.30 – 7.24 (m, 1H), 7.07 (d, *J* = 9.0 Hz, 1H), 4.03 (s, 2H). MS (ESI) *m/z*: 309 (M+H)⁺.

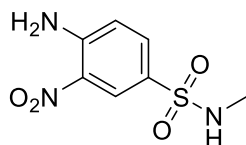
Synthesis of 3-amino-N-(tert-butyl)-4-nitrobenzenesulfonamide (98d)



Compound **98d** was obtained as orange solid (250 mg, 73%) from derivative **96** (420 mg, 1.77 mmol) and the *tert*-butylamine **97d** (0.746 mL, 7.09 mmol) according to the procedure described for **98b**.

^1H NMR (400 MHz, DMSO- d_6) δ 8.38 (d, J = 2.2 Hz, 1H), 7.95 (s, 2H), 7.70 (dd, J = 9.0, 2.2 Hz, 1H), 7.44 (s, 1H), 7.11 (d, J = 9.0 Hz, 1H), 1.10 (s, 9H). MS (ESI) m/z : 274 (M+H) $^+$.

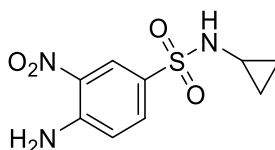
Synthesis of 4-amino-N-methyl-3-nitrobenzenesulfonamide (98e)



Compound **98e** was obtained as yellow solid (260 mg, 70%) from derivative **96** (380 mg, 1.61 mmol) and 2 M THF solution of methylamine **97e** (3.22 mL, 6.44 mmol) according to the procedure described for **98b**.

^1H NMR (400 MHz, DMSO- d_6) δ 8.36 – 8.29 (m, 1H), 7.99 (s, 2H), 7.66 (dd, J = 9.0, 2.2 Hz, 1H), 7.38 – 7.34 (m, 1H), 7.14 (d, J = 9.0 Hz, 1H), 2.39 (d, J = 4.8 Hz, 3H). MS (ESI) m/z : 232 (M+H) $^+$

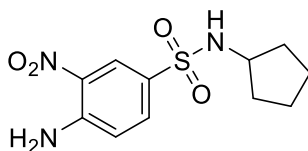
Synthesis of 4-amino-N-cyclopropyl-3-nitrobenzenesulfonamide (98f)



Compound **98f** was obtained as yellow solid (450 mg, 85%) from derivative **96** (488 mg, 2.06 mmol) and cyclopropylamine **97f** (0.571 mL, 8.25 mmol) according to the procedure described for **98b**.

^1H NMR (400 MHz, $\text{DMSO-}d_6$) δ 8.37 (d, $J = 2.2$ Hz, 1H), 8.00 (s, 2H), 7.80 (d, $J = 2.9$ Hz, 1H), 7.68 (dd, $J = 9.0, 2.2$ Hz, 1H), 7.15 (d, $J = 9.0$ Hz, 1H), 2.16 – 2.08 (m, 1H), 0.53 – 0.46 (m, 2H), 0.39 – 0.34 (m, 2H). MS (ESI) m/z : 258 ($\text{M}+\text{H}$) $^+$.

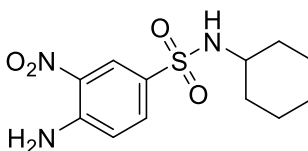
Synthesis of 4-amino-N-cyclopentyl-3-nitrobenzenesulfonamide (98g)



Compound **98g** was obtained as orange solid (387 mg, 70%) from derivative **96** (468 mg, 1.97 mmol) and cyclopentylamine **97g** (0.780 mL, 7.9 mmol) according to the procedure described for **98b**.

^1H NMR (400 MHz, $\text{DMSO-}d_6$) δ 8.36 (d, $J = 2.2$ Hz, 1H), 7.97 (s, 2H), 7.68 (dd, $J = 9.0, 2.2$ Hz, 1H), 7.55 (d, $J = 7.0$ Hz, 1H), 7.13 (d, $J = 9.0$ Hz, 1H), 3.38 – 3.35 (m, 1H), 1.66 – 1.48 (m, 4H), 1.42 – 1.25 (m, 4H). MS (ESI) m/z : 286 ($\text{M}+\text{H}$) $^+$.

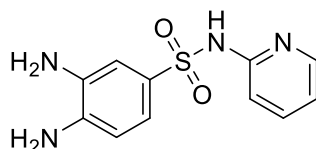
Synthesis of 4-amino-N-cyclohexyl-3-nitrobenzenesulfonamide (98h)



Compound **98h** was obtained as yellow solid (950 mg, 63%) from derivative **96** (1.2 g, 5.07 mmol) and cyclohexylamine **97h** (2.32 mL, 20.28 mmol) according to the procedure described for **98b**.

^1H NMR (400 MHz, $\text{DMSO-}d_6$) δ 8.36 (d, $J = 2.2$ Hz, 1H), 7.96 (s, 2H), 7.70 (dd, $J = 9.0, 2.2$ Hz, 1H), 7.56 (d, $J = 7.2$ Hz, 1H), 7.12 (d, $J = 9.0$ Hz, 1H), 2.94 – 2.85 (m, 1H), 1.62 – 1.52 (m, 5H), 1.19 – 1.09 (m, 5H). MS (ESI) m/z : 300 ($\text{M}+\text{H}$) $^+$.

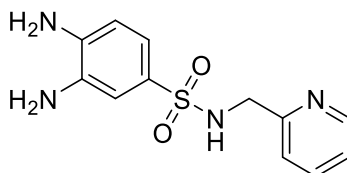
Synthesis of 3,4-diamino-*N*-(pyridin-2-yl)benzenesulfonamide (99a)



Compound **98a** (440 mg, 1.5 mmol) was dissolved in 7.20 mL of AcOH and Zn dust (977 mg, 1.5 mmol) was added portionwise. The reaction mixture was stirred for 1.5 h at room temperature until starting material disappearance. Then, the insoluble salts are filtered and the filtrate, concentrated under reduced pressure. The residual semisolid was taken up with water: the aqueous phase (20 mL) was extracted with EtOAc (3 x 15 mL) and the collected organic phases were washed with saturated solution of NaHCO_3 (3 x 15 mL) brine, dried over sodium sulfate, filtered and evaporated to dryness. The title compound was obtained as light brown solid (257 mg, 64%).

^1H NMR (400 MHz, $\text{DMSO-}d_6$) δ 10.86 (s, 1H), 8.09 (d, $J = 5.2$ Hz, 1H), 7.66 – 7.60 (m, 1H), 7.08 (s, 1H), 7.00 (s, 1H), 6.97 – 6.87 (m, 2H), 6.48 (dd, $J = 8.3, 1.2$ Hz, 1H), 5.23 (s, 2H), 4.82 (s, 2H). MS (ESI) m/z : 265 ($\text{M}+\text{H}$) $^+$.

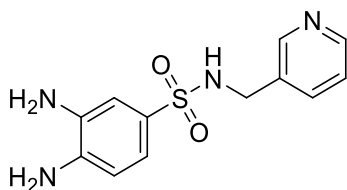
Synthesis of 3,4-diamino-*N*-(pyridin-2-ylmethyl)benzenesulfonamide (99b)



To a solution of **98b** (300 mg, 0.973 mmol) in 10 mL of EtOAc, 10% Pd/C was added. The mixture was stirred under a hydrogen atmosphere (balloon) for 18 h. Then, the solvent was evaporated and the title compound was obtained as light brown solid (250 mg, 92%).

^1H NMR (400 MHz, DMSO- d_6) δ 8.44 (d, $J = 4.7$ Hz, 1H), 7.75 (t, $J = 7.6$ Hz, 1H), 7.60 (t, $J = 6.5$ Hz, 1H), 7.39 (d, $J = 7.6$ Hz, 1H), 7.24 (dd, $J = 7.6, 4.7$ Hz, 1H), 6.96 (d, $J = 2.4$ Hz, 1H), 6.86 (dd, $J = 8.1, 2.4$ Hz, 1H), 6.55 (d, $J = 8.1$ Hz, 1H), 5.22 (brs, 2H), 4.84 (brs, 2H), 3.96 (d, $J = 6.2$ Hz, 2H). MS (ESI) m/z : 279 (M+H) $^+$.

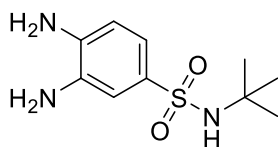
Synthesis of 3,4-diamino-N-(pyridin-3-ylmethyl)benzenesulfonamide (99c)



Compound **99c** was obtained as a yellow solid (85 mg, 94%) from derivative **98c** (100 mg, 0.324 mmol) according to the procedure described for **99b**.

^1H NMR (400 MHz, DMSO- d_6) δ 8.42 (d, $J = 2.0$ Hz, 1H), 7.69 – 7.57 (m, 2H), 7.31 (dd, $J = 7.8, 4.8$ Hz, 1H), 6.95 (d, $J = 2.2$ Hz, 1H), 6.86 (dd, $J = 8.1, 2.2$ Hz, 1H), 6.55 (d, $J = 8.2$ Hz, 1H), 5.23 (brs, 2H), 4.84 (brs, 2H), 3.90 (d, $J = 6.3$ Hz, 2H). MS (ESI) m/z : 279 (M+H) $^+$.

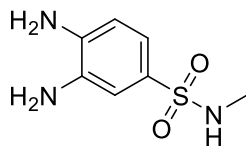
Synthesis of 3-amino-N-(tert-butyl)-4-nitrobenzenesulfonamide (99d)



Compound **99d** was obtained as orange solid (240 mg, 89%) from derivative **98d** (283 mg, 1.03 mmol) according to the procedure described for **99b**.

^1H NMR (400 MHz, DMSO- d_6) δ 6.96 (d, $J = 2.1$ Hz, 1H), 6.90–6.84 (m, 2H), 6.53 (d, $J = 8.2$ Hz, 1H), 5.13 (brs, 2H), 4.79 (brs, 2H), 1.08 (s, 9H). MS (ESI) m/z : 244 (M+H) $^+$

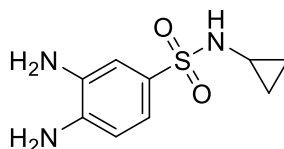
Synthesis of 4-amino-N-methyl-3-nitrobenzenesulfonamide (99e)



Compound **99e** was obtained as yellow solid (80 mg, 92%) from derivative **98e** (100 mg, 0.432 mmol) according to the procedure described for **99b**.

¹H NMR (400 MHz, DMSO-*d*₆) δ 6.90 (d, *J* = 2.2 Hz, 1H), 6.83 – 6.78 (m, 2H), 6.55 (d, *J* = 8.1 Hz, 1H), 5.19 (s, 2H), 4.83 (s, 2H), 2.32 (d, *J* = 5.2 Hz, 3H). MS (ESI) *m/z*: 202 (M+H)⁺.

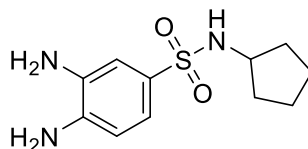
Synthesis of 3,4-diamino-N-cyclopropylbenzenesulfonamide (99f)



Compound **99f** was obtained as brown oil (340 mg, 97%) from derivative **98f** (400 mg, 1.55 mmol) according to the procedure described for **99b**.

¹H NMR (400 MHz, DMSO-*d*₆) δ 7.32 (d, *J* = 2.4 Hz, 1H), 6.94 (d, *J* = 2.1 Hz, 1H), 6.85 (dd, *J* = 8.2, 2.1 Hz, 1H), 6.55 (d, *J* = 8.2 Hz, 1H), 5.20 (s, 2H), 4.82 (s, 2H), 2.04 – 1.99 (m, 1H), 0.46 – 0.32 (m, 4H). MS (ESI) *m/z*: 228 (M+H)⁺.

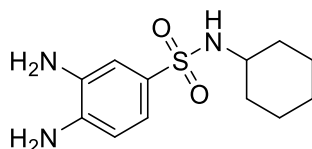
Synthesis of 3,4-diamino-N-cyclopentylbenzenesulfonamide (99g)



Compound **99g** was obtained as orange solid (0.320 g, 92%) from derivative **98g** (0.387 g, 1.36 mmol) according to the procedure described for **99b**.

^1H NMR (400 MHz, $\text{DMSO-}d_6$) δ 6.99 (d, $J = 6.8$ Hz, 1H), 6.92 (d, $J = 2.1$ Hz, 1H), 6.83 (dd, $J = 8.1, 2.2$ Hz, 1H), 6.53 (d, $J = 8.1$ Hz, 1H), 5.16 (brs, 2H), 4.83 (brs, 2H), 3.29 – 3.21 (m, 1H), 1.63 – 1.46 (m, 4H), 1.40 – 1.24 (m, 4H). MS (ESI) m/z : 256 (M+H) $^+$.

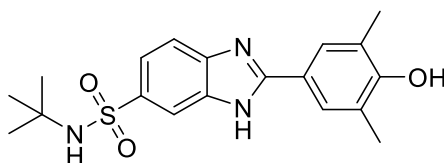
Synthesis of 3,4-diamino-N-cyclohexylbenzenesulfonamide (99h)



Compound **99h** was obtained as light brown solid (420 mg, 94%) from derivative **98h** (496 mg, 1.66 mmol) according to the procedure described for **99b**.

^1H NMR (400 MHz, $\text{DMSO-}d_6$) δ 6.98 (d, $J = 7.3$ Hz, 1H), 6.92 (d, $J = 2.2$ Hz, 1H), 6.83 (dd, $J = 8.1, 2.2$ Hz, 1H), 6.52 (d, $J = 8.1$ Hz, 1H), 5.14 (brs, 2H), 4.80 (brs, 2H), 2.79 (s, 1H), 1.62 – 1.39 (m, 5H), 1.14 – 0.94 (m, 5H). MS (ESI) m/z : 270 (M+H) $^+$.

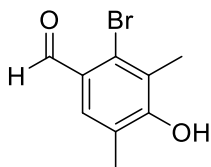
Synthesis of N-(tert-butyl)-2-(4-hydroxy-3,5-dimethylphenyl)-1H-benzodimidazole-6-sulfonamide (100)



Compound **99d** (300 mg, 1.24 mmol) was solubilized in 12 mL of dry DMF and 4-hydroxy-3,5-dimethylbenzaldehyde **76a** (186 mg, 1.24 mmol) and $\text{Na}_2\text{S}_2\text{O}_5$ (335 mg, 1.61 mmol) were added. The resulting mixture was heated at 80 °C and stirred at this temperature for 18 h. After cooling at room temperature, water was added. The brown precipitate formed was recovered by filtration and was washed several times with water. After recrystallization from EtOH, compound **100** was obtained as light yellow solid (295 mg, 64%).

^1H NMR (400 MHz, DMSO- d_6) δ 7.96 (s, 1H), 7.79 (s, 2H), 7.63 (s, 2H), 7.42 (s, 1H), 2.27 (s, 6H), 1.08 (s, 9H). MS (ESI) m/z : 374 (M+H) $^+$.

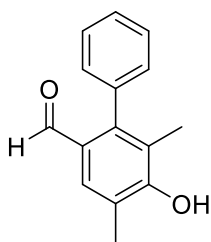
Synthesis of 2-bromo-4-hydroxy-3,5-dimethylbenzaldehyde (101)



To a solution of **76a** (1 g, 6.66 mmol) in 3.33 mL of H_2SO_4 , N-bromosuccinimide (3.55 g, 19.98 mmol) was added portionwise with continuous stirring. The resulting mixture was heated at 60 $^\circ\text{C}$ and stirred for 6 hours. Then water was added and the resulting precipitate was filtered and washed several time with water affording the title compound as red solid (290 mg, 20%).

^1H NMR (400 MHz, CDCl_3) δ 10.29 (s, 1H), 7.64 (s, 1H), 2.41 (s, 3H), 2.26 (s, 3H). MS (ESI) m/z : 228 (M+H) $^+$, 230 (M + H + 2) $^+$

Synthesis of 5-hydroxy-4,6-dimethyl-[1,1'-biphenyl]-2-carbaldehyde (103a)

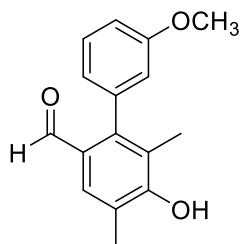


In a 20 mL CEM pressure vessel equipped with a stirrer bar, compound **101** (100 mg, 0.436 mmol) was dissolved in 8.8 mL of EtOH. Then, phenylboronic acid **102a** (64 mg, 0.524 mmol), Tetrakis(triphenylphosphine)palladium (23 mg, 0.022 mmol) and K_2CO_3 (157 mg, 1.13 mmol) were added. The microwave vial was sealed and heated in a CEM Discover microwave synthesizer to 80 $^\circ\text{C}$ for 30 min. After cooling to room temperature, the reaction mixture was filtered and the filtrate concentrated under vacuo. The residual semisolid was taken up with EtOAc (30 mL) and the organic phase was washed with water (3 x 15 mL), brine, dried over

sodium sulfate and filtered. The solvent was removed under reduced pressure and the resulting crude material was purified by silica gel chromatography (hex/EtOAc 95:5 to 50:50) to give compound **103a** a light brown solid (70 mg, 70%).

^1H NMR (400 MHz, CDCl_3) δ 9.51 (s, 1H), 7.73 (s, 1H), 7.48 – 7.38 (m, 3H), 7.23 – 7.18 (m, 2H), 2.35 (s, 3H), 2.00 (s, 3H). MS (ESI) m/z : 227 ($\text{M}+\text{H}$) $^+$.

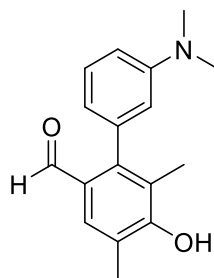
Synthesis of 5-hydroxy-3'-methoxy-4,6-dimethyl-[1,1'-biphenyl]-2-carbaldehyde (103b)



Compound **103b** was obtained as orange solid (75 mg, 67%) from derivative **101** (100 mg, 0.436 mmol) and **102b** (80 mg, 0.524 mmol) according to the procedure described for **103a**.

^1H NMR (400 MHz, $\text{DMSO}-d_6$) δ 9.36 (s, 1H), 7.54 (s, 1H), 7.39 (t, $J = 8.1$ Hz, 1H), 7.08 – 6.95 (m, 1H), 6.81 – 6.73 (m, 1H), 6.38 – 6.27 (m, 1H), 3.78 (s, 3H), 3.68 (s, 2H), 2.27 (s, 2H). MS (ESI) m/z : 257 ($\text{M}+\text{H}$) $^+$.

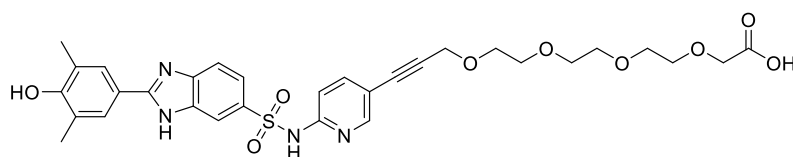
Synthesis of 3'-(dimethylamino)-5-hydroxy-4,6-dimethyl-[1,1'-biphenyl]-2-carbaldehyde (103c)



Compound **103c** was obtained as orange solid (55 mg, 67%) from derivative **101** (70 mg, 0.305 mmol) and **102c** (61 mg, 0.367 mmol) according to the procedure described for **103a**.

^1H NMR (400 MHz, CDCl_3) δ 9.56 (s, 1H), 7.72 (s, 1H), 7.31 – 7.28 (m, 1H), 6.76 (dd, $J = 8.6$, 2.6 Hz, 1H), 6.58 – 6.53 (m, 1H), 6.51 (d, $J = 2.3$ Hz, 1H), 2.96 (s, 6H), 2.34 (s, 3H), 2.04 (s, 3H). MS (ESI) m/z : 270 ($\text{M}+\text{H}$) $^+$.

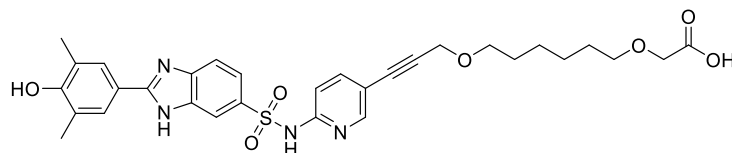
Synthesis of 15-(6-((2-(4-hydroxy-3,5-dimethylphenyl)-1H-benzo[d]imidazole)-6-sulfonamido)pyridin-3-yl)-3,6,9,12-tetraoxapentadec-14-ynoic acid (106)



Compound **119** (9 mg, 0.013 mmol) was dissolved in 0.200 mL of a solution DCM/TFA (1:1) and the mixture was stirred for 30 min and monitored by LC-MS. Then, solvent was evaporated, and the resulting solid was used for the next step without further purification (8 mg, 96%).

LC/MS 1.2-1.25 min, m/z : 639.2 ($\text{M}+\text{H}$) $^+$

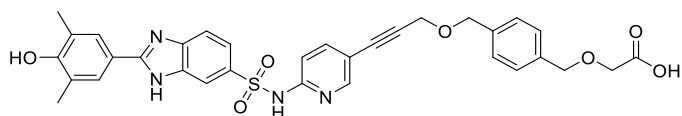
Synthesis of 2-((6-((3-(6-((2-(4-hydroxy-3,5-dimethylphenyl)-1H-benzo[d]imidazole)-6-sulfonamido)pyridin-3-yl)prop-2-yn-1-yl)oxy)hexyl)oxy)acetic acid (107)



Compound **107** was obtained as brown solid (8 mg, 96%) from compound **120** (7 mg, 0.011 mmol) according to the procedure described for **106**.

LC/MS 1.3-1.4 min, m/z : 607.2 ($\text{M}+\text{H}$) $^+$

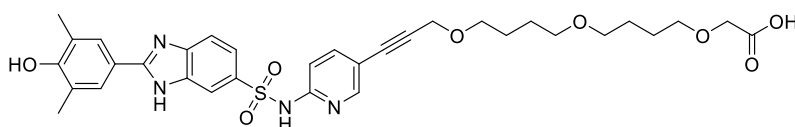
Synthesis of 2-((4-(((3-(6-((2-(4-hydroxy-3,5-dimethylphenyl)-1H-benzo[d]imidazole)-6-sulfonamido)pyridin-3-yl)prop-2-yn-1-yl)oxy)methyl)benzyl)oxy)acetic acid (108)



Compound **108** was obtained as brown solid (6 mg, 96%) from compound **121** (7 mg, 0.010 mmol) according to the procedure described for **106**.

LC/MS 1.35-1.45 min, m/z : 627.2 (M+H)⁺

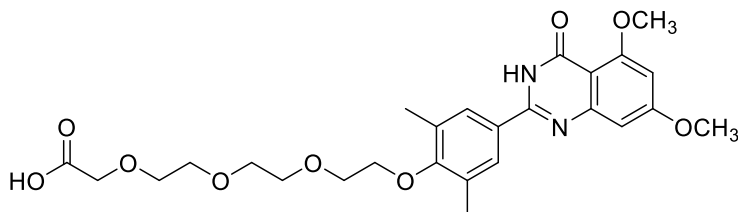
Synthesis of 2-(4-(4-(((3-(6-((2-(4-hydroxy-3,5-dimethylphenyl)-1H-benzo[d]imidazole)-6-sulfonamido)pyridin-3-yl)prop-2-yn-1-yl)oxy)butoxy)butoxy)acetic acid (109)



Compound **109** was obtained as brown solid (13 mg, 95%) from compound **122** (16 mg, 0.021 mmol) according to the procedure described for **106**.

LC/MS 1.3-1.4 min, m/z : 651.2 (M+H)⁺

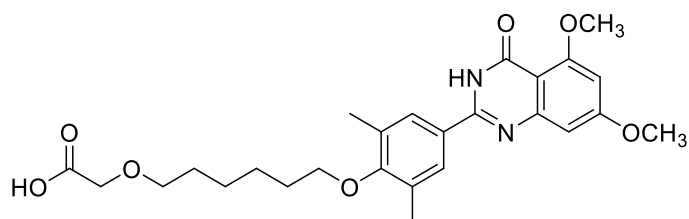
Synthesis of 2-(2-(2-(2-(4-(5,7-dimethoxy-4-oxo-3,4-dihydroquinazolin-2-yl)-2,6-dimethyl phenoxy)ethoxy)ethoxy)ethoxy)acetic acid (110)



Compound **110** was obtained as yellow solid (47 mg, 98%) from compound **141** (53 mg, 0.093 mmol) according to the procedure described for **106**.

LC/MS 1.3-1.4, m/z : 517.1 (M+H)⁺

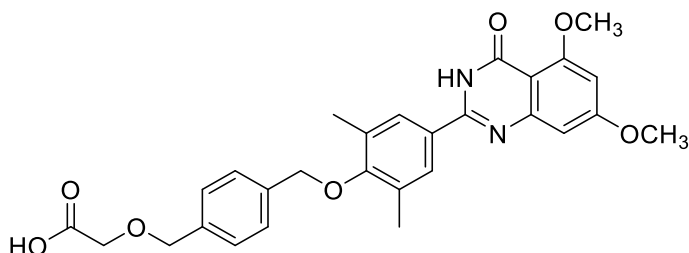
Synthesis of 2-((6-(4-(5,7-dimethoxy-4-oxo-3,4-dihydroquinazolin-2-yl)-2,6-dimethylphenoxy)hexyl)oxy)acetic acid (111)



Compound **111** was obtained as yellow solid (59 mg, 99%) from compound **142** (60 mg, 0.111 mmol) according to the procedure described for **106**.

LC/MS 1.5-1.6 min, m/z : 485.1 (M+H)⁺

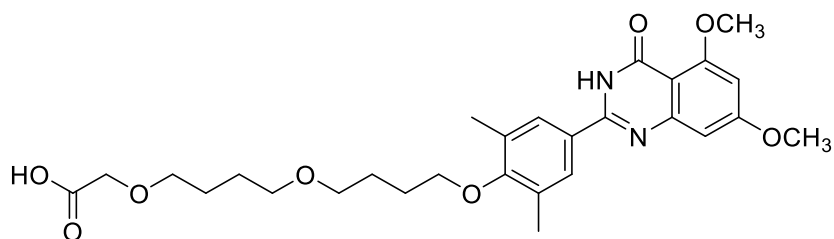
Synthesis of 2-((4-((4-(5,7-dimethoxy-4-oxo-3,4-dihydroquinazolin-2-yl)-2,6-dimethylphenoxy)methyl)benzyl)oxy)acetic acid (112)



Compound **112** was obtained as yellow solid (45 mg, 99%) from compound **143** (50 mg, 0.09 mmol) according to the procedure described for **106**.

LC/MS 1.7-1.8 min, m/z : 505.2 (M+H)⁺

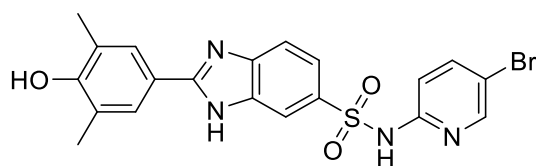
Synthesis of 2-((4-((4-(4-(5,7-dimethoxy-4-oxo-3,4-dihydroquinazolin-2-yl)-2,6-dimethylphenoxy)butoxy)butoxy)acetic acid (113)



Compound **113** was obtained as brown solid (43 mg, 97%) from compound **144** (49 mg, 0.084 mmol) according to the procedure described for **106**.

LC/MS 1.5-1.6 min, m/z : 529.2 (M+H)⁺

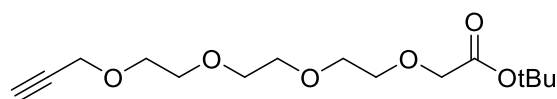
Synthesis of N-(5-bromopyridin-2-yl)-2-(4-hydroxy-3,5-dimethylphenyl)-1H-benzo[d]imidazole-6-sulfonamide (114)



Compound **114** was obtained as brown solid (380 mg, 56%) from derivative **124** (560 mg, 1.5 mmol) and the intermediate **76a** (225 mg, 1.5 mmol) according to the procedure described for **100**.

¹H NMR (400 MHz, DMSO-d₆) δ 11.16 (s, 1H), 8.86 – 8.84 (m, 1H), 8.26 (d, J = 2.5 Hz, 1H), 8.10 (s, 1H), 7.88 (d, J = 8.6 Hz, 1H), 7.77 (s, 2H), 7.73 – 7.55 (m, 1H), 7.10 (dd, J = 8.6, 5.1 Hz, 1H), 2.26 (s, 6H). LC/MS: 1.3 min m/z 473 (M+H)⁺, 475 (M + H + 2)⁺

Synthesis of tert-butyl 3,6,9,12-tetraoxapentadec-14-ynoate (115)

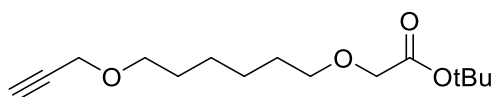


To a cooled solution of **125** (700 mg, 3.72 mmol) in 8 mL of dry THF, NaH 60% in mixture (178 mg, 4.46 mmol) was added and the resulting mixture was stirred at 0 °C for 30 min. Then, *tert*-butyl 2-bromoacetate (0.660 mL, 4.46 mmol) was added and the final suspension was continuously stirred for 14 h at room temperature. Then, the solvent was removed under reduced pressure and the residual was taken up with saturated solution of NH₄Cl (30 mL): the aqueous phase was extracted with EtOAc (3 x 20 mL). The collected organic phases were washed with brine, dried over sodium sulfate, filtered and concentrated. The product **115** was obtained after

purification filtration on a silica gel flash-chromatography column (heptane-EtOAc 70:30 to 0:100) to yield a colorless oil (570 mg, 50%).

$^1\text{H NMR}$ (400 MHz, CDCl_3) δ 4.20 (s, 2H), 4.02 (s, 2H), 3.75 – 3.64 (m, 12H), 2.42 (s, 1H), 1.48 (s, 9H).

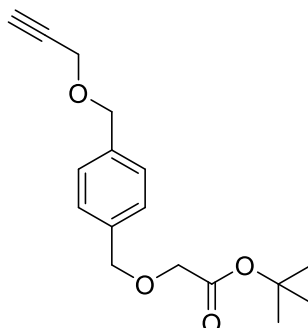
Synthesis of tert-butyl 2-((6-(prop-2-yn-1-yloxy)hexyl)oxy)acetate (116)



Compound **127** (100 mg, 0.640 mmol) and rhodium acetate (15 mg, 0.032 mmol) were dissolved in 0.810 mL of dry DCM under nitrogen atmosphere and the resulting green suspension was cooled at 0°C. Then, *tert*-Butyl diazoacetate (0.100 mL, 0.768 mmol) was added dropwise under 1 hour. Then, the reaction was allowed to reach room temperature and was stirred for 18 h. The crude was purified on a silica gel flash-chromatography column (heptane- EtOAc 90:10 to 40:60) to yield the title compound as colorless oil (115 mg, 66%).

$^1\text{H NMR}$ (400 MHz, CDCl_3) δ 4.03 (d, $J = 2.4$ Hz, 2H), 3.85 (s, 2H), 3.42 (t, $J = 6.6$ Hz, 4H), 2.35 (t, $J = 2.4$ Hz, 1H), 1.59 – 1.44 (m, 4H), 1.39 (s, 9H), 1.31 (q, $J = 3.9$ Hz, 4H).

Synthesis of tert-butyl 2-((4-((prop-2-yn-1-yloxy)methyl)benzyl)oxy)acetate (117)

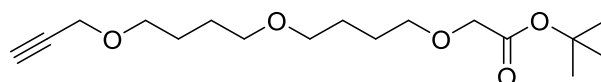


A solution of propargyl alcohol (0.040 mL, 0.698 mmol) in 10 mL of dry DMF was cooled at 0 °C and NaH 60% in mixture (28 mg, 0.698 mmol) was added. The resulting mixture was stirred at 0 °C for 30 min under nitrogen atmosphere. Then, compound **130** (200 mg, 0.634

mmol) was added and the final suspension was continuously stirred for 14 h at room temperature. The crude was concentrated under reduced pressure and the residual was taken up with saturated solution of NH₄Cl (30 mL): the aqueous phase was extracted with EtOAc (3 x 20 mL). The collected organic phases were washed with brine, dried over sodium sulfate, filtered and concentrated. The product **117** was obtained after purification filtration on a silica gel flash-chromatography column (heptane-EtOAc 90:10 to 50:50) to yield a colorless oil (110 mg, 60%).

¹H NMR (400 MHz, CDCl₃) δ 7.40 – 7.32 (m, 4H), 4.61 (d, *J* = 3.9 Hz, 2H), 4.17 (d, *J* = 2.4 Hz, 2H), 3.98 (s, 2H), 2.46 (t, *J* = 2.4 Hz, 1H), 1.48 (s, 9H).

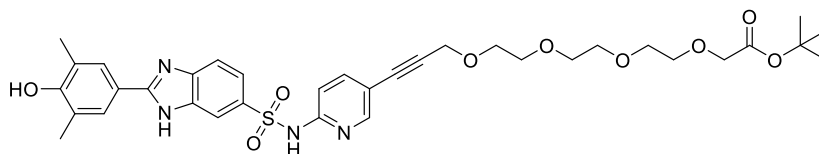
Synthesis of tert-butyl 2-(4-(4-(prop-2-yn-1-yloxy)butoxy)butoxy)acetate (118)



Compound **118** was obtained as colorless oil (15 mg, 30 %) from compound **136** (62 mg, 0.160 mmol) and propargyl alcohol (0.011 mL, 0.176 mmol) according to the procedure described for **117**.

¹H NMR (400 MHz, CDCl₃) δ 4.12 (d, *J* = 2.4 Hz, 2H), 3.93 (s, 2H), 3.52 (td, *J* = 6.3, 1.6 Hz, 4H), 3.46 – 3.38 (m, 4H), 2.40 (t, *J* = 2.3 Hz, 1H), 1.70 – 1.61 (m, 8H), 1.47 (s, 9H).

Synthesis of tert-butyl 15-(6-((2-(4-hydroxy-3,5-dimethylphenyl)-1H-benzo[d]imidazole)-6-sulfonamido)pyridin-3-yl)-3,6,9,12-tetraoxapentadec-14-ynoate (119)



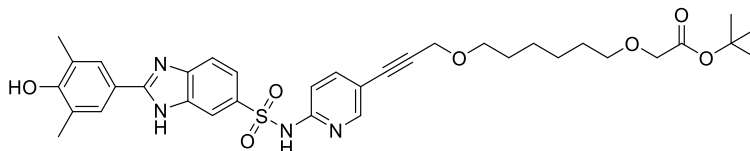
A solution of compound **114** (50 mg, 0.106 mmol) in 1 mL of dry DMF was added to K₂CO₃ (44 mg, 0.318 mmol) and CuI (6 mg, 0.027 mmol) under argon atmosphere. Then, compound

115 (48 mg, 0.158 mmol), tri-*tert*-butylphosphine (0.011 mL, 0.042 mmol) bis(tri-*tert*-butylphosphine)palladium(0) (40 mg, 0.078 mmol) were added and the resulting black suspension was stirred at 100 °C for 18 h. Then, the solvent was removed under reduced pressure and the solid residual was taken up with a mixture of DCM/MeOH (9:1) and filtered on a path of celite. The filtrate was evaporated under reduced pressure and the crude was purified on silica gel flash-chromatography column (DCM-MeOH 97:3 to 80:20) to give the title compound as brown solid (9 mg, 13%).

¹H NMR (400 MHz, CD₃OD) δ 8.44 (s, 1H), 8.18 (d, *J* = 2.3 Hz, 2H), 7.81 (dd, *J* = 8.6, 1.8 Hz, 1H), 7.72 (s, 2H), 7.67 (dd, *J* = 8.6, 2.3 Hz, 1H), 7.62 (d, *J* = 8.6 Hz, 1H), 7.21 – 7.16 (m, 1H), 4.37 (s, 2H), 4.00 (s, 2H), 3.77 – 3.55 (m, 12H), 2.31 (s, 6H), 1.43 (s, 9H).

LC/MS: 1.47 min *m/z* 695.3 (M+H)⁺

Synthesis of tert-butyl 2-((6-((3-((2-(4-hydroxy-3,5-dimethylphenyl)-1H-benzo[d]imidazole)-6-sulfonamido)pyridin-3-yl)prop-2-yn-1-yl)oxy)hexyl)oxy)acetate (120)

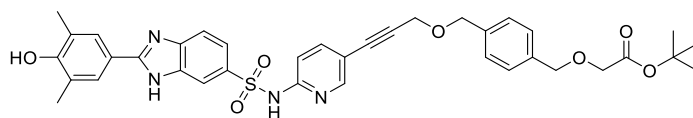


Compound **120** was obtained as brown solid (8 mg, 11%) from compound **114** (50 mg, 0.106 mmol) and intermediate **116** (43 mg, 0.159 mmol) according to the procedure described for **119**.

¹H NMR (400 MHz, CD₃OD) δ 8.21 – 8.14 (m, 3H), 7.81 (dd, *J* = 8.6, 1.7 Hz, 1H), 7.71 (s, 2H), 7.67 (dd, *J* = 8.7, 2.2 Hz, 1H), 7.62 (d, *J* = 8.6 Hz, 1H), 7.19 (dd, *J* = 8.7, 0.9 Hz, 1H), 4.30 (s, 2H), 3.92 (s, 2H), 3.53 (t, *J* = 6.4 Hz, 2H), 3.46 (t, *J* = 6.4 Hz, 2H), 2.31 (s, 6H), 1.57 – 1.54 (m, 4H), 1.45 (s, 9H), 1.38 – 1.35 (m, 4H).

LC/MS: 1.64 min *m/z* 663.3 (M+H)⁺

Synthesis of tert-butyl 2-((4-(((3-(6-((2-(4-hydroxy-3,5-dimethylphenyl)-1H-benzo[d]imidazole)-6-sulfonamido)pyridin-3-yl)prop-2-yn-1-yl)oxy)methyl)benzyl)oxy)acetate (121)

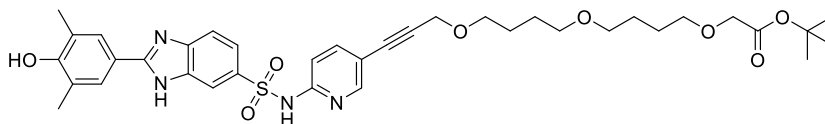


Compound **121** was obtained as brown solid (10 mg, 14%) from compound **114** (50 mg, 0.106 mmol) and intermediate **117** (46 mg, 0.159 mmol) according to the procedure described for **119**.

¹H NMR (400 MHz, CD₃OD) δ 8.20 – 8.15 (m, 2H), 7.81 (dd, *J* = 8.5, 1.8 Hz, 1H), 7.71 (s, 2H), 7.67 (dd, *J* = 8.5, 2.3 Hz, 1H), 7.62 (d, *J* = 8.5 Hz, 1H), 7.34 (s, 4H), 7.19 (dd, *J* = 8.7, 0.9 Hz, 1H), 4.60 (s, 2H), 4.55 (s, 2H), 4.35 (s, 2H), 3.99 (s, 2H), 2.31 (s, 6H), 1.47 (s, 9H).

LC/MS: 1.72 min *m/z* 683.2 (M+H)⁺

Synthesis of tert-butyl 2-(4-(4-(((3-(6-((2-(4-hydroxy-3,5-dimethylphenyl)-1H-benzo[d]imidazole)-6-sulfonamido)pyridin-3-yl)prop-2-yn-1-yl)oxy)butoxy)butoxy)acetate (122)

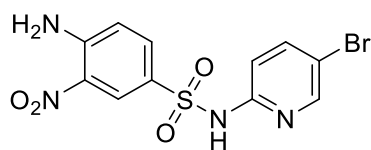


Compound **122** was obtained as brown solid (15 mg, 20%) from compound **114** (50 mg, 0.106 mmol) and intermediate **118** (46 mg, 0.159 mmol) according to the procedure described for **119**.

¹H NMR (400 MHz, CD₃OD) δ 8.16 (s, 2H), 7.79 (d, *J* = 8.6 Hz, 2H), 7.71 (s, 2H), 7.61 (d, *J* = 8.6 Hz, 2H), 7.20 – 7.02 (m, 2H), 4.29 (s, 2H), 3.92 (s, 2H), 3.57 – 3.51 (m, 2H), 3.46 (d, *J* = 5.9 Hz, 2H), 3.43 – 3.36 (m, 4H), 2.31 (s, 6H), 1.68 – 1.54 (m, 8H), 1.45 (s, 9H).

LC/MS: 1.72 min *m/z* 707.3 (M+H)⁺

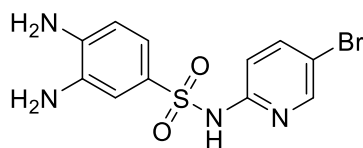
Synthesis of 4-amino-N-(5-bromopyridin-2-yl)-3-nitrobenzenesulfonamide (123)



Compound **123** was obtained as yellow solid (1 g, 23%) from derivative **96** (2.85 g, 12.05 mmol) and 2-amino-5-bromopyridine **97i** (1.87 g, 10.85 mmol) according to the procedure described for **98a**.

^1H NMR (400 MHz, DMSO- d_6) δ 11.18 (s, 1H), 8.51 (d, $J = 2.2$ Hz, 1H), 8.28 (d, $J = 2.5$ Hz, 1H), 8.00 (s, 2H), 7.90 (dd, $J = 8.8, 2.5$ Hz, 1H), 7.79 (d, $J = 2.2$ Hz, 1H), 7.09 (d, $J = 9.0$ Hz, 1H), 6.99 (d, $J = 8.8$ Hz, 1H). LC/MS: 1.5-1.6 min, m/z 372.8 ($\text{M}+\text{H}$) $^+$, 374.8 ($\text{M} + \text{H} + 2$) $^+$

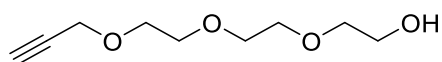
Synthesis of 3,4-diamino-N-(5-bromopyridin-2-yl)benzenesulfonamide (124)



Compound **124** was obtained as brown solid (514 mg, 98%) from derivative **123** (560 mg, 1.5 mmol) according to the procedure described for **99a**.

^1H NMR (400 MHz, DMSO- d_6) δ 10.75 (s, 1H), 8.26 (d, $J = 2.6$ Hz, 1H), 7.28 – 7.22 (m, 1H), 7.17 (d, $J = 7.7$ Hz, 1H), 7.07 – 6.98 (m, 2H), 6.97 – 6.91 (m, 1H), 5.29 (brs, 2H), 4.84 (brs, 2H). LC/MS: 1.2 min, m/z 343 ($\text{M}+\text{H}$) $^+$, 345 ($\text{M} + \text{H} + 2$) $^+$

Synthesis of 2-(2-(2-(prop-2-yn-1-yloxy)ethoxy)ethoxy)ethan-1-ol (125)

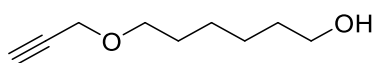


To a suspension of potassium *tert*-butoxide (1.12 g, 9.99 mmol) in 50 mL of anhydrous THF, **70c** (3 g, 19.97 mmol) was added and the resulting white suspension was stirred for 30 min. Then, propargyl bromide was added (1.11 mL, 9.99 mmol) and the resulting mixture was stirred

at room temperature for 18 h. Then, the insoluble salts were removed by filtration and the filtrate was concentrated in vacuo and purified on a silica gel flash-chromatography column (heptane-EtOAc 40:60 to 0:100) affording the title compound (1.5 g, 80%).

$^1\text{H NMR}$ (400 MHz, CDCl_3) δ 4.21 (s, 2H), 3.76 – 3.67 (m, 10H), 3.65 – 3.57 (m, 2H), 2.43 (q, $J = 2.1$ Hz, 1H).

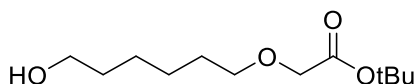
Synthesis of 6-(prop-2-yn-1-yloxy)hexan-1-ol (127)



To a cooled solution of **126** (3 g, 25.39 mmol) in 20 mL of dry DMF, NaH 60% in mixture (406 mg, 10.15 mmol) was added under nitrogen atmosphere and the resulting mixture was stirred at 0 °C for 30 min. Then, propargyl bromide (0.754 mL, 8.46 mmol) was added and the final suspension was continuously stirred for 14 h at room temperature. The crude was concentrated and the residual was taken up with saturated solution of NH_4Cl (30 mL): the aqueous phase was extracted with EtOAc (3 x 20 mL). The collected organic phases were washed with brine, dried over sodium sulfate, filtered and concentrated. The product **127** was obtained after purification by filtration on a silica gel flash-chromatography column (heptane-EtOAc 70:30 to 0:100) to yield a colorless oil (1 g, 76%).

$^1\text{H NMR}$ (400 MHz, CDCl_3) δ 4.13 (d, $J = 2.4$ Hz, 2H), 3.68 – 3.62 (m, 2H), 3.52 (t, $J = 6.6$ Hz, 2H), 2.41 (t, $J = 2.4$ Hz, 1H), 1.64 – 1.54 (m, 4H), 1.44 – 1.35 (m, 4H).

Synthesis of tert-butyl 2-((6-hydroxyhexyl)oxy)acetate (128)

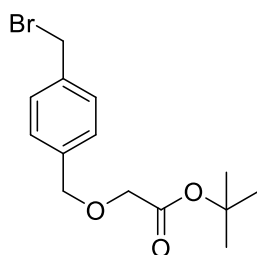


NaH 60% in mixture (203 mg, 5.08 mmol) was added under nitrogen atmosphere to a solution of **126** (1.5 g, 12.7 mmol) in 12 mL of dry DMF at 0 °C. The resulting mixture was stirred at 0 °C for 30 min. Then, *tert*-butyl 2-bromoacetate (0.624 mL, 4.23 mmol) was added and the final

suspension was continuously stirred for 14 h at room temperature. The crude was concentrated and the residual was taken up with saturated solution of NH_4Cl (30 mL): the aqueous phase was extracted with EtOAc (3 x 20 mL). The collected organic phases were washed with brine, dried over sodium sulfate, filtered and concentrated. The product **128** was obtained after purification filtration on a silica gel flash-chromatography column (heptane-EtOAc 70:30 to 0:100) to yield a colorless oil (394 mg, 40%).

^1H NMR (400 MHz, CDCl_3) δ 3.94 (s, 2H), 3.68 – 3.61 (m, 2H), 3.51 (t, $J = 6.5$ Hz, 2H), 1.69 – 1.54 (m, 4H), 1.48 (s, 9H), 1.43 – 1.38 (m, 4H).

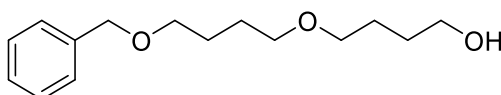
Synthesis of tert-butyl 2-((4-(bromomethyl)benzyl)oxy)acetate (130)



Compound **130** was obtained as colorless oil (420 mg, 67%) from derivative (4-(bromomethyl)phenyl)methanol **129** (400 mg, 2 mmol) according to the procedure described for **116**.

^1H NMR (400 MHz, CDCl_3) δ 7.46 – 7.27 (m, 4H), 4.61 (s, 2H), 4.49 (s, 2H), 3.99 (s, 2H), 1.49 (s, 9H).

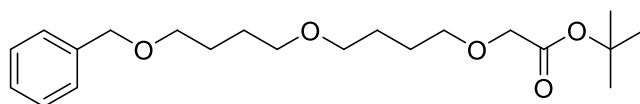
Synthesis of 4-(4-(benzyloxy)butoxy)butan-1-ol (133)



To a cooled solution of 1,4-butanediol **132** (1.04 mL, 12.34 mmol) in 6 mL of dry DMF NaH 60% in mixture (197 mg, 4.93 mmol) was added. The resulting mixture was stirred at 0 °C for 30 min under nitrogen atmosphere. Then, 4-benzyloxy-1-butanol **131** (0.781 mL g, 4.11 mmol)

was added and the final suspension was continuously stirred for 14 h at room temperature. The crude was concentrated under reduced pressure and the residual was taken up with saturated solution of NH_4Cl (30 mL): the aqueous phase was extracted with EtOAc (3 x 20 mL). The collected organic phases were washed with brine, dried over sodium sulfate, filtered and concentrated. The product **133** was obtained after purification filtration on a silica gel flash-chromatography column (heptane-EtOAc 90:10 to 50:50) to yield a yellow oil (870 mg, 84%). ^1H NMR (400 MHz, CDCl_3) δ 7.35 – 7.27 (m, 5H), 4.50 (s, 2H), 3.64 (d, $J = 5.2$ Hz, 2H), 3.55 – 3.40 (m, 6H), 1.72 – 1.64 (m, 8H).

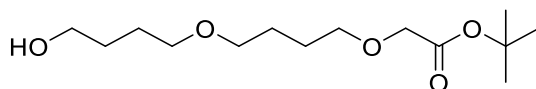
Synthesis of tert-butyl 2-(4-(4-(benzyloxy)butoxy)butoxy)acetate (134)



Compound **134** was obtained as colorless oil (297 mg, 75%) from 4-(4-(benzyloxy)butoxy)butan-1-ol **133** (250 mg, 0.990 mmol) according to the procedure described for **116**.

^1H NMR (400 MHz, CDCl_3) δ 7.36 – 7.28 (m, 5H), 4.50 (s, 2H), 3.94 (s, 2H), 3.58 – 3.47 (m, 4H), 3.42 – 3.39 (m, 4H), 1.72 – 1.62 (m, 8H), 1.48 (s, 9H).

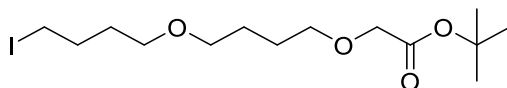
Synthesis of tert-butyl 2-(4-(4-hydroxybutoxy)butoxy)acetate (135)



Compound **135** (430 mg, 1.17 mmol) was solubilized in 3 mL of MeOH and 10% Pd/C was added. The mixture was stirred under a hydrogen atmosphere (balloon) for 18 h. Then, the mixture was filtered and the filtrate evaporated to give the title compound as colorless oil (310 mg, 96%).

^1H NMR (400 MHz, CDCl_3) δ 3.94 (s, 2H), 3.67 – 3.62 (m, 2H), 3.55 – 3.51 (m, 2H), 3.49 – 3.43 (m, 4H), 1.72 – 1.66 (m, 8H), 1.47 (s, 9H).

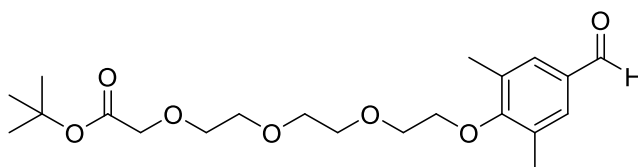
Synthesis of tert-butyl 2-(4-(4-iodobutoxy)butoxy)acetate (136)



Iodine (465 mg, 1.83 mmol) was added to triphenylphosphine (480 mg, 1.83 mmol) and imidazole (124 mg, 1.83 mmol) in 14 mL of dry DCM at 0 °C. The resulting mixture was stirred at room temperature for 5 min, then was cooled to 0 °C. A solution of compound **135** (390 mg, 1.41 mmol) in 9 mL of dichloromethane was added to the reaction mixture at 0 °C and the resulting mixture was stirred at room temperature for 3 h. The reaction was quenched with saturated Na_2SO_3 solution (5 mL): the aqueous phase was extracted with EtOAc (3 x 5 mL). The combined organic phases were washed with brine, dried over sodium sulfate, filtered and evaporated to dryness. The crude material was purified by column chromatography (heptane-EtOAc 70:30 to 20:80) to afford the title compound as colorless oil (305 mg, 56%).

^1H NMR (400 MHz, CDCl_3) δ 3.94 (s, 2H), 3.55 – 3.51 (m, 2H), 3.42 – 3.38 (m, 4H), 3.21 (t, $J = 7.0$ Hz, 2H), 1.96 – 1.86 (m, 2H), 1.70 – 1.63 (m, 6H), 1.48 (s, 9H).

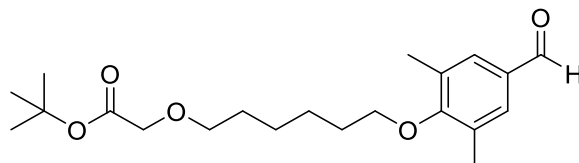
Synthesis of tert-butyl 2-(2-(2-(2-(4-formyl-2,6-dimethylphenoxy)ethoxy)ethoxy)ethoxy)acetate (137)



Compound **137** was obtained as a pale yellow solid (450 mg, 80%) from derivative 4-hydroxy-3,5-dimethylbenzaldehyde **76a** (237 mg, 1.58 mmol) and intermediate **146** (600 mg, 1.43 mmol) according to the procedure described for **61**.

^1H NMR (400 MHz, CDCl_3) δ 9.87 (s, 1H), 7.55 (s, 2H), 4.02 (s, 2H), 3.84 (t, $J = 5.7, 3.8$ Hz, 2H), 3.77 – 3.66 (m, 10H), 2.35 (s, 6H), 1.47 (s, 9H). LC/MS: 1.68 min m/z 397.2 ($\text{M}+\text{H}$) $^+$

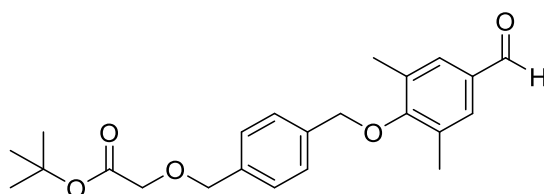
Synthesis of tert-butyl 2-((6-(4-formyl-2,6-dimethylphenoxy)hexyl)oxy)acetate (138)



Compound **138** was obtained as a pale yellow solid (260 mg, 70%) from derivative 4-hydroxy-3,5-dimethylbenzaldehyde **76a** (170 mg, 1.13 mmol) and intermediate **147** (400 mg, 1.03 mmol) according to the procedure described for **61**.

^1H NMR (400 MHz, CDCl_3) δ 9.87 (s, 1H), 7.55 (s, 2H), 3.96 (s, 2H), 3.81 (t, $J = 6.6$ Hz, 2H), 3.53 (t, $J = 6.5$ Hz, 2H), 2.33 (s, 6H), 1.88 – 1.80 (m, 2H), 1.72 – 1.64 (m, 2H), 1.60 – 1.51 (m, 2H), 1.48 (s, 9H), 1.35 – 1.21 (m, 2H). LC/MS: 1.5 min m/z 365.2 ($\text{M}+\text{H}$) $^+$

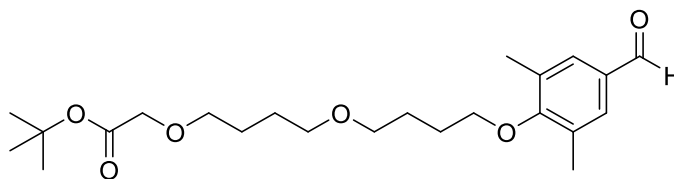
Synthesis of tert-butyl 2-(4-((4-formyl-2,6-dimethylphenoxy)methyl)phenyl)acetate (139)



Compound **139** was obtained as a pale yellow solid (235 mg, 96%) from derivative 4-hydroxy-3,5-dimethylbenzaldehyde **76a** (105 mg, 0.698 mmol) and intermediate **130** (200 mg, 0.634 mmol) according to the procedure described for **61**.

^1H NMR (400 MHz, CDCl_3) δ 9.90 (s, 1H), 7.58 (s, 2H), 7.48 – 7.39 (m, 4H), 4.87 (s, 2H), 4.65 (s, 2H), 4.01 (s, 2H), 2.35 (s, 6H), 1.50 (s, 9H). LC/MS: 1.4 min m/z 385 ($\text{M}+\text{H}$) $^+$

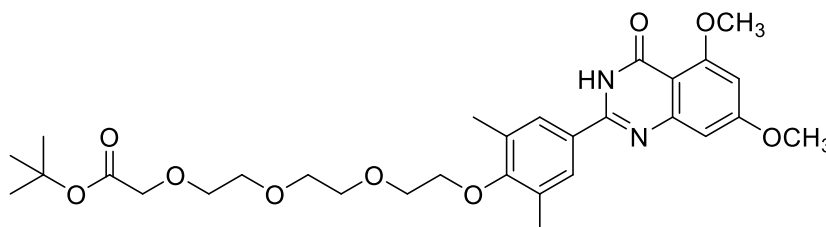
Synthesis of tert-butyl 2-(4-(4-(4-formyl-2,6-dimethylphenoxy)butoxy)butoxy)acetate (140)



Compound **140** was obtained as a pale yellow solid (155 mg, 96%) from derivative 4-hydroxy-3,5-dimethylbenzaldehyde **76a** (59 mg, 0.394 mmol) and intermediate **148** (154 mg, 0.358 mmol) according to the procedure described for **61**.

^1H NMR (400 MHz, CDCl_3) δ 9.87 (s, 1H), 7.54 (s, 2H), 3.93 (s, 2H), 3.84 (t, $J = 6.4$ Hz, 2H), 3.55 – 3.51 (m, 2H), 3.50 – 3.44 (m, 2H), 2.32 (s, 6H), 1.93 – 1.85 (m, 2H), 1.83 – 1.75 (m, 2H), 1.69 – 1.63 (m, 4H), 1.47 (s, 9H). LC/MS: 1.5 min m/z 409 (M+H) $^+$

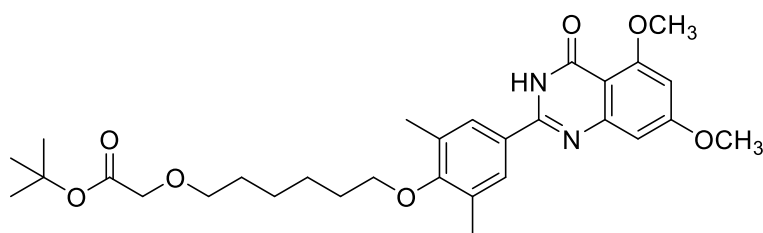
Synthesis of tert-butyl 2-(2-(2-(2-(4-(5,7-dimethoxy-4-oxo-3,4-dihydroquinazolin-2-yl)-2,6-dimethylphenoxy)ethoxy)ethoxy)ethoxy)acetate (141)



To a solution of compound **137** (240 mg, 0.605 mmol) in 4 ml of dry DMF, derivative **64** (119 mg, 0.605 mmol) and $\text{Na}_2\text{S}_2\text{O}_5$ (152 mg, 0.726 mmol) were added. The resulting mixture was heated at 80 °C and stirred at this temperature for 18 h. After cooling at room temperature, water was added (15 mL). The aqueous phase was extracted with EtOAc (3 x 10 mL). The collected organic phases were washed with saturated solution of NaHCO_3 (3 x 10 mL), brine, dried over sodium sulfate and filtered. After purification on silica gel flash-chromatography column (DCM-MeOH 97:3 to 80:20), the title compound was obtained as pale yellow solid (430 mg, 68%).

^1H NMR (400 MHz, CDCl_3) δ 9.46 (s, 1H), 7.69 (s, 2H), 6.83 (d, $J = 2.3$ Hz, 1H), 6.46 (d, $J = 2.3$ Hz, 1H), 4.03 (s, 3H), 4.02 – 3.99 (m, 2H), 3.98 (s, 3H), 3.93 (s, 2H), 3.88 – 3.83 (m, 2H), 3.78 – 3.68 (m, 8H), 2.38 (s, 6H), 1.47 (s, 9H). LC/MS: 1.4 min m/z 573 ($\text{M}+\text{H}$) $^+$

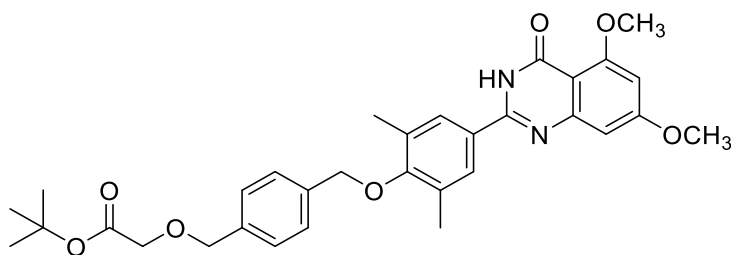
Synthesis of tert-butyl 2-((6-(4-(5,7-dimethoxy-4-oxo-3,4-dihydroquinazolin-2-yl)-2,6-dimethylphenoxy)hexyl)oxy)acetate (142)



Compound **142** was obtained as a pale yellow solid (331 mg, 86%) from derivative **138** (260 mg, 0.713 mmol) and intermediate **64** (140 mg, 0.713 mmol) according to the procedure described for **141**.

^1H NMR (400 MHz, CDCl_3) δ 9.75 (s, 1H), 7.72 (s, 2H), 6.83 (d, $J = 2.3$ Hz, 1H), 6.45 (d, $J = 2.3$ Hz, 1H), 3.97 (s, 2H), 3.95 (s, 2H), 3.93 (s, 2H), 3.81 (t, $J = 6.5$ Hz, 2H), 3.54 (t, $J = 6.6$ Hz, 2H), 2.36 (s, 6H), 1.90 – 1.80 (m, 2H), 1.74 – 1.63 (m, 2H), 1.63 – 1.51 (m, 4H), 1.48 (s, 9H). LC/MS: 1.5 min m/z 541 ($\text{M}+\text{H}$) $^+$

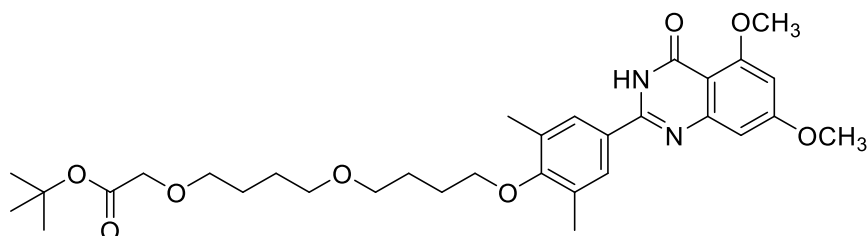
Synthesis of tert-butyl 2-(4-((4-(5,7-dimethoxy-4-oxo-3,4-dihydroquinazolin-2-yl)-2,6-dimethylphenoxy)methyl)phenyl)acetate (143)



Compound **143** was obtained as a pale yellow solid (290 mg, 85%) from derivative **143** (229 mg, 0.647 mmol) and intermediate **64** (127 mg, 0.647 mmol) according to the procedure described for **141**.

^1H NMR (400 MHz, CDCl_3) δ 9.91 (s, 1H), 7.76 (s, 2H), 7.50 – 7.37 (m, 5H), 6.84 (d, $J = 2.3$ Hz, 2H), 6.46 (d, $J = 2.3$ Hz, 2H), 4.86 (s, 2H), 4.65 (s, 2H), 4.01 (s, 2H), 3.97 (s, 3H), 3.93 (s, 3H), 2.37 (s, 6H), 1.49 (s, 9H). LC/MS: 1.6 min m/z 561 ($\text{M}+\text{H}$) $^+$

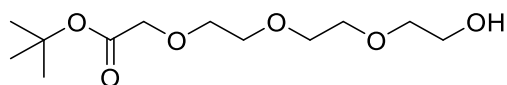
Synthesis of tert-butyl 2-(4-(4-(4-(5,7-dimethoxy-4-oxo-3,4-dihydroquinazolin-2-yl)-2,6-dimethylphenoxy)butoxy)butoxy)acetate (144)



Compound **144** was obtained as a pale yellow solid (190 mg, 86%) from derivative **140** (155 mg, 0.380 mmol) and intermediate **64** (75 mg, 0.380 mmol) according to the procedure described for **141**.

^1H NMR (400 MHz, CDCl_3) δ 9.34 (s, 1H), 7.68 (s, 2H), 6.83 (d, $J = 2.3$ Hz, 1H), 6.46 (d, $J = 2.3$ Hz, 1H), 3.98 (s, 3H), 3.95 (s, 3H), 3.93 (s, 2H), 3.84 (t, $J = 6.4$ Hz, 2H), 3.56 – 3.44 (m, 4H), 2.36 (s, 6H), 1.94 – 1.87 (m, 2H), 1.84 – 1.78 (m, 2H), 1.68 (qt, $J = 4.8, 2.3$ Hz, 6H), 1.48 (s, 9H). LC/MS: 1.6 min m/z 585 ($\text{M}+\text{H}$) $^+$

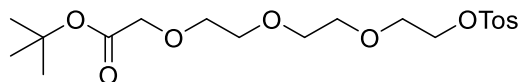
Synthesis of tert-butyl 2-(2-(2-(2-hydroxyethoxy)ethoxy)ethoxy)acetate (145)



Compound **145** was obtained as colorless oil (1.74 g, 60%) from compound **70c** (5 g, 33.3 mmol) according to the procedure described for **128**.

^1H NMR (400 MHz, CDCl_3) δ 4.02 (s, 2H), 3.76 – 3.65 (m, 10H), 3.61 (dd, $J = 5.3, 3.9$ Hz, 2H), 1.47 (s, 9H).

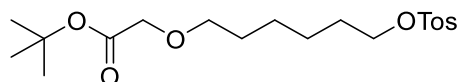
Synthesis of tert-butyl 2-(2-(2-(2-(tosyloxy)ethoxy)ethoxy)ethoxy)acetate (146)



Compound **146** was obtained as colorless oil (785 mg, 64%) from compound **145** (800 mg, 3.02 mmol) according to the procedure described for **74a**.

^1H NMR (400 MHz, CDCl_3) δ 7.80 (d, $J = 8.2$, 2H), 7.34 (d, $J = 8.2$ Hz, 2H), 4.16 (t, $J = 4.9$ Hz, 2H), 4.00 (s, 2H), 3.73 – 3.64 (m, 10H), 2.45 (s, 3H), 1.47 (s, 9H).

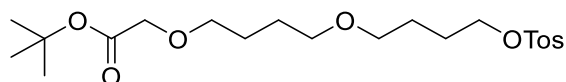
Synthesis of tert-butyl 2-((6-(tosyloxy)hexyl)oxy)acetate (147)



Compound **147** was obtained as colorless oil (206 mg, 62%) from compound **128** (200 mg, 0.861 mmol) according to the procedure described for **74a**.

^1H NMR (400 MHz, CDCl_3) δ 7.79 (d, $J = 8.4$ Hz, 2H), 7.34 (d, $J = 8.4$ Hz, 2H), 4.03 (t, $J = 6.5$ Hz, 2H), 3.92 (s, 2H), 3.47 (t, $J = 6.5$ Hz, 2H), 2.45 (s, 3H), 1.70 – 1.61 (m, 2H), 1.60 – 1.50 (m, 2H), 1.48 (s, 9H), 1.39 – 1.28 (m, 4H).

Synthesis of tert-butyl 2-(4-(4-(tosyloxy)butoxy)butoxy)acetate (148)



Compound **148** was obtained as colorless oil (160 mg, 60%) from compound **135** (182 mg, 0.658 mmol) according to the procedure described for **74a**.

¹H NMR (400 MHz, CDCl₃) δ 7.79 (d, *J* = 8.0 Hz, 2H), 7.34 (d, *J* = 8.0 Hz, 2H), 4.06 (t, *J* = 6.4 Hz, 2H), 3.94 (s, 2H), 3.51 (t, *J* = 6.1 Hz, 2H), 3.43 – 3.27 (m, 4H), 2.45 (s, 3H), 1.80 – 1.52 (m, 8H), 1.48 (s, 9H).

7.3 Biological protocols

7.3.1 FRET assay

Compounds were tested on BD1 and BD2 domains (6xHis-tagged) of each BET protein in a dose–response format measuring binding competition between the compounds and an AlexaFluor647 derivative of JQ1. Compounds were diluted in assay buffer (150 mM HEPES, 150 mM NaCl, 5% glycerol, 1 mM DTT, and 1 mM CHAPS, pH 7.4), starting from a stock solution of 10 mM (100% DMSO). The highest concentration tested was 100 μM and from this concentration 12 threefold dilutions were prepared. 5 μL of each concentration were transferred into a low volume black 384-well plate and, thanking advance of a Thermo Scientific Multidrop Combi, 2 μL of protein (10 nM), 2 μL of AlexaFluor647 derivative of JQ1 (50 nM) and 1 μL of europium chelate-labeled anti-6His antibody (1 nM) were transferred in each well. After an equilibration of 30 min in the dark at rt, the binding of the protein to the fluorescent ligand was detected on BMG Labtech Pherastar luminescence plate reader (excitation = 337 nm; emission 1 = 615 nm; emission 2 = 665 nm; dual wavelength bias dichroic = 400 nm, 630 nm). TR-FRET ratio was calculated using the following equation:

$$\text{ratio} = ((\text{acceptor fluorescence at 665 nm})/(\text{donor fluorescence at 615 nm})) \times 1000$$

Each compound was tested in triplicate and data were analyzed using Graphpad Prism software.

7.3.2 Cell culture, testing compounds and immunoblotting

HeLa cells were cultured (37 °C, 5% CO₂) in DMEM medium (Gibco) supplemented with 10% fetal bovine serum (FBS) (Gibco), L-glutamine (Gibco), penicillin, streptomycin. The cells

were seeded at 1×10^6 per well on a standard 6-well plate. After 24h, cells were treated with compounds at different concentrations (DMSO concentration of 0.1%). After the proper incubation time (6 h and 16 h) cells were washed with PBS twice and lysed with RIPA buffer (Sigma), supplemented with protease inhibitor cocktail (Roche), Benzodase (Merck), and 0.5 mM MgCl₂. Lysate was briefly sonicated and centrifuged at 20000 g for 10 min at 4 °C. From each sample, supernatant was collected and protein concentration measured by BCA assay.

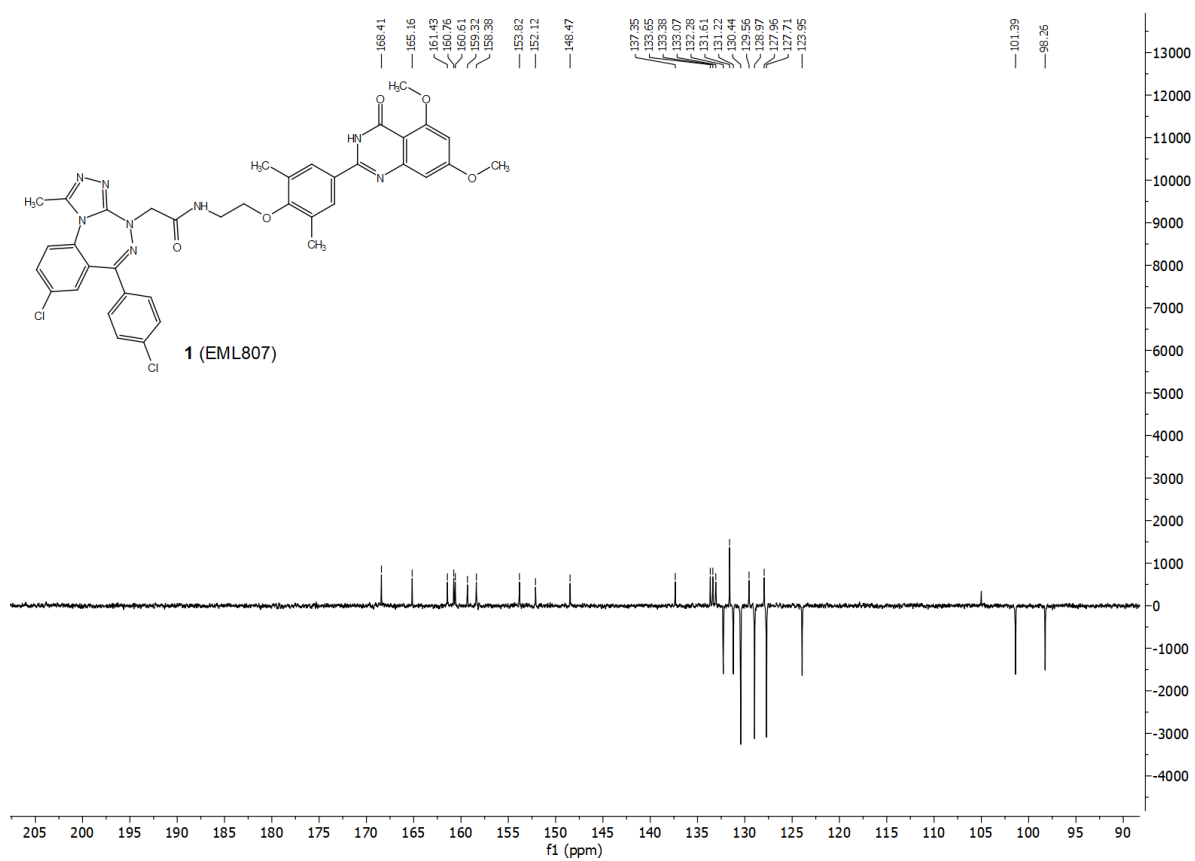
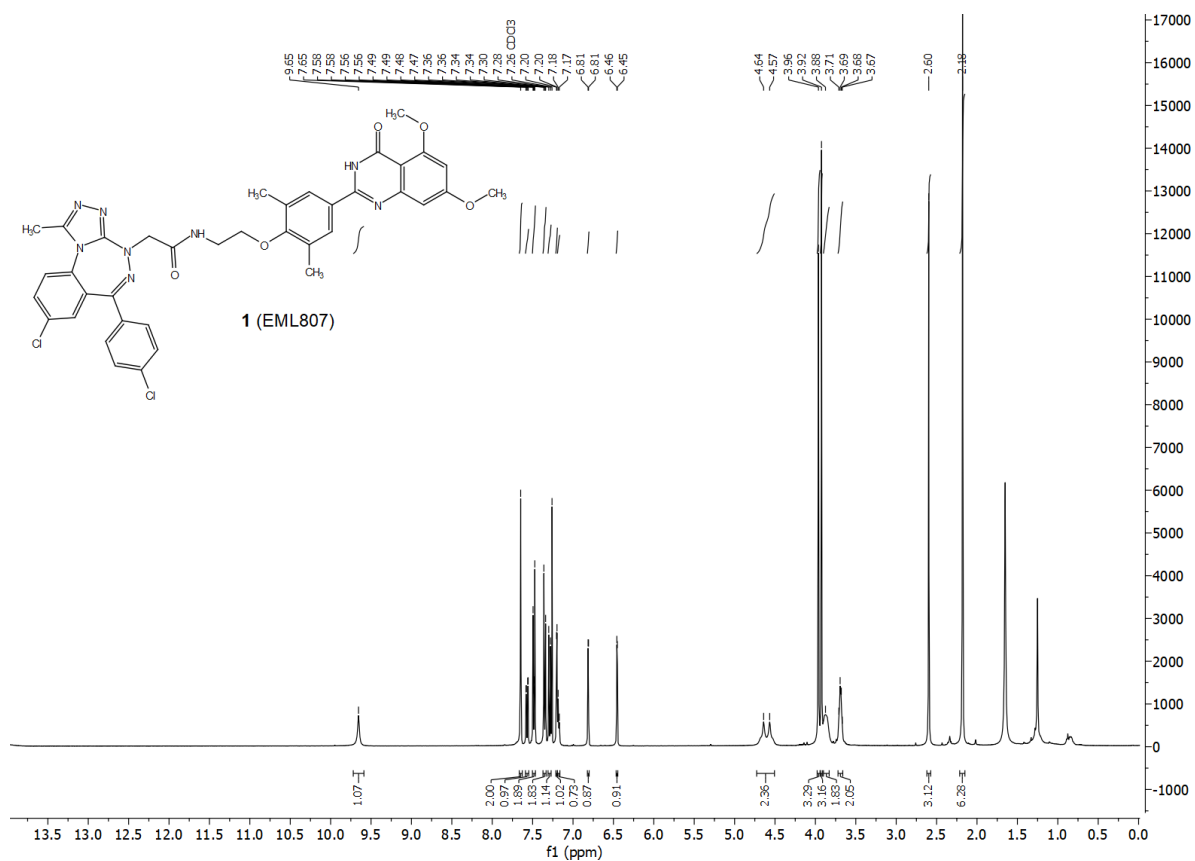
Regarding the classic Western-blot procedure, proteins were resolved by SDS-PAGE on NuPage 4–12% Bis-Tris Midi Gel (Invitrogen) and transferred to Amersham Protran 0.45 NC nitrocellulose membrane (GE Healthcare) using wet transfer. The membrane was blocked with 5% w/v milk in Tris-buffered saline (TBS) with 0.1% w/v Tween-20. Blots were probed with anti-Brd4 (AbCam, ab128874), anti-Brd3 (AbCam, ab50818), anti-Brd2 (AbCam, ab139690), and hFAB Rhodamine anti-tubulin IgG (BioRAD #12004166). Blots were developed with IRDye secondary antibody (Licor) anti-mouse or anti-rabbit and bands visualized using ChemiDoc imaging system (Bio-Rad). ImageLab software was used for densitometric analysis. Regarding the use of the instrument Simple Western™ Jess, samples were prepared and analyzed following the standard protocol reported.

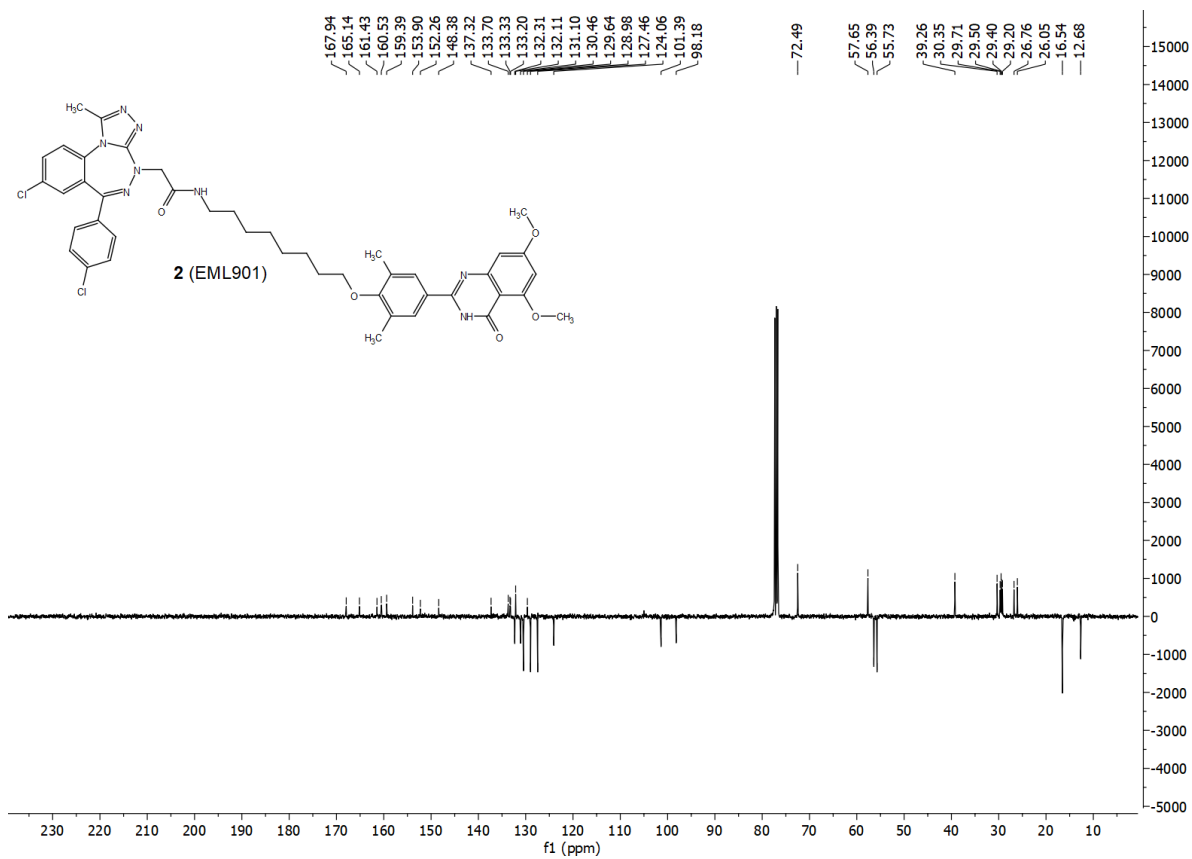
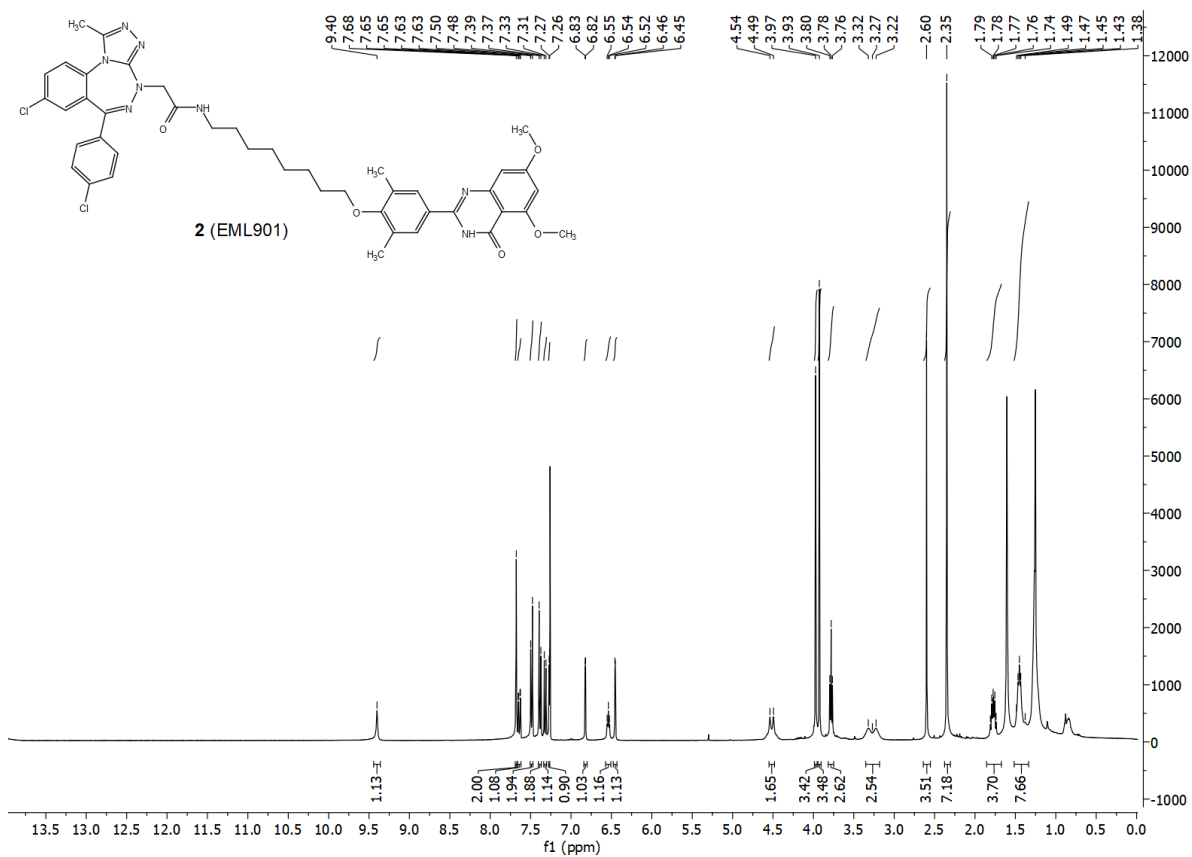
7.3.2 Cell viability assay

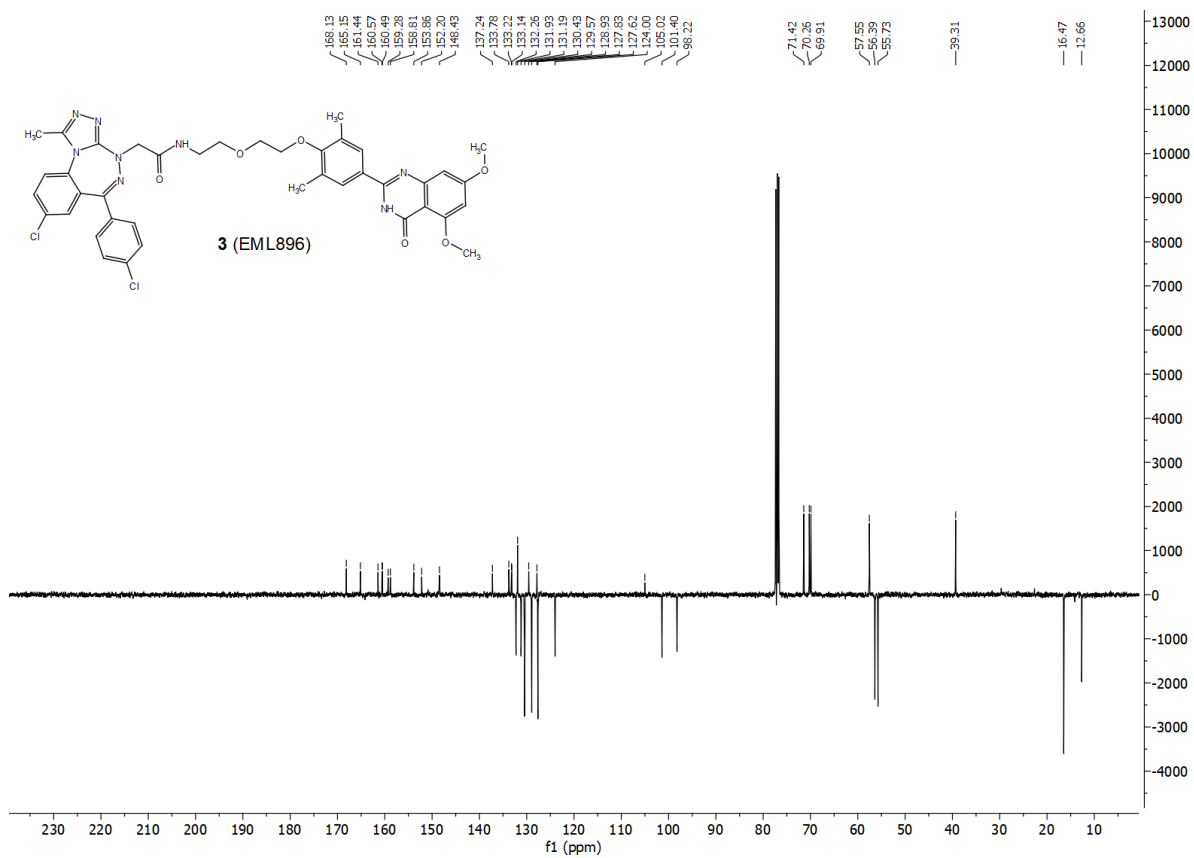
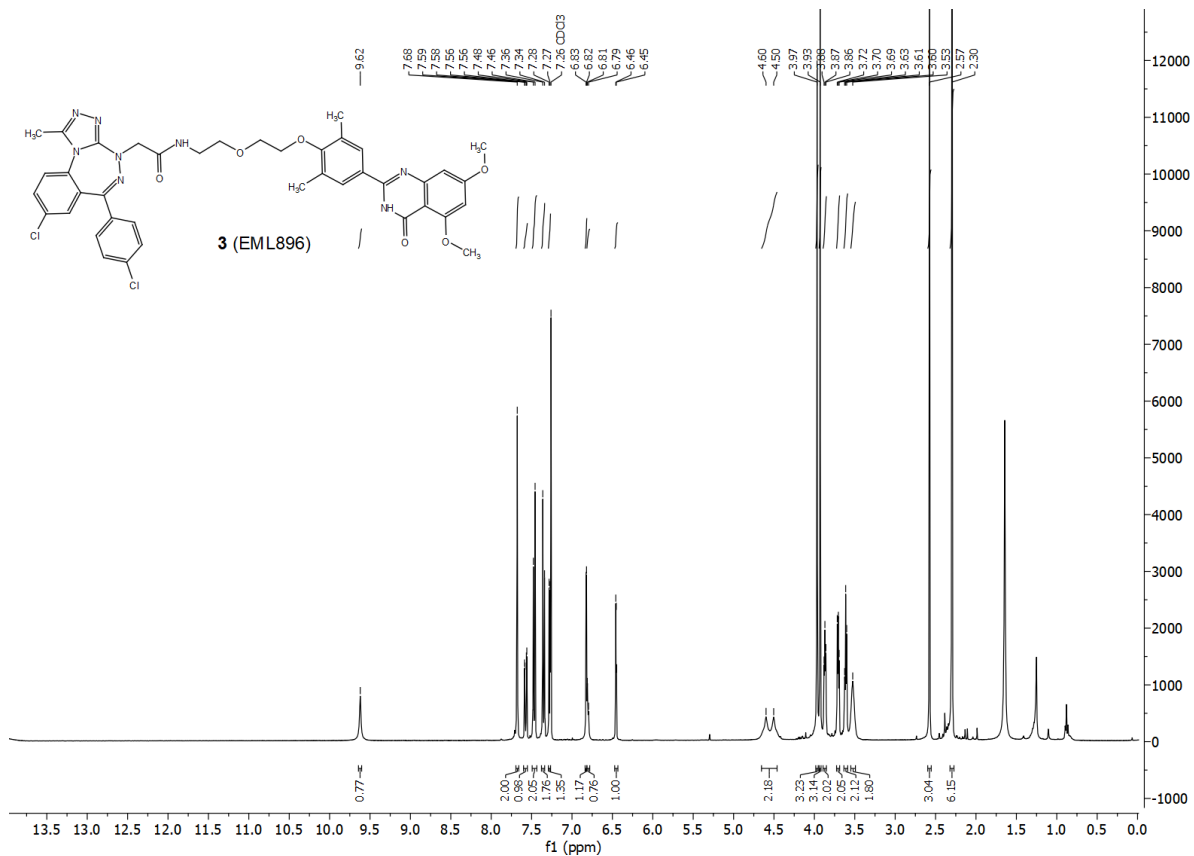
MV4-11 cells were grown in RPMI (Gibco) supplemented with 10% fetal bovine serum (FBS) and L-glutamine. MV4-11 cells were seeded into a clear-bottomed 384-well plate (Sigma – Greiner CELLSTAR) at $\sim 0.6 \times 10^5$ cells/mL in 25 μ L of media. Under sterile conditions, each test compound (stock solution 20 mM, 100% DMSO) was diluted in RPMI media to reach 0.1% DMSO. Each compound was tested at 12 concentrations (from 20 μ M to 2 nM), and each condition was performed in triplicate. For the no-cell control 25 μ L of plain RPMI was dispensed into ~ 2 rows of the plate. The assay plate was incubated at 37°C 5% CO₂ for 48 h. After the treatment, cell viability was measured with Promega CellTiter-Glo luminescent cell

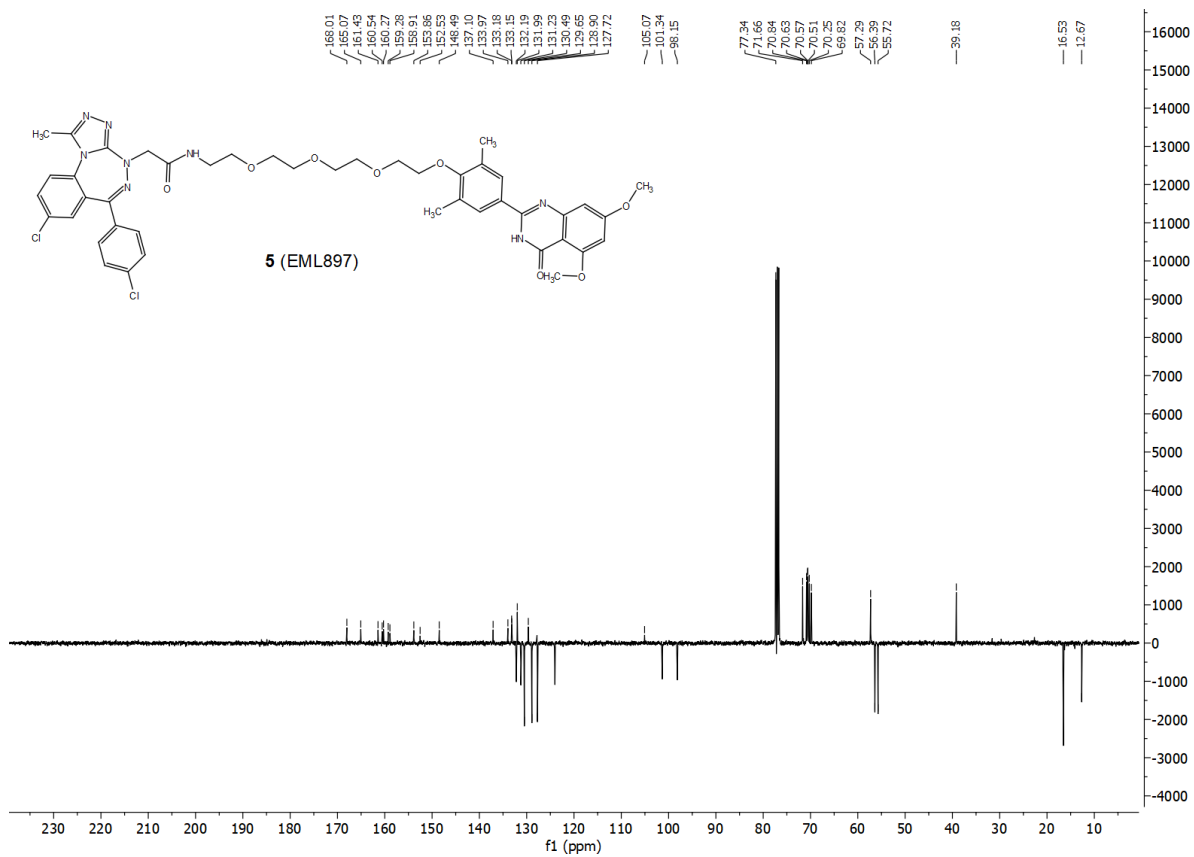
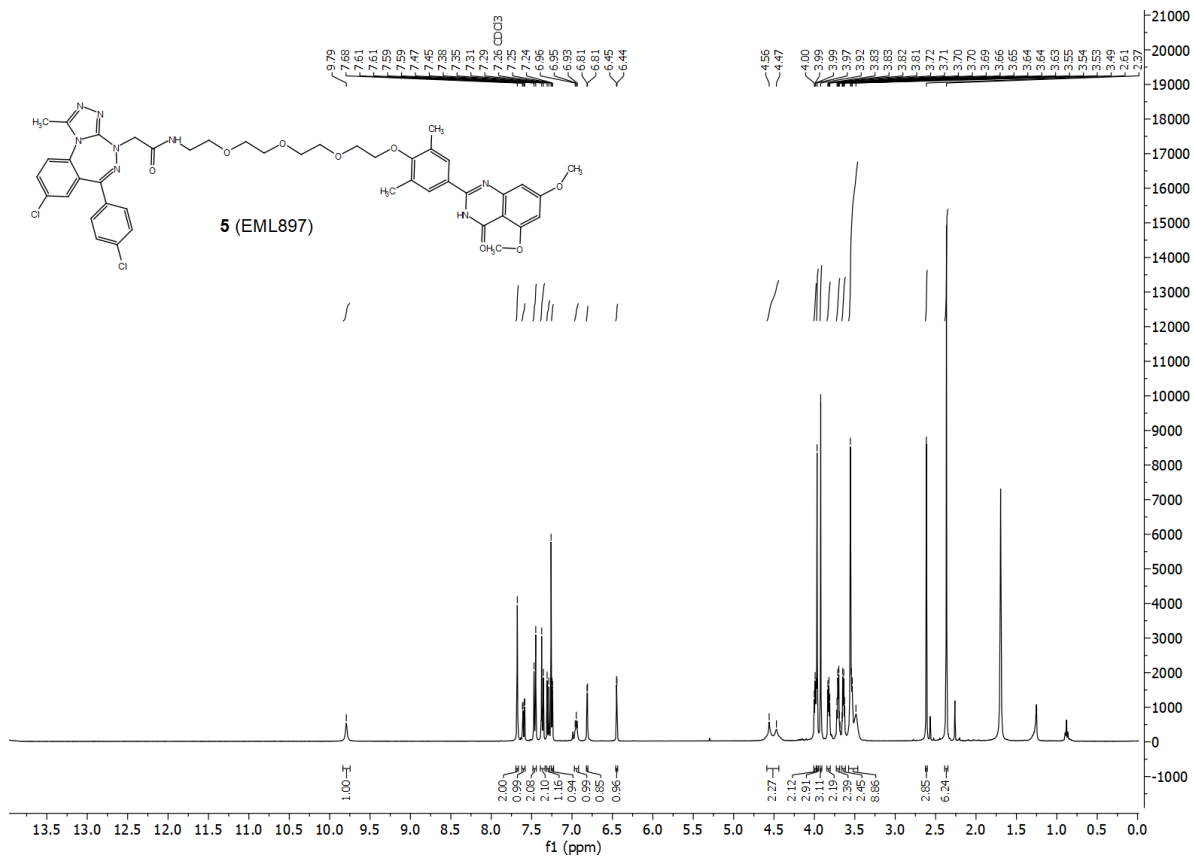
viability assay kit according to the manufacturer instructions. Signal was recorded on a BMG Labtech Pherastar luminescence plate reader with recommended settings. Data were analyzed with Graphpad Prism software.

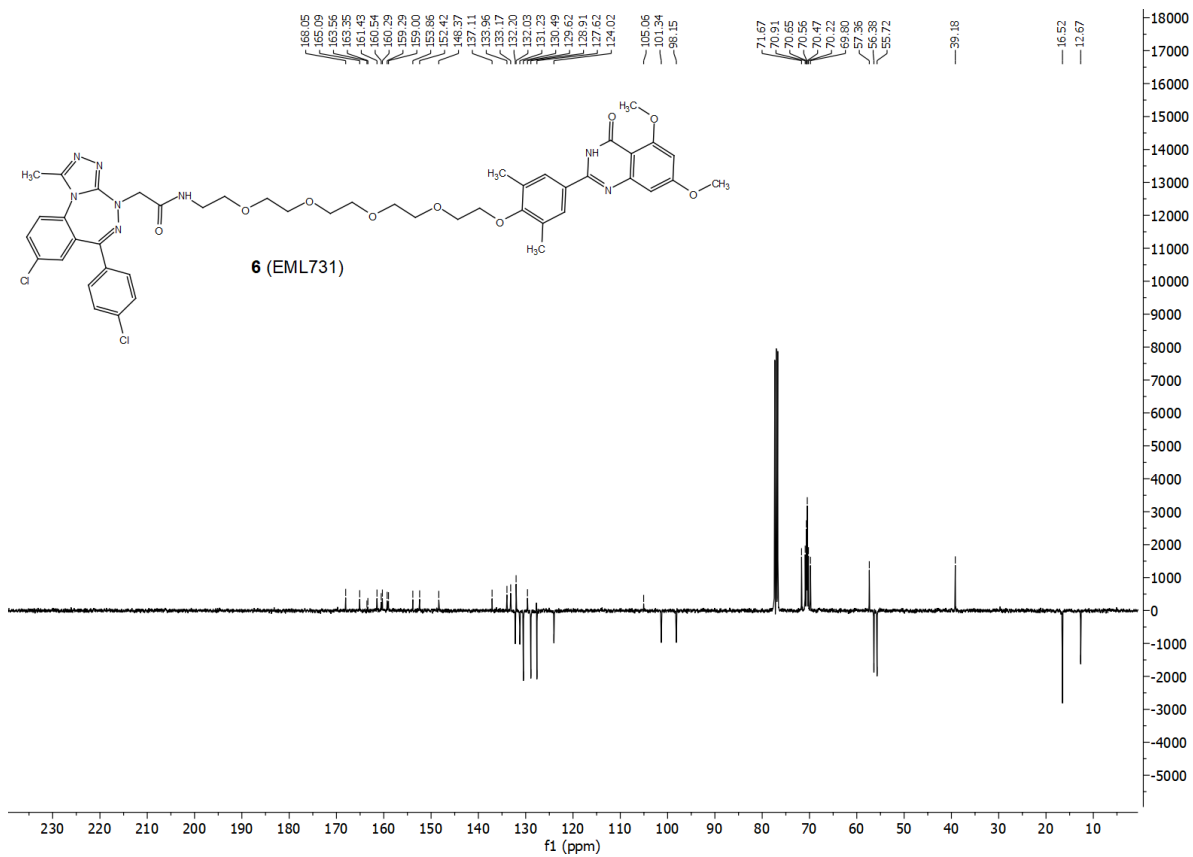
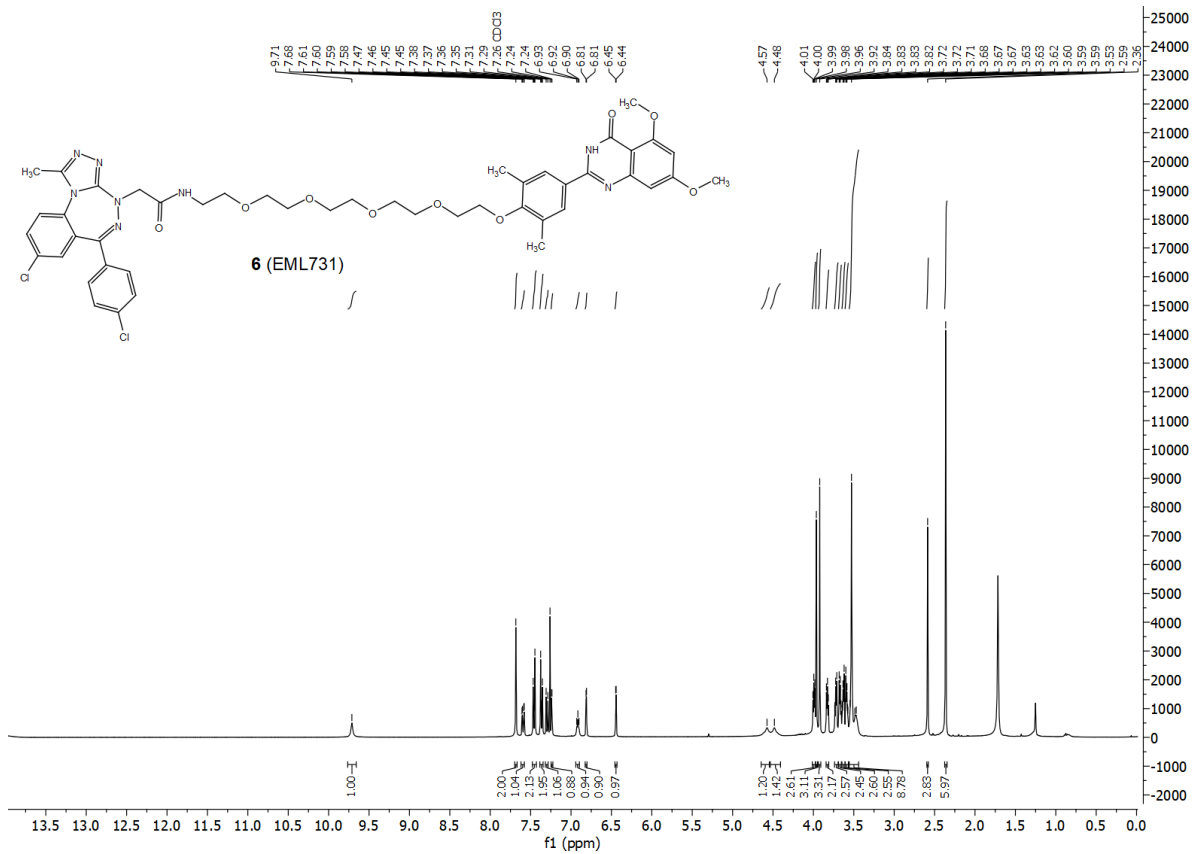
7.4 NMR Data

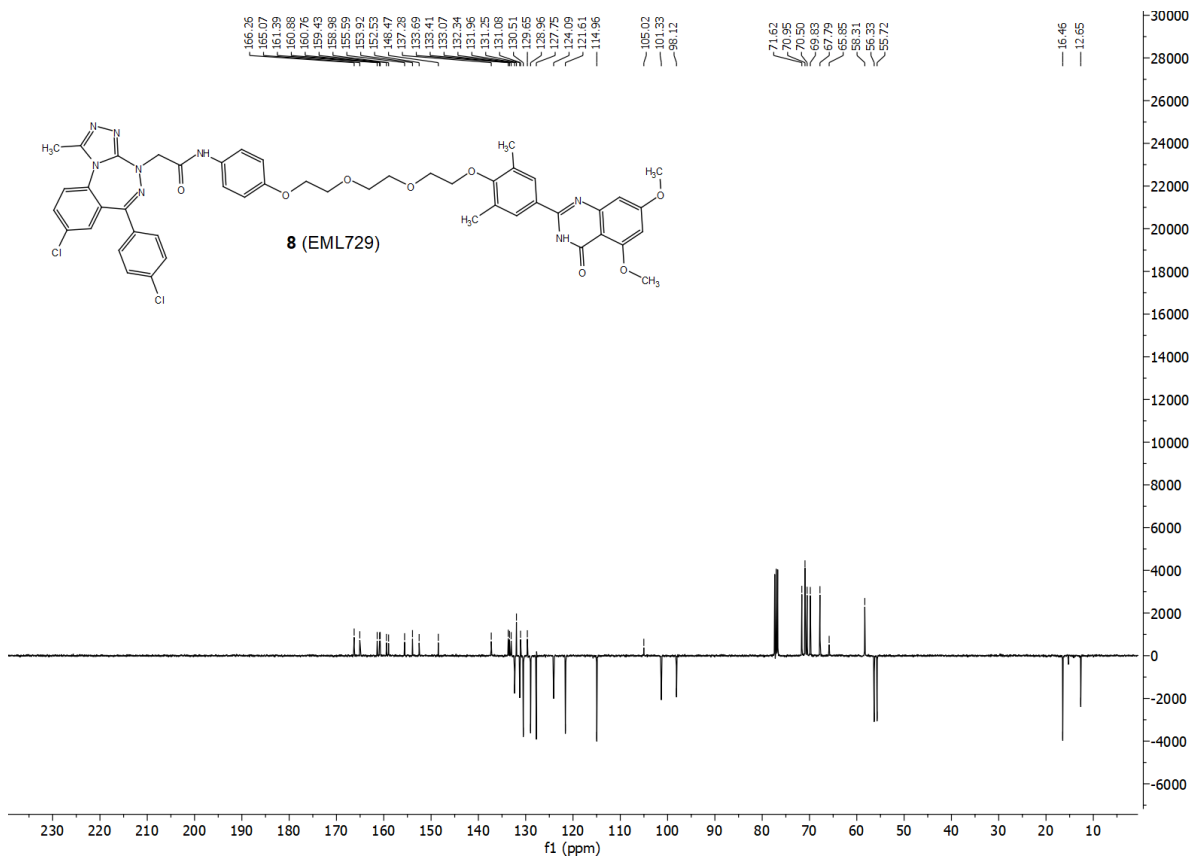
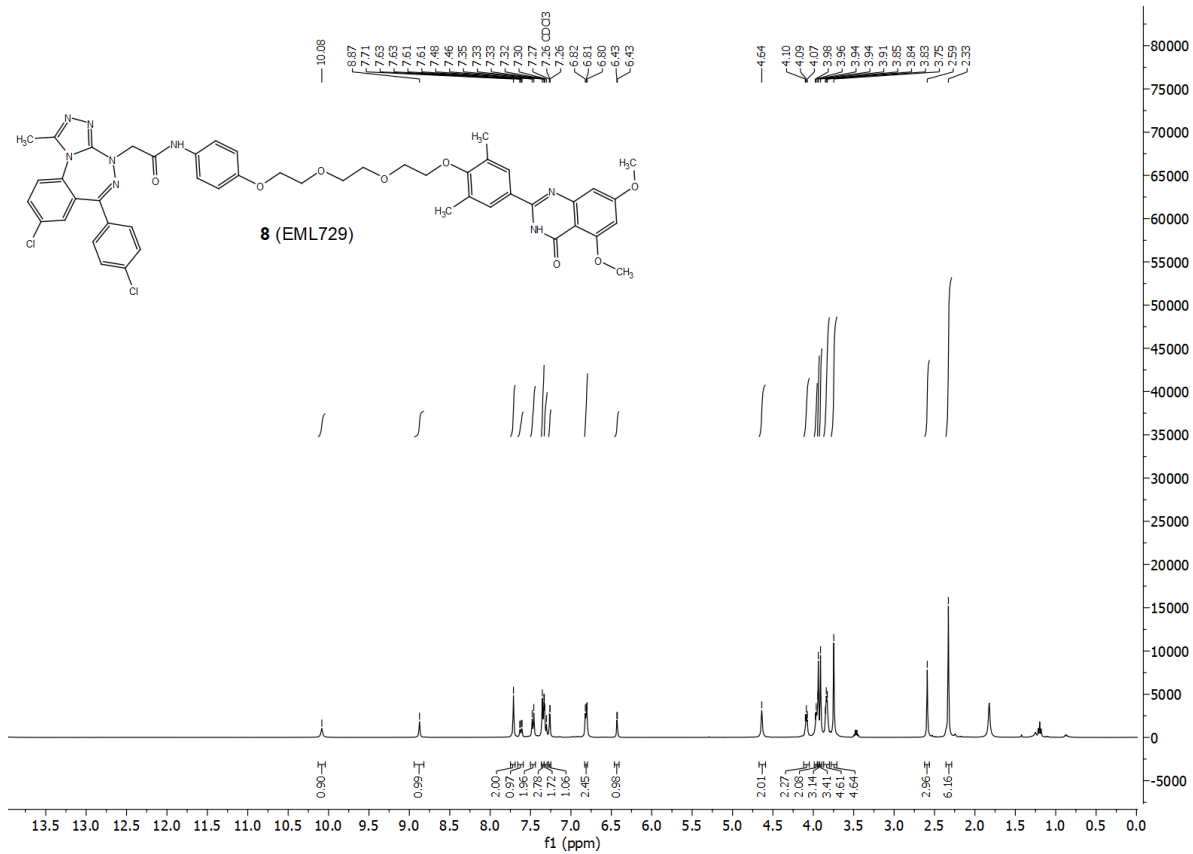


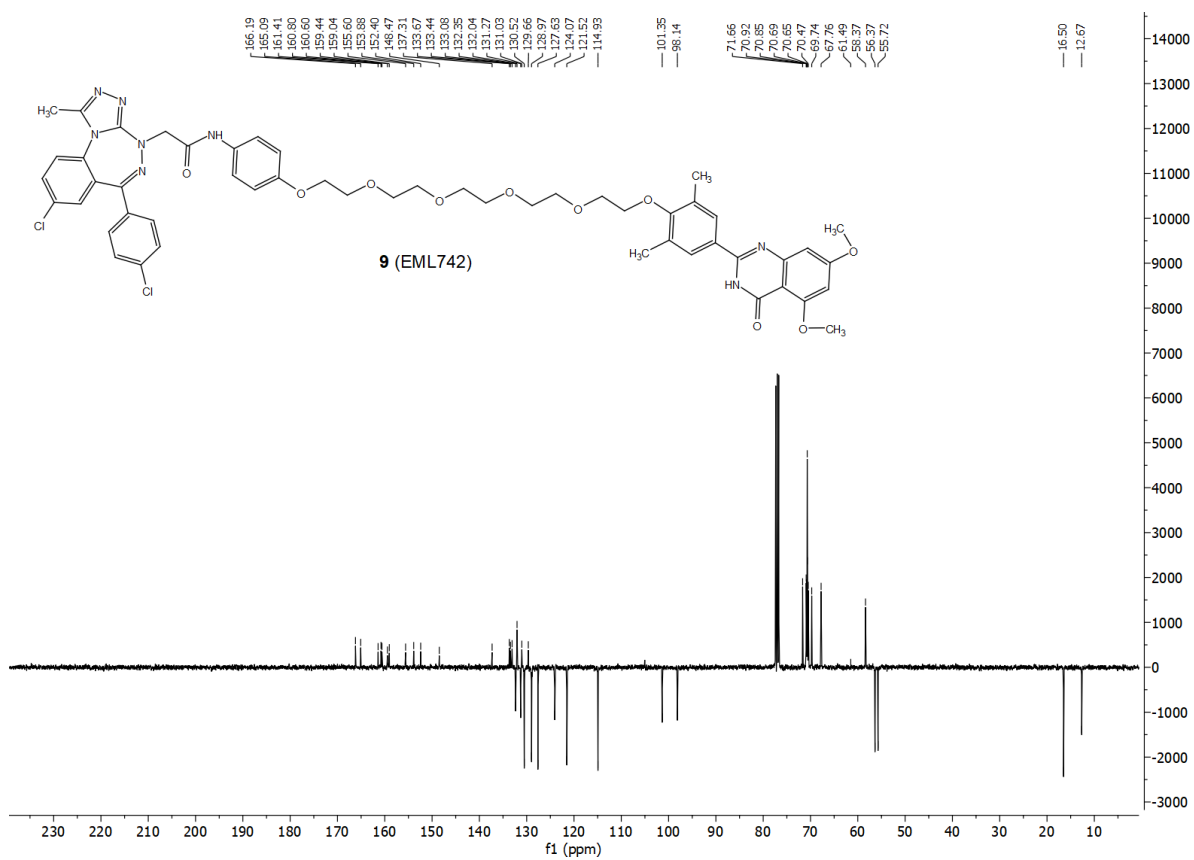
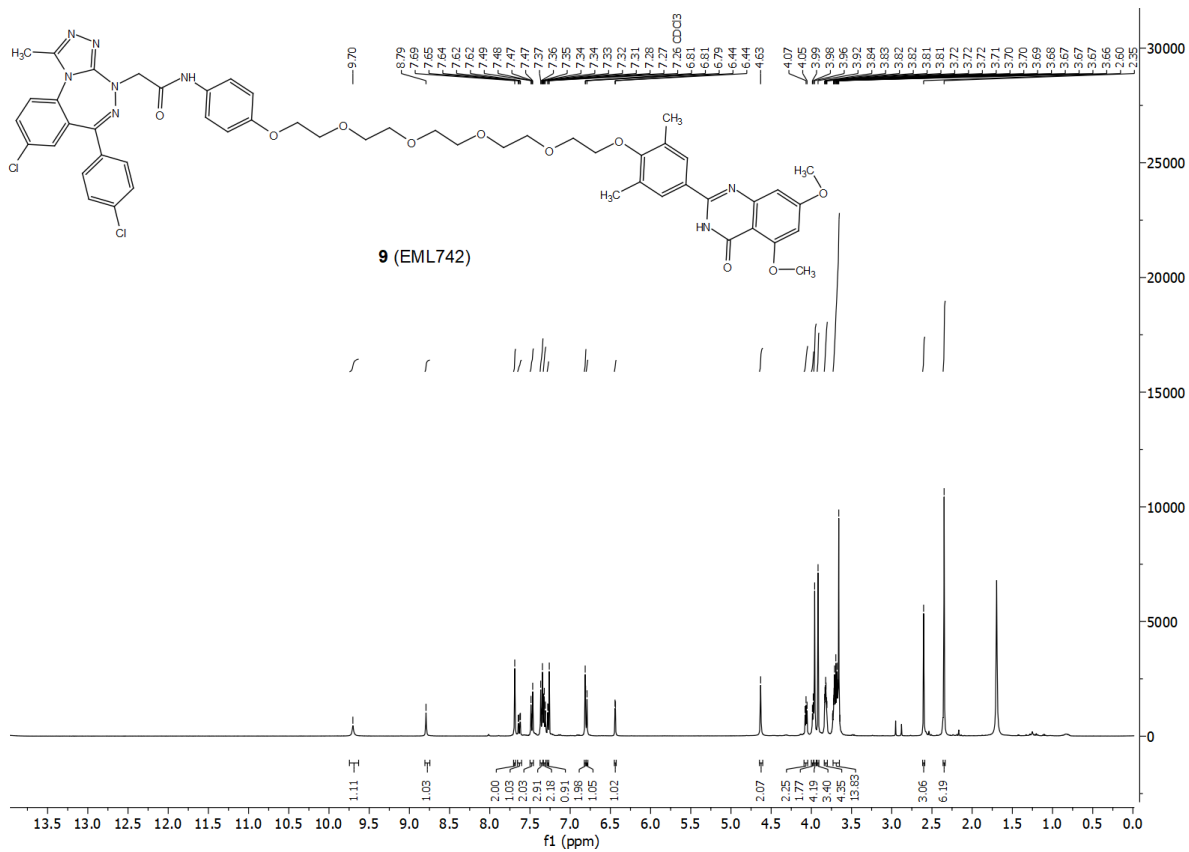


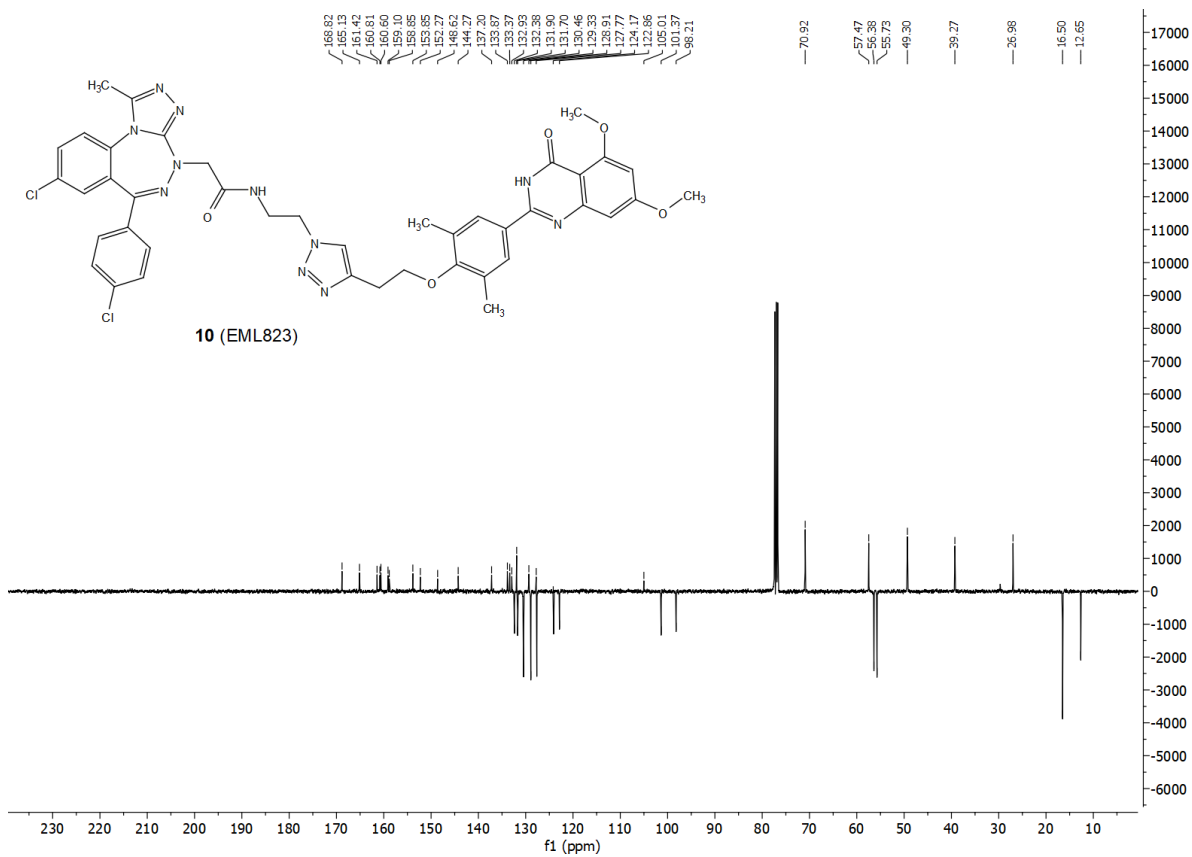
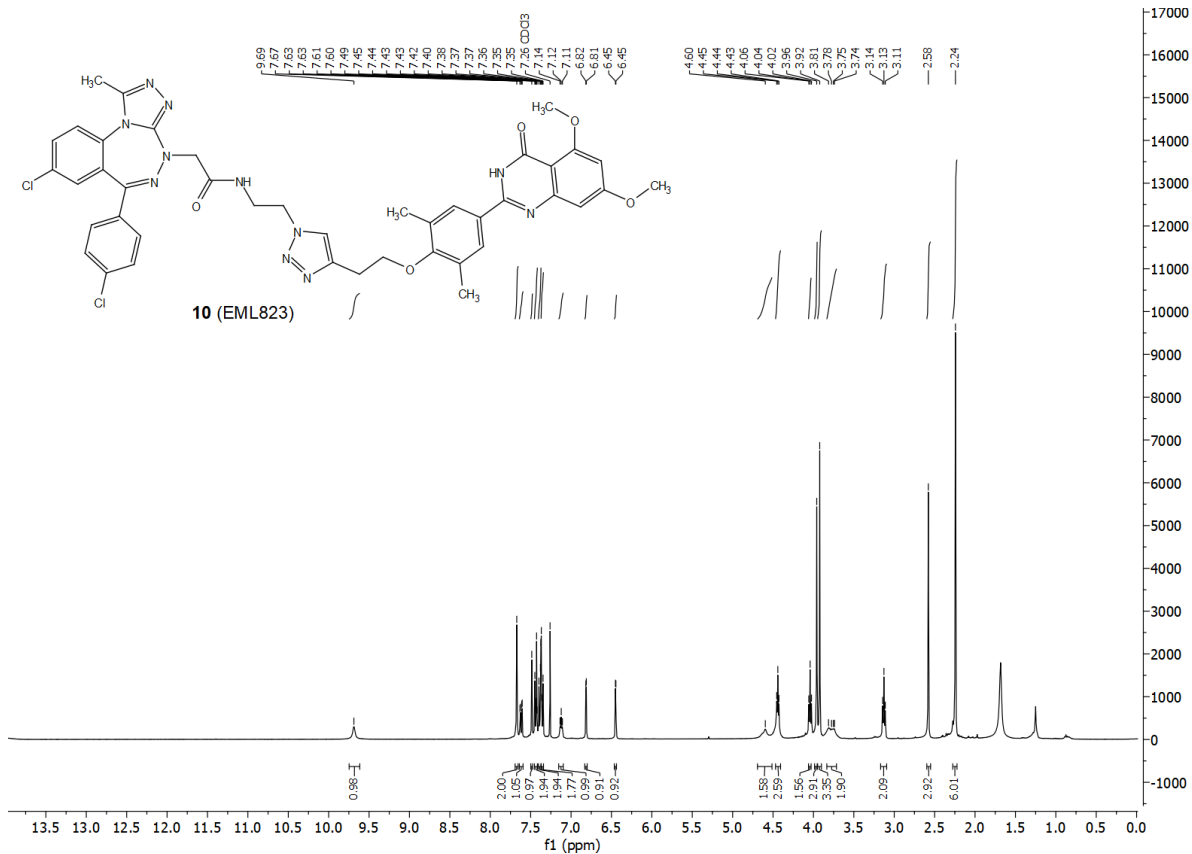


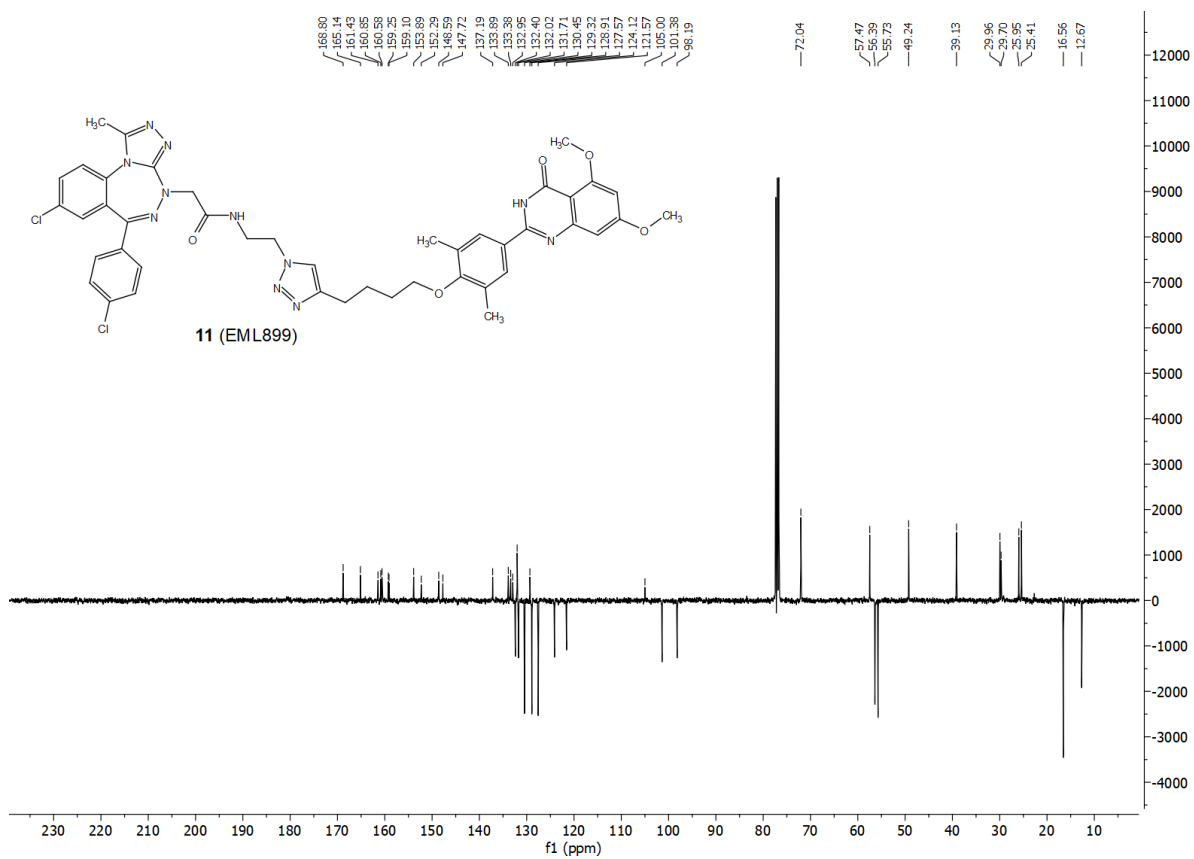
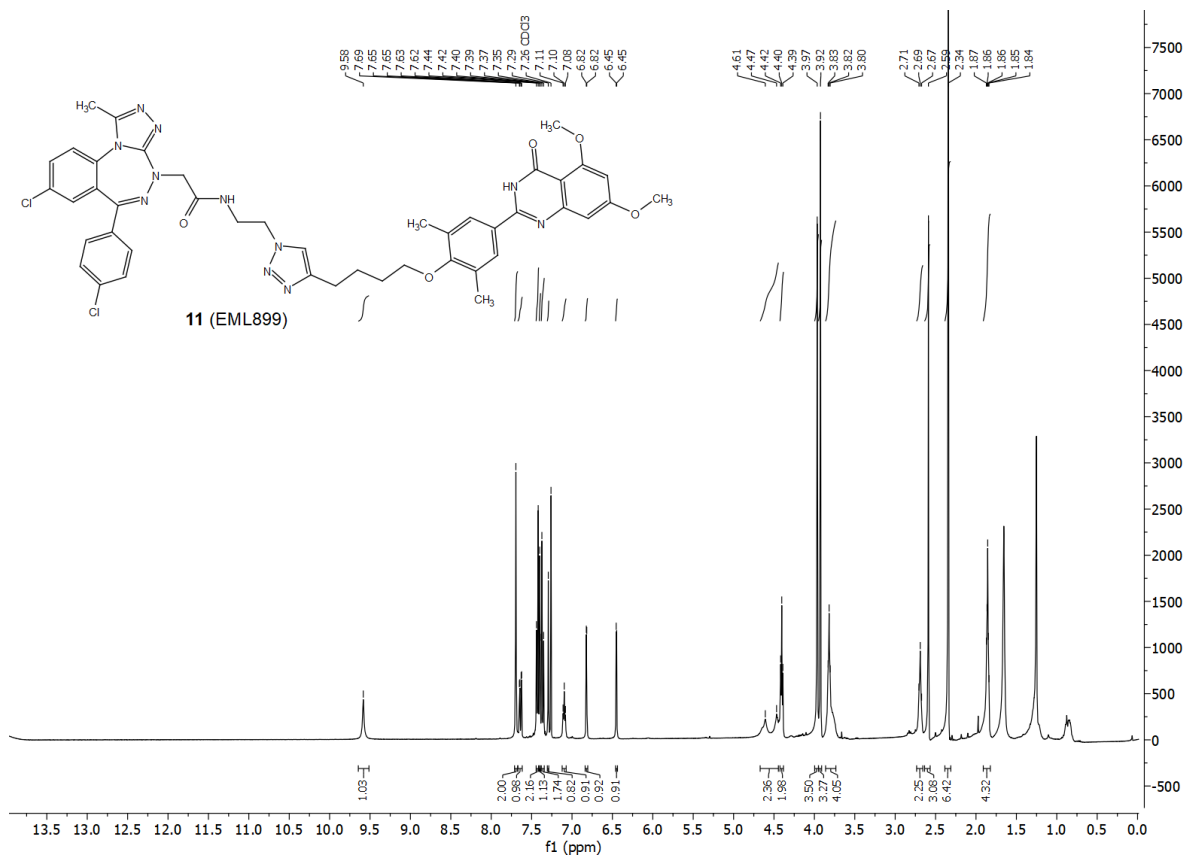


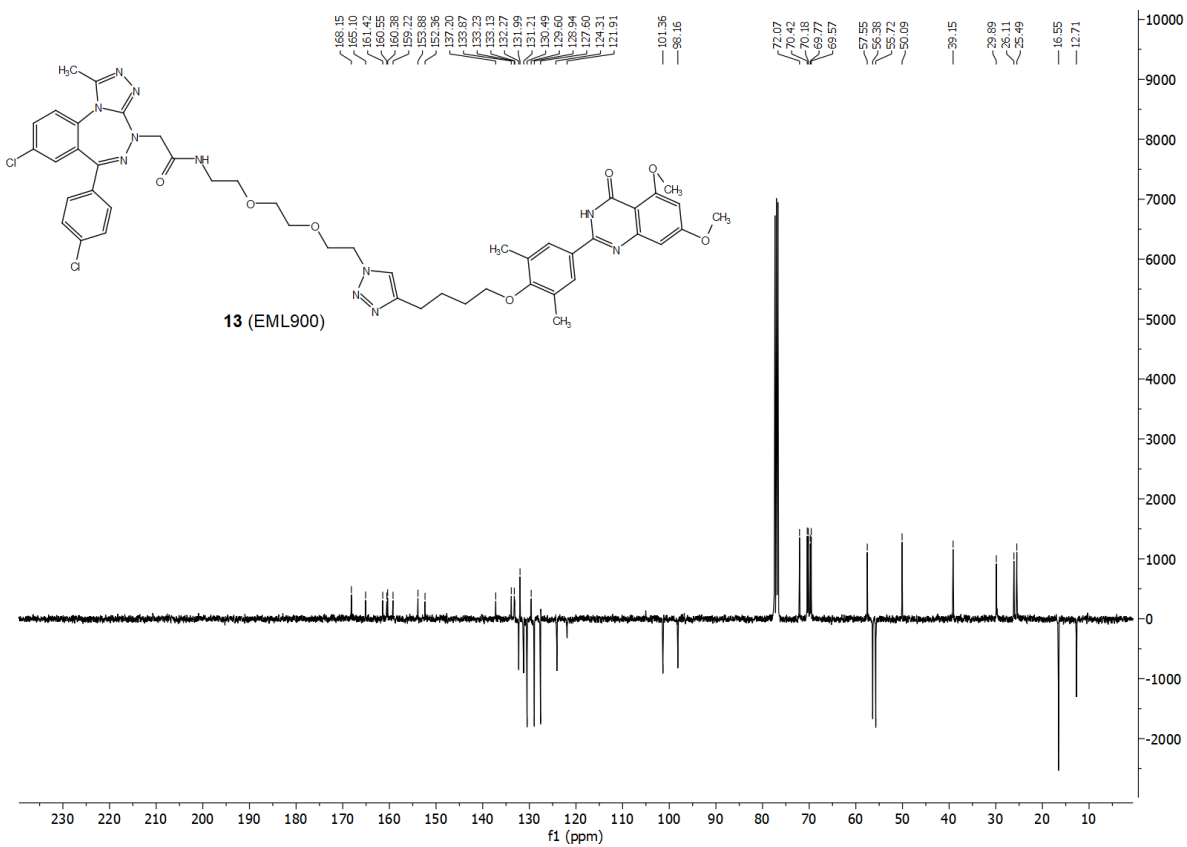
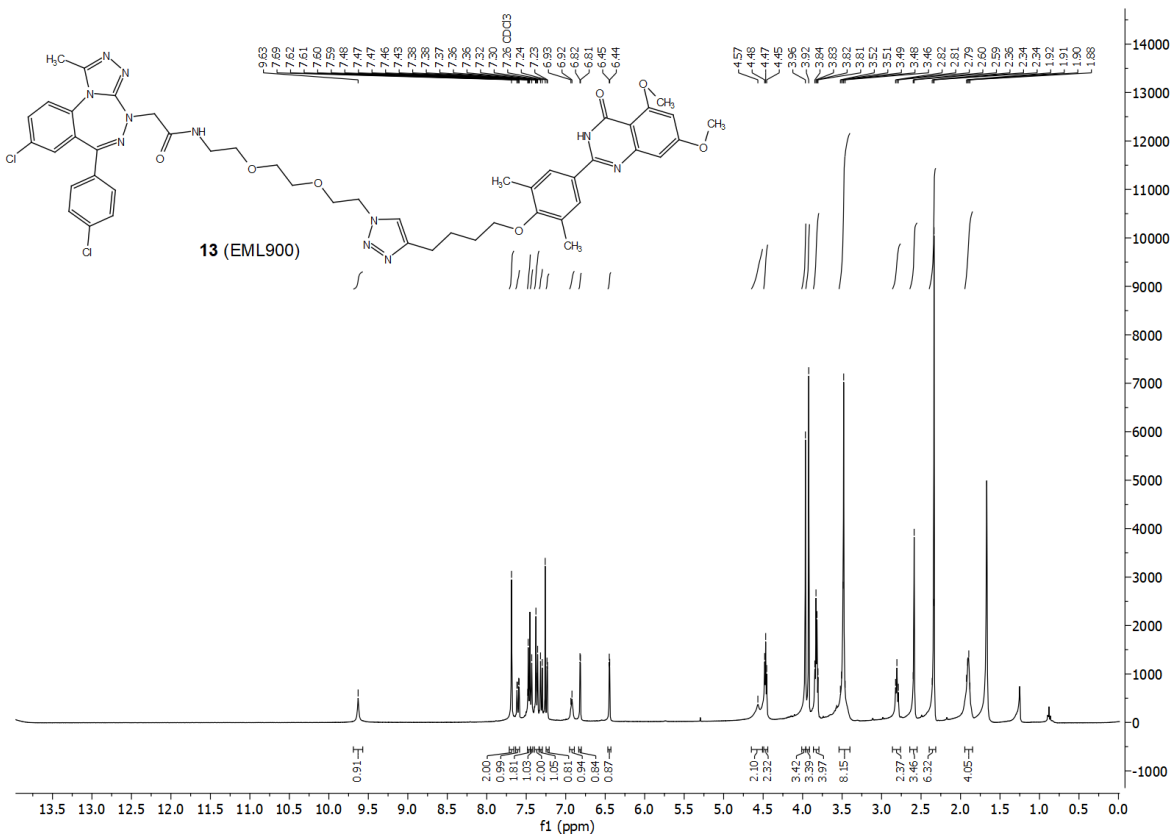


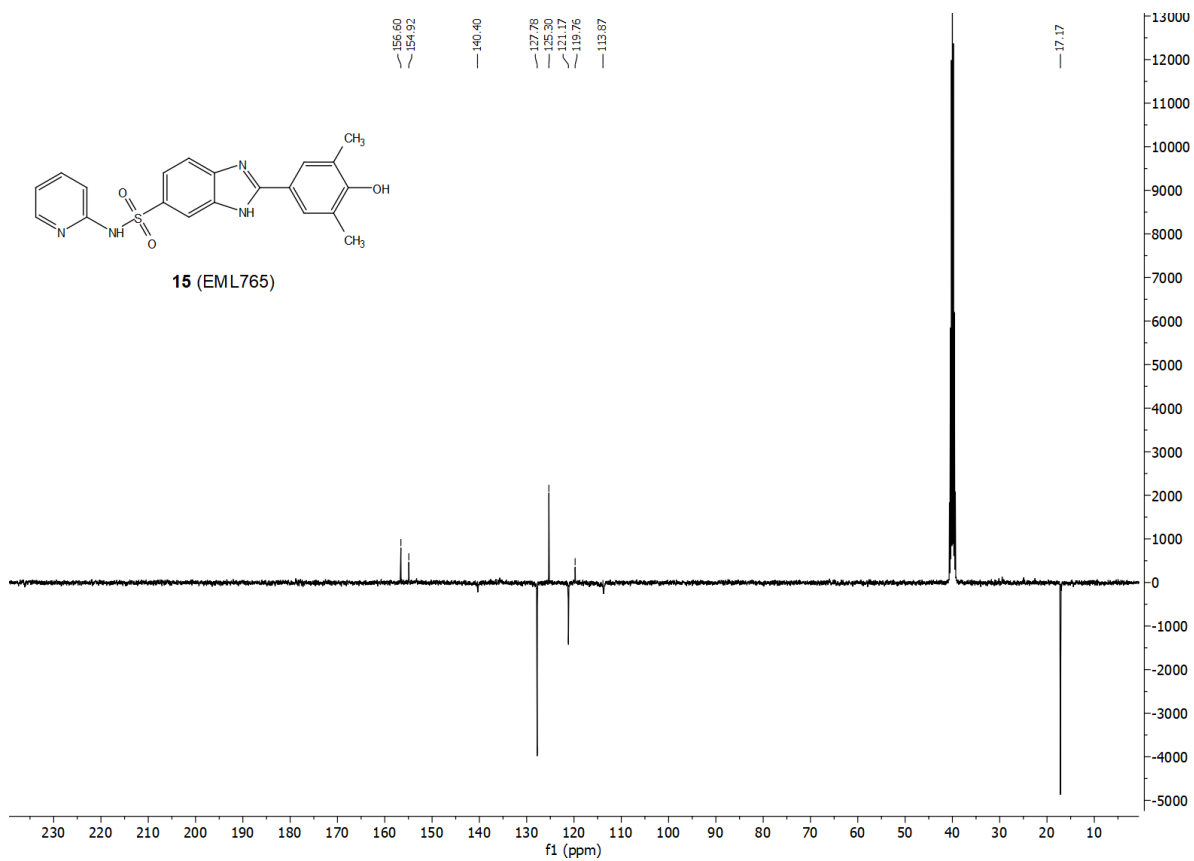
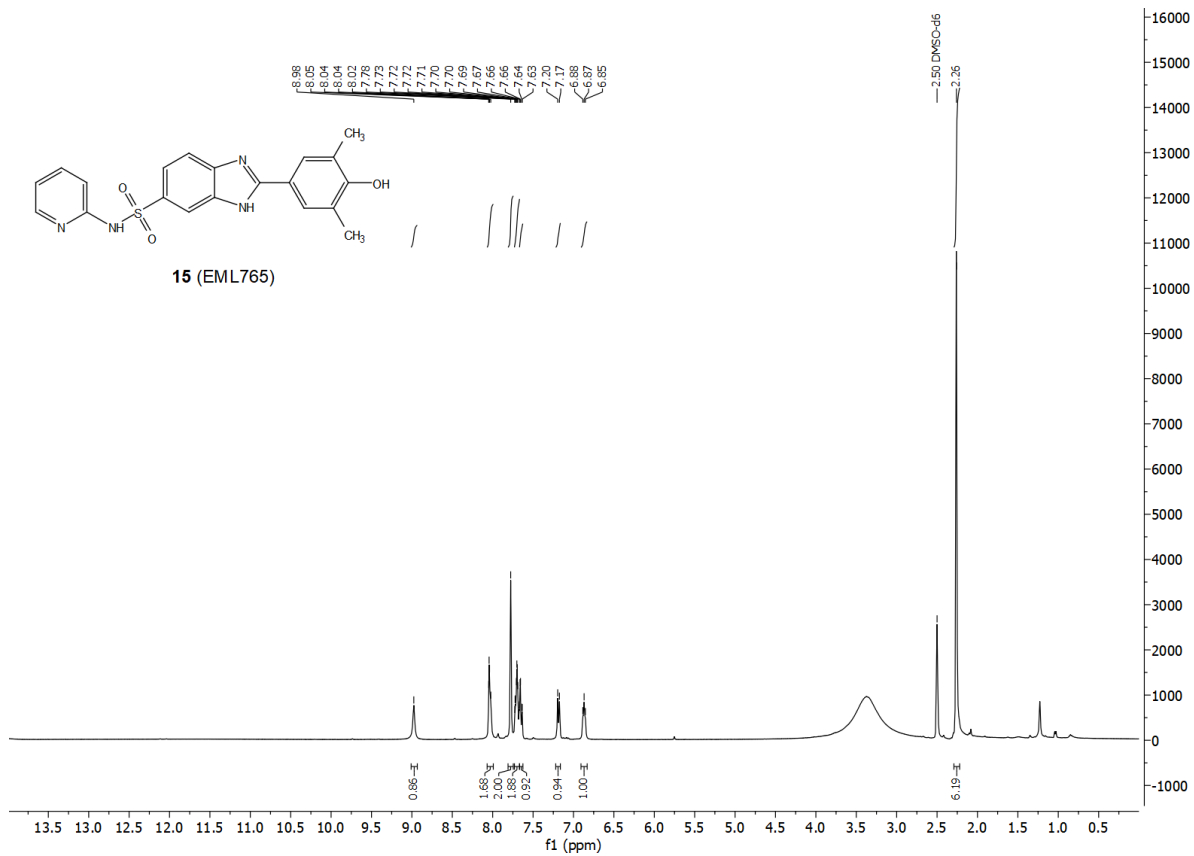


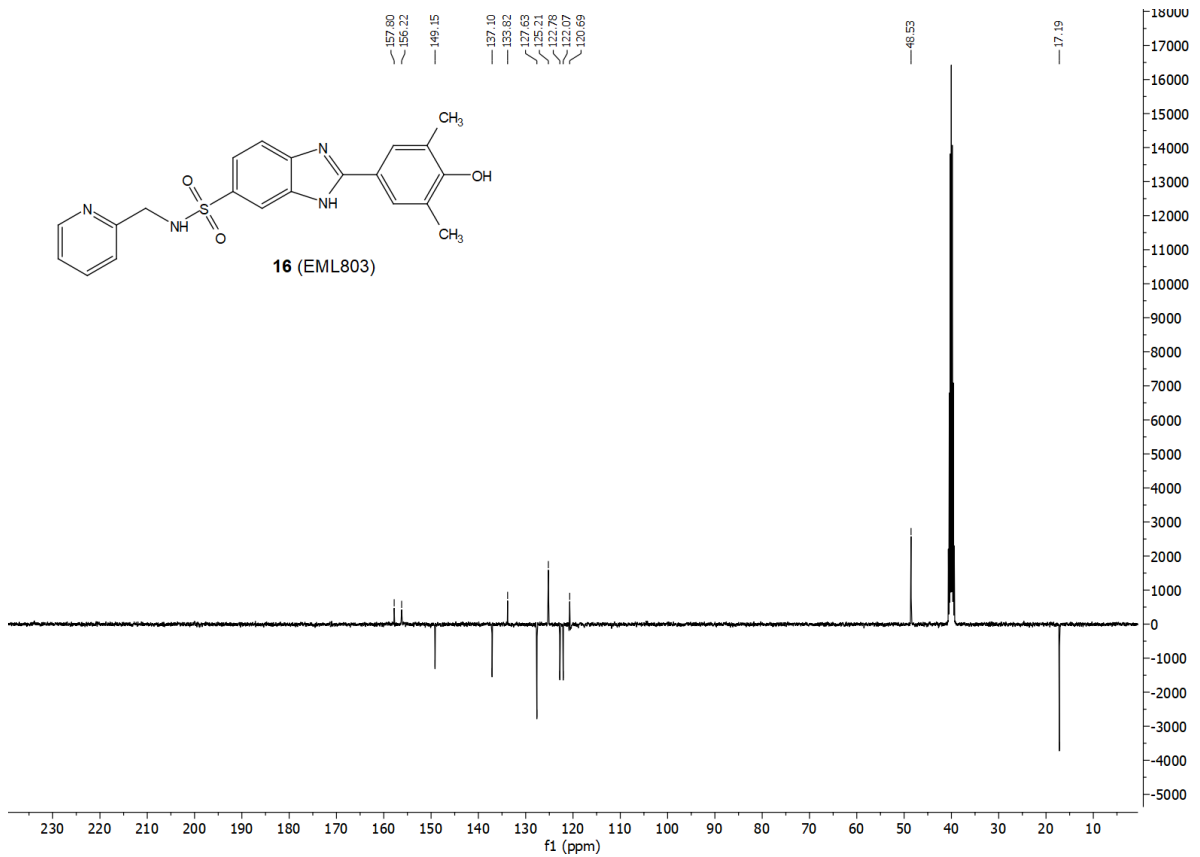
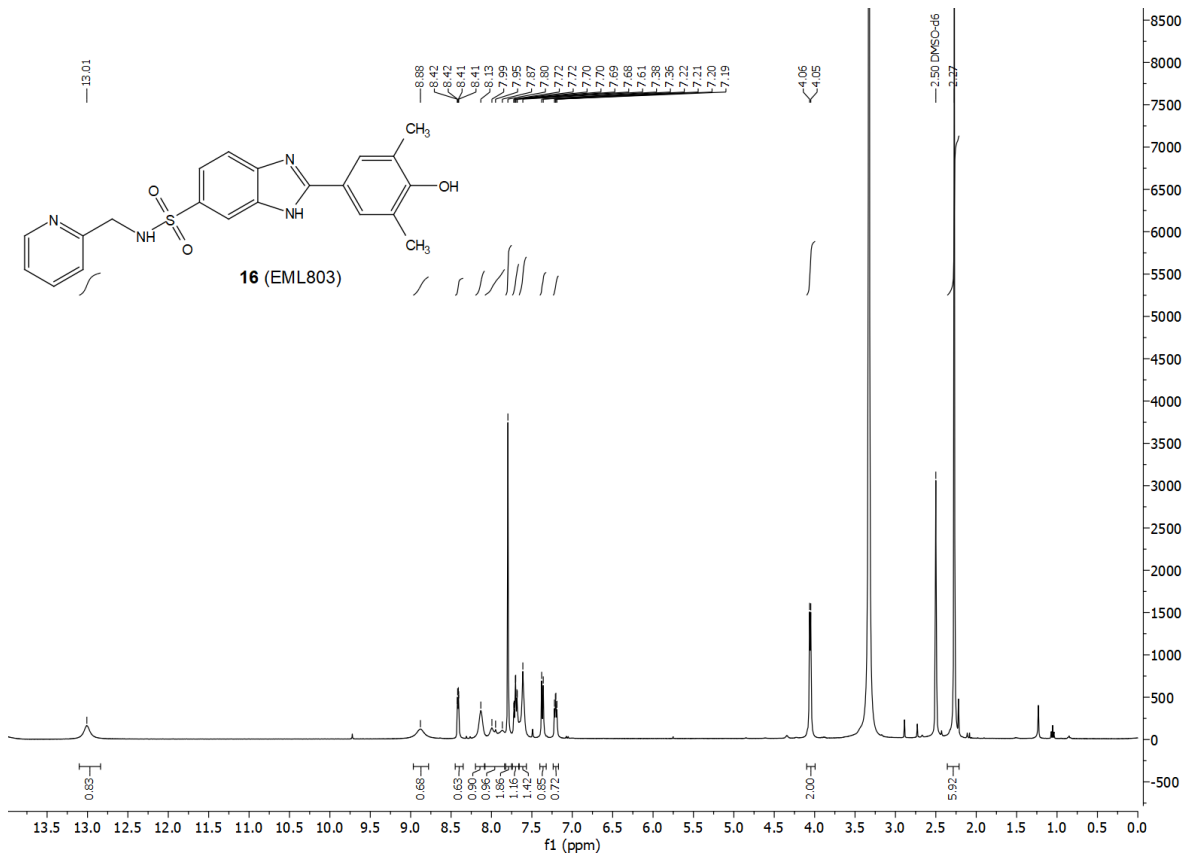


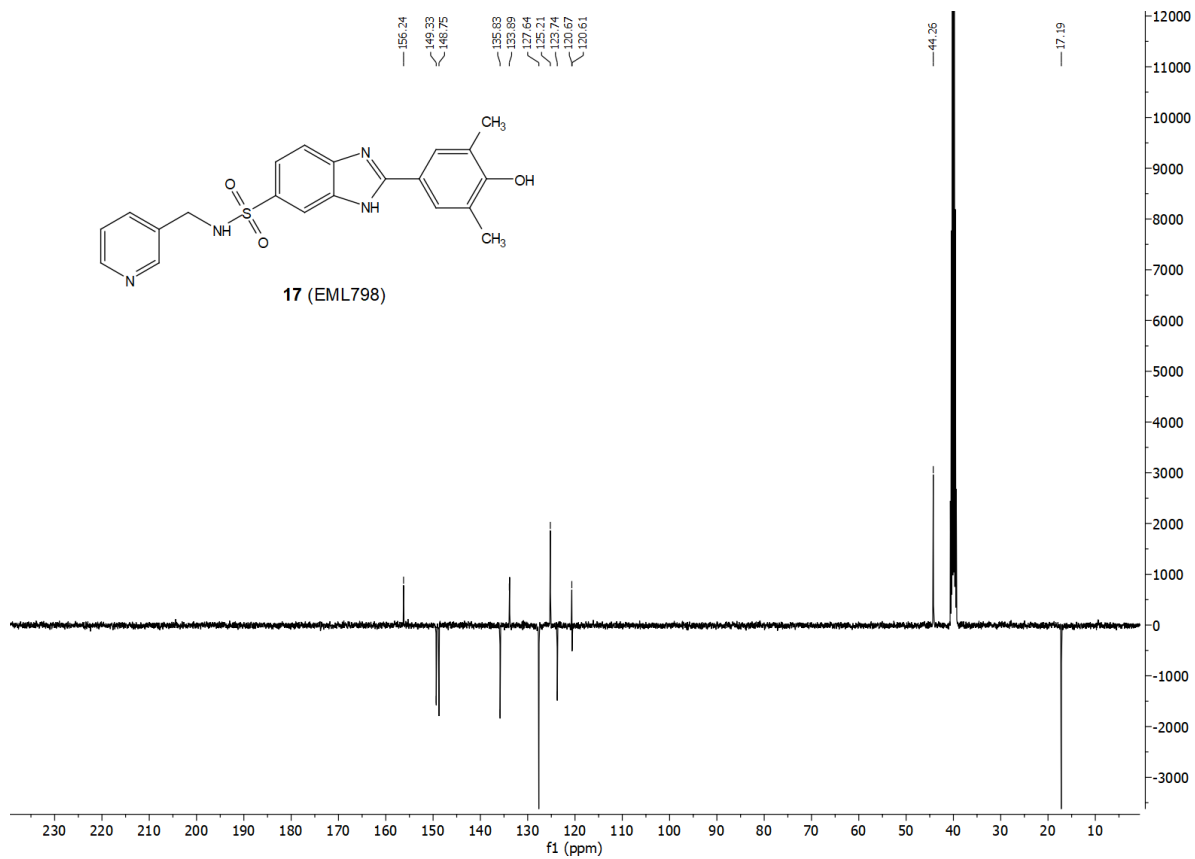
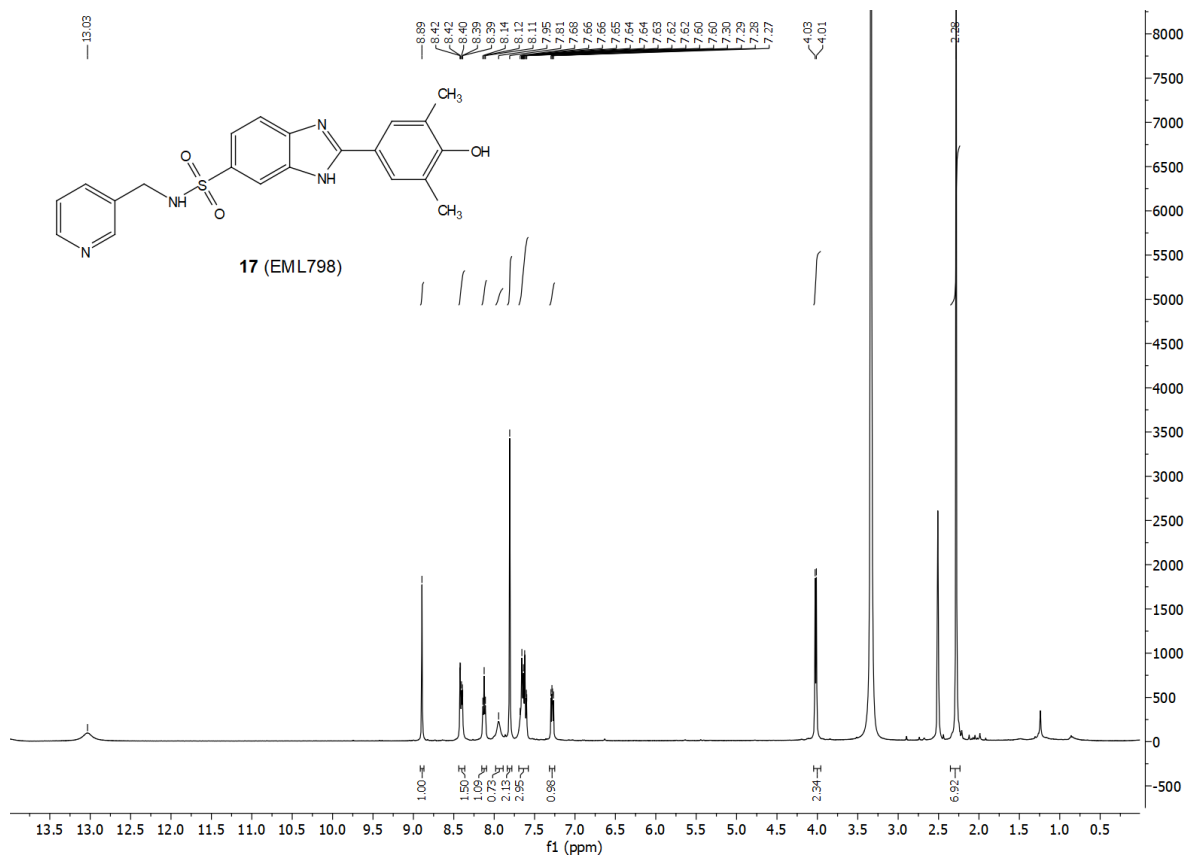


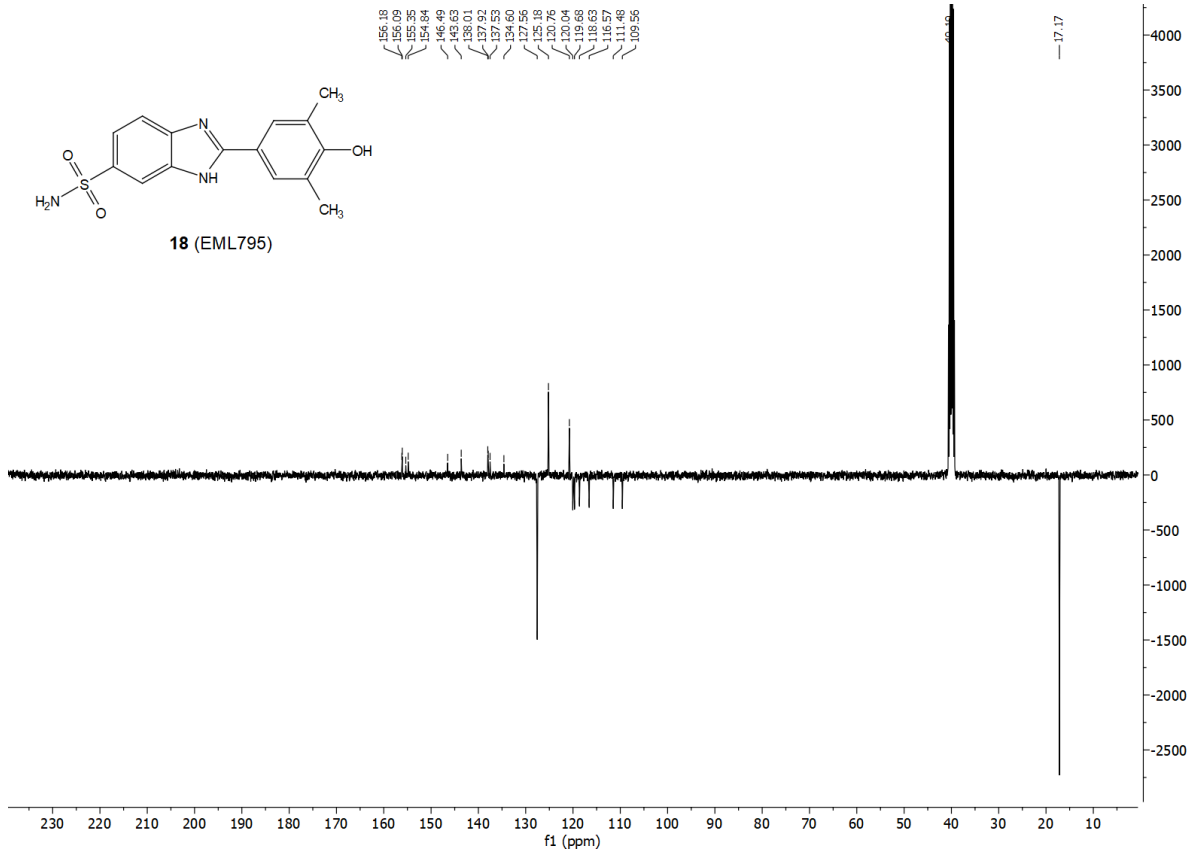
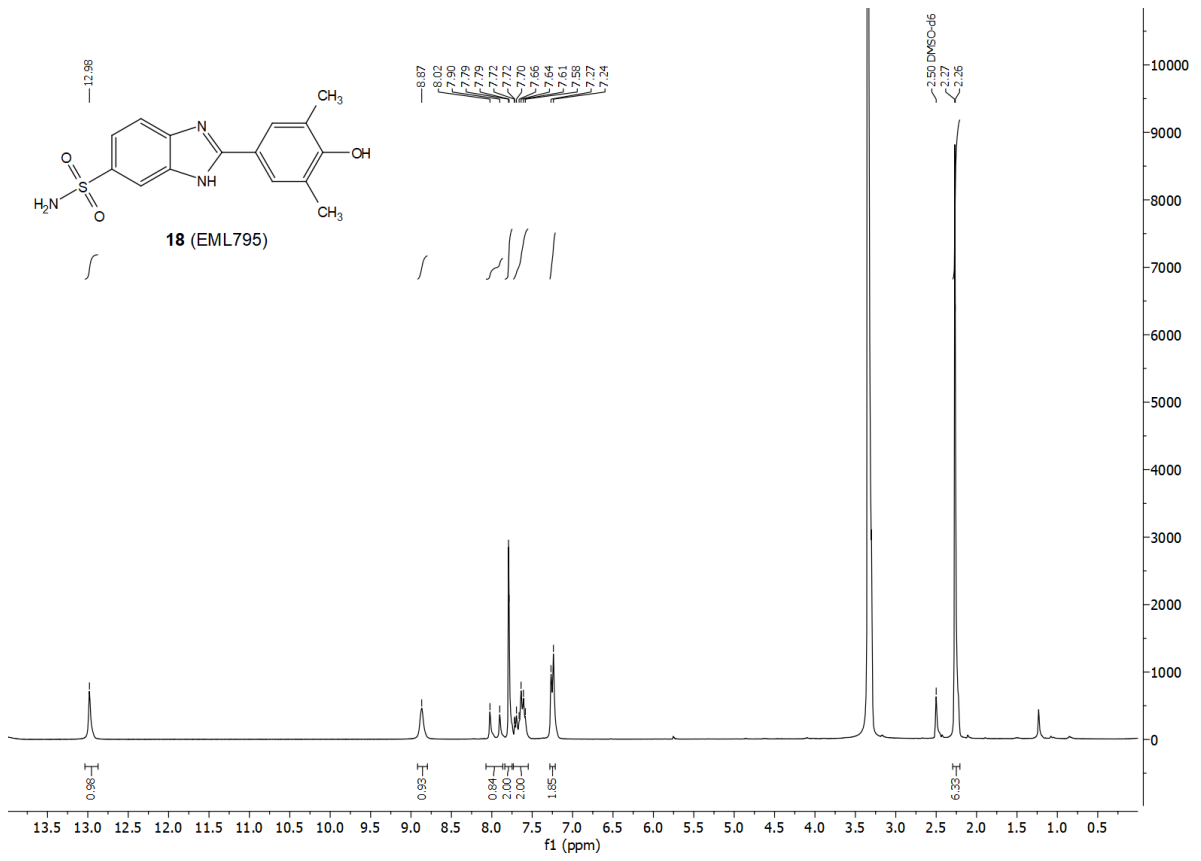


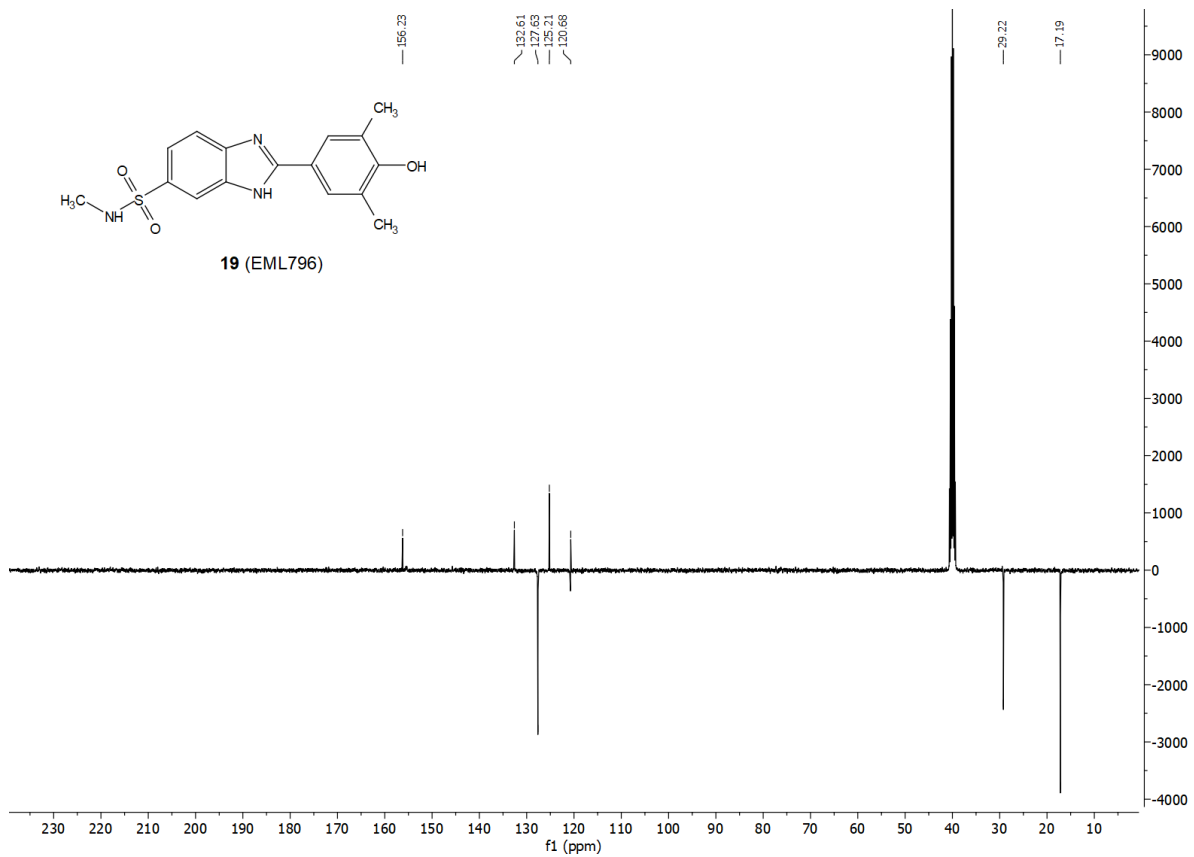
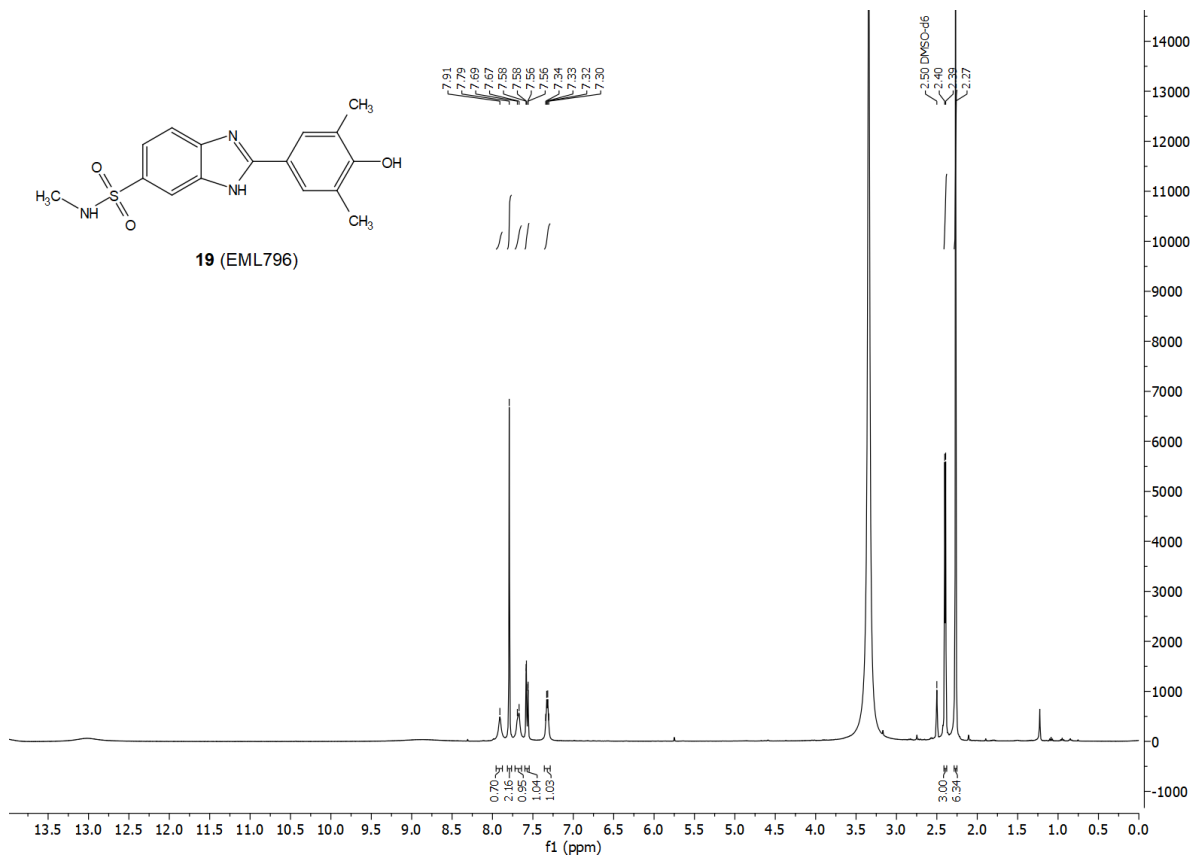


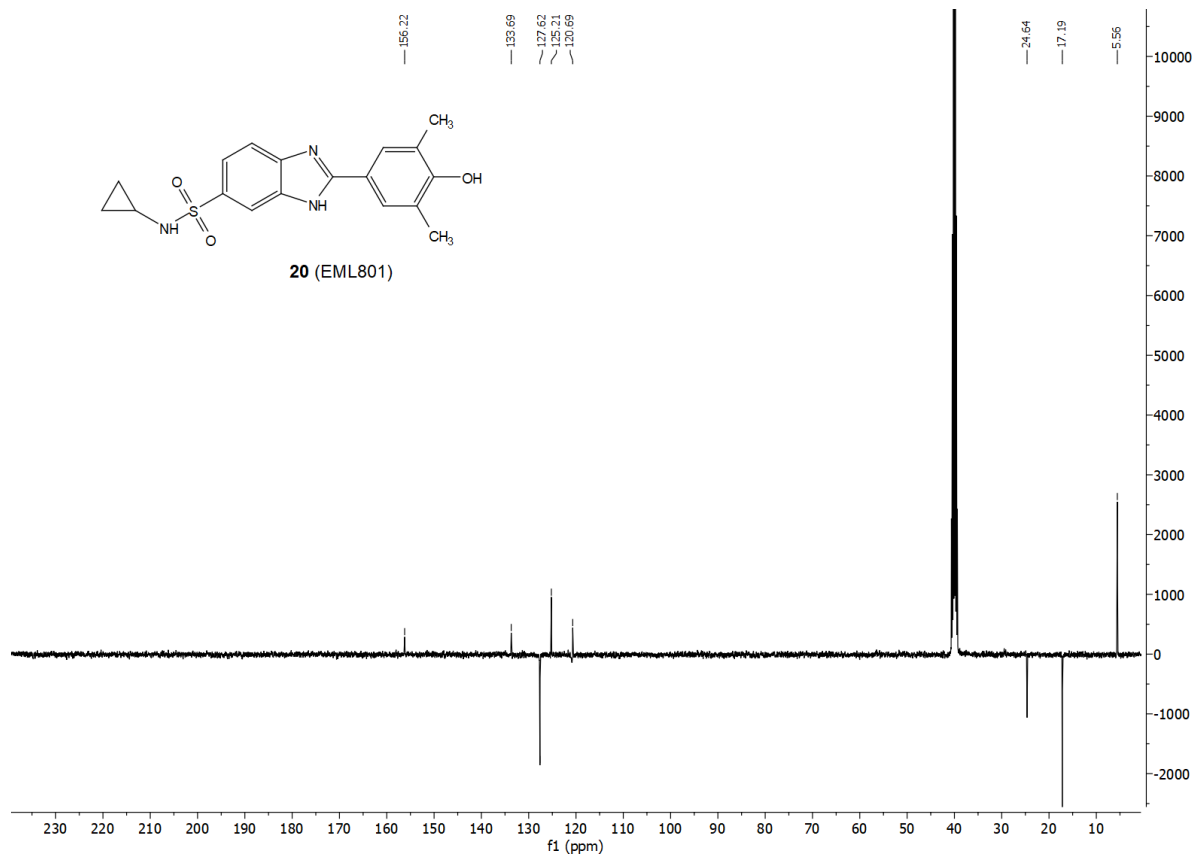
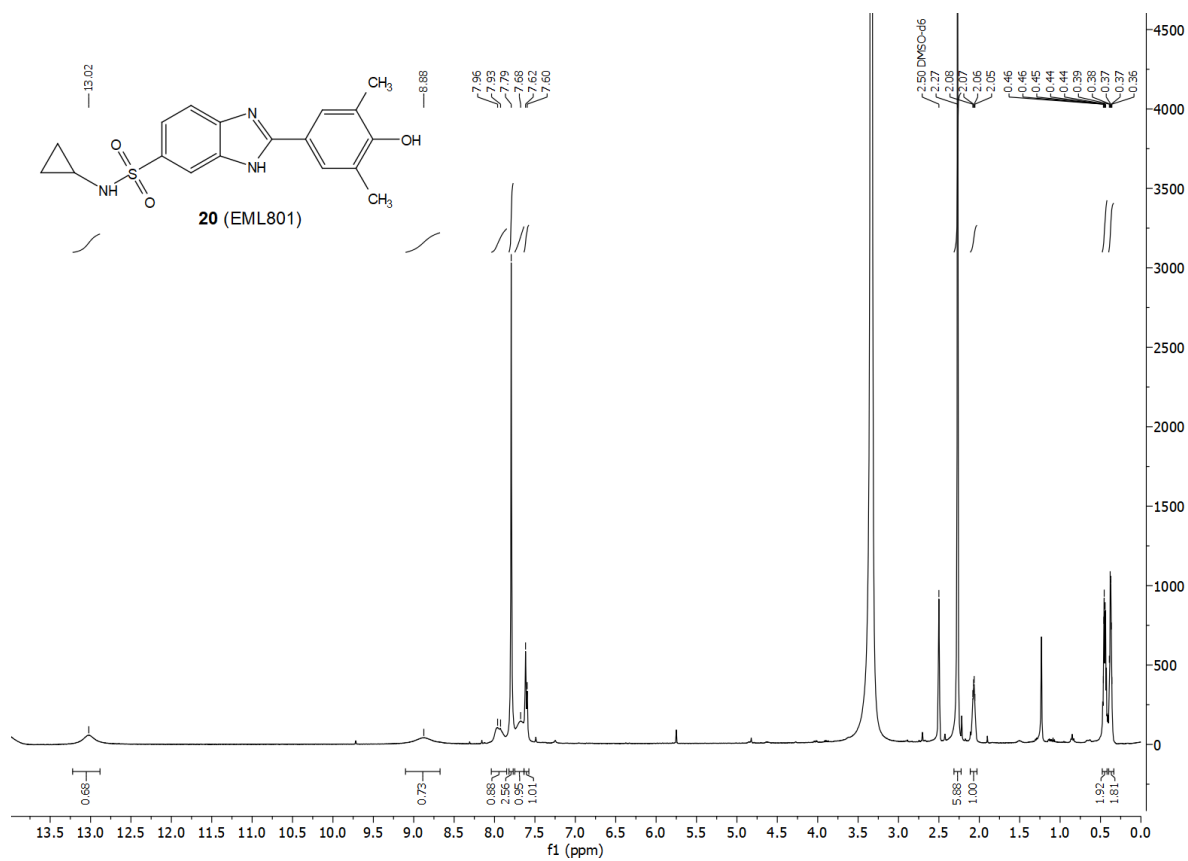


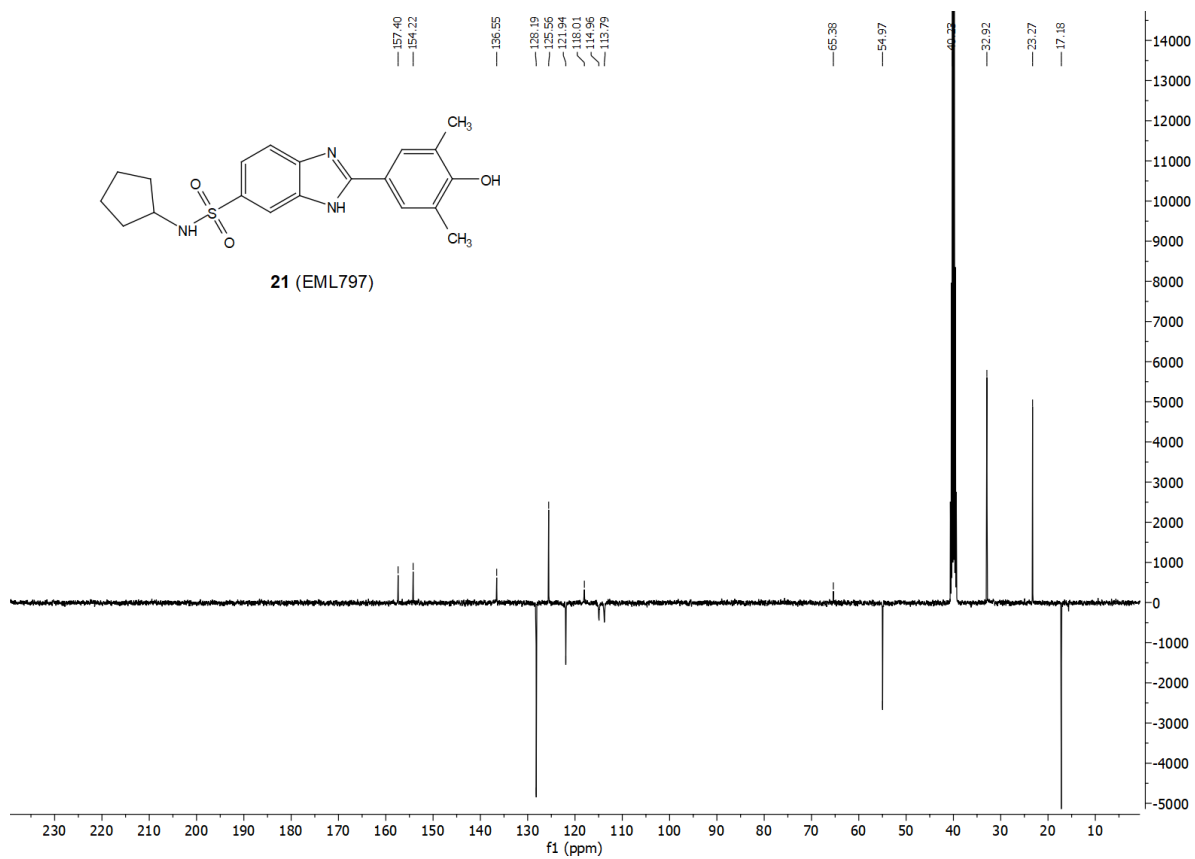
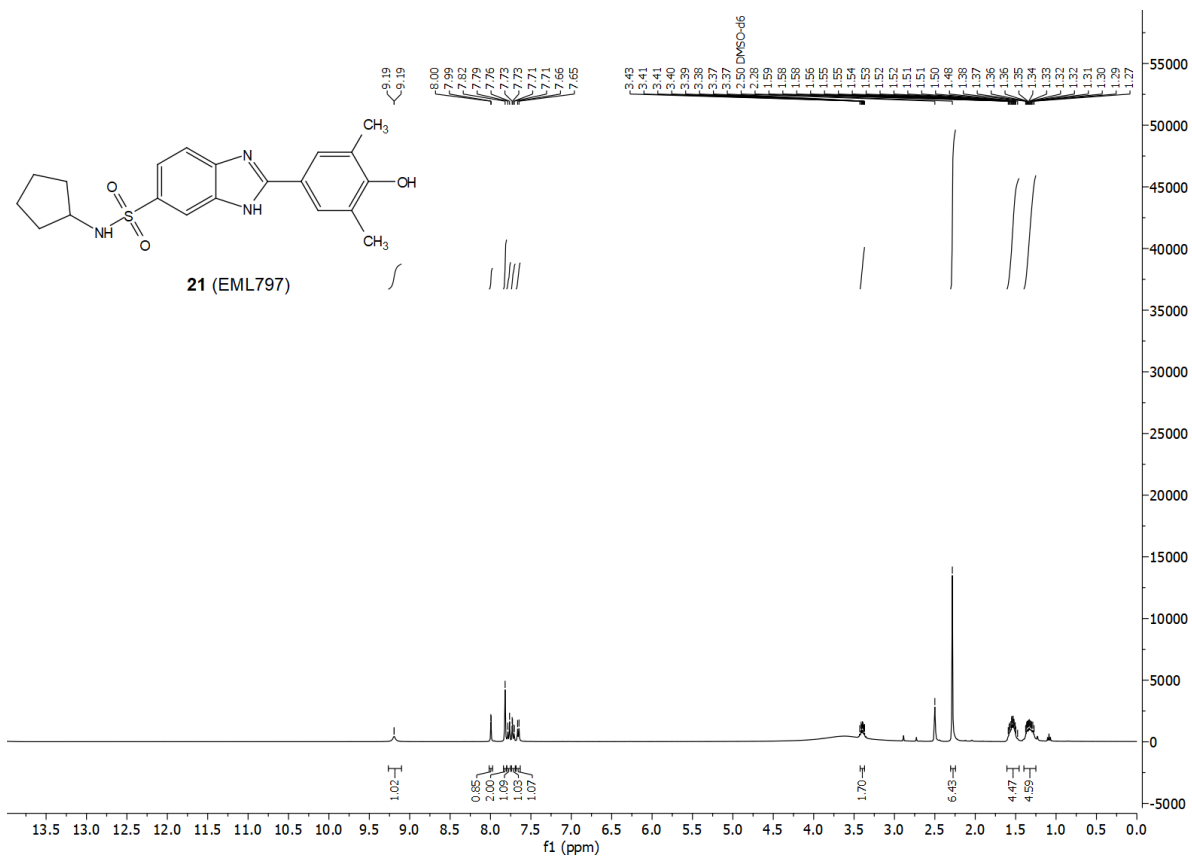


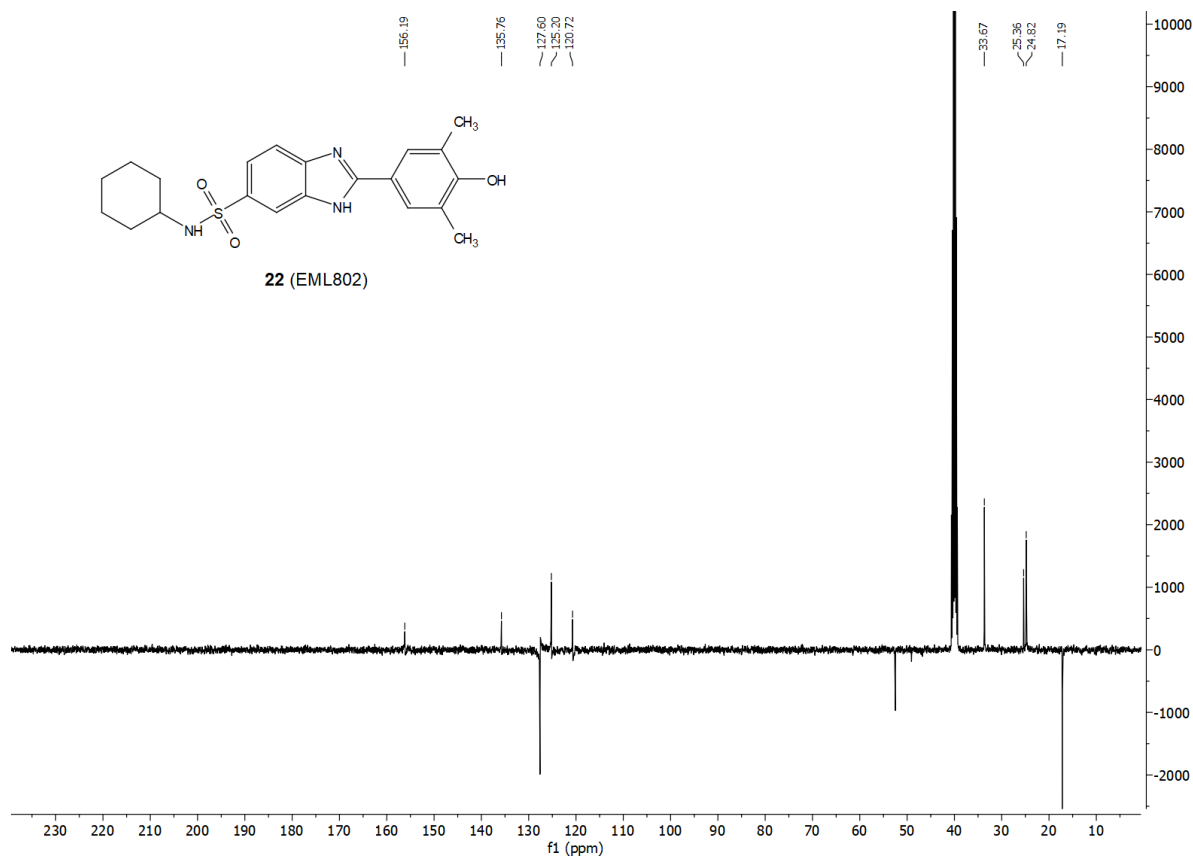
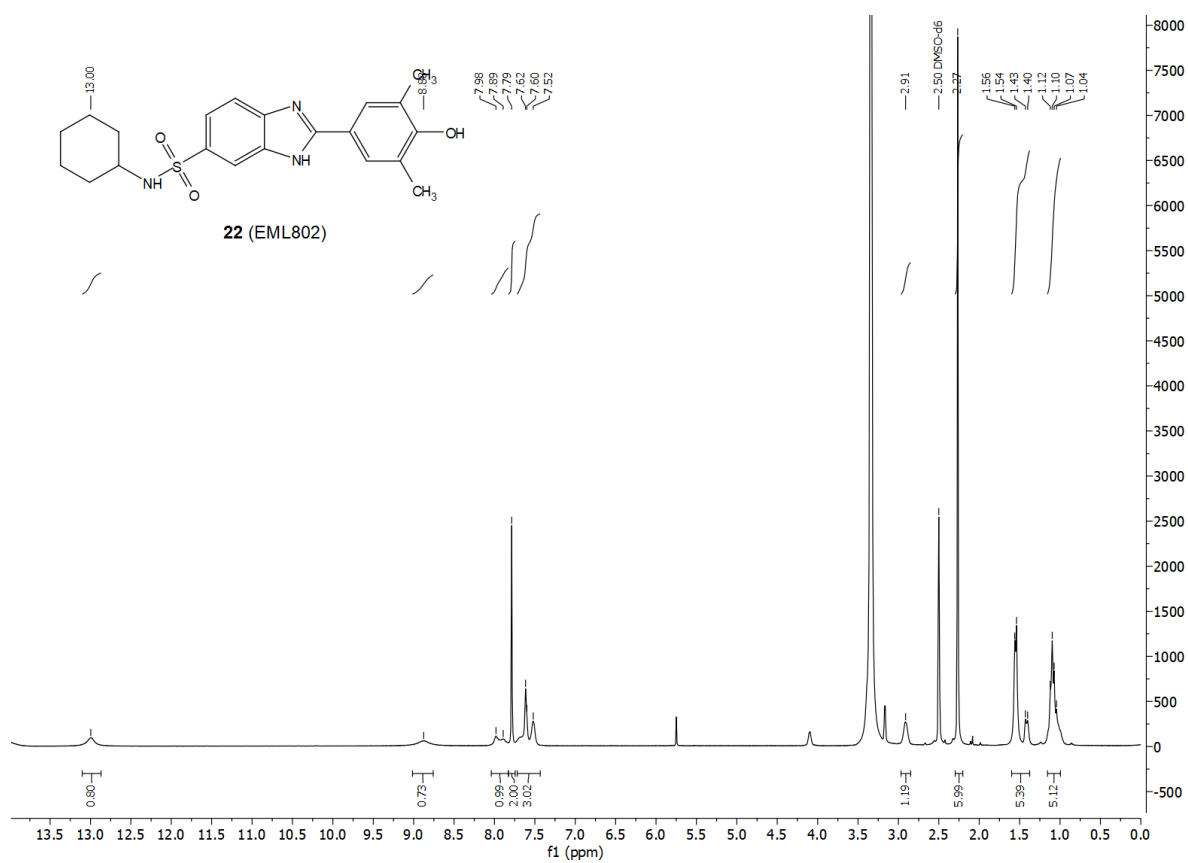


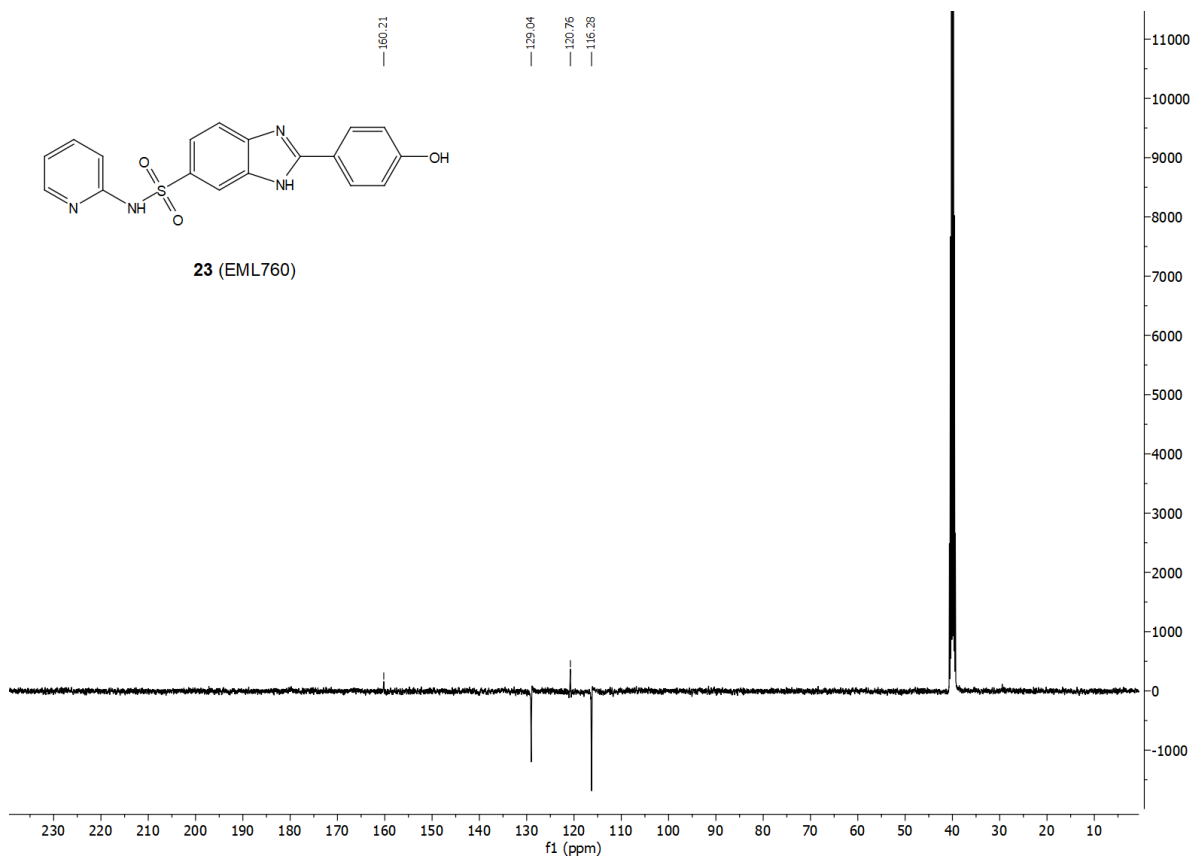
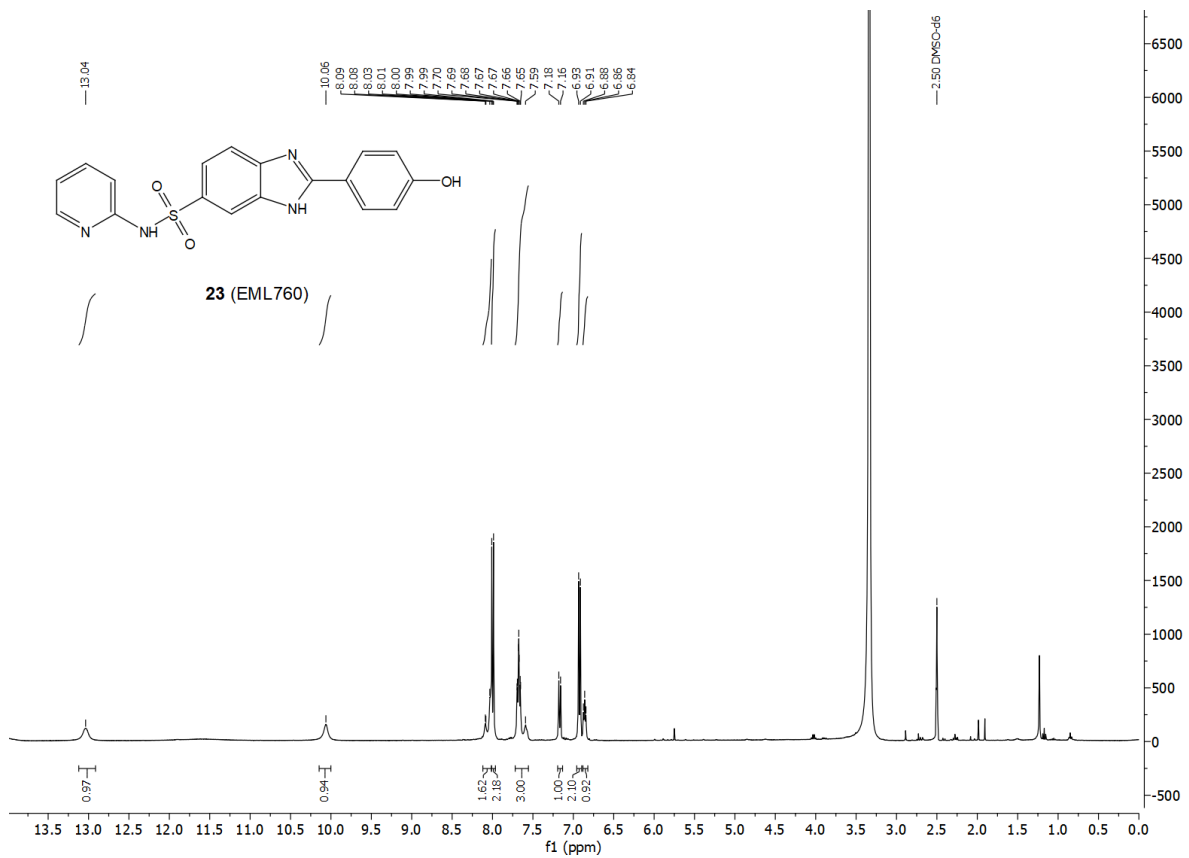


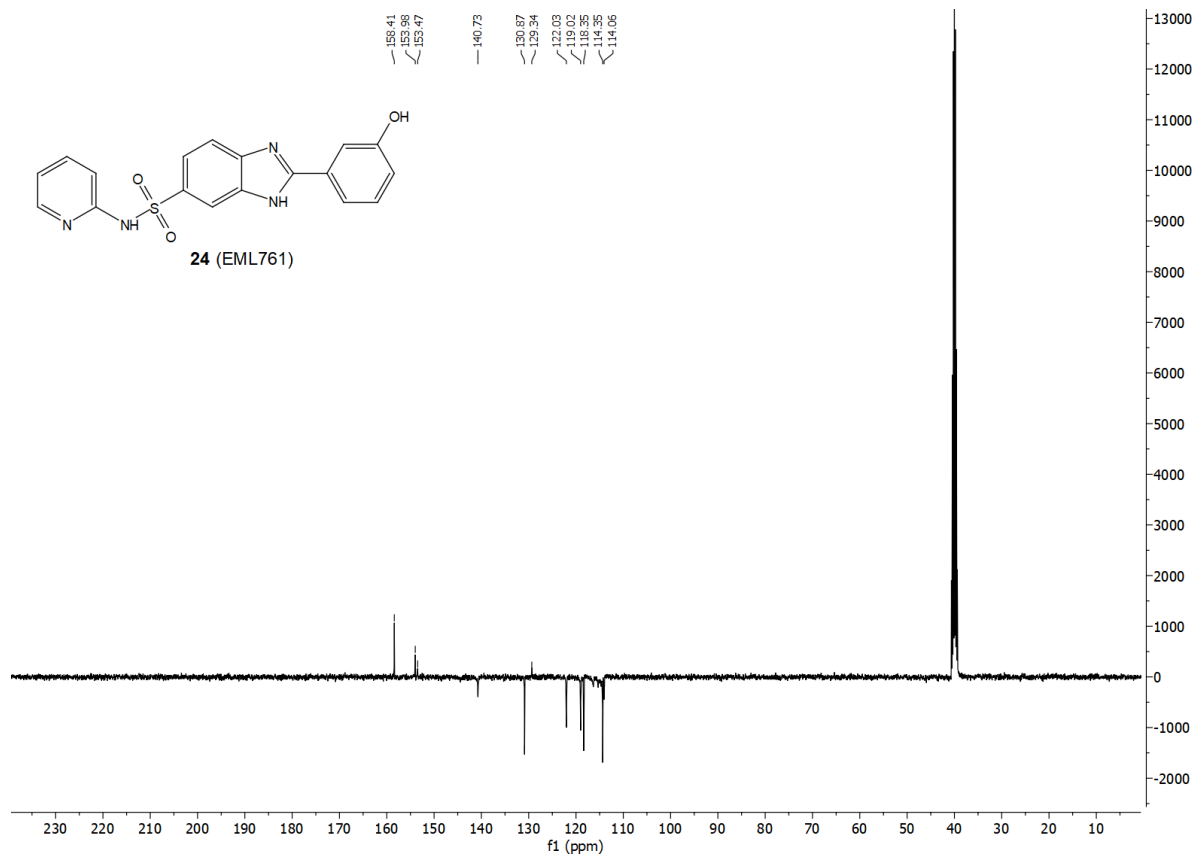
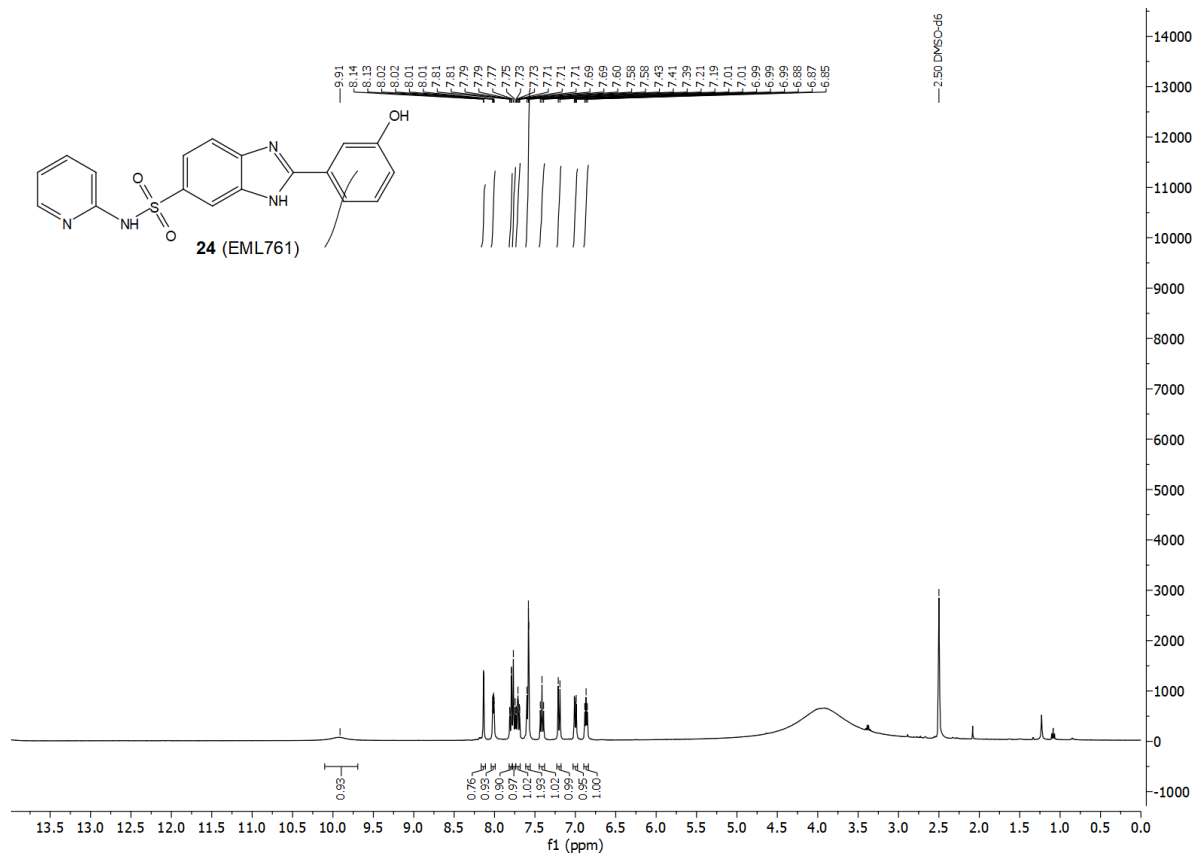


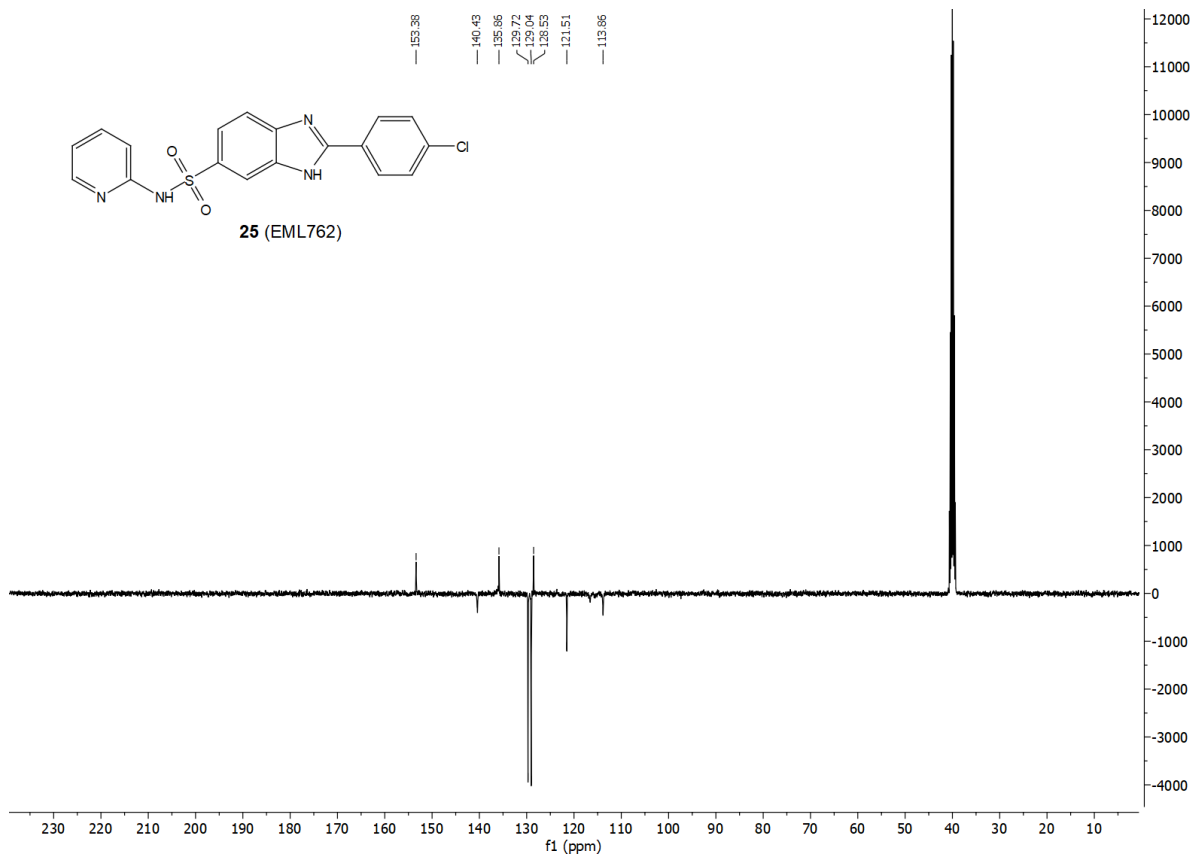
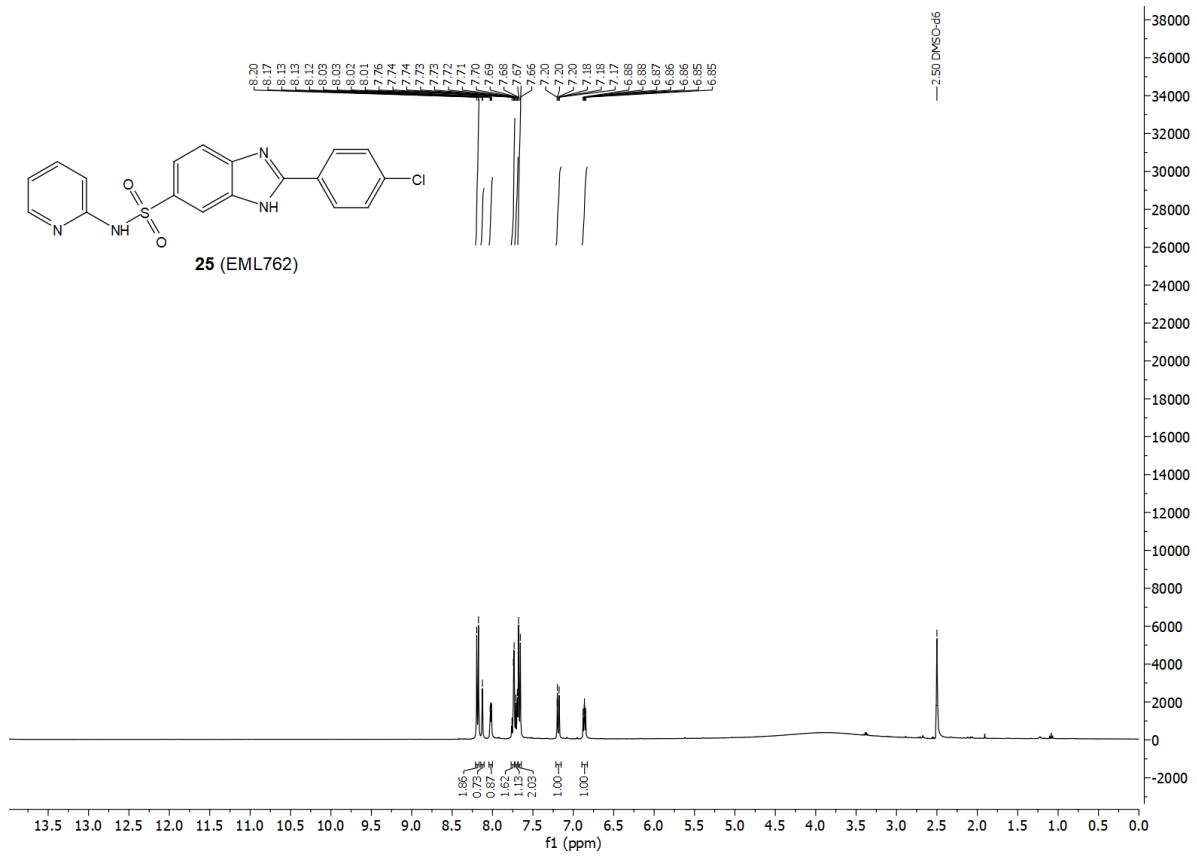


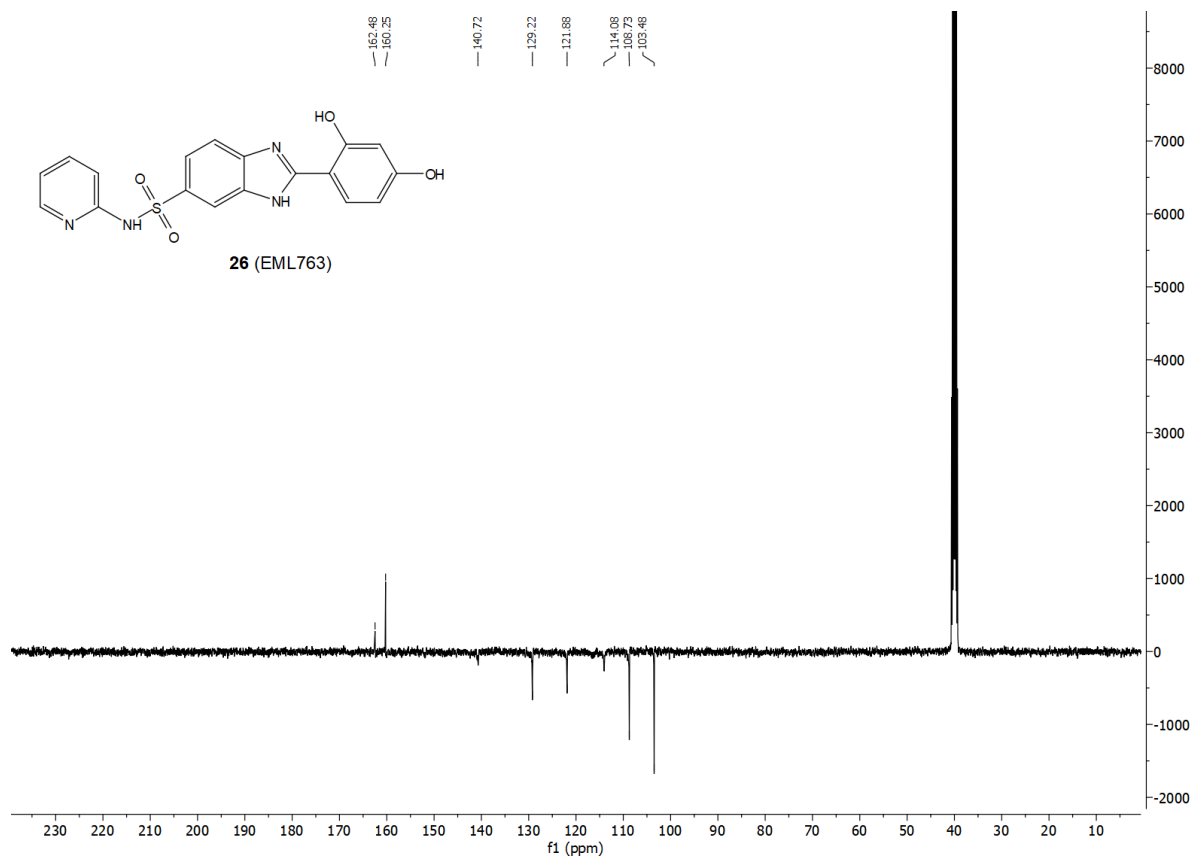
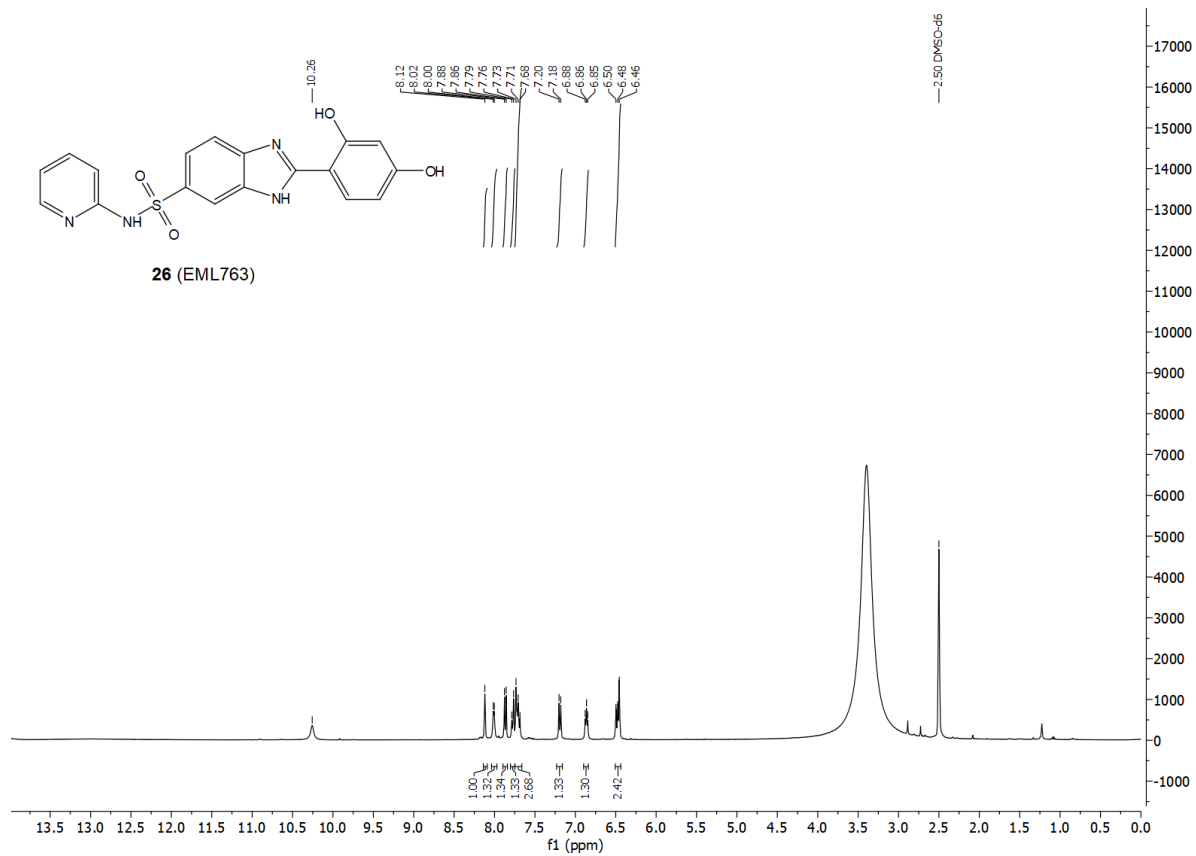


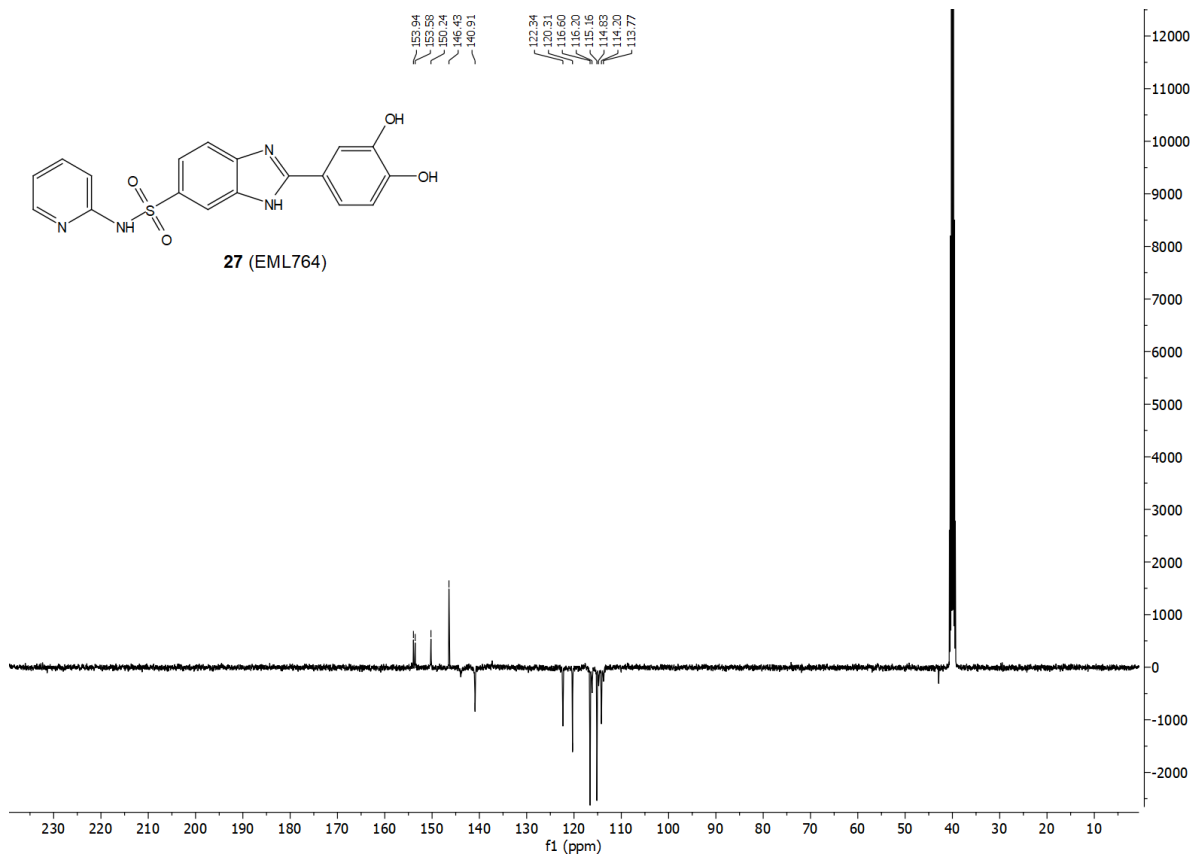
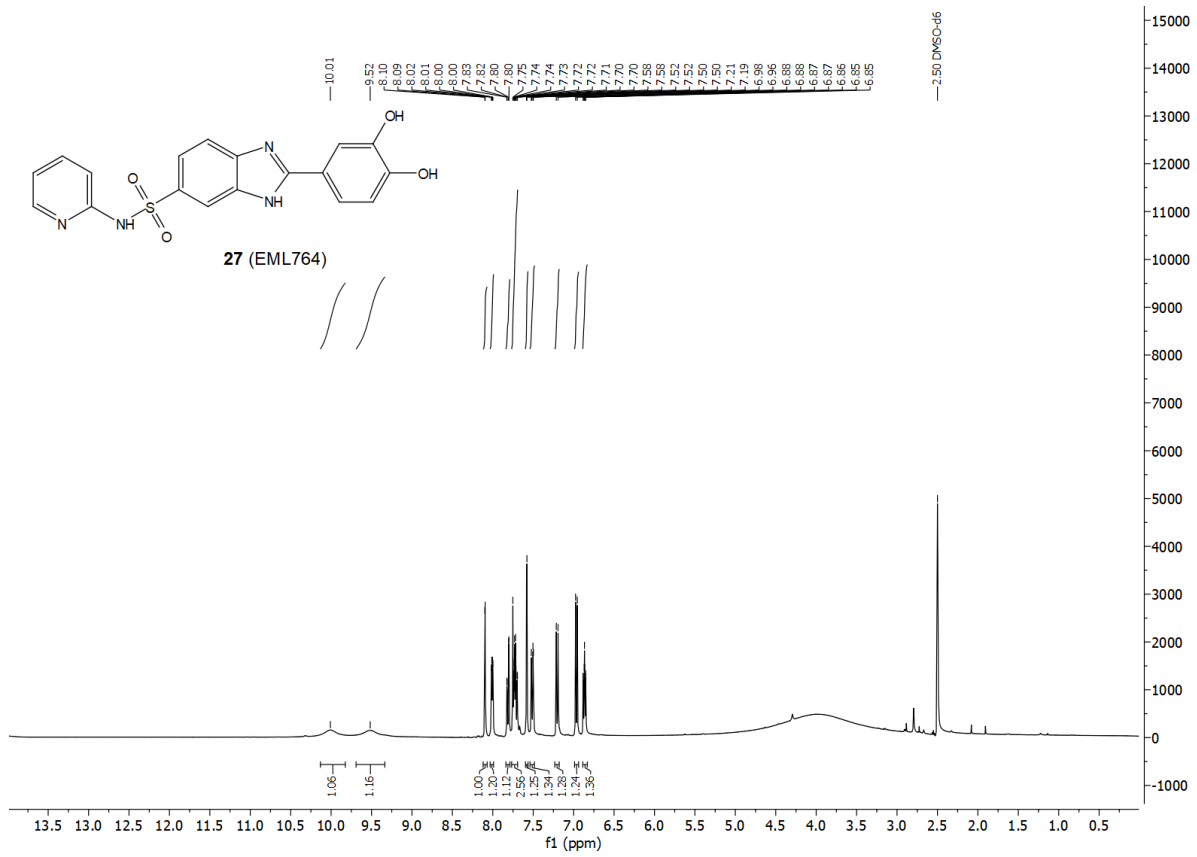


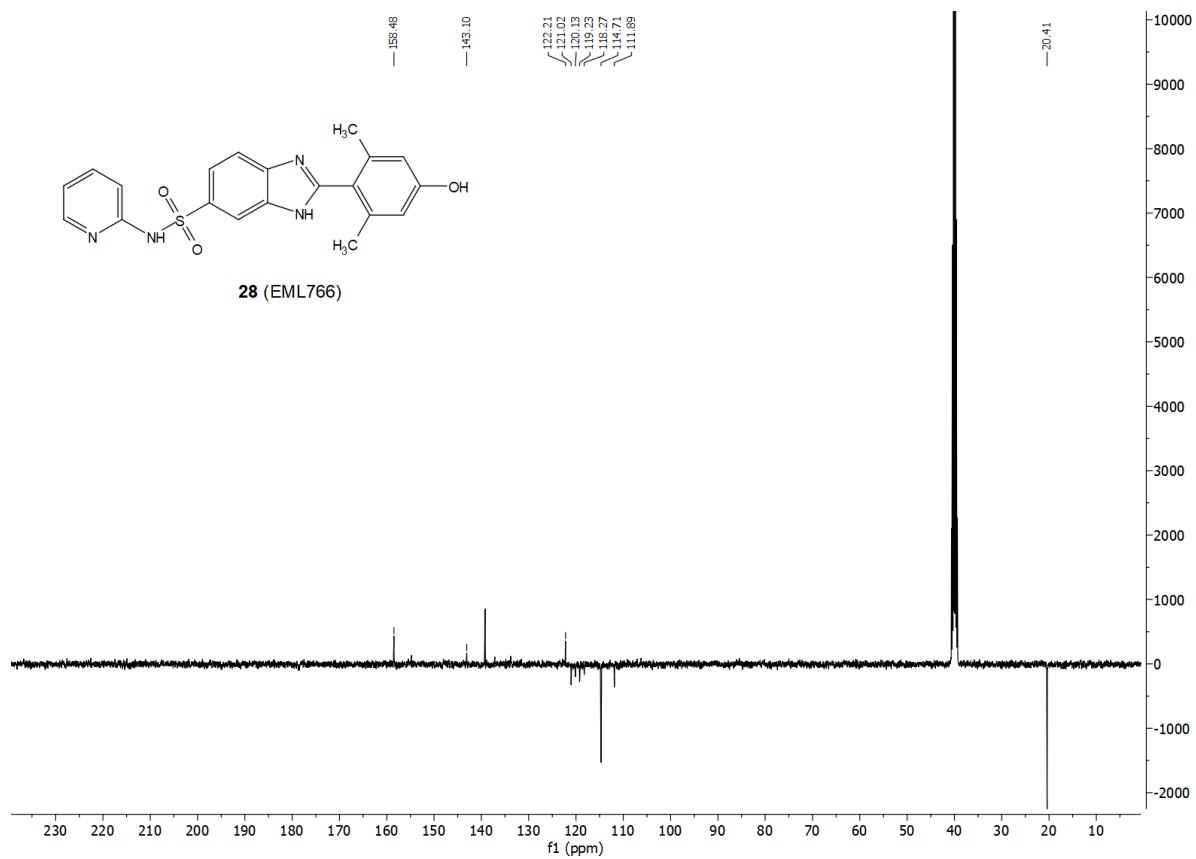
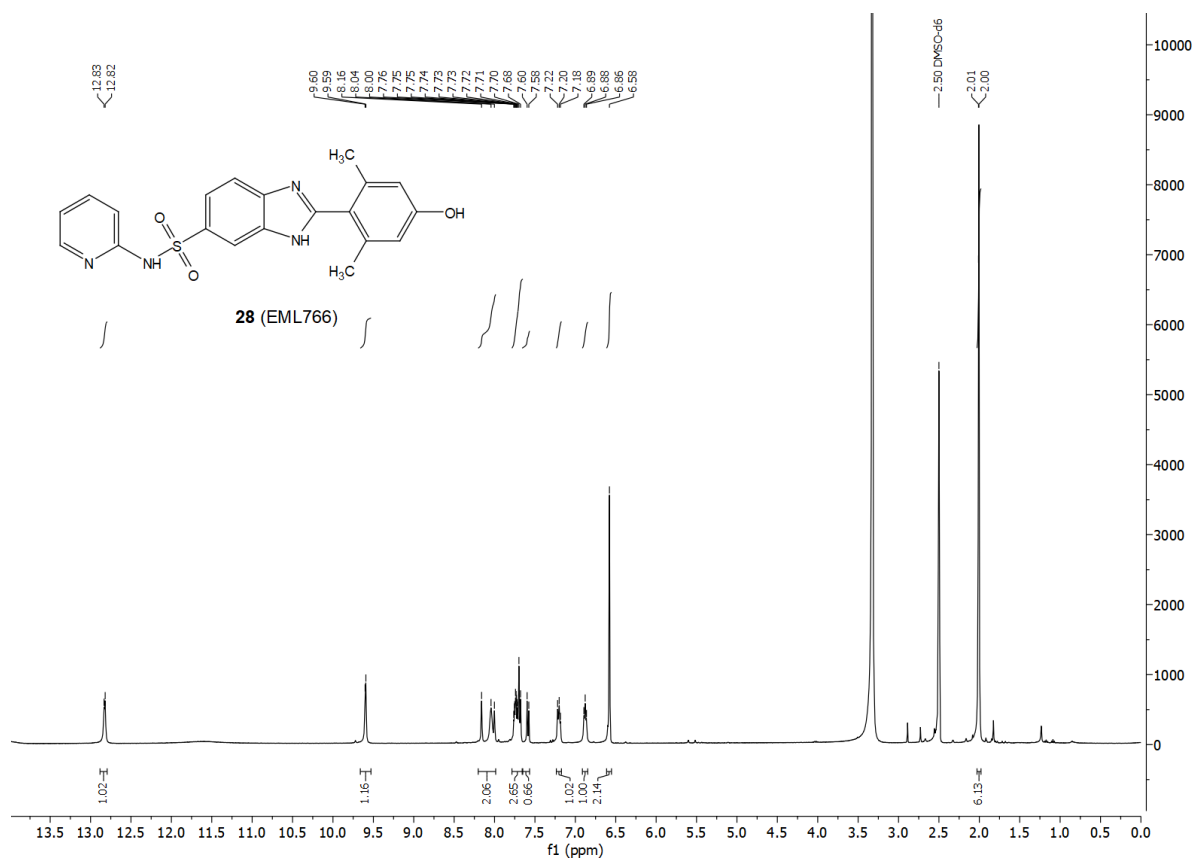


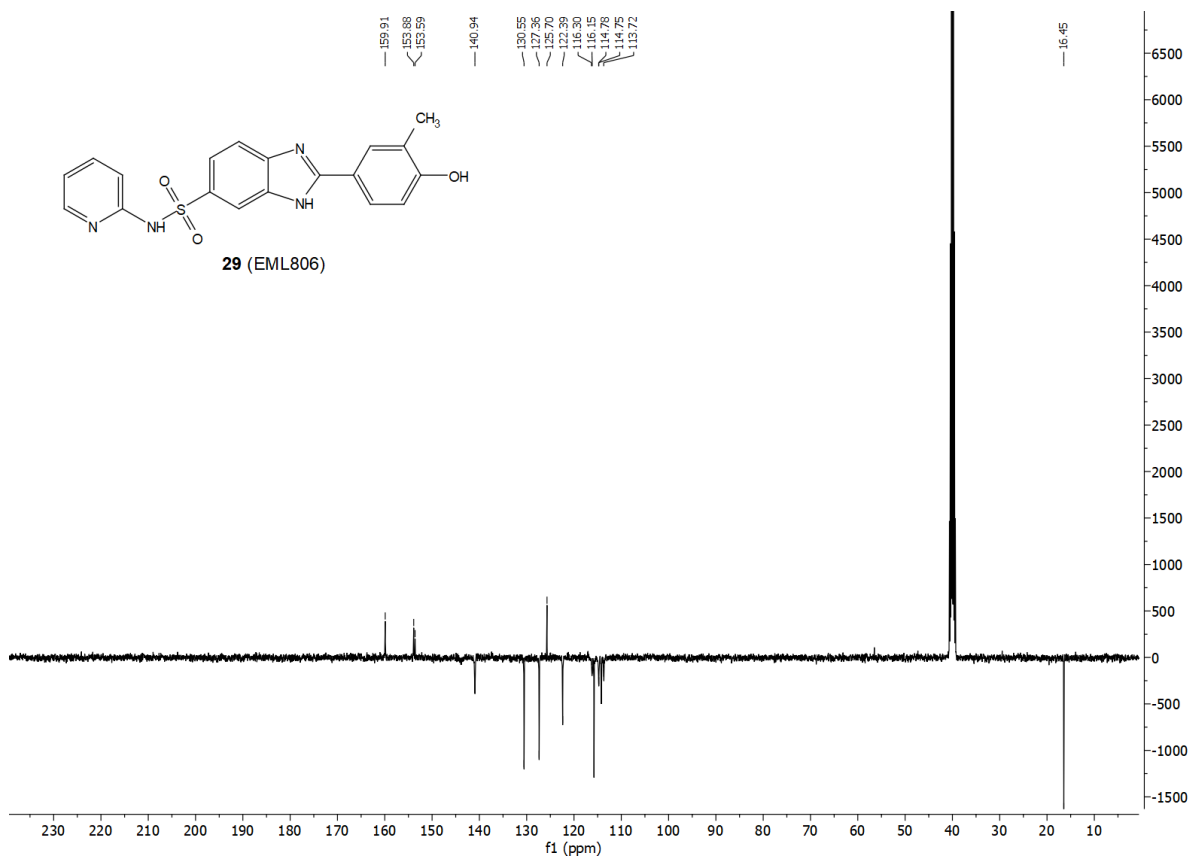
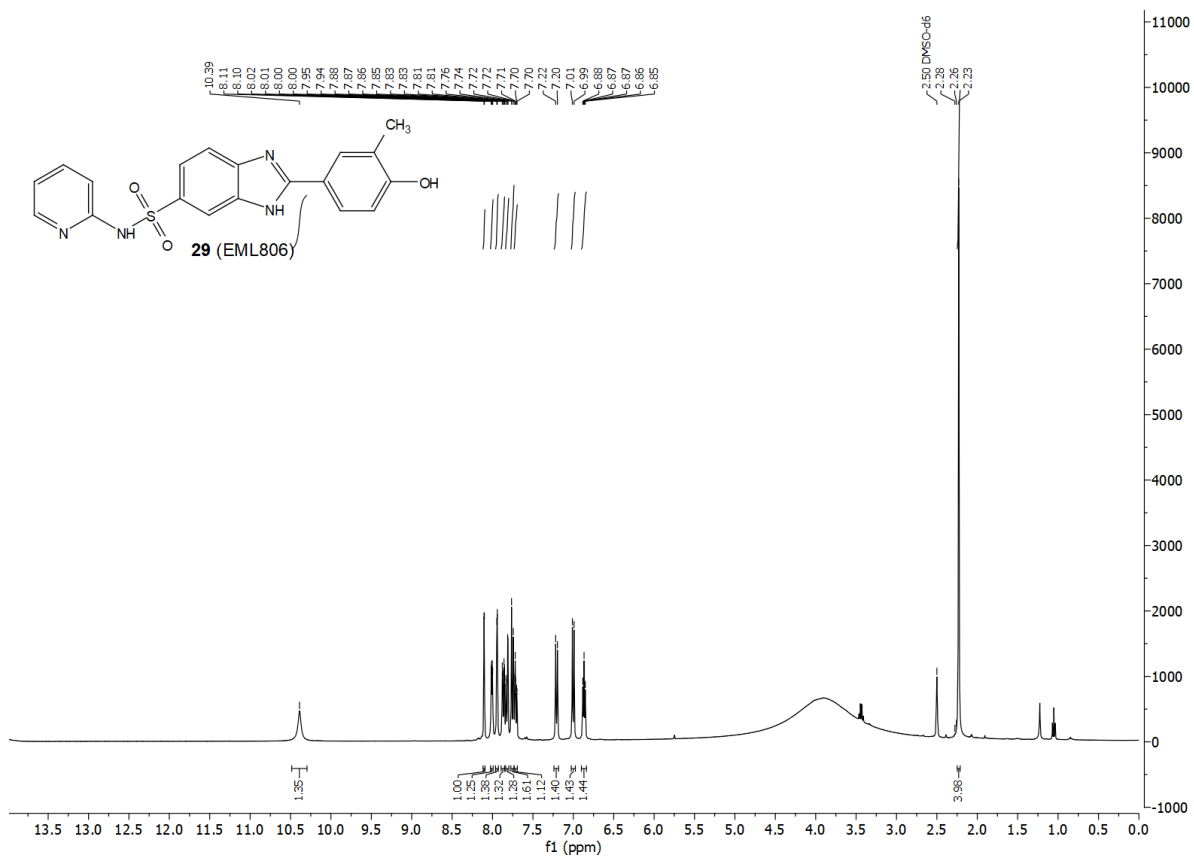


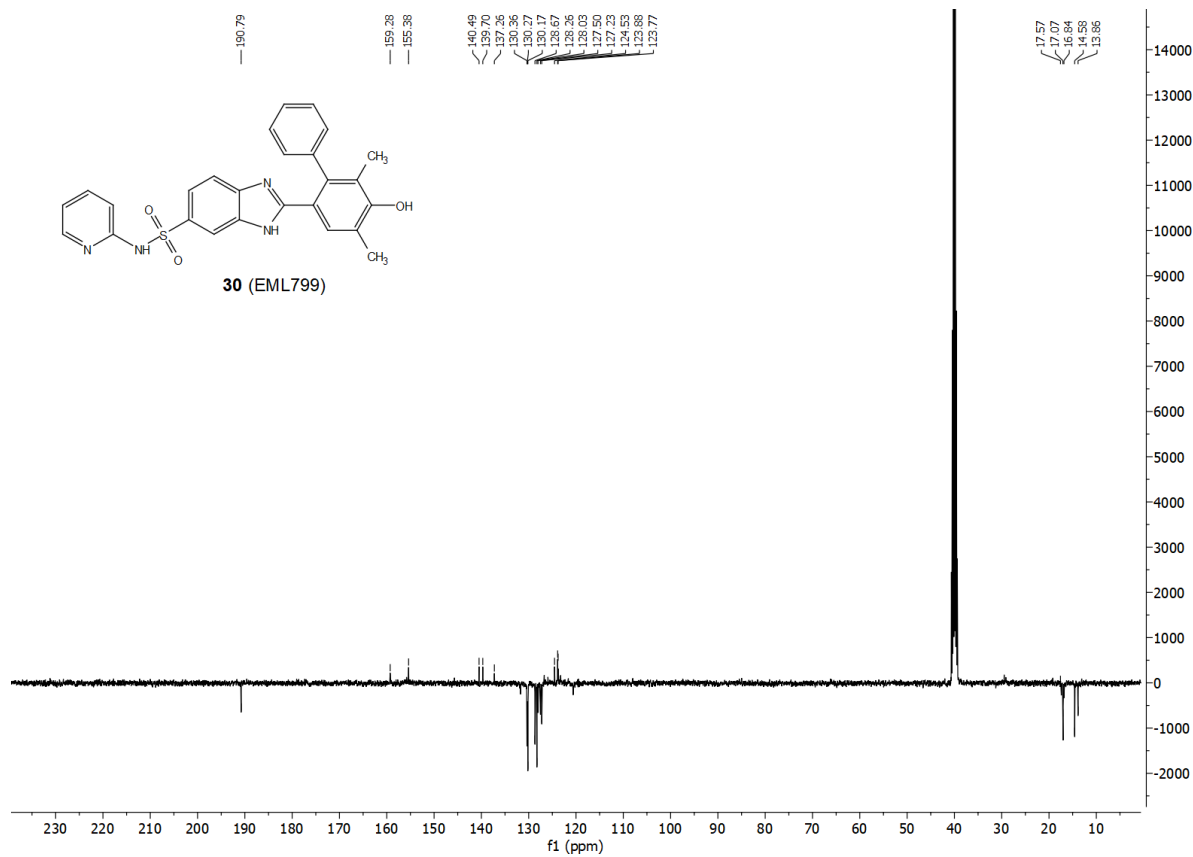
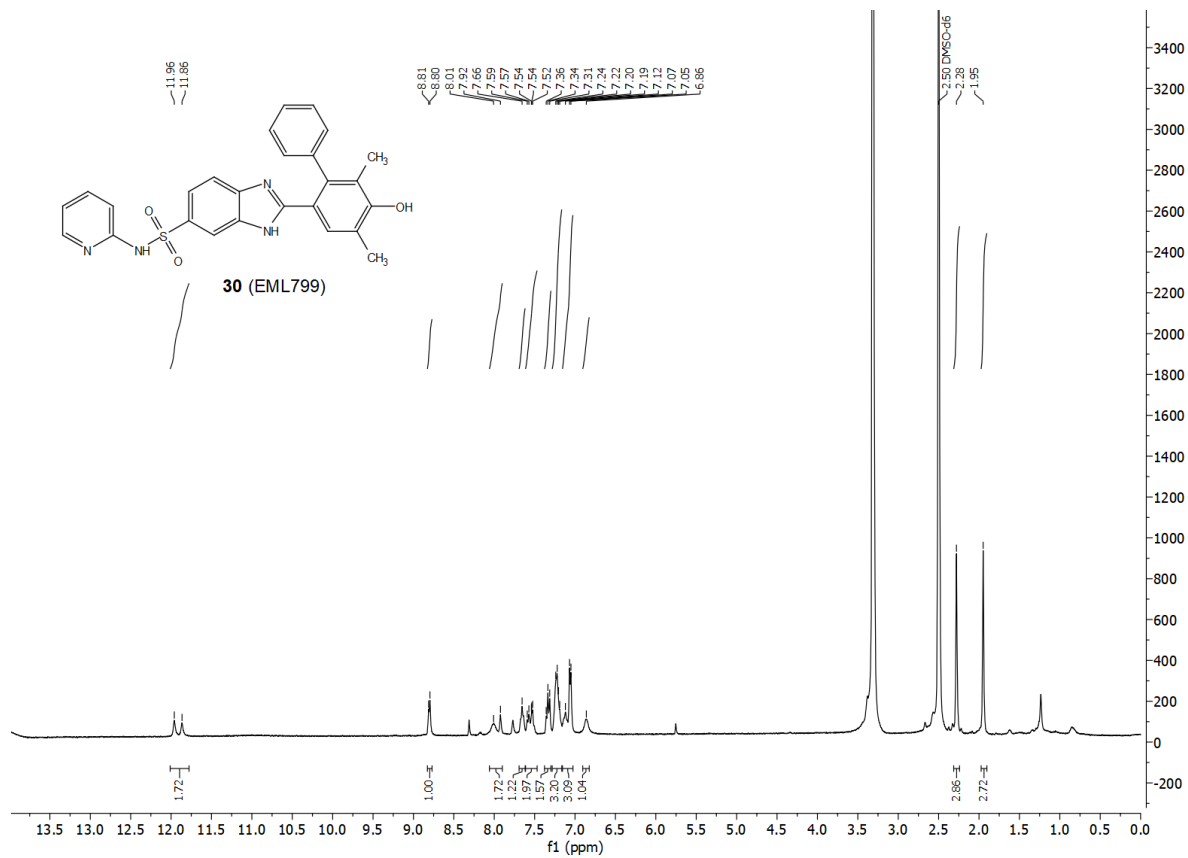


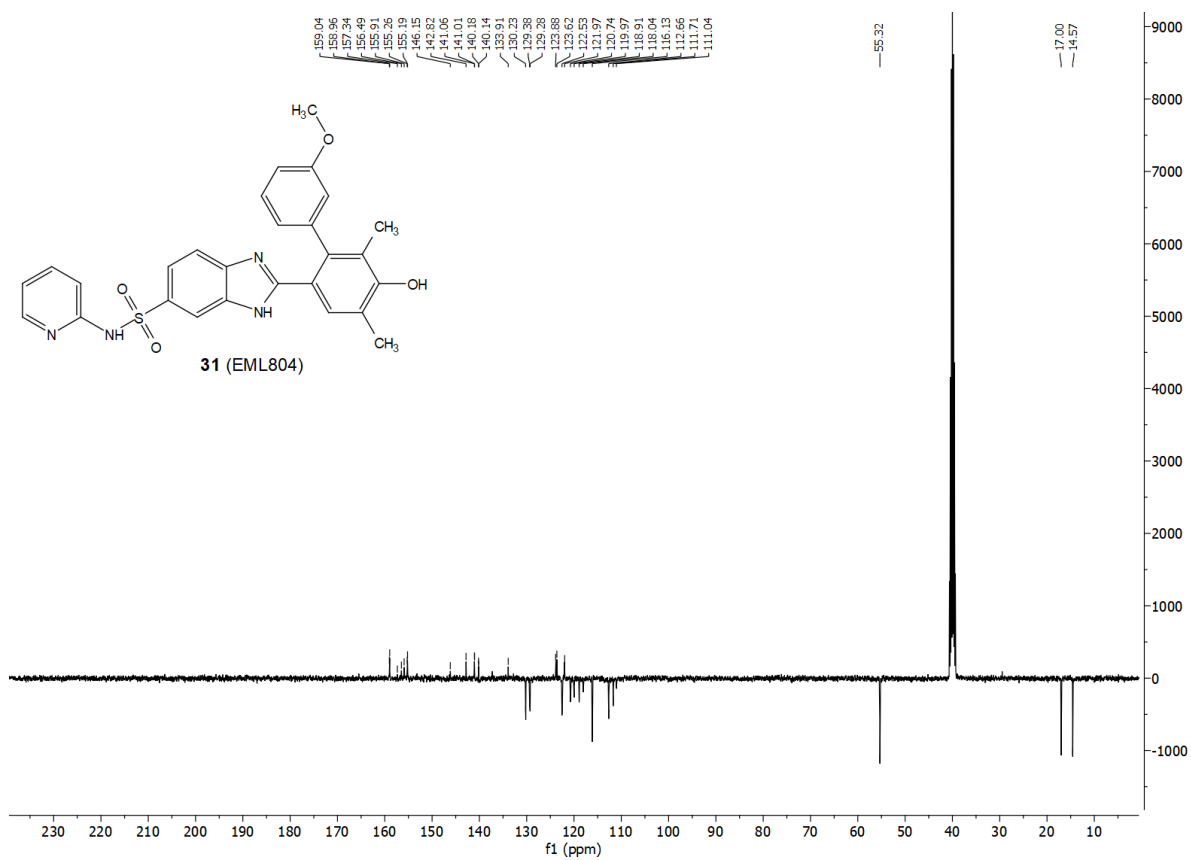
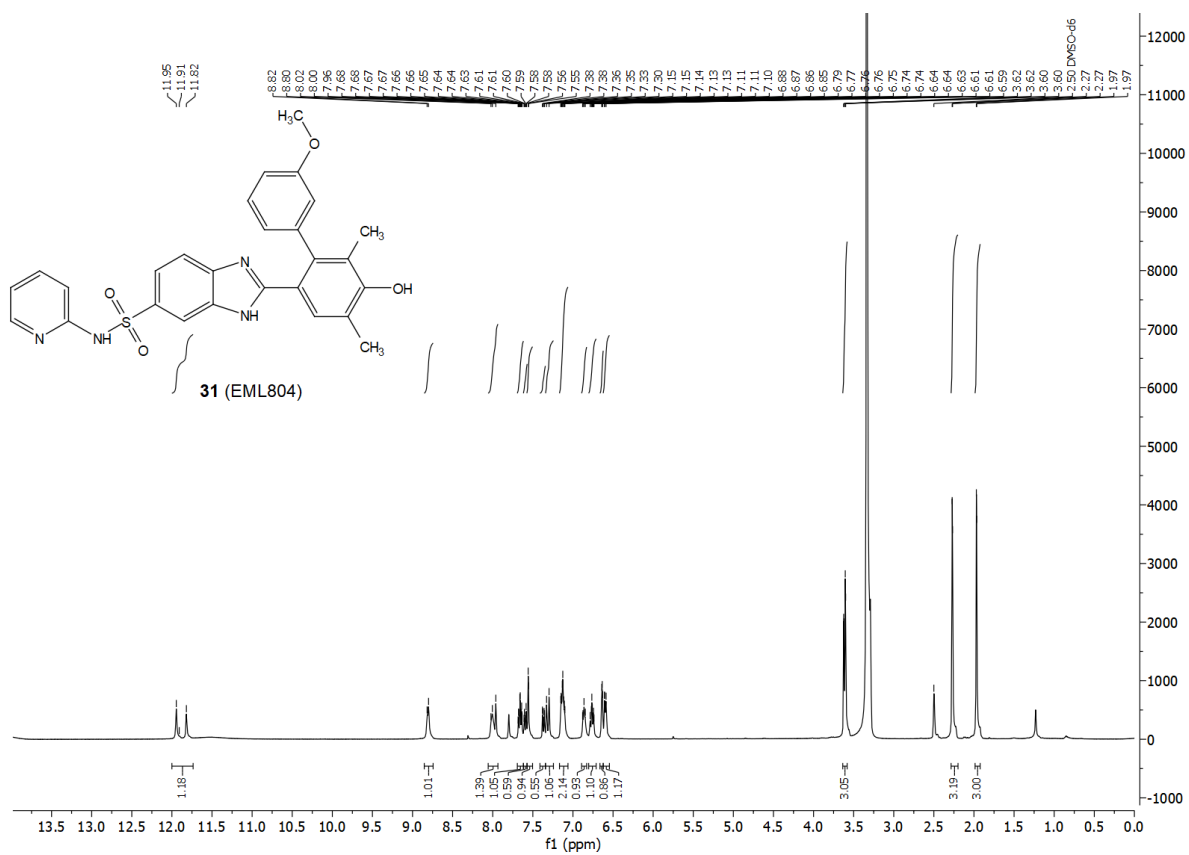


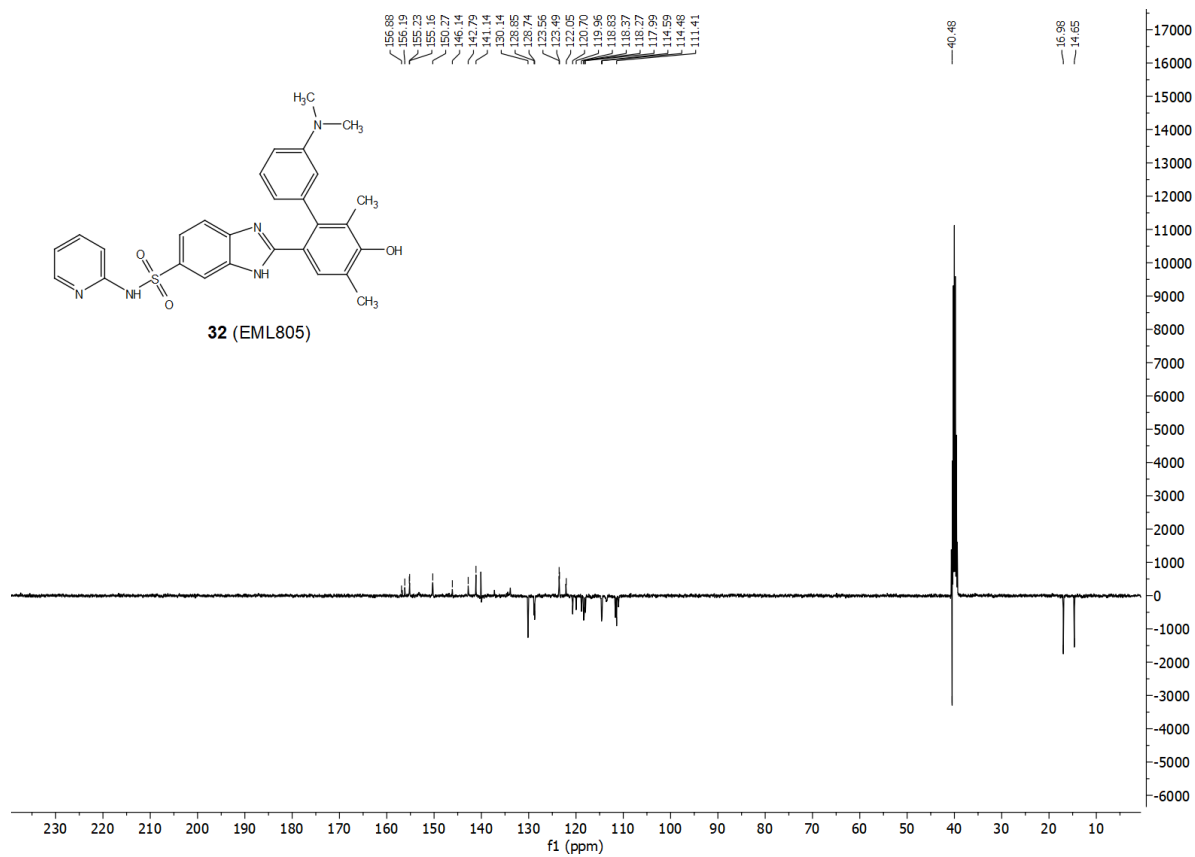
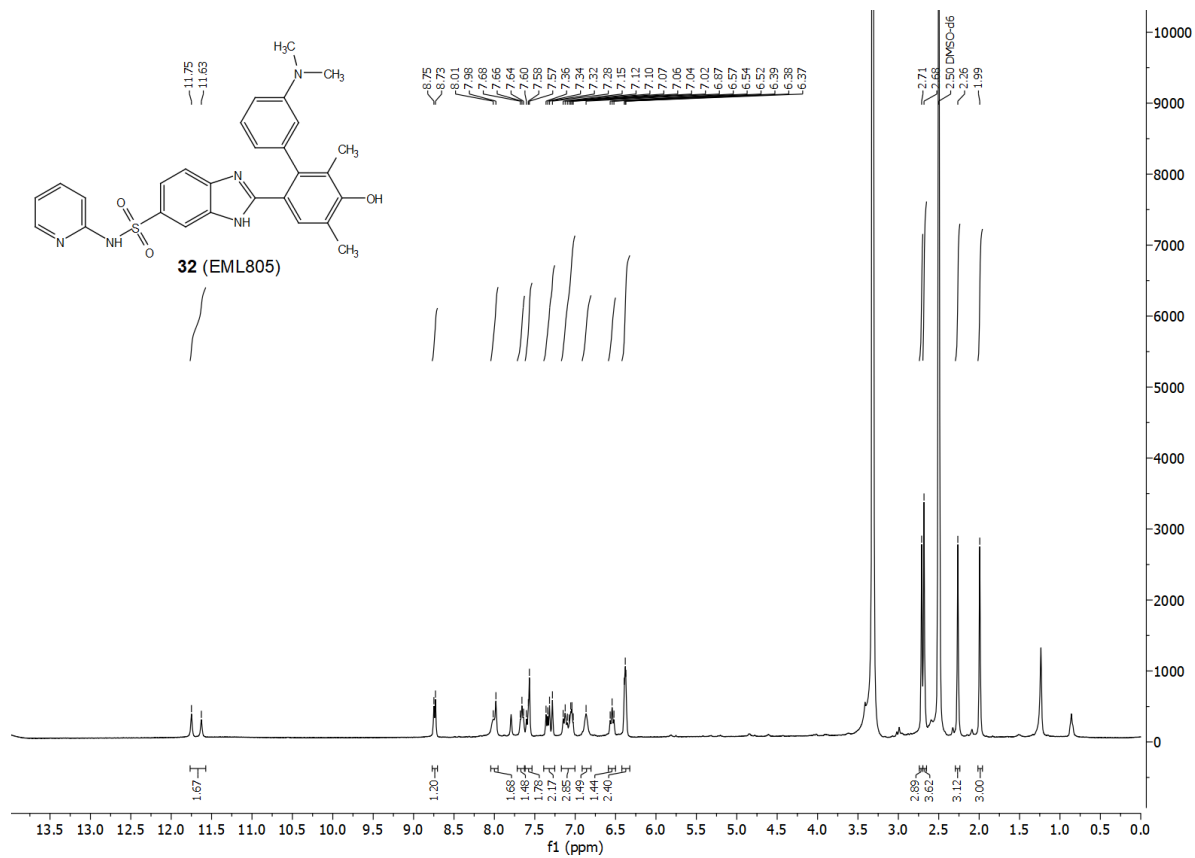


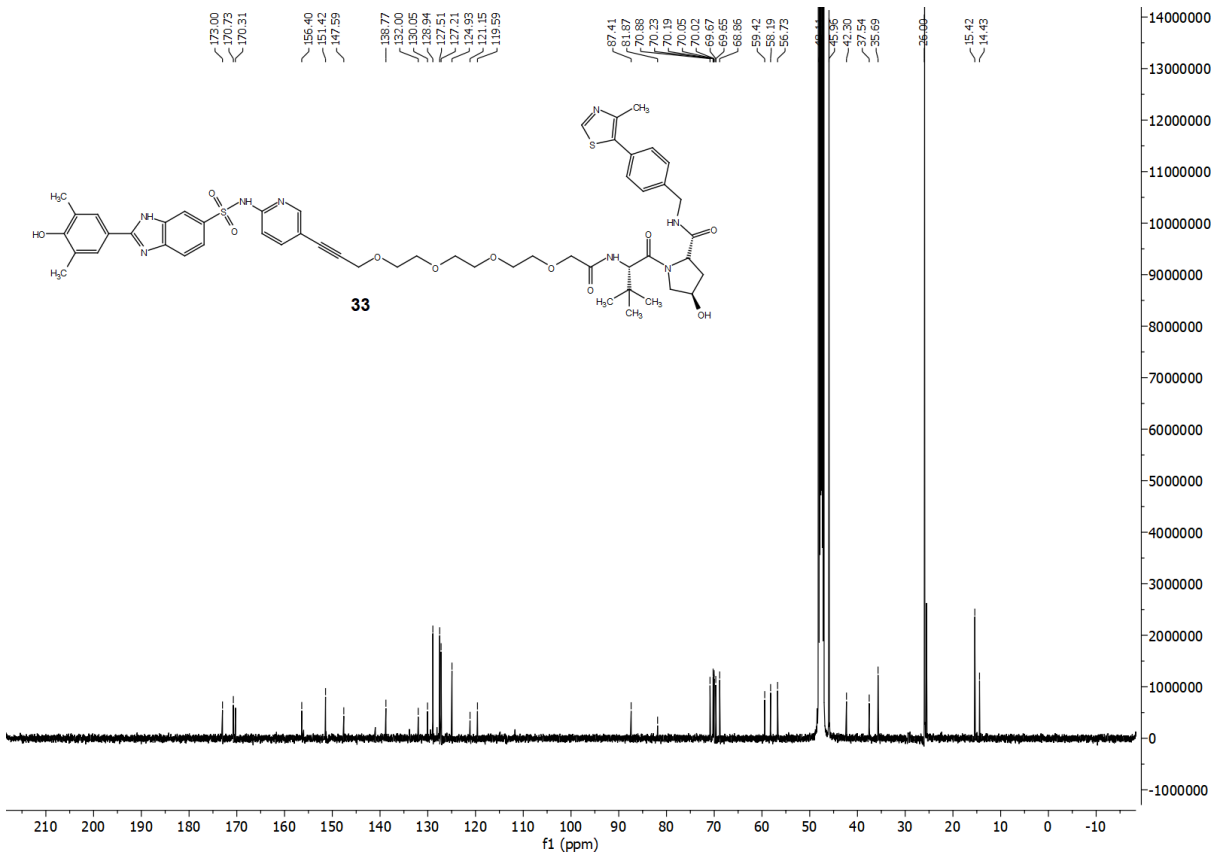
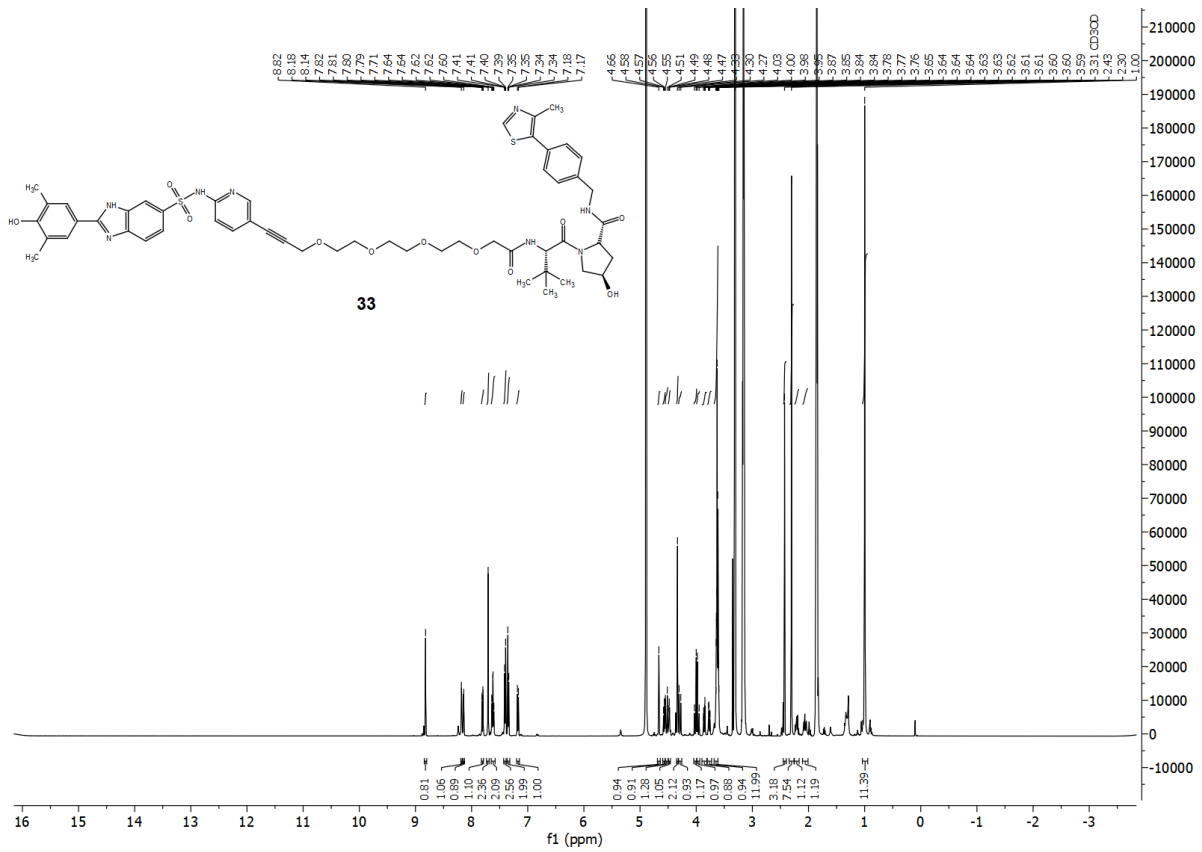


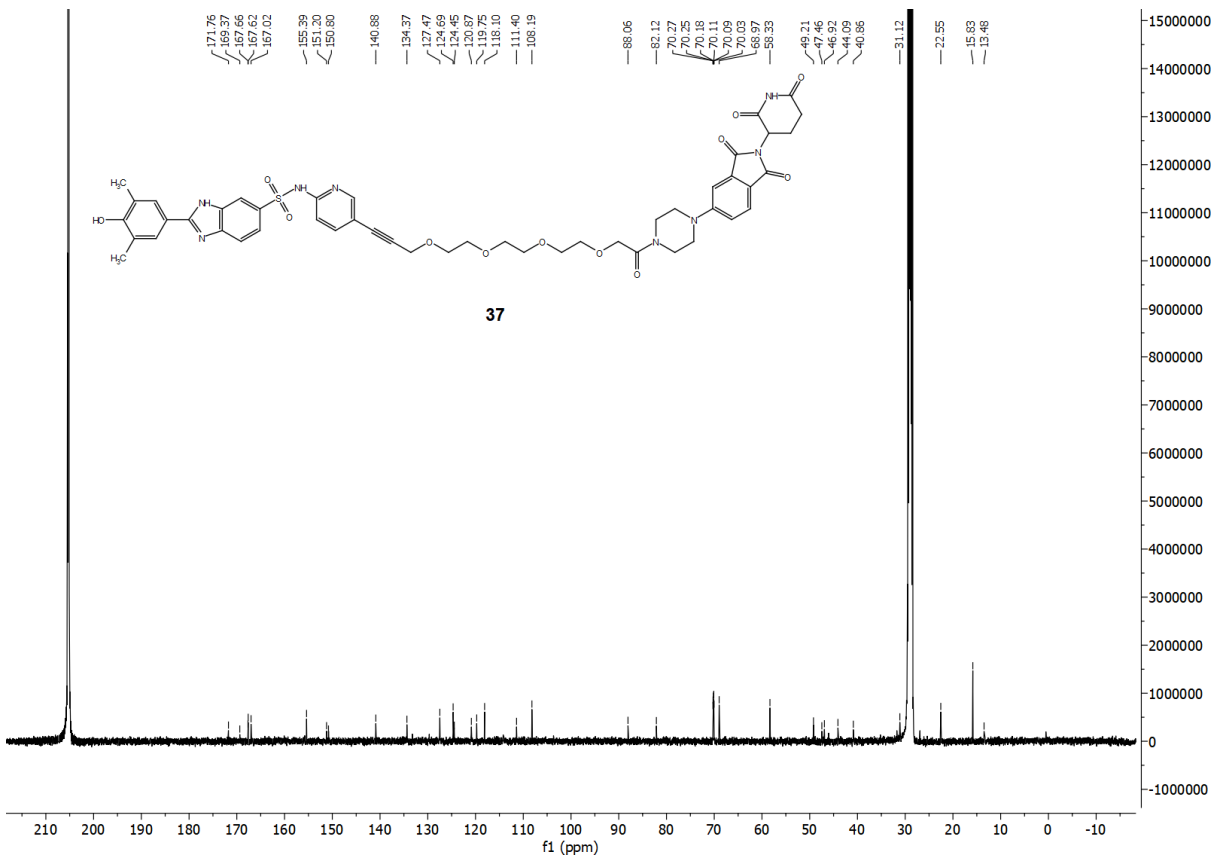
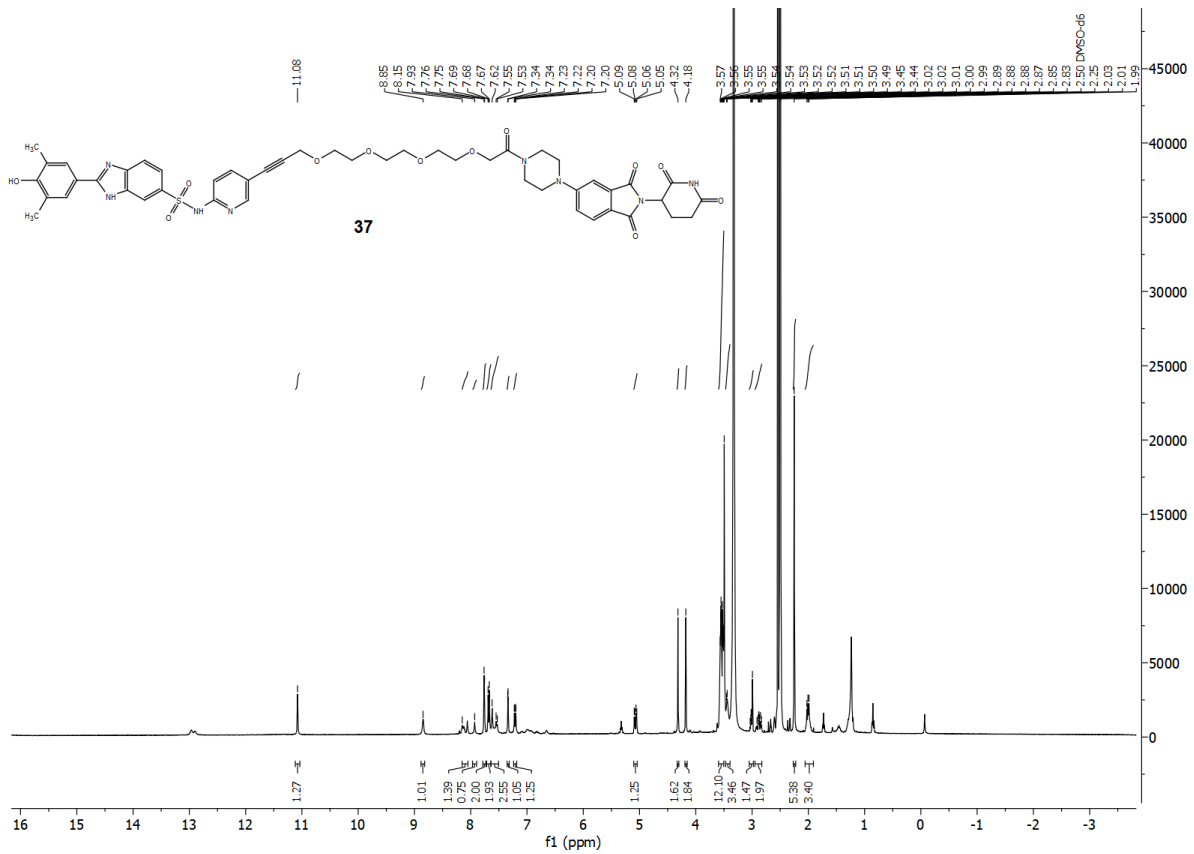


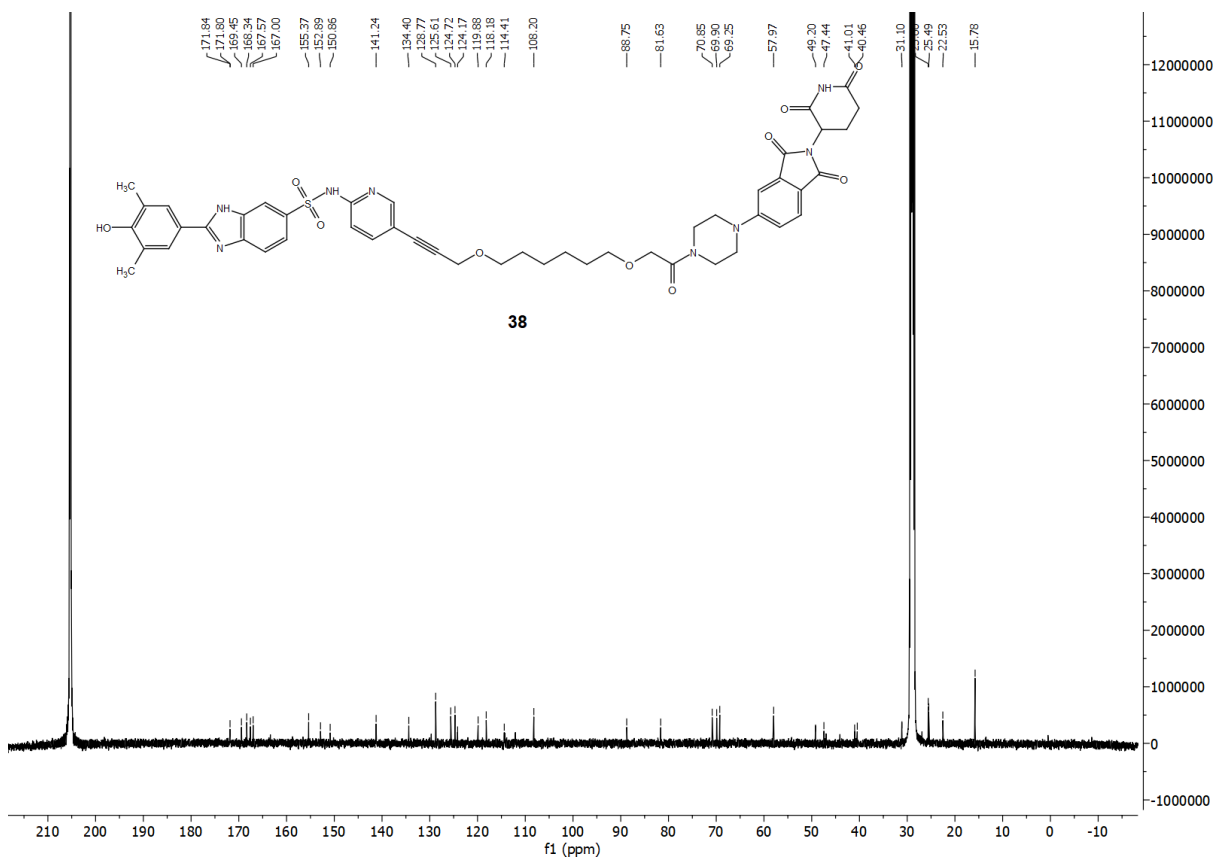
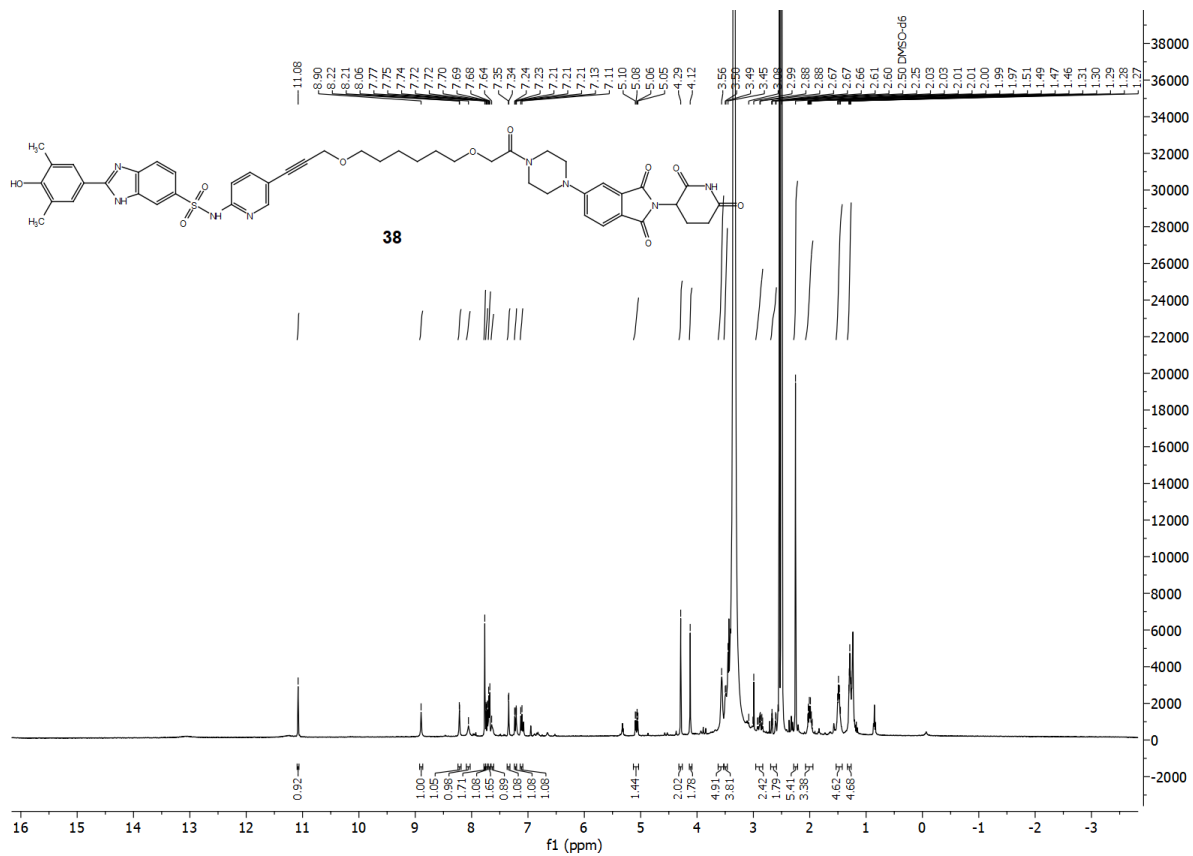


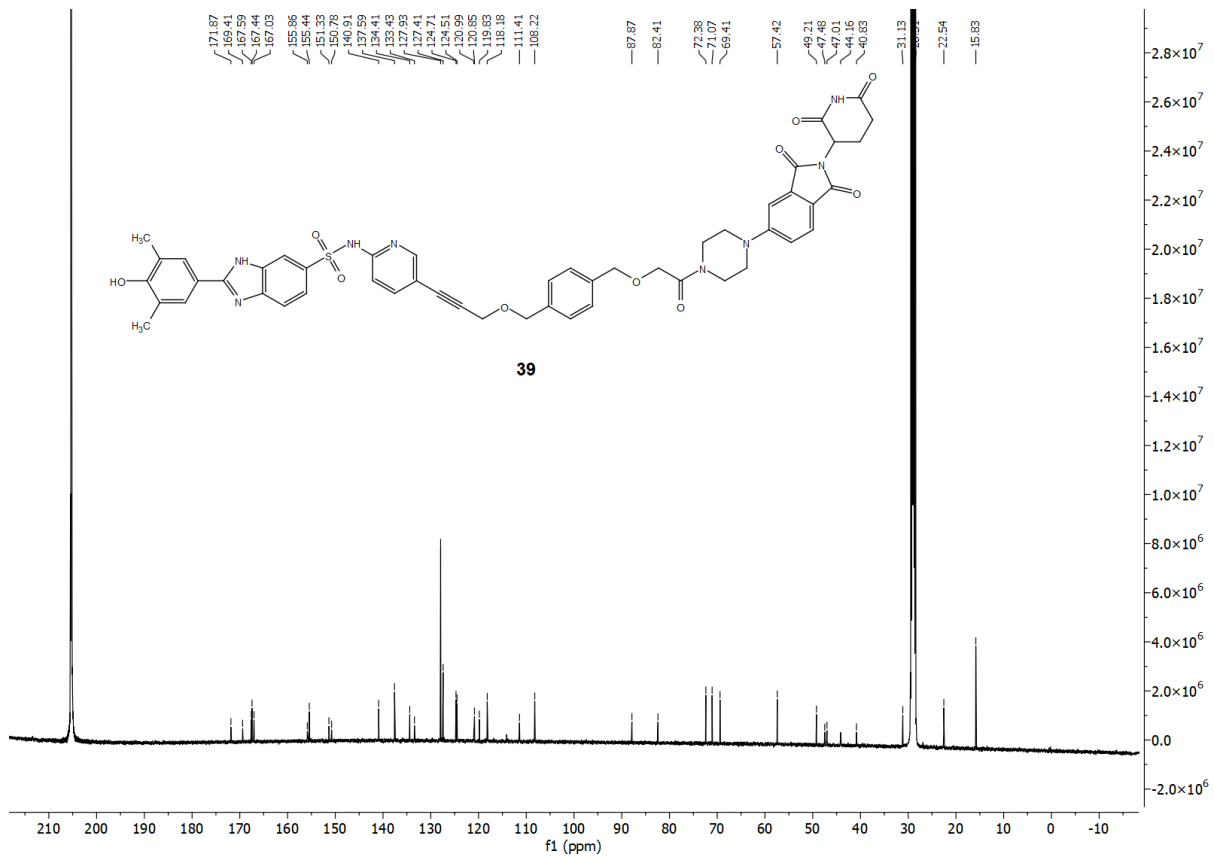
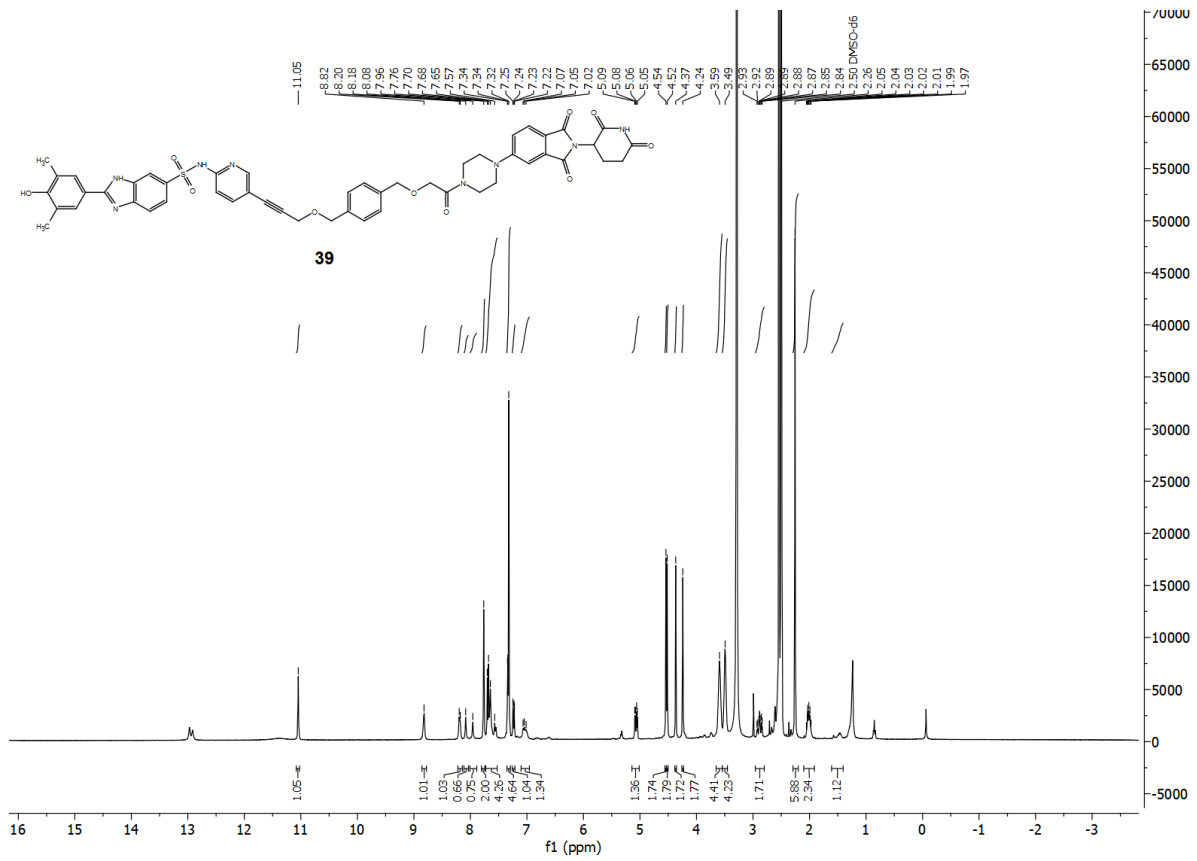


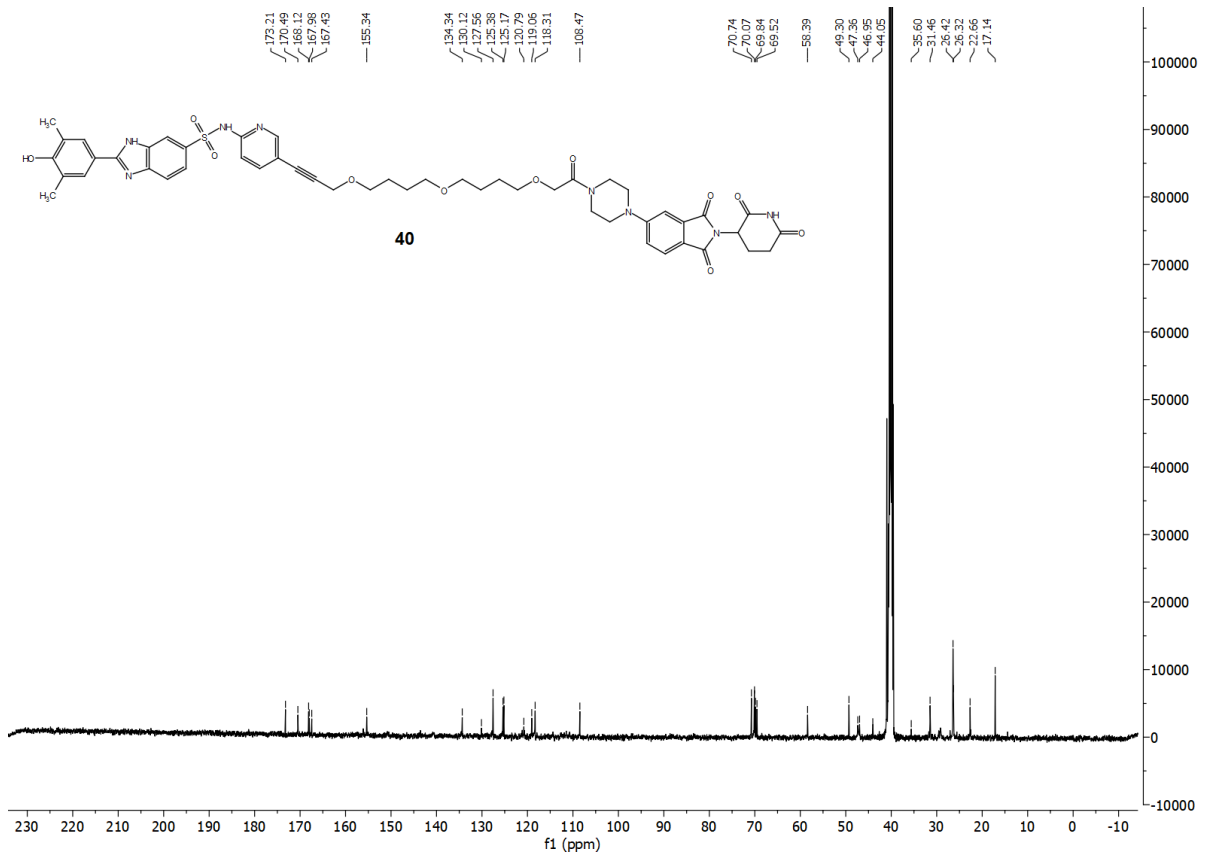
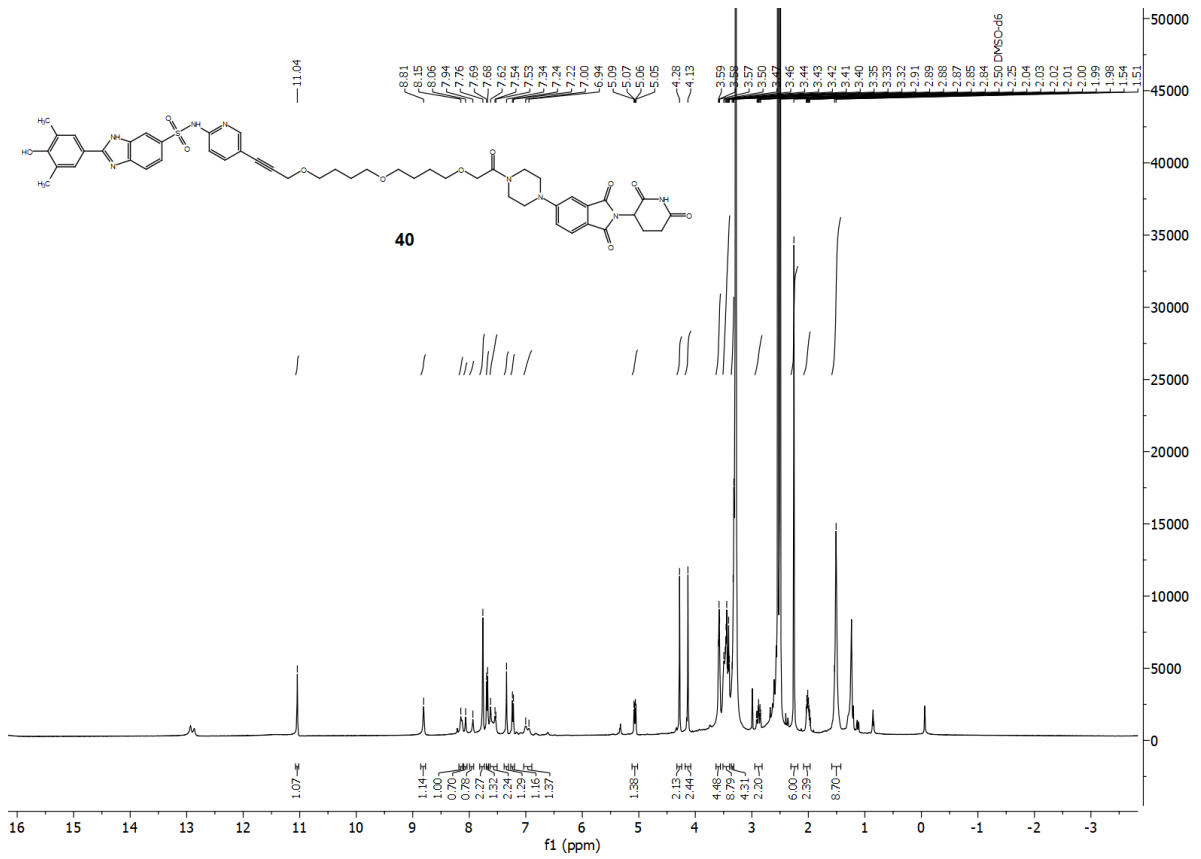


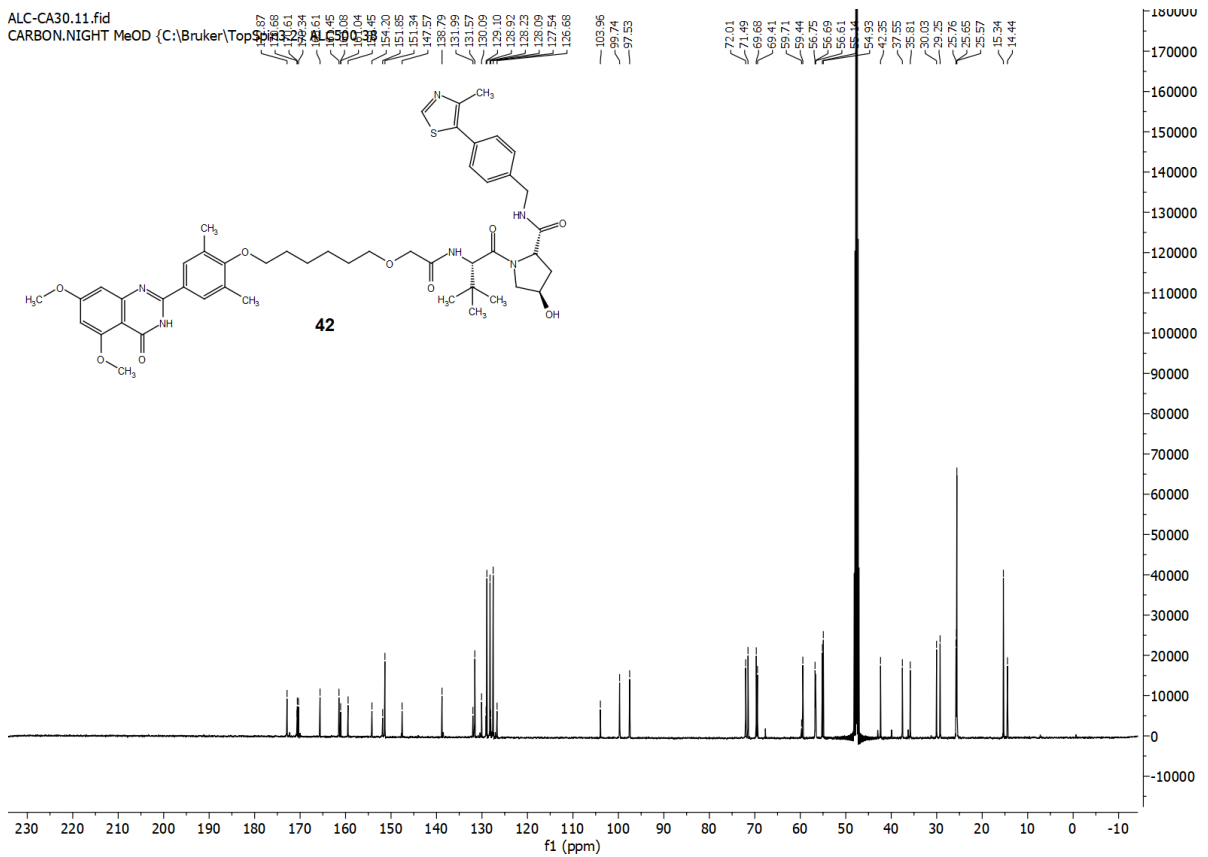
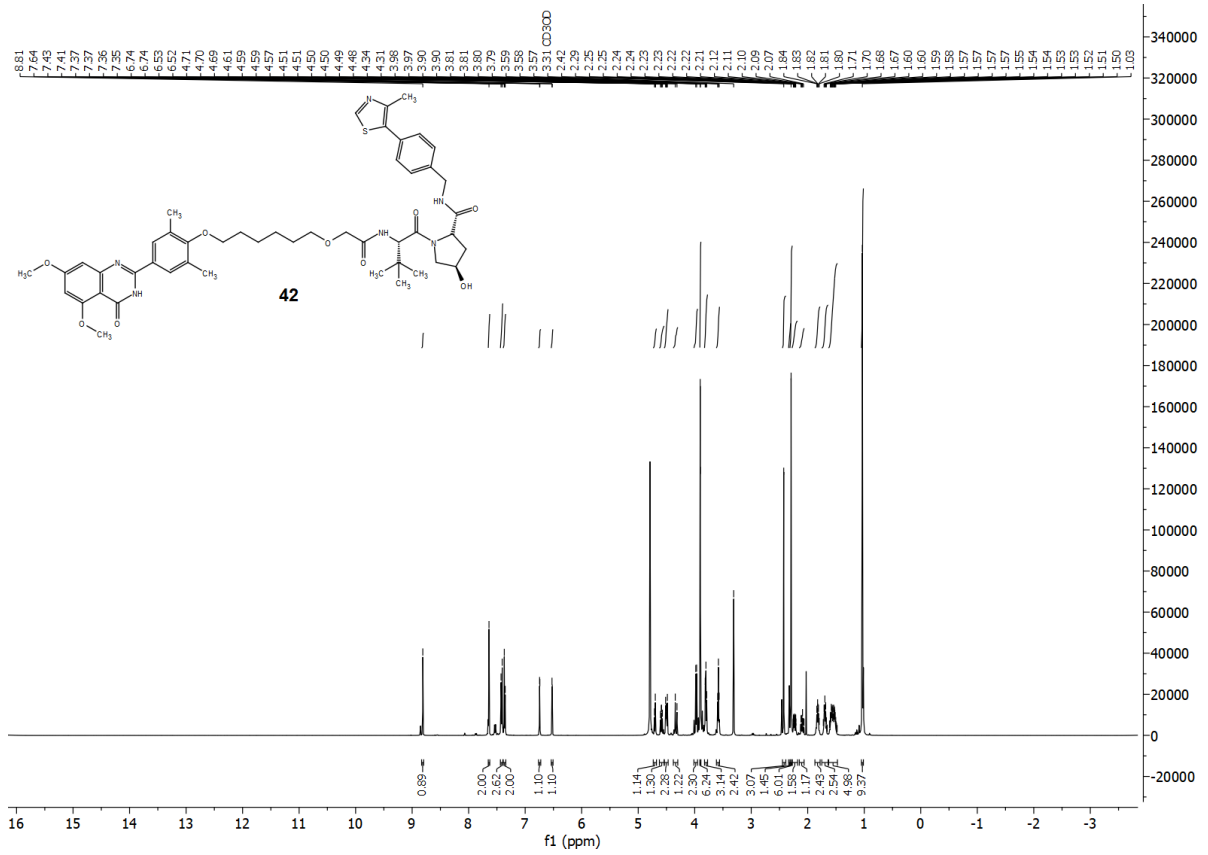


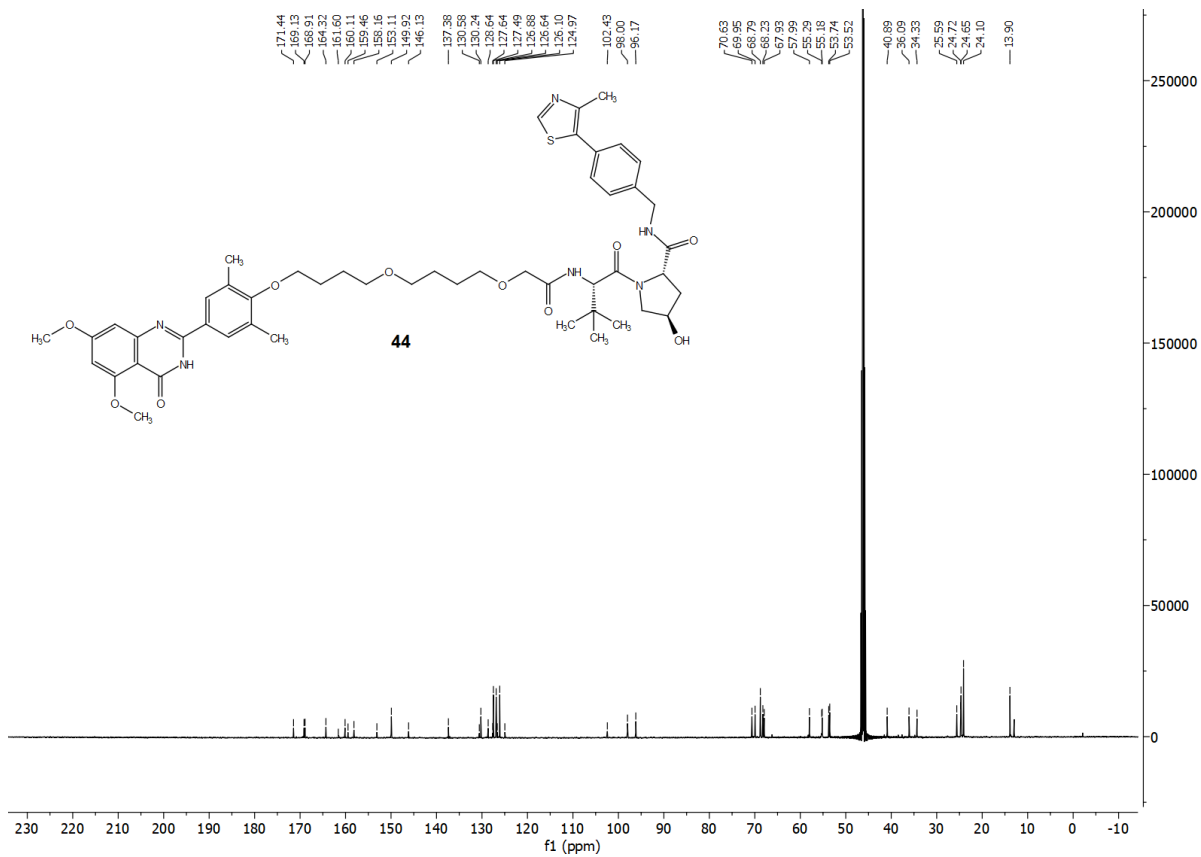
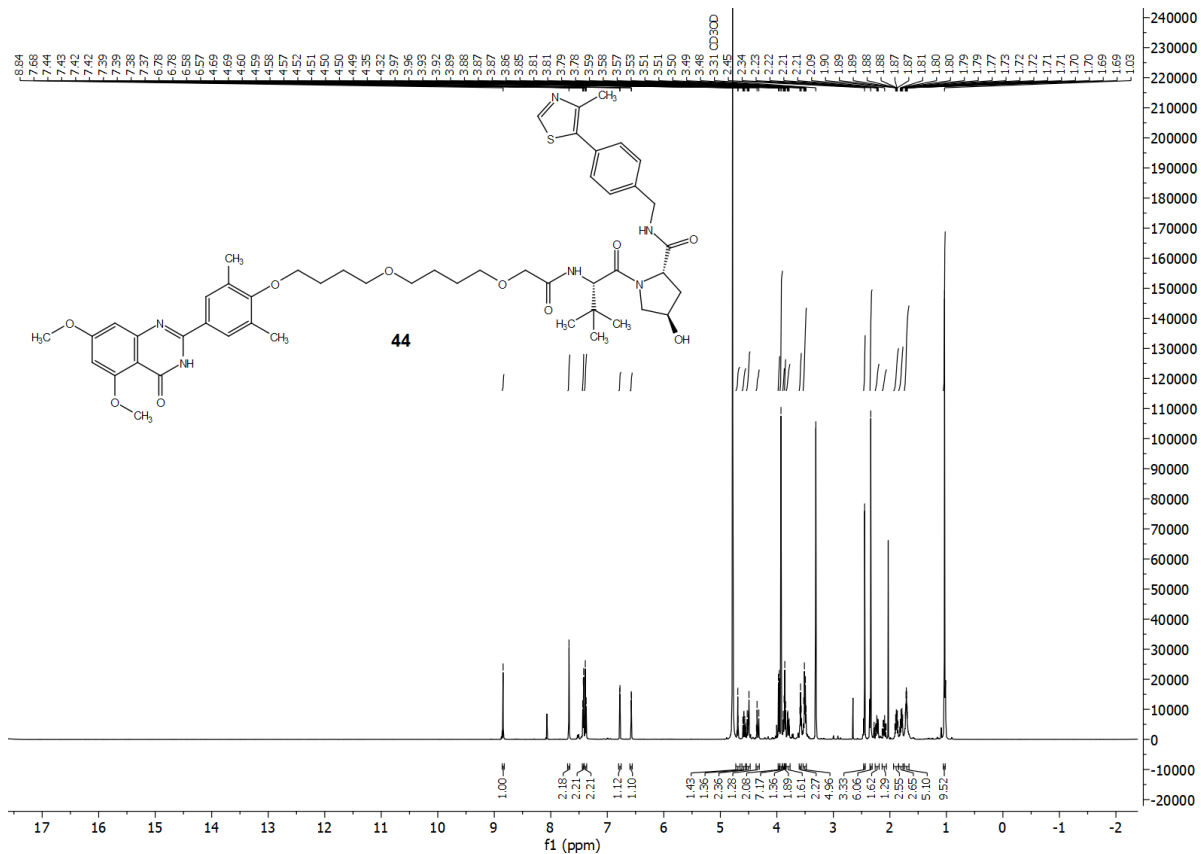


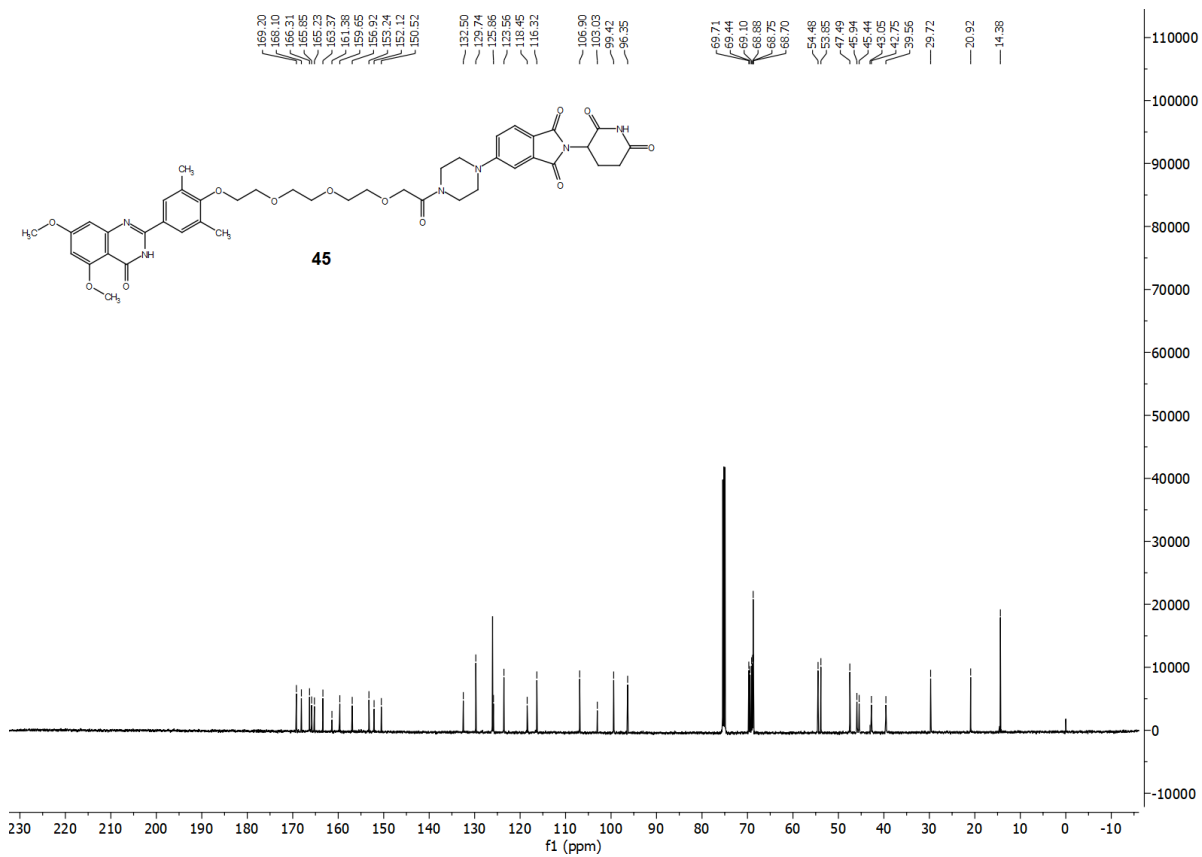
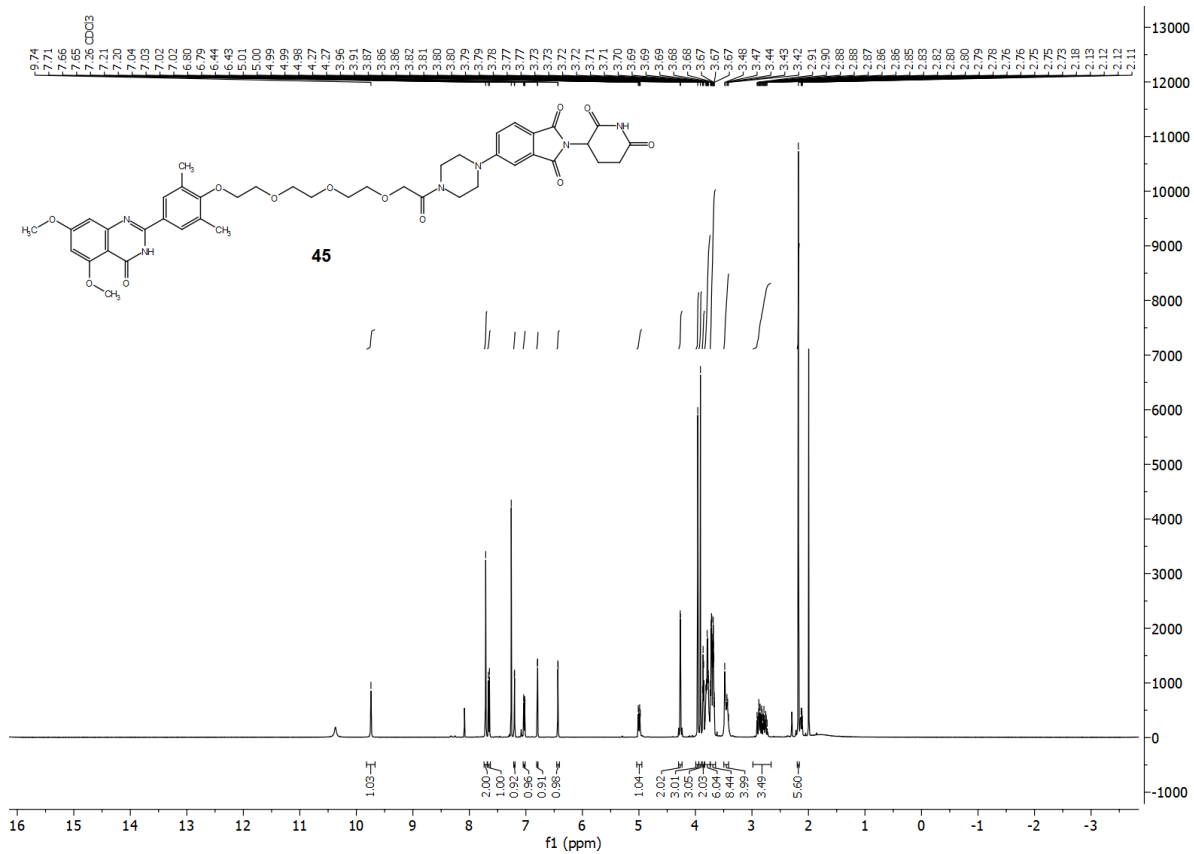


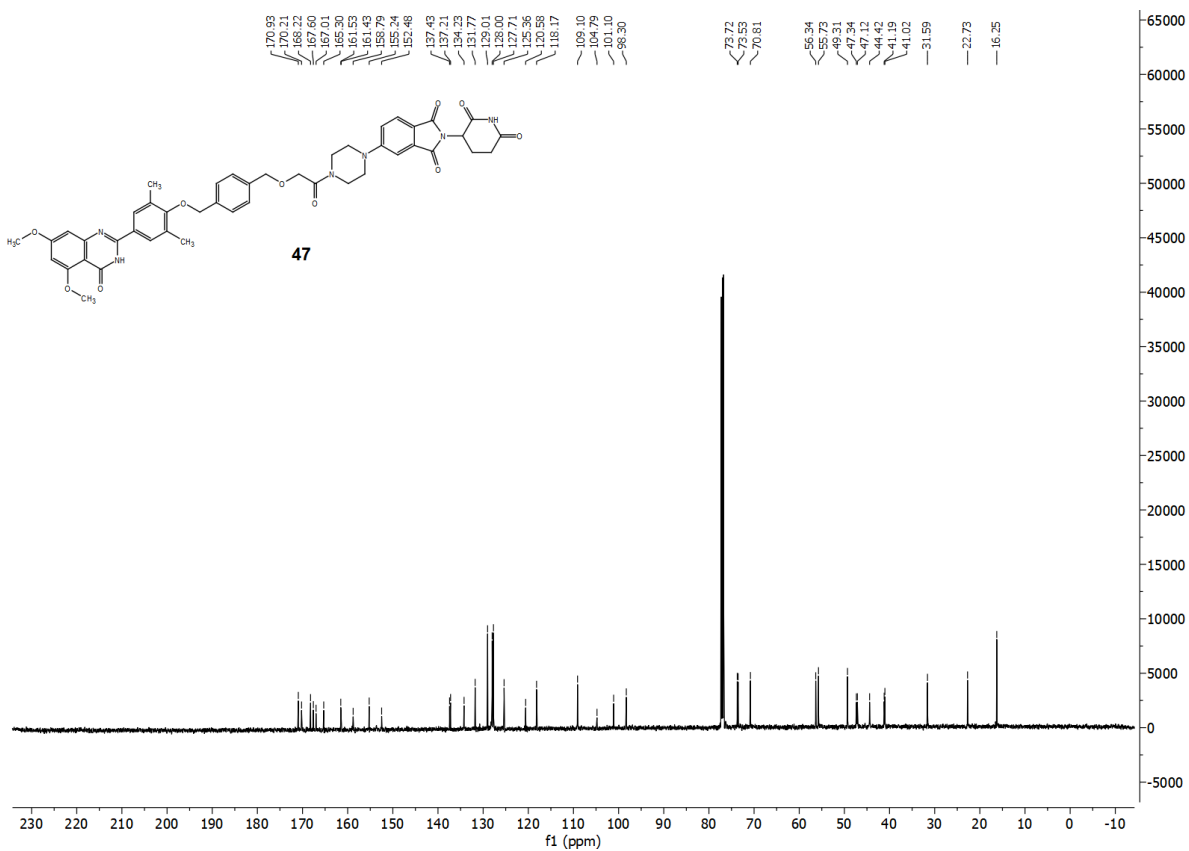
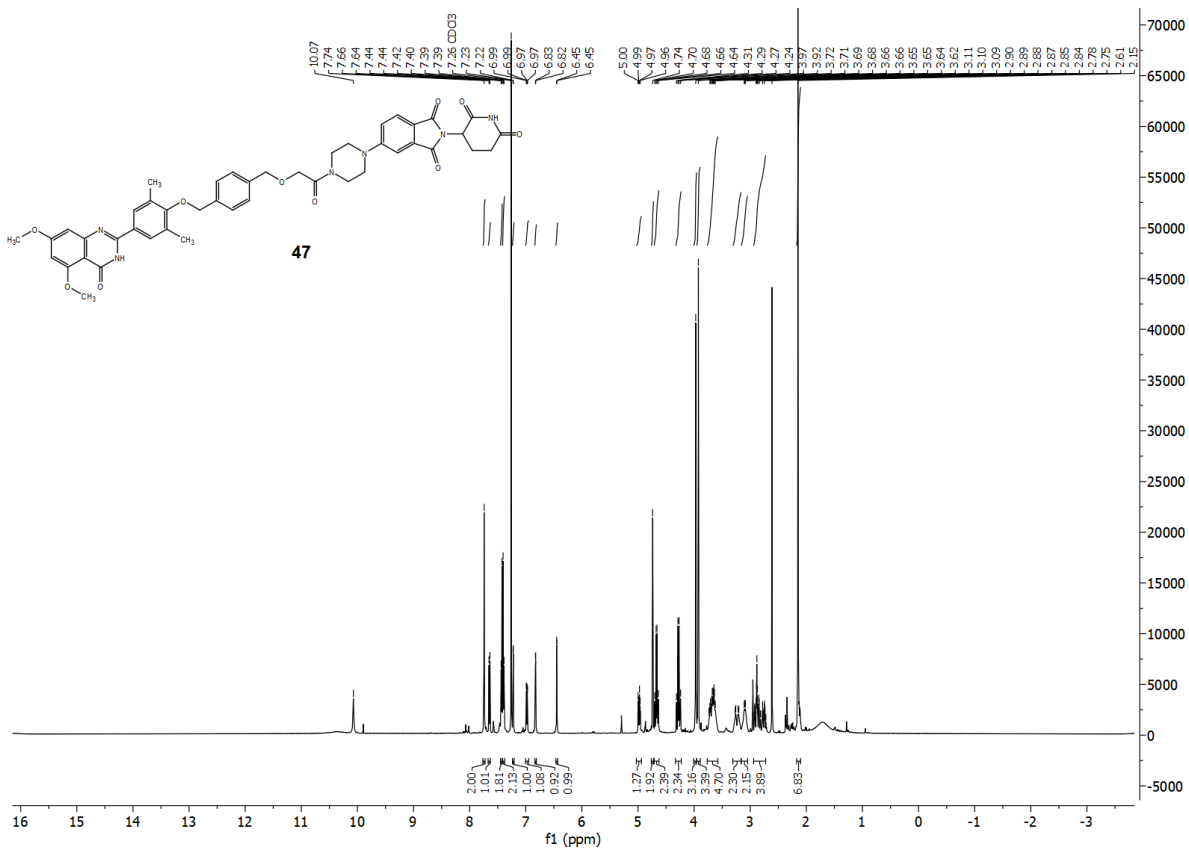












REFERENCES

1. Simo-Riudalbas, L.; Esteller, M.; Esteller, M.; Esteller, M., Targeting the histone orthography of cancer: drugs for writers, erasers and readers. *Br J Pharmacol* **2015**, *172* (11), 2716-32.
2. Williamson, A. K.; Zhu, Z.; Yuan, Z.-M., Epigenetic mechanisms behind cellular sensitivity to DNA damage. *Cell Stress* **2018**, *2* (7), 176-180.
3. Arrowsmith, C. H.; Bountra, C.; Fish, P. V.; Lee, K.; Schapira, M., Epigenetic protein families: a new frontier for drug discovery. *Nat Rev Drug Discov* **2012**, *11* (5), 384-400.
4. Sbardella, G., Histone acetyltransferases: targets and inhibitors. *Methods Princ. Med. Chem.* **2018**, *74* (Epigenetic Drug Discovery), 297-345.
5. Choudhary, C.; Weinert, B. T.; Nishida, Y.; Verdin, E.; Mann, M., The growing landscape of lysine acetylation links metabolism and cell signalling. *Nat Rev Mol Cell Biol* **2014**, *15* (8), 536-50.
6. Biswas, S.; Rao, C. M., Epigenetic tools (The Writers, The Readers and The Erasers) and their implications in cancer therapy. *Eur. J. Pharmacol.* **2018**, *837*, 8-24.
7. Di, M. M.; Del, B. D.; Triscioglio, D., The multifaceted role of lysine acetylation in cancer: prognostic biomarker and therapeutic target. *Oncotarget* **2016**, *7* (34), 55789-55810.
8. Timmermann, S.; Lehrmann, H.; Polesskaya, A.; Harel-Bellan, A., Histone acetylation and disease. *Cell Mol Life Sci* **2001**, *58* (5-6), 728-36.
9. Iyer, N. G.; Ozdag, H.; Caldas, C., p300/CBP and cancer. *Oncogene* **2004**, *23* (24), 4225-31.
10. Valor, L. M.; Viosca, J.; Lopez-Atalaya, J. P.; Barco, A., Lysine Acetyltransferases CBP and p300 as Therapeutic Targets in Cognitive and Neurodegenerative Disorders. *Curr. Pharm. Des.* **2013**, *19* (28), 5051-5064.

11. Lu, X.; Deng, Y.; Yu, D.; Cao, H.; Wang, L.; Liu, L.; Yu, C.; Zhang, Y.; Guo, X.; Yu, G., Histone acetyltransferase p300 mediates histone acetylation of PS1 and BACE1 in a cellular model of Alzheimer's disease. *PLoS One* **2014**, *9* (7), e103067/1-e103067/9, 9 pp.
12. Park, S.-Y.; Kim, M.-J.; Kim, Y. J.; Lee, Y.-H.; Bae, D.; Kim, S.; Na, Y.; Yoon, H.-G., Selective PCAF inhibitor ameliorates cognitive and behavioral deficits by suppressing NF- κ B-mediated neuroinflammation induced by A β in a model of Alzheimer's disease. *Int. J. Mol. Med.* **2015**, *35* (4), 1109-1118.
13. Dancy, B. M.; Cole, P. A., Protein Lysine Acetylation by p300/CBP. *Chem. Rev. (Washington, DC, U. S.)* **2015**, *115* (6), 2419-2452.
14. Seto, E.; Yoshida, M., Erasers of histone acetylation: the histone deacetylase enzymes. *Cold Spring Harbor Perspect. Biol.* **2014**, *6* (4), 1-27.
15. Falkenberg, K. J.; Johnstone, R. W., Histone deacetylases and their inhibitors in cancer, neurological diseases and immune disorders. *Nat. Rev. Drug Discovery* **2015**.
16. Suraweera, A.; O'Byrne, K. J.; Richard, D. J.; O'Byrne, K. J., Combination Therapy With Histone Deacetylase Inhibitors (HDACi) for the Treatment of Cancer: Achieving the Full Therapeutic Potential of HDACi. *Front Oncol* **2018**, *8*, 92.
17. Ferri, E.; Petosa, C.; McKenna, C. E., Bromodomains: Structure, function and pharmacology of inhibition. *Biochem. Pharmacol. (Amsterdam, Neth.)* **2016**, *106*, 1-18.
18. Smith, S. G.; Zhou, M.-M., The Bromodomain: A New Target in Emerging Epigenetic Medicine. *ACS Chem. Biol.* **2016**, *11* (3), 598-608.
19. Cochran, A. G.; Conery, A. R.; Sims, I. I. R. J., Bromodomains: a new target class for drug development. *Nat. Rev. Drug Discovery* **2019**, *18* (8), 609-628.
20. Filippakopoulos, P.; Picaud, S.; Mangos, M.; Keates, T.; Lambert, J.-P.; Barsyte-Lovejoy, D.; Felletar, I.; Volkmer, R.; Muller, S.; Pawson, T.; Gingras, A.-C.; Arrowsmith, C.

H.; Knapp, S., Histone Recognition and Large-Scale Structural Analysis of the Human Bromodomain Family. *Cell (Cambridge, MA, U. S.)* **2012**, *149* (1), 214-231.

21. Filippakopoulos, P.; Knapp, S., The bromodomain interaction module. *FEBS Lett.* **2012**, *586* (17), 2692-2704.

22. Zaware, N.; Zhou, M.-M., Bromodomain biology and drug discovery. *Nat. Struct. Mol. Biol.* **2019**, *26* (10), 870-879.

23. Fujisawa, T.; Filippakopoulos, P., Functions of bromodomain-containing proteins and their roles in homeostasis and cancer. *Nat. Rev. Mol. Cell Biol.* **2017**, *18* (4), 246-262.

24. Jin, L.; Garcia, J.; Chan, E.; de la Cruz, C.; Segal, E.; Merchant, M.; Kharbanda, S.; Raisner, R.; Haverty, P. M.; Modrusan, Z.; Ly, J.; Choo, E.; Kaufman, S.; Beresini, M. H.; Romero, F. A.; Magnuson, S.; Gascoigne, K. E., Therapeutic Targeting of the CBP/p300 Bromodomain Blocks the Growth of Castration-Resistant Prostate Cancer. *Cancer Res.* **2017**, *77* (20), 5564-5575.

25. Conery, A. R.; Centore, R. C.; Neiss, A.; Keller, P. J.; Joshi, S.; Spillane, K. L.; Sandy, P.; Hatton, C.; Pardo, E.; Zawadzke, L.; Bommi-Reddy, A.; Gascoigne, K. E.; Bryant, B. M.; Mertz, J. A.; Sims, R. J., Correction: Bromodomain inhibition of the transcriptional coactivators CBP/EP300 as a therapeutic strategy to target the IRF4 network in multiple myeloma. *Elife* **2016**, *5*.

26. Hay, D. A.; Fedorov, O.; Martin, S.; Singleton, D. C.; Tallant, C.; Wells, C.; Picaud, S.; Philpott, M.; Monteiro, O. P.; Rogers, C. M.; Conway, S. J.; Rooney, T. P. C.; Tumber, A.; Yapp, C.; Filippakopoulos, P.; Bunnage, M. E.; Muller, S.; Knapp, S.; Schofield, C. J.; Brennan, P. E., Discovery and Optimization of Small-Molecule Ligands for the CBP/p300 Bromodomains. *J. Am. Chem. Soc.* **2014**, *136* (26), 9308-9319.

27. Hammitzsch, A.; Tallant, C.; Fedorov, O.; O'Mahony, A.; Brennan, P. E.; Hay, D. A.; Martinez, F. O.; Al-Mossawi, M. H.; de Wit, J.; Vecellio, M.; Wells, C.; Wordsworth, P.; Muller, S.; Knapp, S.; Bowness, P., CBP30, a selective CBP/p300 bromodomain inhibitor, suppresses human Th17 responses. *Proc. Natl. Acad. Sci. U. S. A.* **2015**, *112* (34), 10768-10773.

28. Zucconi, B. E.; Makofske, J. L.; Meyers, D. J.; Hwang, Y.; Wu, M.; Kuroda, M. I.; Cole, P. A., Combination targeting of the bromodomain and acetyltransferase active site of p300/CBP. *Biochemistry* **2019**, *58* (16), 2133-2143.
29. Crawford, T. D.; Romero, F. A.; Lai, K. W.; Tsui, V.; Taylor, A. M.; de Leon Boenig, G.; Noland, C. L.; Murray, J.; Ly, J.; Choo, E. F.; Hunsaker, T. L.; Chan, E. W.; Merchant, M.; Kharbanda, S.; Gascoigne, K. E.; Kaufman, S.; Beresini, M. H.; Liao, J.; Liu, W.; Chen, K. X.; Chen, Z.; Conery, A. R.; Cote, A.; Jayaram, H.; Jiang, Y.; Kiefer, J. R.; Kleinheinz, T.; Li, Y.; Maher, J.; Pardo, E.; Poy, F.; Spillane, K. L.; Wang, F.; Wang, J.; Wei, X.; Xu, Z.; Xu, Z.; Yen, I.; Zawadzke, L.; Zhu, X.; Bellon, S.; Cummings, R.; Cochran, A. G.; Albrecht, B. K.; Magnuson, S., Discovery of a Potent and Selective in Vivo Probe (GNE-272) for the Bromodomains of CBP/EP300. *J. Med. Chem.* **2016**, *59* (23), 10549-10563.
30. Romero, F. A.; Murray, J.; Lai, K. W.; Tsui, V.; Albrecht, B. K.; An, L.; Beresini, M. H.; de Leon Boenig, G.; Bronner, S. M.; Chan, E. W.; Chen, K. X.; Chen, Z.; Choo, E. F.; Clagg, K.; Clark, K.; Crawford, T. D.; Cyr, P.; de Almeida Nagata, D.; Gascoigne, K. E.; Grogan, J. L.; Hatzivassiliou, G.; Huang, W.; Hunsaker, T. L.; Kaufman, S.; Koenig, S. G.; Li, R.; Li, Y.; Liang, X.; Liao, J.; Liu, W.; Ly, J.; Maher, J.; Masui, C.; Merchant, M.; Ran, Y.; Taylor, A. M.; Wai, J.; Wang, F.; Wei, X.; Yu, D.; Zhu, B.-Y.; Zhu, X.; Magnuson, S., GNE-781, A Highly Advanced Potent and Selective Bromodomain Inhibitor of Cyclic Adenosine Monophosphate Response Element Binding Protein, Binding Protein (CBP). *J. Med. Chem.* **2017**, *60* (22), 9162-9183.
31. Bono, J. S. D.; Cojocar, E.; Plummer, E. R.; Knuroski, T.; Clegg, K.; Ashby, F.; Pegg, N.; West, W.; Brooks, A. N., An open label phase I/IIa study to evaluate the safety and efficacy of CCS1477 as monotherapy and in combination in patients with advanced solid/metastatic tumors. *Journal of Clinical Oncology* **2019**, *37* (15), TPS5089-TPS5089.
32. Moustakim, M.; Clark, P. G. K.; Trulli, L.; Fuentes de Arriba, A. L.; Ehebauer, M. T.; Chaikuad, A.; Murphy, E. J.; Mendez-Johnson, J.; Daniels, D.; Hou, C.-F. D.; Lin, Y.-H.; Walker, J. R.; Hui, R.; Yang, H.; Dorrell, L.; Rogers, C. M.; Monteiro, O. P.; Fedorov, O.; Huber, K. V. M.; Knapp, S.; Heer, J.; Dixon, D. J.; Brennan, P. E., Discovery of a PCAF Bromodomain Chemical Probe. *Angew. Chem., Int. Ed.* **2017**, *56* (3), 827-831.

33. Mujtaba, S.; He, Y.; Zeng, L.; Farooq, A.; Carlson, J. E.; Ott, M.; Verdin, E.; Zhou, M.-M., Structural basis of lysine-acetylated HIV-1 Tat recognition by PCAF bromodomain. *Mol. Cell* **2002**, *9* (3), 575-586.
34. Wang, X.; Wang, S.; Troisi, E. C.; Howard, T. P.; Haswell, J. R.; Wolf, B. K.; Hawk, W. H.; Ramos, P.; Oberlick, E. M.; Tzvetkov, E. P.; Vazquez, F.; Hahn, W. C.; Park, P. J.; Roberts, C. W. M., BRD9 defines a SWI/SNF sub-complex and constitutes a specific vulnerability in malignant rhabdoid tumors. *Nat. Commun.* **2019**, *10* (1), 1-11.
35. Clark, P. G. K.; Vieira, L. C. C.; Tallant, C.; Fedorov, O.; Singleton, D. C.; Rogers, C. M.; Monteiro, O. P.; Bennett, J. M.; Baronio, R.; Mueller, S.; Daniels, D. L.; Mendez, J.; Knapp, S.; Brennan, P. E.; Dixon, D. J., LP99: Discovery and Synthesis of the First Selective BRD7/9 Bromodomain Inhibitor. *Angew. Chem., Int. Ed.* **2015**, *54* (21), 6217-6221.
36. Theodoulou, N. H.; Bamborough, P.; Bannister, A. J.; Becher, I.; Bit, R. A.; Che, K. H.; Chung, C.-w.; Dittmann, A.; Drewes, G.; Drewry, D. H.; Gordon, L.; Grandi, P.; Leveridge, M.; Lindon, M.; Michon, A.-M.; Molnar, J.; Robson, S. C.; Tomkinson, N. C. O.; Kouzarides, T.; Prinjha, R. K.; Humphreys, P. G., Discovery of I-BRD9, a Selective Cell Active Chemical Probe for Bromodomain Containing Protein 9 Inhibition. *J. Med. Chem.* **2016**, *59* (4), 1425-1439.
37. Kraemer, K. F.; Moreno, N.; Fruehwald, M. C.; Kerl, K., BRD9 inhibition, alone or in combination with cytostatic compounds as a therapeutic approach in rhabdoid tumors. *Int. J. Mol. Sci.* **2017**, *18* (7), 1537/1-1537/12.
38. Martin, L. J.; Koegl, M.; Bader, G.; Cockcroft, X.-L.; Fedorov, O.; Fiegen, D.; Gerstberger, T.; Hofmann, M. H.; Hohmann, A. F.; Kessler, D.; Knapp, S.; Knesl, P.; Kornigg, S.; Mueller, S.; Nar, H.; Rogers, C.; Rumpel, K.; Schaaf, O.; Steurer, S.; Tallant, C.; Vakoc, C. R.; Zeeb, M.; Zoephel, A.; Pearson, M.; Boehmelt, G.; McConnell, D., Structure-Based Design of an in Vivo Active Selective BRD9 Inhibitor. *J. Med. Chem.* **2016**, *59* (10), 4462-4475.
39. Bevill, S. M.; Olivares-Quintero, J. F.; Sciaky, N.; Golitz, B. T.; Singh, D.; Beltran, A. S.; Rashid, N. U.; Stuhlmiller, T. J.; Hale, A.; Moorman, N. J.; Santos, C. M.; Angus, S. P.;

Zawistowski, J. S.; Johnson, G. L., GSK2801, a BAZ2/BRD9 bromodomain inhibitor, synergizes with BET inhibitors to induce apoptosis in triple-negative breast cancer. *Mol. Cancer Res.* **2019**, *17* (7), 1503-1518.

40. Filippakopoulos, P.; Knapp, S., Targeting bromodomains: epigenetic readers of lysine acetylation. *Nat. Rev. Drug Discovery* **2014**, *13* (5), 337-356.

41. Brand, M.; Measures, A. R.; Wilson, B. G.; Cortopassi, W. A.; Alexander, R.; Hoss, M.; Hewings, D. S.; Rooney, T. P. C.; Paton, R. S.; Conway, S. J., Small Molecule Inhibitors of Bromodomain-Acetyl-lysine Interactions. *ACS Chem. Biol.* **2015**, *10* (1), 22-39.

42. Taniguchi, Y., The bromodomain and extra-terminal domain (BET) family: functional anatomy of BET paralogous proteins. *Int. J. Mol. Sci.* **2016**, *17* (11), 1849/1-1849/24.

43. Liu, Z.; Wang, P.; Chen, H.; Wold, E. A.; Tian, B.; Brasier, A. R.; Zhou, J., Drug Discovery Targeting Bromodomain-Containing Protein 4. *J. Med. Chem.* **2017**, *60* (11), 4533-4558.

44. Shi, J.; Vakoc, C. R., The Mechanisms behind the Therapeutic Activity of BET Bromodomain Inhibition. *Mol. Cell* **2014**, *54* (5), 728-736.

45. Muller, S.; Filippakopoulos, P.; Knapp, S., Bromodomains as therapeutic targets. *Expert Rev. Mol. Med.* **2011**, *13*, e29/1-e29/21.

46. Fu, L.-l.; Tian, M.; Li, X.; Li, J.-j.; Ouyang, L.; Zhang, Y.; Liu, B.; Huang, J.; Zhang, Y., Inhibition of BET bromodomains as a therapeutic strategy for cancer drug discovery. *Oncotarget* **2015**, *6* (8), 5501-16.

47. Gallenkamp, D.; Gelato, K. A.; Haendler, B.; Weinmann, H., Bromodomains and Their Pharmacological Inhibitors. *ChemMedChem* **2014**, *9* (3), 438-464.

48. Lamonica, J. M.; Deng, W.; Kadauke, S.; Campbell, A. E.; Gamsjaeger, R.; Wang, H.; Cheng, Y.; Billin, A. N.; Hardison, R. C.; MacKay, J. P.; Blobel, G. A., Bromodomain protein

Brd3 associates with acetylated GATA1 to promote its chromatin occupancy at erythroid target genes. Author Summary. *Proc. Natl. Acad. Sci. U. S. A.* **2011**, *108* (22), 8927-8928.

49. Wadhwa, E.; Nicolaides, T., Bromodomain Inhibitor Review: Bromodomain and Extra-terminal Family Protein Inhibitors as a Potential New Therapy in Central Nervous System Tumors. *Cureus* **2016**, *8* (5), e620.

50. Nicodeme, E.; Jeffrey, K. L.; Schaefer, U.; Beinke, S.; Dewell, S.; Chung, C.-w.; Chandwani, R.; Marazzi, I.; Wilson, P.; Coste, H.; White, J.; Kirilovsky, J.; Rice, C. M.; Lora, J. M.; Prinjha, R. K.; Lee, K.; Tarakhovsky, A., Suppression of inflammation by a synthetic histone mimic. *Nature (London, U. K.)* **2010**, *468* (7327), 1119-1123.

51. Brown, J. D.; Feldman, Z. B.; Doherty, S. P.; Reyes, J. M.; Rahl, P. B.; Lin, C. Y.; Sheng, Q.; Duan, Q.; Federation, A. J.; Kung, A. L.; Haldar, S. M.; Young, R. A.; Plutzky, J.; Bradner, J. E., BET bromodomain proteins regulate enhancer function during adipogenesis. *Proc. Natl. Acad. Sci. U. S. A.* **2018**, *115* (9), 2144-2149.

52. Filippakopoulos, P.; Qi, J.; Picaud, S.; Shen, Y.; Smith, W. B.; Fedorov, O.; Morse, E. M.; Keates, T.; Hickman, T. T.; Felletar, I.; Philpott, M.; Munro, S.; McKeown, M. R.; Wang, Y.; Christie, A. L.; West, N.; Cameron, M. J.; Schwartz, B.; Heightman, T. D.; La Thangue, N.; French, C.; Wiest, O.; Kung, A. L.; Knapp, S.; Bradner, J. E., Selective inhibition of BET bromodomains. *Nature (London, U. K.)* **2010**, *468* (7327), 1067-1073.

53. Alqahtani, A.; Choucair, K.; Ashraf, M.; Hammouda, D. M.; Alloghbi, A.; Khan, T.; Senzer, N.; Nemunaitis, J., Bromodomain and extra-terminal motif inhibitors: a review of preclinical and clinical advances in cancer therapy. *Future Sci. OA* **2019**, *5* (3), 1-20.

54. Theodoulou, N. H.; Tomkinson, N. C. O.; Prinjha, R. K.; Humphreys, P. G., Clinical progress and pharmacology of small molecule bromodomain inhibitors. *Curr. Opin. Chem. Biol.* **2016**, *33*, 58-66.

55. Amorim, S.; Stathis, A.; Zucca, E.; Gleeson, M.; Iyengar, S.; Cunningham, D.; Magarotto, V.; Palumbo, A.; Leleu, X.; Morschhauser, F.; Facon, T.; Karlin, L.; Salles, G.; Broussais, F.; Rezai, K.; Lokiec, F.; Herait, P.; Kahatt, C.; Thieblemont, C., Bromodomain

inhibitor OTX015 in patients with lymphoma or multiple myeloma: a dose-escalation, open-label, pharmacokinetic, phase 1 study. *Lancet Haematol* **2016**, *3* (4), e196-204.

56. Mirguet, O.; Gosmini, R.; Toum, J.; Clement, C. A.; Barnathan, M.; Brusq, J.-M.; Mordaunt, J. E.; Grimes, R. M.; Crowe, M.; Pineau, O.; Ajakane, M.; Daugan, A.; Jeffrey, P.; Cutler, L.; Haynes, A. C.; Smithers, N. N.; Chung, C.-w.; Bamborough, P.; Uings, I. J.; Lewis, A.; Witherington, J.; Parr, N.; Prinjha, R. K.; Nicodeme, E., Discovery of Epigenetic Regulator I-BET762: Lead Optimization to Afford a Clinical Candidate Inhibitor of the BET Bromodomains. *J. Med. Chem.* **2013**, *56* (19), 7501-7515.

57. Chung, C.-w.; Coste, H.; White, J. H.; Mirguet, O.; Wilde, J.; Gosmini, R. L.; Delves, C.; Magny, S. M.; Woodward, R.; Hughes, S. A.; Boursier, E. V.; Flynn, H.; Bouillot, A. M.; Bamborough, P.; Brusq, J.-M. G.; Gellibert, F. J.; Jones, E. J.; Riou, A. M.; Homes, P.; Martin, S. L.; Uings, I. J.; Toum, J.; Clement, C. A.; Boullay, A.-B.; Grimley, R. L.; Blandel, F. M.; Prinjha, R. K.; Lee, K.; Kirilovsky, J.; Nicodeme, E., Discovery and characterization of small molecule inhibitors of the BET family bromodomains. *J. Med. Chem.* **2011**, *54* (11), 3827-3838.

58. Filippakopoulos, P.; Picaud, S.; Fedorov, O.; Keller, M.; Wrobel, M.; Morgenstern, O.; Bracher, F.; Knapp, S., Benzodiazepines and benzotriazepines as protein interaction inhibitors targeting bromodomains of the BET family. *Bioorg. Med. Chem.* **2012**, *20* (6), 1878-1886.

59. Dawson, M. A.; Prinjha, R. K.; Dittman, A.; Giotopoulos, G.; Bantscheff, M.; Chan, W.-I.; Robson, S. C.; Chung, C.-w.; Hopf, C.; Savitski, M. M.; Huthmacher, C.; Gudgin, E.; Lugo, D.; Beinke, S.; Chapman, T. D.; Roberts, E. J.; Soden, P. E.; Auger, K. R.; Mirguet, O.; Doehner, K.; Delwel, R.; Burnett, A. K.; Jeffrey, P.; Drewes, G.; Lee, K.; Huntly, B. J. P.; Kouzarides, T., Inhibition of BET recruitment to chromatin as an effective treatment for MLL-fusion leukaemia. *Nature (London, U. K.)* **2011**, *478* (7370), 529-533.

60. Radwan, M.; Serya, R., Fragment-Based Drug Discovery in the Bromodomain and Extra-Terminal Domain Family. *Arch. Pharm. (Weinheim, Ger.)* **2017**, *350* (8).

61. Bamborough, P.; Diallo, H.; Goodacre, J. D.; Gordon, L.; Lewis, A.; Seal, J. T.; Wilson, D. M.; Woodrow, M. D.; Chung, C.-w., Fragment-Based Discovery of Bromodomain Inhibitors Part 2: Optimization of Phenylisoxazole Sulfonamides. *J. Med. Chem.* **2012**, *55* (2), 587-596.
62. Jennings, L. E.; Schiedel, M.; Hewings, D. S.; Picaud, S.; Laurin, C. M. C.; Bruno, P. A.; Bluck, J. P.; Scorch, A. R.; See, L.; Reynolds, J. K.; Moroglu, M.; Mistry, I. N.; Hicks, A.; Guzanov, P.; Clayton, J.; Evans, C. N. G.; Stazi, G.; Biggin, P. C.; Mapp, A. K.; Hammond, E. M.; Humphreys, P. G.; Filippakopoulos, P.; Conway, S. J., BET bromodomain ligands: Probing the WPF shelf to improve BRD4 bromodomain affinity and metabolic stability. *Bioorg. Med. Chem.* **2018**, *26* (11), 2937-2957.
63. Hewings, D. S.; Fedorov, O.; Filippakopoulos, P.; Martin, S.; Picaud, S.; Tumber, A.; Wells, C.; Olcina, M. M.; Freeman, K.; Gill, A.; Ritchie, A. J.; Sheppard, D. W.; Russell, A. J.; Hammond, E. M.; Knapp, S.; Brennan, P. E.; Conway, S. J., Optimization of 3,5-Dimethylisoxazole Derivatives as Potent Bromodomain Ligands. *J. Med. Chem.* **2013**, *56* (8), 3217-3227.
64. Picaud, S.; Da Costa, D.; Thanasopoulou, A.; Filippakopoulos, P.; Fish, P. V.; Philpott, M.; Fedorov, O.; Brennan, P.; Bunnage, M. E.; Owen, D. R.; Bradner, J. E.; Taniere, P.; O'Sullivan, B.; Mueller, S.; Schwaller, J.; Stankovic, T.; Knapp, S., PFI-1, a Highly Selective Protein Interaction Inhibitor, Targeting BET Bromodomains. *Cancer Res.* **2013**, *73* (11), 3336-3346.
65. Gosmini, R.; Nguyen, V. L.; Toum, J.; Simon, C.; Brusq, J.-M. G.; Krysa, G.; Mirguet, O.; Riou-Eymard, A. M.; Boursier, E. V.; Trottet, L.; Bamborough, P.; Clark, H.; Chung, C.-w.; Cutler, L.; Demont, E. H.; Kaur, R.; Lewis, A. J.; Schilling, M. B.; Soden, P. E.; Taylor, S.; Walker, A. L.; Walker, M. D.; Prinjha, R. K.; Nicodeme, E., The Discovery of I-BET726 (GSK1324726A), a Potent Tetrahydroquinoline ApoA1 Up-Regulator and Selective BET Bromodomain Inhibitor. *J. Med. Chem.* **2014**, *57* (19), 8111-8131.
66. Zhao, L.; Cao, D.; Chen, T.; Wang, Y.; Miao, Z.; Xu, Y.; Chen, W.; Wang, X.; Li, Y.; Du, Z.; Xiong, B.; Li, J.; Xu, C.; Zhang, N.; He, J.; Shen, J., Fragment-Based Drug Discovery of 2-Thiazolidinones as Inhibitors of the Histone Reader BRD4 Bromodomain. *J. Med. Chem.* **2013**, *56* (10), 3833-3851.

67. Galdeano, C.; Ciulli, A., Selectivity on-target of bromodomain chemical probes by structure-guided medicinal chemistry and chemical biology. *Future Med. Chem.* **2016**, *8* (13), 1655-1680.
68. Gacias, M.; Gerona-Navarro, G.; Plotnikov, A. N.; Zhang, G.; Zeng, L.; Kaur, J.; Moy, G.; Rusinova, E.; Rodriguez, Y.; Matikainen, B.; Vincek, A.; Joshua, J.; Casaccia, P.; Zhou, M.-M., Selective Chemical Modulation of Gene Transcription Favors Oligodendrocyte Lineage Progression. *Chem. Biol. (Oxford, U. K.)* **2014**, *21* (7), 841-854.
69. Fong, C. Y.; Gilan, O.; Lam, E. Y. N.; Rubin, A. F.; Ftouni, S.; Tyler, D.; Stanley, K.; Sinha, D.; Yeh, P.; Morison, J.; Giotopoulos, G.; Lugo, D.; Jeffrey, P.; Lee, S. C.-W.; Carpenter, C.; Gregory, R.; Ramsay, R. G.; Lane, S. W.; Abdel-Wahab, O.; Kouzarides, T.; Johnstone, R. W.; Dawson, S.-J.; Huntly, B. J. P.; Prinjha, R. K.; Papenfuss, A. T.; Dawson, M. A., BET inhibitor resistance emerges from leukaemia stem cells. *Nature (London, U. K.)* **2015**, *525* (7570), 538-542.
70. Zhang, G.; Plotnikov, A. N.; Rusinova, E.; Shen, T.; Morohashi, K.; Joshua, J.; Zeng, L.; Mujtaba, S.; Ohlmeyer, M.; Zhou, M.-M., Structure-Guided Design of Potent Diazobenzene Inhibitors for the BET Bromodomains. *J. Med. Chem.* **2013**, *56* (22), 9251-9264.
71. Picaud, S.; Wells, C.; Felletar, I.; Brotherton, D.; Martin, S.; Savitsky, P.; Diez-Dacal, B.; Philpott, M.; Bountra, C.; Lingard, H.; Fedorov, O.; Muller, S.; Brennan, P. E.; Knapp, S.; Filippakopoulos, P., RVX-208, an inhibitor of BET transcriptional regulators with selectivity for the second bromodomain. *Proc Natl Acad Sci U S A* **2013**, *110* (49), 19754-9.
72. Cheng, C.; Diao, H.; Zhang, F.; Wang, Y.; Wang, K.; Wu, R., Deciphering the mechanisms of selective inhibition for the tandem BD1/BD2 in the BET-bromodomain family. *Phys. Chem. Chem. Phys.* **2017**, *19* (35), 23934-23941.
73. Baud, M. G. J.; Lin-Shiao, E.; Zengerle, M.; Tallant, C.; Ciulli, A., New Synthetic Routes to Triazolo-benzodiazepine Analogues: Expanding the Scope of the Bump-and-Hole Approach for Selective Bromo and Extra-Terminal (BET) Bromodomain Inhibition. *J. Med. Chem.* **2016**, *59* (4), 1492-1500.

74. Law, R. P.; Atkinson, S. J.; Bamborough, P.; Chung, C.-w.; Demont, E. H.; Gordon, L. J.; Lindon, M.; Prinjha, R. K.; Watson, A. J. B.; Hirst, D. J., Discovery of Tetrahydroquinoxalines as Bromodomain and Extra-Terminal Domain (BET) Inhibitors with Selectivity for the Second Bromodomain. *J. Med. Chem.* **2018**, *61* (10), 4317-4334.
75. Nicholls, S. J.; Ray, K. K.; Johansson, J. O.; Gordon, A.; Sweeney, M.; Halliday, C.; Kulikowski, E.; Wong, N.; Kim, S. W.; Schwartz, G. G., Selective BET Protein Inhibition with Apabetalone and Cardiovascular Events: A Pooled Analysis of Trials in Patients with Coronary Artery Disease. *Am. J. Cardiovasc. Drugs* **2018**, *18* (2), 109-115.
76. Fidanze, S. D.; Hasvold, L. A.; Liu, D.; McDaniel, K. F.; Pratt, J.; Schrimpf, M.; Sheppard, G. S.; Wang, L.; Li, B. Arylpyrrolo[2,3-c]pyridinones as bromodomain inhibitors and their preparation. WO2017177955A1, **2017**.
77. Wang, L.; Sheppard, G.; Fidanze, S.; Hasvold, L.; Liu, D.; Pratt, J.; Bui, M.-H.; Faivre, E.; Huang, X.; Lin, X.; Wilcox, D.; Shen, Y.; Albert, D.; Kati, W.; Mc Daniel, K. In *Structure based design: Identification of the clinical candidate ABBV-744, a first-in-class highly BDII-selective BET bromodomain inhibitor*, American Chemical Society: 2018; pp MEDI-22.
78. Jiang, F.; Hu, Q.; Zhang, Z.; Li, H.; Li, H.; Zhang, D.; Li, H.; Ma, Y.; Xu, J.; Chen, H.; Cui, Y.; Zhi, Y.; Zhang, Y.; Xu, J.; Zhu, J.; Lu, T.; Chen, Y., Discovery of Benzo[cd]indol-2(1H)-ones and Pyrrolo[4,3,2-de]quinolin-2(1H)-ones as Bromodomain and Extra-Terminal Domain (BET) Inhibitors with Selectivity for the First Bromodomain with Potential High Efficiency against Acute Gouty Arthritis. *J. Med. Chem.* **2019**, *62* (24), 11080-11107.
79. Tanaka, M.; Roberts, J. M.; Seo, H.-S.; Souza, A.; Paulk, J.; Scott, T. G.; DeAngelo, S. L.; Dhe-Paganon, S.; Bradner, J. E., Design and characterization of bivalent BET inhibitors. *Nat. Chem. Biol.* **2016**, *12* (12), 1089-1096.
80. Ren, C.; Zhang, G.; Han, F.; Fu, S.; Cao, Y.; Zhang, F.; Zhang, Q.; Meslamani, J.; Xub, Y.; Ji, D.; Cao, L.; Zhou, Q.; Cheung, K.-L.; Sharma, R.; Babault, N.; Yic, Z.; Zhang, W.; Walsh, M. J.; Zeng, L.; Zhou, M.-M., Spatially constrained tandem bromodomain inhibition bolsters sustained repression of BRD4 transcriptional activity for TNBC cell growth. *Proc. Natl. Acad. Sci. U. S. A.* **2018**, *115* (31), 7949-7954.

81. Waring, M. J.; Chen, H.; Rabow, A. A.; Walker, G.; Bobby, R.; Boiko, S.; Bradbury, R. H.; Callis, R.; Clark, E.; Dale, I.; Daniels, D. L.; Dulak, A.; Flavell, L.; Holdgate, G.; Jowitt, T. A.; Kikhney, A.; McAlister, M.; Mendez, J.; Ogg, D.; Patel, J.; Petteruti, P.; Robb, G. R.; Robers, M. B.; Saif, S.; Stratton, N.; Svergun, D. I.; Wang, W.; Whittaker, D.; Wilson, D. M.; Yao, Y., Potent and selective bivalent inhibitors of BET bromodomains. *Nat. Chem. Biol.* **2016**, *12* (12), 1097-1104.
82. Bradbury, R. H.; Callis, R.; Carr, G. R.; Chen, H.; Clark, E.; Feron, L.; Glossop, S.; Graham, M. A.; Hattersley, M.; Jones, C.; Lamont, S. G.; Ouvry, G.; Patel, A.; Patel, J.; Rabow, A. A.; Roberts, C. A.; Stokes, S.; Stratton, N.; Walker, G. E.; Ward, L.; Whalley, D.; Whittaker, D.; Wrigley, G.; Waring, M. J., Optimization of a Series of Bivalent Triazolopyridazine Based Bromodomain and Extraterminal Inhibitors: The Discovery of (3R)-4-[2-[4-[1-(3-Methoxy-[1,2,4]triazolo[4,3-b]pyridazin-6-yl)-4-piperidyl]phenoxy]ethyl]-1,3-dimethyl-piperazin-2-one (AZD5153). *J. Med. Chem.* **2016**, *59* (17), 7801-7817.
83. Paiva, S.-L.; Crews, C. M., Targeted protein degradation: elements of PROTAC design. *Curr. Opin. Chem. Biol.* **2019**, *50*, 111-119.
84. Lee, M. J.; Lee, J. H.; Rubinsztein, D. C., Tau degradation: The ubiquitin-proteasome system versus the autophagy-lysosome system. *Prog. Neurobiol. (Oxford, U. K.)* **2013**, *105*, 49-59.
85. Wertz, I. E.; Wang, X., From Discovery to Bedside: Targeting the Ubiquitin System. *Cell Chem. Biol.* **2019**, *26* (2), 156-177.
86. Nakayama, K. I.; Nakayama, K., Ubiquitin ligases: cell-cycle control and cancer. *Nat. Rev. Cancer* **2006**, *6* (5), 369-381.
87. Sarikas, A.; Hartmann, T.; Pan, Z.-Q., The cullin protein family. *Genome Biol.* **2011**, *12*, 220.

88. Collins, I.; Wang, H.; Caldwell, J. J.; Chopra, R., Chemical approaches to targeted protein degradation through modulation of the ubiquitin-proteasome pathway. *Biochem. J.* **2017**, *474* (7), 1127-1147.
89. Ito, T.; Ando, H.; Suzuki, T.; Ogura, T.; Hotta, K.; Imamura, Y.; Yamaguchi, Y.; Handa, H., Identification of a Primary Target of Thalidomide Teratogenicity. *Science (Washington, DC, U. S.)* **2010**, *327* (5971), 1345-1350.
90. Crew, A. P.; Qian, Y.; Dong, H.; Wang, J.; Hornberger, K. R.; Crews, C. M. Tetrahydronaphthalene and tetrahydroisoquinoline derivatives as estrogen receptor degraders and their preparation. WO2018102725A1, 2018.
91. Fischer, E. S.; Bohm, K.; Lydeard, J. R.; Yang, H.; Stadler, M. B.; Cavadini, S.; Nagel, J.; Serluca, F.; Acker, V.; Lingaraju, G. M.; Tichkule, R. B.; Schebesta, M.; Forrester, W. C.; Schirle, M.; Hassiepen, U.; Ottl, J.; Hild, M.; Beckwith, R. E. J.; Harper, J. W.; Jenkins, J. L.; Thoma, N. H., Structure of the DDB1-CRBN E3 ubiquitin ligase in complex with thalidomide. *Nature (London, U. K.)* **2014**, *512* (7512), 49-53.
92. Nguyen, H. C.; Yang, H.; Fribourgh, J. L.; Wolfe, L. S.; Xiong, Y., Insights into Cullin-RING E3 Ubiquitin Ligase Recruitment: Structure of the VHL-EloBC-Cul2 Complex. *Structure (Oxford, U. K.)* **2015**, *23* (3), 441-449.
93. Buckley, D. L.; Van Molle, I.; Gareiss, P. C.; Tae, H. S.; Michel, J.; Noblin, D. J.; Jorgensen, W. L.; Ciulli, A.; Crews, C. M., Targeting the von Hippel-Lindau E3 Ubiquitin Ligase Using Small Molecules To Disrupt the VHL/HIF-1 α Interaction. *J. Am. Chem. Soc.* **2012**, *134* (10), 4465-4468.
94. Galdeano, C.; Gadd, M. S.; Soares, P.; Scaffidi, S.; Van Molle, I.; Birced, I.; Hewitt, S.; Dias, D. M.; Ciulli, A., Structure-Guided Design and Optimization of Small Molecules Targeting the Protein-Protein Interaction between the von Hippel-Lindau (VHL) E3 Ubiquitin Ligase and the Hypoxia Inducible Factor (HIF) Alpha Subunit with in Vitro Nanomolar Affinities. *J. Med. Chem.* **2014**, *57* (20), 8657-8663.

95. Soares, P.; Gadd, M. S.; Frost, J.; Galdeano, C.; Ellis, L.; Epemolu, O.; Rocha, S.; Read, K. D.; Ciulli, A., Group-Based Optimization of Potent and Cell-Active Inhibitors of the von Hippel-Lindau (VHL) E3 Ubiquitin Ligase: Structure-Activity Relationships Leading to the Chemical Probe (2S,4R)-1-((S)-2-(1-Cyanocyclopropanecarboxamido)-3,3-dimethylbutanoyl)-4-hydroxy-N-(4-(4-methylthiazol-5-yl)benzyl)pyrrolidine-2-carboxamide (VH298). *J. Med. Chem.* **2018**, *61* (2), 599-618.
96. Schapira, M.; Calabrese, M. F.; Bullock, A. N.; Crews, C. M., Targeted protein degradation: expanding the toolbox. *Nat. Rev. Drug Discovery* **2019**.
97. Lu, J.; Qian, Y.; Altieri, M.; Dong, H.; Wang, J.; Raina, K.; Hines, J.; Winkler, J. D.; Crew, A. P.; Coleman, K.; Crews, C. M., Hijacking the E3 Ubiquitin Ligase Cereblon to Efficiently Target BRD4. *Chem. Biol. (Oxford, U. K.)* **2015**, *22* (6), 755-763.
98. Winter, G. E.; Buckley, D. L.; Paulk, J.; Roberts, J. M.; Souza, A.; Dhe-Paganon, S.; Bradner, J. E., Phthalimide conjugation as a strategy for in vivo target protein degradation. *Science (Washington, DC, U. S.)* **2015**, *348* (6241), 1376-1381.
99. Zhou, B.; Hu, J.; Xu, F.; Chen, Z.; Bai, L.; Fernandez-Salas, E.; Lin, M.; Liu, L.; Yang, C.-Y.; Zhao, Y.; McEachern, D.; Przybranowski, S.; Wen, B.; Sun, D.; Wang, S., Discovery of a Small-Molecule Degradator of Bromodomain and Extra-Terminal (BET) Proteins with Picomolar Cellular Potencies and Capable of Achieving Tumor Regression. *J. Med. Chem.* **2018**, *61* (2), 462-481.
100. Qin, C.; Hu, Y.; Zhou, B.; Fernandez-Salas, E.; Yang, C.-Y.; Liu, L.; McEachern, D.; Przybranowski, S.; Wang, M.; Stuckey, J.; Meagher, J.; Bai, L.; Chen, Z.; Lin, M.; Yang, J.; Ziazadeh, D. N.; Xu, F.; Hu, J.; Xing, W.; Huang, L.; Li, S.; Wen, B.; Sun, D.; Wang, S., Discovery of QCA570 as an Exceptionally Potent and Efficacious Proteolysis Targeting Chimera (PROTAC) Degradator of the Bromodomain and Extra-Terminal (BET) Proteins Capable of Inducing Complete and Durable Tumor Regression. *J. Med. Chem.* **2018**, *61* (15), 6685-6704.
101. Zengerle, M.; Chan, K.-H.; Ciulli, A., Selective Small Molecule Induced Degradation of the BET Bromodomain Protein BRD4. *ACS Chem. Biol.* **2015**, *10* (8), 1770-1777.

102. Gadd, M. S.; Testa, A.; Lucas, X.; Chan, K.-H.; Chen, W.; Lamont, D. J.; Zengerle, M.; Ciulli, A., Structural basis of PROTAC cooperative recognition for selective protein degradation. *Nat. Chem. Biol.* **2017**, *13* (5), 514-521.
103. Testa, A.; Hughes, S. J.; Lucas, X.; Wright, J. E.; Ciulli, A., Structure-based design of a macrocyclic PROTAC. *ChemRxiv* **2019**, 1-13.
104. Raina, K.; Lu, J.; Qian, Y.; Altieri, M.; Gordon, D.; Rossi, A. M. K.; Wang, J.; Chen, X.; Dong, H.; Siu, K.; Winkler, J. D.; Crew, A. P.; Crews, C. M.; Coleman, K. G., PROTAC-induced BET protein degradation as a therapy for castration-resistant prostate cancer. *Proc. Natl. Acad. Sci. U. S. A.* **2016**, *113* (26), 7124-7129.
105. Chan, K.-H.; Zengerle, M.; Testa, A.; Ciulli, A., Impact of Target Warhead and Linkage Vector on Inducing Protein Degradation: Comparison of Bromodomain and Extra-Terminal (BET) Degraders Derived from Triazolodiazepine (JQ1) and Tetrahydroquinoline (I-BET726) BET Inhibitor Scaffolds. *J. Med. Chem.* **2018**, *61* (2), 504-513.
106. Churcher, I., Protac-Induced Protein Degradation in Drug Discovery: Breaking the Rules or Just Making New Ones? *J. Med. Chem.* **2018**, *61* (2), 444-452.
107. Edmondson, S. D.; Yang, B.; Fallan, C., Proteolysis targeting chimeras (PROTACs) in 'beyond rule-of-five' chemical space: Recent progress and future challenges. *Bioorg. Med. Chem. Lett.* **2019**, *29* (13), 1555-1564.
108. Li, J. J.; Holsworth, D. D.; Hu, L.-Y., Molecular properties that influence the oral bioavailability of drug candidates. *Chemtracts* **2003**, *16* (7), 439-442.
109. Selig, R.; Goettert, M.; Schattel, V.; Schollmeyer, D.; Albrecht, W.; Laufer, S., A Frozen Analogue Approach to Aminopyridinylimidazoles Leading to Novel and Promising p38 MAP Kinase Inhibitors. *J. Med. Chem.* **2012**, *55* (19), 8429-8439.
110. Huggins, D. J.; Sherman, W.; Tidor, B., Rational Approaches to Improving Selectivity in Drug Design. *J. Med. Chem.* **2012**, *55* (4), 1424-1444.

111. Niesen, F. H.; Berglund, H.; Vedadi, M., The use of differential scanning fluorimetry to detect ligand interactions that promote protein stability. *Nat. Protoc.* **2007**, *2* (9), 2212-2221.
112. Cole, J. L.; Lary, J. W.; Thomas, P. M.; Laue, T. M., Analytical ultracentrifugation: sedimentation velocity and sedimentation equilibrium. *Methods Cell Biol* **2008**, *84*, 143-79.
113. Su, H.; Xu, Y., Application of ITC-based characterization of thermodynamic and kinetic association of ligands with proteins in drug design. *Front. Pharmacol.* **2018**, *9*, 1133.
114. McDaniel, K. F.; Wang, L.; Soltwedel, T.; Fidanze, S. D.; Hasvold, L. A.; Liu, D.; Mantei, R. A.; Pratt, J. K.; Sheppard, G. S.; Bui, M. H.; Faivre, E. J.; Huang, X.; Li, L.; Lin, X.; Wang, R.; Warder, S. E.; Wilcox, D.; Albert, D. H.; Magoc, T. J.; Rajaraman, G.; Park, C. H.; Hutchins, C. W.; Shen, J. J.; Edalji, R. P.; Sun, C. C.; Martin, R.; Gao, W.; Wong, S.; Fang, G.; Elmore, S. W.; Shen, Y.; Kati, W. M., Discovery of N-(4-(2,4-Difluorophenoxy)-3-(6-methyl-7-oxo-6,7-dihydro-1H-pyrrolo[2,3-c]pyridin-4-yl)phenyl)ethanesulfonamide (ABBV-075/Mivebresib), a Potent and Orally Available Bromodomain and Extraterminal Domain (BET) Family Bromodomain Inhibitor. *J. Med. Chem.* **2017**, *60* (20), 8369-8384.
115. Cortes, E. C.; Franco, R. S.; Mellado, O. G., Synthesis and spectral properties of 2-[(o- and p-substituted)phenylamino]-3H-5-[(o- and p-substituted)phenyl]-7-chloro-1,4-benzodiazepines. *J. Heterocycl. Chem.* **2001**, *38* (3), 663-669.
116. McDonald, I. M.; Austin, C.; Buck, I. M.; Dunstone, D. J.; Griffin, E.; Harper, E. A.; Hull, R. A. D.; Kalindjian, S. B.; Linney, I. D.; Low, C. M. R.; Pether, M. J.; Spencer, J.; Wright, P. T.; Adatia, T.; Bashall, A., Novel, Achiral 1,3,4-Benzotriazepine Analogues of 1,4-Benzodiazepine-Based CCK2 Antagonists That Display High Selectivity over CCK1 Receptors. *J. Med. Chem.* **2006**, *49* (7), 2253-2261.
117. Bouzide, A.; Sauve, G., Silver(I) Oxide Mediated Highly Selective Monotosylation of Symmetrical Diols. Application to the Synthesis of Polysubstituted Cyclic Ethers. *Org. Lett.* **2002**, *4* (14), 2329-2332.
118. Davila, J.; Chassepot, A.; Longo, J.; Boulmedais, F.; Reisch, A.; Frisch, B.; Meyer, F.; Voegel, J.-C.; Mesini, P. J.; Senger, B.; Metz-Boutigue, M.-H.; Hemmerle, J.; Lavallo, P.;

Schaaf, P.; Jierry, L., Cyto-mechanoresponsive Polyelectrolyte Multilayer Films. *J. Am. Chem. Soc.* **2012**, *134* (1), 83-86.

119. Milite, C.; Amendola, G.; Nocentini, A.; Bua, S.; Cipriano, A.; Barresi, E.; Feoli, A.; Novellino, E.; Da Settimo, F.; Supuran, C. T.; Castellano, S.; Cosconati, S.; Taliani, S., Novel 2-substituted-benzimidazole-6-sulfonamides as carbonic anhydrase inhibitors: synthesis, biological evaluation against isoforms I, II, IX and XII and molecular docking studies. *J. Enzyme Inhib. Med. Chem.* **2019**, *34* (1), 1697-1710.

120. Crew, A. P.; Berlin, M.; Flanagan, J. J.; Dong, H.; Ishchenko, A. Preparation of tau-protein targeting bifunctional compounds (PROTACS) as E3 ubiquitin ligase binding useful in treatment and prevention of diseases. US20180125821A1, **2018**.